Collapsin Response Mediator Protein and Rho GTPases in neuronal differentiation

A thesis by

Matthew David Brown

Submitted to

University College London

for the

Degree of Doctor of Philosophy, Ph.D.

2004

Department of Molecular Neuroscience
Institute of Neurology
University College London
Queens Square
London WC1N 3BG

ProQuest LLC
789 East Eisenhower Parkway
P.O. Box 1346
Ann Arbor, MI 48106-1346

Acknowledgements

I wish to thank Professor Louis Lim for giving me the opportunity to undertake my Ph.D in his lab, and enabling me to work in Singapore and attend conferences around the world. I would also like to express my thanks to Christine Hall for her constant encouragement, support and supervision for the duration of my project. Thanks also go to the members of Lim Lab for their help and advice over the past few years.

I wish to say a huge thank you to all my family, in particular Mum, Geoff, Dad and Elaine. Without their constant support and encouragement over the years I would never have got this far. Finally a big thank you to Sarah for all the support, encouragement and the occasional technical suggestion throughout the project and during the writing up.

Thesis Abstract

In the developing nervous system the modelling of axons and their growth cones is dependent on the dynamic regulation of the Rho family of GTPases, which play a crucial role in the regulation of the actin cytoskeleton. The guidance cues controlling axon path finding, either repulsive or attractive, require the Rho GTPases to effect changes in morphology. The signalling pathways linking the guidance molecules, and their receptors, to the Rho family GTPases remain unclear.

Collapsin Response Mediator Protein-2 (CRMP-2) is a neurospecific protein involved in axonal outgrowth and the semaphorin3A collapse pathway. CRMP-2 is also a Rho kinase substrate, suggesting an involvement with the Rho GTPases. To investigate this, CRMP-2 was co-expressed in the neuroblastoma cell line, N1E-115, with active and inactive GTPase mutants. Cells expressing dominant active Rac1 and CRMP-2 became contracted, normally a RhoA effect, while co-expression of dominant active RhoA and CRMP-2 resulted in a phenotype typically associated with Rac1 signalling.

CRMP-2 could bind directly to RhoA and Rac1, and, to a much lesser extent, Cdc42 in an overlay assay. *In vivo* CRMP-2 associated with active RhoA, but immunoprecipitated with active and inactive Rac1 mutants.

Cdk5 inhibitors, but not Rho-kinase inhibitors blocked semaphorin3A-induced collapse in dorsal root ganglion neurones and N1E-115. Mutation of the Cdk5 phosphorylation site in CRMP-2 also inhibited sema3A collapse, suggesting a specific role of Cdk5 and CRMP-2 in the semaphorin3A growth cone collapse pathway.

These results show CRMP-2 can switch RhoA and Rac1, and may link the guidance cues to the Rho-GTPases, which define growth cone morphology through their regulation of the actin cytoskeleton. Downstream of sema3A, CRMP-2 plays a crucial role in growth cone collapse, in a pathway involving Cdk5, and possibly phosphorylation at serine 522.

Table of contents

List of Figures

Abbreviations

ADF	Actin Depolymerising Factor
ADP	Adenosine Diphosphate
Arp2/3	Actin Related Proteins 2/3
ATP	Adenosine Triphosphate
BCR	Breakpoint Cluster Region
BDNF	Brain Derived Nerve Factor
BSA	Bovine Serum Albumin
cAMP	Cyclic Adenosine Monophosphate
Cdc42	Cell Division Cycle 42
Cdk5	Cyclin Dependant Kinase 5
cGMP	Cyclic Guanosine Monophosphate
CNS	Central Nervous System
CRAM	CRMP Associated Molecular
CRIB	Cdc42/Rac Interacting Domain
CRIK	Citron Rho-Interacting Kinase
CRMP	Collapsin Response Mediator Protein
CSPG	Chondroitin Sulphate Proteoglycan
DCC	Deleted in Colorectal Cancer
DH domain	Dbl homology domain
DMEM	Dulbeccos Modified Eagles Medium
DMSO	Dimethyl Sulphoxide
Drg	Dorsal Root Ganglion

DTT	Dithiothretiol
E.coli	Escherichia Coli
ECL	Enhanced Chemiluminescence
ECM	Extra Cellular Matrix
EDTA	Ethylenediamine Tetraacetic Acid
EVH	Ena/VASP homology
F-actin	Filamentous Actin
FAK	Focal Adhesion Kinase
FCS	Foetal Calf Serum
FITC	Fluorescein Isothiocyanate
G-actin	Globular Actin
GAP	GTPase Activating Protein
GDI	Guanosine Disassociation Inhibitor
GDP	Guanosine Diphosphate
GEF	Guanosine Exchange Factor
GSK	Glycogen synthase kinase
GST	Gluathione-S-Transferase
GTP	Guanosine Triphosphqate
HA	Haemagglutinin Antigen
HBSS	Hanks Buffered Saline Solution
HCl	Hydrochloric Acid
Ig	Immunoglobin

IPTG	Isopropyl-thio-D-galactoside
LIM Kinase	LIN-1, ISL-1, MEC-3 Kinase
LPA	Lysophosphatidic Acid
MAG	Myelin Associated Glycoprotein
MBS	Myosin Binding Subunit (of Myosin phosphatase)
MDia	Mammalian Diaphanous
MLC	Myosin Light Chain
MLCK	MLC Kinase
NGF	Nerve Growth Factor
NP-1	Neuropilin-1
N-WASP	Neuronal WASP
OTK	Off Track
PAGE	Polyacrylamide Gel Electrophoresis
PAK	p21 Activated Kinase
PBS	Phosphate Buffered Saline
PCR	Polymerase Chain Reaction
PDGF	Platelet Derived Growth Factor
PDZ domain	PSD-95, Dlg, ZO1 domain
PH	Pleckstrin homology domain
PIX	PAK Interacting Exchange Factor
PKA	Protein Kinase A
PKC	Protein Kinase C

PKG	Protein Kinase G
PLD	Phospholipase D
PMA	Phorbol Myristate Acetate
PMSF	Phenylmethyl-Sulfonyl Fluoride
PNS	Peripheral Nervous System
PSD-95	Postsynaptic density 95
PVDF	Polyvinylidene Fluoride Transfer Membrane
Rac1	Ras-related C3 botulinum toxin substrate 1
RGS	Regulator of heteromeric G-protein Signalling
RhoA	Ras homologous A
ROK	Rho Kinase
ROS	Reactive Oxygen Species
SDS	Sodium Doedecyl Sulphate
Sema	Semaphorin
Ser	Serine
SH2	Src homology domain 2
SH3	Src homology domain 3
Thr	Threonine
Tiam-1	T Lymphoma Invasion and Metastasis
TOAD	Turned On After Division
TRITC	Tetramethyl Rhodamine Isothiocyanate

Unc	Uncoordinated
WASP	Wiskott Aldrich Protein
WIP	WASP Interacting Protein

Chapter 1

Introduction

1.1 The Actin Cytoskeleton

Actins, and actin filaments, form a crucial component of the cytoskeleton, allowing cells to maintain or change morphology and to migrate in response to environmental factors. They are very abundant proteins in most cells, often consisting of 5% or more of total cell protein. The actin in mammalian tissues is divided into 3 different classes; α-actin, which is found in various types of muscle tissue, while β and γ-actin are non-muscle actins.

1.1.1 Actin

Actin exists in two forms, G-actin and F-actin. G-actin, or globular actin, consists of the monomer actin units, each a single peptide of 375 amino acids. When these monomers polymerise they form filamentous actin, or F-actin, in a process requiring ATP. Each monomer binds a single ATP molecule that is hydrolysed to ADP when the monomers polymerise (Figure 1). The ADP is trapped in the actin monomer once it is incorporated into the filament. However when the monomer is removed during depolymerisation, the ADP is removed and replaced with ATP, ready for re-incorporation.

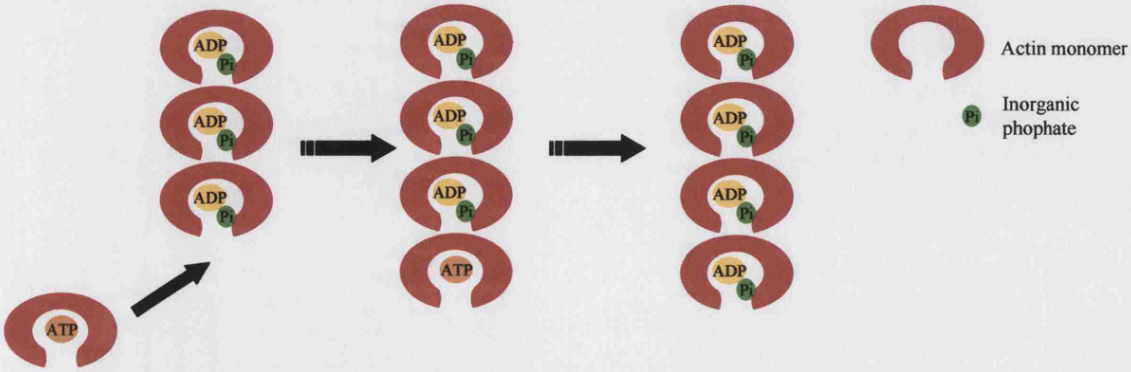

Figure 1.1 Assembly of actin monomers into filaments, and hydrolysis of ATP.

The two ends of F-actin filaments have different polymerising properties. The barbed end polymerises up to 10 times faster than the pointed end. Due to the different polymerisation abilities of the different ends, each has a different critical concentration for polymerisation (Kd). This is the concentration of monomers required to induce spontaneous polymerisation *in vitro*. Under physiological salt conditions the Kd for the barbed end is 0.1μM, and 0.6μM for the pointed end (reviewed in Pollard, 1999). At a monomer concentration between the two Kd, there is a net polymerisation at the barbed end, and a net loss at the pointed end. When these two reactions proceed at an identical rate, the actin filament undergoes a process called treadmilling. Here, although there is a net influx of actin monomers, the filament does not change in length.

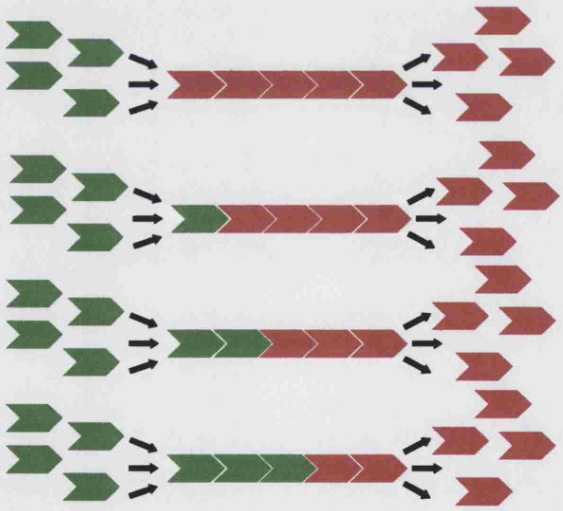

Figure 1.2. Diagram of actin treadmilling.

The elongation of actin filaments is a balance between the available actin monomers and the exposed ends of actin filaments. Regulation of polymerisation can be achieved by regulating the availability of either component.

1.1.2 Formation of new actin filaments

Spontaneous formation of actin filaments from actin monomers is an unfavourable reaction because of the instability of the dimers and trimers. Although actin monomers have been shown to polymerise *in vitro* under physiological salt conditions, this is a slow reaction.

In vivo, the formation of new actin filaments from actin monomers, termed nucleation, is regulated by accessory proteins, which either promote or inhibit the process. Some of the best studied accessory proteins are those in the Arp2/3 complex. The Arp2/3 complex consists of 7 subunits, Actin-related proteins (ARP) 2 and 3, and five novel proteins, p40, p35, p19, p18 and p14. Proteins in the Arp2/3 complex are very abundant, and highly conserved (Kelleher et al, 1995; Welch et al, 1997). Once activated by the WASP/scar proteins (see section 1.1.4), Arp2/3 binds directly to actin monomers, allowing barbed ends to become exposed, and hence the nucleation of new actin filaments (Rohatgi et al, 1999).

After nucleation, the Arp2/3 is incorporated into the new filament network (Yarar et al, 1999), allowing the addition of new filaments onto the side of the first filament. Consequently, Arp2/3 enables the anchoring of end-to-side branches, which takes place during nucleation (Blanchoin et al, 2000). These side branches are formed at 70^{o} angle from the main branch (Mullins et al, 1998), which can also be seen in the actin structures at the leading edge of membrane protrusions, where the actin forms filaments at 70^{o} from the side filaments. In addition to being able to nucleate the formation of new filaments, Arp2/3 can also bind to existing filaments, and serve as an additional nucleation site on the side of filaments. This is another way by which

Arp2/3 can allow side branches to form and permit cross-linking between actin filaments. The formation of filopodia involves different processes because they consist of parallel bundles of actin filaments, which are held together by cross-linking proteins, such as fimbrin (Matsudaira et al, 1983). There are no cross-linking or side actin filament branches in these structures, although the Arp2/3 complex still appears to play a role (Goldberg et al, 2000; Vignjevic et al, 2003).

1.1.3 Regulation of the actin monomer pool

Many cell types can contain cellular concentrations of actin monomers of around 100μM (Pollard, 1999). However, *in vitro*, these monomers would spontaneously polymerise, until a concentration of 0.1μM, the Kd for the barbed end, was reached. Therefore cells have developed methods to maintain these high concentration actin monomer pools.

The two main actin monomer binding proteins in vertebrate cells are thymosin-β4 and profilin. Thymosin-β4, a small protein of 42 residues, sequesters actin monomers (Safer et al, 1994), and has a 50 fold higher affinity for ATP-actin than for ADP-actin (Carlier et al, 1993; Pantaloni et al, 1993). Once bound to thymosin-β4, the actin monomers cannot polymerise and so thymosin-β4 is thought to play an important role in maintaining the high concentration of actin monomers present in many cells types. Thymosin-β4 competes for the actin monomers with profilin, the only actin monomer binding protein present in lower organisms, such as protozoa and fungi. Profilin binds to actin monomers and transports them to the barbed filament ends, to allow polymerisation (Pantaloni et al, 1993). Profilin also facilitates the exchange of ADP for ATP in released monomers, allowing them to be returned to the actin monomer

pool. ATP-actin is exchanged between thymosin-β4 and profilin to regulate actin filament elongation. The concentration of the proteins, and their affinity for the actin monomers determines how much actin is available for elongation.

Profilin is important in maintaining an available pool of ATP-actin ready to elongate free barbed ends. However, if all the actin filaments in a cell had free barbed ends, elongation would soon deplete the available pool of ATP-actin monomers. Therefore many of the barbed ends are capped by capping protein or gelsolin (Schafer et al, 1996). These proteins bind to the barbed end to prevent addition of new actin monomers. As a result, the concentration of free barbed ends is maintained low. Therefore, the combination of thymosin-β4, profilin and capping protein/gelsolin enable cells to regulate the actin monomer pool.

1.1.4 Signalling to the Arp2/3 complex

Many external stimuli, such as growth factors and growth cone guidance cues, are able to influence actin polymerisation by activating the Arp2/3 complex and drive actin filament elongation. There are many signal transduction pathways that can affect actin regulation, but many are thought to converge on the WASP proteins. These proteins transduce signals carried from the Rho family GTPsaes, Rac and Cdc42 (Machesky et al, 1999), as well as binding to receptor tyrosine kinases, such as PDGF and EGF receptors via the adaptor molecules Nck and Grb2.

WASP, the defective protein in Wiskott-Aldrich syndrome, is expressed in platelets and white blood cells (H. D. Ochs, 1998). N-WASP was originally isolated from the

brain and thought to be neurospecific (Miki et al, 1996), but has since shown to be ubiquitously expressed. A group of similar proteins, containing three members, has been identified and termed WAVE (Miki et al, 1998). The WASP and WAVE proteins share sequence similarity in the C-terminal, with all three containing an EVH1 (Ena/VASP homology) domain, an Acidic (A) domain and a proline rich central region, which interacts with profilin or SH3 domains. The A domain consists of 30 conserved residues, and interacts with the p19 subunit of the Arp2/3 complex (Machesky et al, 1998). EVH2, also 30 residues in length, binds to and prevents actin monomer addition to pointed ends, but not to barbed ends (Higgs et al, 1999). Both these domains are required for activation of the Arp2/3 complex. However the WASP and WAVE proteins differ in the N-terminal third, where WASP/N-WASP contain an EVH1 domain, which interacts with proline rich targets such as WASP Interacting Protein (WIP), and a Cdc42/Rac interactive Binding domain, (CRIB), which binds to Cdc42. WAVE appears to have very few functionally recognised domains in the N-terminal. The WASP proteins also interact with, and are activated by PIP2 (Miki et al, 1996; Rozelle et al, 2000).

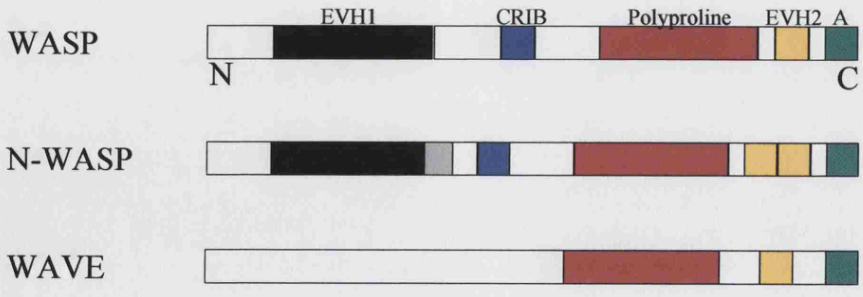

Figure 1.3. Domain structure of the three members of the WASP family.

There is some strong evidence to point to these proteins as upstream Arp2/3 activators. WASP and N-WASP bind Cdc42 and are required for Cdc42 induced actin polymerisation (Rohatgi et al, 1999; Yarar et al, 1999) and this Cdc42-induced polymerisation is dependent on the Arp2/3 complex (Ma et al, 1998).

1.1.5 The Ena/VASP proteins

The Ena/VASP proteins have also been shown to play an important role in the regulation of actin polymerisation. They are related to the WASP family, and contain a conserved EVH1 domain (Ena/VASP homology) and proline rich domain. The EVH1 region in the Ena/VASP proteins interacts with ligands such as vinculin and zyxin, and the poly-proline region interacts with similar targets to the WASP proteins, such as profilin and the SH3 domains of Abl, Lyn and Src (Lambrechts et al, 2000). Unlike the WASP proteins, Ena/VASP contain an EVH2 domain, which mediates tetramerisation of the protein and F-actin binding.

Ena/VASP co-localise with the Arp2/3 at the leading edge of membrane protrusions, as well as other areas of actin assembly such as focal adhesions, and have been shown to catalyse the elongation of newly formed actin filaments (Laurent et al, 1999). They recruit the actin monomers to the filaments via their interaction with profilin, and are then able to promote elongation via their interaction with the monomers and the filaments.

1.1.6 Depolymerisation of actin filament

In order for cells to undergo morphology changes or migration, there must be a rapid turnover of the actin. ADF (actin depolymerisation factor) and cofilin promote the recycling of the actin from filaments (Carlier et al, 1988). Although these are two distinct proteins, their activities exert very similar effects on actin dynamics, and usually co-localise in cells.

They have been shown to enhance the actin dynamics in the actin comet tail in the endocytic bacteria *Listeria monocytogenes* (Rosenblatt et al, 1997), which polymerise the actin of their host cell to move around the cell, and between cells.

Figure 1.4. *Listeria monocytogenes* (green) forming actin tails (red) in a host cell. Image from Portnoy laboratory homepage. http://mcb.berkeley.edu/labs/portnoy/

In addition ADF and cofilin have been shown to depolymerise pure actin filaments *in vitro* (Bamburg et al, 1980). There are two possible mechanisms for these proteins to cause depolymerisation. Firstly they may sever the filaments directly, and secondly, they may increase the subunit dissociation at either or both ends. Either method would result in the depolymerisation of the filament.

The ability of ADF/cofilin to depolymerise actin filaments, allows them to co-operate with profilin to accelerate actin treadmilling, which is an important process during cell motility. Cofilin accelerates the removal of actin monomers from the barbed end of the filament, because of its high affinity for ADP actin, and allows them to be recycled by profilin, which facilitates exchange of ADP for ATP, returning them to the pointed end for re-polymerisation (reviewed Pollard, 2003).

The ADF/cofilins can be regulated downstream of the Rho family GTPases, just like the Arp2/3. The downstream effector of Rac or Cdc42, p21 activated kinase (PAK), and the RhoA effector Rho kinase, both phosphorylate and activate LIM-kinase (Edwards et al, 1999; Ohashi et al, 2000; Sumiet al, 2001), which then phosphorylates cofilin (Yang et al, 1998; Maekawa et al, 1999). The result of this phosphorylation is a reduction in the affinity of cofilin for actin, and therefore stabilises the filaments.

The capping protein, gelsolin has been shown to sever actin filaments in response to Ca^{2+} ions. Once severed, the new barbed end is then capped by gelsolin to prevent elongation. Breaking up an actin network is an important process in a number of cellular processes. One example is the fusion of a phagosome with a lysosome following phagocytosis, which requires the breakdown of the dense actin network surrounding the phagosome.

1.1.7 Actin and the plasma membrane

In order to effect changes in cell morphology, or induce cell migration, the actin filaments must be able to impose a force on the plasma membrane, and push it forwards. The way actin does this is still yet to be confirmed, but there are two main

theories at present. First, the polymerisation of actin will itself exert a force on the membrane, allowing the filaments to push outwards (Tilney et al, 1981). There is some evidence for this idea. Firstly, giant liposomes containing pure actin will undergo some membrane deformation. If actin cross-linking proteins are added, this deformation is quite severe (Miyata et al, 1999). Also, in *Listeria monocytogenes* assembly of the actin filaments is sufficient to move the bacteria through the cell. The only proteins required for this process other than actin are Arp2/3, ADF/cofilin and capping protein (Loisel et al, 1999). None of these are force-producing proteins, and so the polymerisation of the actin is sufficient to produce the force.

An alternative theory, suggests that the filaments act like springs, and move side to side due to thermal motion, before exerting a force and springing back to their original position (Mogilner and Oster, 1996). When moving to the side they are away from the membrane, and it is here when the actin monomers are added to the barbed end. When the filament returns to its original position, the extra actin units push the membrane outwards (Mogilner and Oster, 1996). One important observation that supports this idea is that actin filaments are 45° from the direction of protrusion, and this is the optimum angle to transmit force by this method (Svitkina et al, 1997). In addition the cross links produced by the Arp2/3 complex are quite stiff, also enabling the force to be transmitted through the side chains (Blanchoin et al, 2000).

1.1.8 Myosin

Myosin is an actin associated motor protein allowing actin filaments or other cellular structures to be moved. All myosins contain a conserved "head" domain, which is the motor unit that hydrolyses ATP in order to induce the force (Reviewed in Tyska and

Warshaw, 2002). In addition to the motor domain, myosins contain additional domains, which vary depending on the myosin type and function. Some bind to plasma membrane to allow vesicle movement, while others bind to actin filaments to allow filaments to move with respect to each other. In addition, myosins bind to microtubules, and enable movement of vesicles or organelles, which plays an important role in axonal transport in neurones (Reviewed in Bridgeman, 2004). When moving along actin filaments, all myosins move along the filaments from the pointed end towards the barbed end, with one exception, myosin 6 (Wells et al, 1999), which plays a role in endocytosis.

1.1.9 The actin cytoskeleton and integrins

One prominent component of the actin cytoskeleton, especially in fibroblasts, are actin stress fibres. These dense actin bundles are anchored at one end at specialised sites called focal adhesions, while the other end is anchored to other focal adhesions or to intermediate filaments around the nucleus, allowing the cell to exert tension on the matrix. The focal adhesions are areas where the membrane is in very close proximity to the extracellular matrix, and consequently is firmly attached. The transmembrane linkers for these sites of adhesion are the integrins (Choquet et al, 1997). These proteins contain an extracellular domain, which binds to the matrix, a single transmembrane domain, and an intracellular domain, which interacts with components of actin regulation. Integrins play an important role in actin regulation, linking the extracellular matrix to the actin cytoskeleton and generating traction during migration but also allowing biochemical signals to be transmitted across the membrane directly to the actin cytoskeleton.

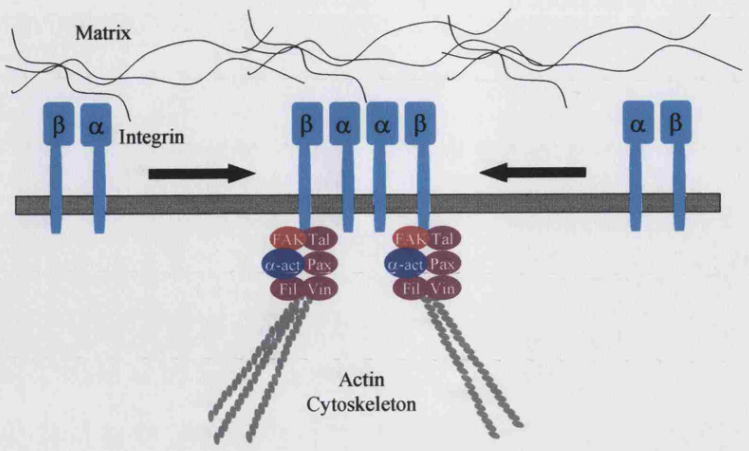

Figure 1.5. The integrins, linking the extracellular matrix to the actin cytoskeleton (Adapted from Burridge and Chrzanowska-Wodnicka, 1999)

There are two main families of integrins, α and β integrins, which form heterodimers (Reviewed in Burridge et al, 1996). The cytoplasmic tail from the β integrins is sufficient to link the integrins to the actin filaments, but there is evidence to suggest that the tails from the two integrin heterodimers interact, and that this interaction is under the regulation of ligand binding (Haas et al, 1996; Leisner et al, 1999). At the site of focal adhesions, the integrins cluster to allow the anchoring of the stress fibres, although this interaction is indirect (Burridge et al, 1996).

There are a number of proteins required to link the cytoplasmic tails of the integrins to the actin bundles. Talin is an important component of focal adhesions and has been shown to co-localise with the integrins. During the formation of focal adhesions, Talin has been shown to accumulate early in the process (Moulder et al, 1996), which requires the presence of the integrins, but not other interacting proteins such as vinculin. Talin contains two 270kDa subunits, which form an anti-parallel homodimer, and has binding sites for actin, vinculin, focal adhesion kinase, phospholipids and the transmembrane protein laylin (Jockusch et al, 1995; Borowsky

et al, 1998). Talin binds to β1, β2, and β3 integrins at regions at either end of the protein, suggesting that Talin can bind to two or more integrins at once (Pfaff et al, 1998).

Filamin is another β-integrin binding protein that is present in focal adhesions. These proteins comprise of two parallel 250kDa subunits and an N-terminal actin-binding domain. They cross-link actin filaments, and reinforce loose actin filament networks or tight actin bundles like stress fibres (Loo et al, 1998). It is not exclusive to focal adhesions, and is also found associated with actin filaments throughout the cell, and along the stress fibres (Jockusch et al, 1995).

Two further proteins associated with the focal adhesions are α-actinin and vinculin. α-actinin forms rod-like 100kDa monomers which localise to focal adhesions, by interacting with the tail of β-integrin tails (Cattelino et al, 1999). Vinculin, a 120kDa protein, is one of the most abundant in focal adhesions. It can interact with F-actin, Talin, α-actinin, paxilin and VASP (Bubeck et al, 1997), but can not interact directly with the integrins, and is not absolutely required for the integrin-actin linkage (Priddle et al, 1998).

As well as allowing anchorage of the cell membrane to the matrix, the focal adhesions allow the transduction of signals between the matrix and the actin cytoskeleton. This signal transduction moves in both directions, with intracellular signals also able to regulate the adhesions of the integrins to the matrix, in a process referred to as inside out signalling, as well as signalling from the matrix to the actin filaments (Hughes and Pfaff, 1998). The proteins most likely to play a role in transducing signals from the

integrins to the actin cytoskeleton are members of the Ena/VASP family. Their EVH1 domain allows binding to vinculin a major component of the focal adhesions, and they localise to areas of actin assembly, including focal adhesions. Once Ena/VASP have been recruited, the other key proteins involved in actin assembly are recruited such as the WASP proteins and the Arp2/3 complex. With all these proteins present, actin polymerisation can take place.

1.1.10 The actin cytoskeleton and the nervous system

The precise regulation of the actin cytoskeleton plays a crucial role in the developing nervous system. Neurones migrate to their correct destination, and then differentiate to produce neurites and growth cones that must respond to many guidance cues in order to innervate their correct targets.

The growth cone is a very sensitive cellular structure that can respond to many guidance cues, such as semaphorins, and shows similar features to an independent migrating cell. There are however some differences in the actin regulation between neuronal growth cones and fibroblasts. The actin in a growth cone is different from that seen in fibroblasts, with bundles of actin filaments that radiate from the leading edge towards a central area of the lamellipodia (Lewis and Bridgeman, 1992). N-WASP and Arp2/3 are crucial components in the actin regulation in all cells types, and they are involved in the mechanisms behind neurite growth. The p34 and p21 subunits of the Arp2/3 complex are concentrated in actin filaments of NGF-stimulated growth cones of rat sympathetic neurones and PC12 cells (Goldberg et al, 2000). Also mutations in the Arp3 and p40 subunits of the Arp2/3 have been shown to cause abnormal neuronal development (Zallen et al, 2002)

N-WASP was first isolated from brain (Miki et al 1996), but has since shown to be ubiquitously expressed. N-WASP is found throughout the brain, but is concentrated at nerve terminals (Fukuoka et al, 1997). Mutation of the EVH2 region of N-WASP blocks NGF stimulated neurite growth in PC12 cells and hippocampal neurones. In addition, mutation of the CRIB to prevent Cdc42 binding blocks neurite growth altogether, (Banzai et al, 2000). Interestingly, mutations in *Drosophila* WASP have no effect on neuronal development, but instead affect cell fate determination, suggesting the two WASP proteins play different roles in the regulation of the actin cytoskeleton (Ben-Yaacov et al, 2001).

The Ena/VASP proteins have been shown to be concentrated to F-actin rich regions of NGF-stimulated sympathetic growth cones (Goldberg et al, 2000), and are also highly expressed in the developing cortical plate (Goh et al, 2002). When Ena/VASP function is inhibited before cortical neuron migration, early neurones migrate too far, reaching the superficial layers of the cortex, which is normally inhabited by older neurones. Neurone morphology remains normal, suggesting Ena/VASP proteins function *in vivo* to correctly position migrating cortical neurones (Goh et al, 2002).

The mammalian homologue of Ena, Mena, has been shown to play an important role in neuronal development. Mena knockout mice show severe brain defects, suggesting Mena is essential for correct development (Lanier et al, 1999). Mena knockout mice, also heterozygous for profiling knockout show even more severe phenotypes and die *in utero*. Further examination showed defects in the formation of the neural crest, and neural tube, suggesting together Mena and profilin are crucial during neuronal growth

and correct path finding (Lanier et al, 1999). Taken together these observations show that correct actin regulation is crucial for normal neuronal development.

Another class of actin associated proteins, ADF/cofilin also play a role in the nervous system. Both proteins were originally identified from brain, with ADF isolated from chick brain (Bamburg et al, 1980) and cofilin isolated from porcine brain (Nishida et al, 1984). ADF is expressed in cerebella neurones and in the dendrites of Purkinje cells (Lena et al 1991), and has been shown to travel with actin monomers in axonal transport, and so may function in some transport capacity (Bray et al, 1992).

ADF has been suggested to play some role in neurodegeneration. In some cases of Alzheimer's disease, there is a large loss of synapses, potentially up to 50%, without a corresponding loss of the neurones themselves. Further examination has shown that, in some cases, there is a disruption in the axonal transport of these neurones resulting in a loss of processes (Masliah et al, 1989). This disruption to axonal transport may also play some role in degeneration caused by the superoxide dismutase mutation, responsible for 15% of cases of familial amyotrophic lateral sclerosis (Williamson et al, 1999). The disruption to axonal transport appears to be due to rod like structures containing actin, ADF and cofilin in the axon. These rods can be induced in cultured hippocampal neurones, by overexpressing ADF/cofilin. When these rods become large enough, they span the width of the axon, and disrupt the microtubules, affecting axonal transport (Minamide et al, 2000).

LIM kinase, which regulates cofilin by phosphorylation, is highly expressed in the brain (Mizuno et al, 1994) and plays an important role in the regulation of the actin

cytoskeleton. Inactive LIM kinase can block Rac1 or insulin induced lamellipodia (Yang et al, 1998) as well as blocking RhoA induced stress fibres and Cdc42 induced filopodia (Sumai et al, 1999). LIM kinase is phosphorylated at the same site by the Rac/Cdc42 effector PAK (Edwards et al, 1999) and the RhoA effector ROK (Maekawa et al, 1999). Once phosphorylated, LIM kinase becomes active and phosphorylates cofilin inactivating it, and so stabilising actin filaments.

The phosphorylation of cofilin by LIM kinases has been shown to be important in the semaphorin3A (sema3A) guidance pathway. Following treatment with sema3A, there is an increase in the phosphorylation of cofilin, followed by a decrease in the phosphorylation. This phosphorylation is probably due to LIM kinase, as inhibition of LIM kinase inhibits the sema3A collapse (Aizawa et al, 2000). Finally, the LIM kinase gene is one of those lost in William's syndrome, caused by the deletion of a segment on chromosome 11 spanning several genes (Donnai and Karniloff-Smith, 2000). As a result of this deletion, there are some developmental abnormalities and cognitive impairment, although it is difficult to access the role the loss of LIM kinase plays in this disorder.

1.1.11 Microtubules

Another component of the cytoskeleton is microtubules. These structural proteins show some similarities with actin. They consist of large chains composed of polymerised subunits, and the rates of polymerisation and depolymerisation regulate the growth or shrinkage of the microtubules. The monomer units are tubulin dimers consisting of α and β subunits. Tubulin polymerises more quickly at the plus end, which is terminated by the β subunit, while the minus end, which is terminated by the

α unit, polymerises more slowly. Another form of tubulin, γ-tubulin, forms the centrosome, a ring of tubulin that acts as a nucleation site for microtubules, during cell division (Reviewed in Howard and Hyman, 2003). Once assembled, microtubules act as tracks for the transport of cell organelles and chromosomes, through the motor protein, kinesin. However, microtubules can themselves, provide forces, and polymerisation of tubulin can exert forces on the cell membrane (Reviewed in Howard and Hyman, 2003).

The microtubule dynamics are driven by GTP hydrolysis. Tubulin is a GTPase (David-Pfeuty et al, 1977), and this enzymatic activity is promoted by polymerisation of the tubulin (Carlier and Pantaloni, 1982). However, the β-tubulin contains the GTP binding domain, but the α-tubulin contains the hydrolysing activity, and hydrolysis of GTP only occurs once two tubulin dimers polymerise (Nogales et al, 1999).

Recently, there has been found to be an interplay between the regulation of microtubules and the actin cytoskeleton through RhoGTPases. A member of the Rho family of GTPases, Rac1, binds directly to tubulin (Best et al, 1996), and a downstream kinase of Rac1 and Cdc42, PAK, phosphorylates stathmin, preventing it from destabilising microtubules (Daub et al, 2001). The downstream RhoA effector, mDia stabilises microtubules in fibroblasts, in a Rho-kinase independent fashion (Palazzo et al, 2001).

In neuronal growth cones, a large bundle of microtubules are located in the centre of growth cones, with a few dynamic microtubule processes extending towards to periphery of the growth cone, where actin forms filopodia and lamellipodia (Reviewed Rodriguez et al, 2003). Inhibition of actin polymerisation in the growth

cone causes the microtubules to advance into the growth cone periphery, suggesting that microtubule dynamics and actin dynamics are closely linked (Forscher et al, 1988). The dynamics of actin and microtubules are functionally linked in developing growth cones, where the inhibition polymerisation of one, prevents the polymerisation of the other (Dent and Kalil, 2001). Also, the inhibition of either actin or microtubule dynamics prevents axonal branching, but not axonal elongation. As the axonal elongation is undirected, this points to a role for actin and microtubule dynamics in axonal pathfinding (Dent and Kalil, 2001). In fact, local and specific disruption of actin bundles in the growth cone causes microtubule growth into the areas where actin bundles remain, resulting in growth cone turning (Zhou et al, 2002).

1.2 The Rho family of GTPases

Some of the most important, and best characterised regulators of the actin cytoskeleton are Rho GTPases. This family of small enzymes belong to the larger Ras superfamily of GTPases, and hydrolyse GTP to GDP, and so cycle between GTP and GDP bound forms. When bound to GDP they are inactive, but when they bind GTP a conformational change takes place, allowing the GTPases to bind to and activate downstream effectors.

The Rho family can be divided into six groups. Rho (comprising RhoA, RhoB, and RhoC,) Rac (comprising Rac1, Rac2, Rac3 and RhoG), Cdc42 (comprising Cdc42, G25K and TC10), Rnd (comprising RhoE/Rnd3, Rnd1/Rho6 and Rnd2/Rho7), RhoD and TTF. Of these Rho GTPases, the best studied are Rac1, RhoA and Cdc42.

1.2.1 The morphological effects of the Rho GTPases

In Swiss 3T3 fibroblasts, it has been shown that RhoA is activated in response to external factors, such as Lysophosphatidic acid (LPA), resulting in the formation of actin stress fibres and focal adhesions (Ridley and Hall, 1992). Rac1 was shown to respond to platelet-derived growth factor (PDGF), resulting in the formation of membrane ruffles and lamellipodia (Ridley et al, 1992). There is also some cross talk between RhoA and Rac1. Treating fibroblasts with PDGF causes membrane ruffling, but after 10-15 minutes, some stress fibres and focal adhesions are formed.

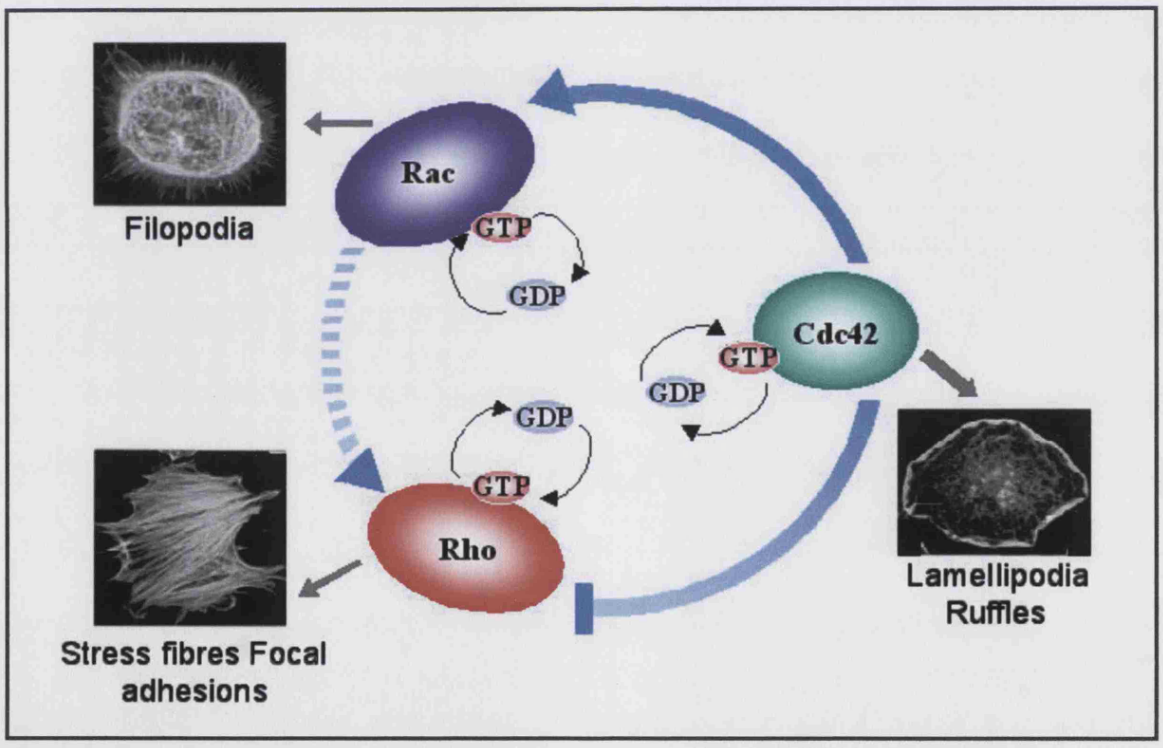

Figure 1.6. The morphological effects and the hierarchal relationship of the Rho GTPases. (Cell images taken from Hall, 1998; diagram adapted from Lim et al, 1996)

These stress fibres and focal adhesions have been shown to be RhoA dependant (Ridley and Hall, 1992), suggesting that RhoA can be activated downstream of Rac1. In addition to the ability of Rac1 to regulate actin polymerisation, an involvement in microtubules regulation was suggested with the ability of GTP Rac1 to bind to tubulin (Best et al, 1996), and Rac1 has also been implicated in the production of reactive oxygen species (ROS) (Ozaki et al, 2000). Swiss 3T3 fibroblasts were used to show Cdc42 could be activated in response to bradykinin to induce the formation of actin microspikes and filopodia (Kozma et al, 1995). Further evidence of the cross talk between the GTPases was demonstrated by the formation of Rac1-dependant membrane ruffles and lamellipodia following Cdc42 activation suggesting Rac1 can be activated downstream of Cdc42 (Kozma et al, 1995).

1.2.2 Effectors of the Rho GTPases

In order for the Rho GTPases to activate their signalling pathways, they bind to and activate a large number of downstream effectors. These effectors only bind to Rho proteins when GTP bound, and can be either kinases or non-kinases. A large number of effectors have been identified, although only some have been suggested to play a role in neuronal development, are discussed here.

1.2.2.1 PAK

p21-activated kinase, PAK, was isolated as a Rac1 and Cdc42 effector. Both GTP Rac1 and GTP Cdc42 bind PAK causing auto-phosphorylation and increase in kinase activity (Manser et al, 1994). A region crucial to the binding of GTP bound Rac1 or Cdc42 was identified as a 16 amino acid sequence (Manser et al, 1993; Manser et al, 1994). It was subsequently found in other proteins and termed Cdc42/Rac interactive

binding (CRIB) (Burbelo et al, 1995). Rac1 and Cdc42 have been shown to recruit PAK to focal complexes, where it exerts its kinase activity. In addition, activated PAK results in loss of stress fibres and focal adhesions (Manser et al, 1997). These effects are similar to those observed by activating Rac1 and Cdc42 (Manser et al, 1997)

A number of other proteins have now been identified by their interactions with PAK. A novel Rac1 exchange factor was identified by its direct interaction with PAK, and termed PAK-interacting exchange factor (PIX). This protein can induce Rac1-dependant membrane ruffling, and because PAK is an effector for both Rac1 and Cdc42, suggests a role for PIX in the cross talk signalling between Cdc42 and Rac1 (Manser et al, 1998; Obermeier et al, 1998).

PAK has also been shown to phosphorylate and activate LIM kinase (Edwards et al, 1999), in a pathway that can link Rac1 and Cdc42 to regulation of the actin cytoskeleton. LIM kinase was first identified as a novel kinase highly expressed in developing nervous tissue (Mizuno et al, 1994), although an additional LIM kinase has since been identified, LIM kinase 2, which is more widely expressed (Okano et al, 1995). Phosphorylation of LIM kinases by PAK results in increased kinase activity towards cofilin, an important component of actin recycling. Activation of Rac1 and Cdc42 causes an increased interaction between PAK and LIM kinase. Kinase inactive LIM kinase can interfere with Rac1, Cdc42 or PAK induced cytoskeletal changes (Edwards et al, 1999). This phosphorylation pathway suggests one way in which Rac1 and Cdc42 can induce their changes in cell morphology.

LIM kinase also provides a convergence point between Rac1/Cdc42 and RhoA signalling pathways. As well as being a substrate for PAK, LIM kinase is also a substrate for the RhoA effector Rho kinase. Rho kinase phosphorylates LIM kinase on the same site as PAK, threonine 508, also increasing the kinase activity towards cofilin (Maekawa et al, 1999; Ohashi et al, 2000). Therefore LIM kinase offers one pathway by which the Rho GTPases can effect changes to the actin cytoskeleton.

1.2.2.2 WASP (See section 1.1.4)

The protein responsible for Wiskott Aldrich syndrome, WASP is an effector for Cdc42, but does not bind to either RhoA or Rac1 (Aspenstrom et al, 1996; Symons et al, 1996). WASP, and the related protein N-WASP both bind directly to the Arp2/3 complex and facilitate the formation of actin filaments, and so form a bridge between Cdc42 and reorganisation of the actin cytoskeleton. A WASP related protein, WAVE, has been shown to play a role in Rac1 induced ruffles and lamellipodia (Miki et al, 1998) although this protein is not a Rac1 effector, and does not bind the GTPase.

1.2.2.3 Rho-kinase

Another key effector is Rho-kinase-α (ROKα). ROK-α was first identified as a kinase that binds to GTP RhoA and is translocated to the membrane, (Leung at al, 1995; Mitsui et al, 1996). In addition to binding to RhoA, ROK-α was shown to bind RhoB and RhoC, but not to Rac1 or Cdc42, and induces stress fibres and focal adhesions in a kinase dependant manner (Leung et al, 1996; Amano et al, 1997). The RhoA binding domain was narrowed to a 30 amino acid sequence, and shown to be essential for GTPase binding. A second member of the Rho kinase family, termed ROK-β was

identified, with 90% homology in the kinase domain. Of the 30 amino acids comprising the Rho-binding domain, 20 are identical between the two sequences (Leung et al, 1996), emphasising the importance of sequence for RhoA binding.

Further studies have shown that ROK-α also binds to RhoE (Rnd3), although this interaction is quite different from that with RhoA. Although RhoA and RhoE cannot interact with ROK-α simultaneously, the RhoE binding site was localised to the kinase domain. In addition, RhoE can inhibit the Rho kinase-α induced stress fibres and focal adhesions, suggesting RhoE has an inhibitory role in the regulation of ROK-α (Riento et al, 2003).

ROK is activated by lysophosphatidic acid, which signals thorugh the G protein G_{13} (Gohla et al, 1998). Activation of this G protein results in activation of the Guanosine Exchange Factor, p115 RhoGEF (Hart et al, 1998), which upregulates RhoA GTP (Kranenburg et al, 1999). The down stream targets of the ROK-α are components of the myosin contraction machinery. ROK-α phosphorylates the myosin-binding subunit of myosin phosphatase, resulting in inactivation. As a result of inactivation of myosin phosphatase, there is an increase in the phosphorylation levels of myosin light chain, causing contraction in muscle, and interaction between actin and myosin in non-muscle cells (Kimura et al, 1996; Kureishi et al, 1997).

Some evidence for the interplay between different effectors has been shown between ROK-α and another RhoA effector mDia. mDia is the mammalian homologue of the *Drosophila* gene, Diaphanous, which was shown to be required for cytokinesis during development (Castrillon and Wasserman, 1994). mDia is a RhoA effector, which

binds to profilin (Watanabe et al, 1997), and stabilises microtubules in fibroblasts (Palazzo et al, 2001). mDia co-operates with ROK-α in the formation the RhoA associated actin structures, stress fibres and focal adhesions (Watanabe et al, 1999), but is antagonised by ROK-α in the Rho-dependant activation of Rac1, and the Rac1-induced lamellipodia (Tsuji et al, 2002).

1.2.2.4 Citron

Further searches for novel RhoA effectors discovered citron, and the related effectors, CRIK and CRIK-SK. It would appear these three proteins are splice variants from the same gene. Citron was discovered in a yeast two hybrid system, and was found to interact with both RhoA and Rac1, but not Cdc42 (Maduale et al, 1995). This 183 kDa protein has no kinase domain, and as yet no function has been assigned to it. However two related proteins were identified. CRIK, citron Rho-interacting kinase, consists of a kinase domain fused onto the whole of the citron sequence, while CRIK-SK consists only of the kinase domain (Di Cun et al, 1998). No substrate has been found for these effectors, and they have limited effect on the actin cytoskeleton. Expression of these effectors is limited mainly to brain and testis, suggesting a more specific and selective function than ROK-α.

1.2.3 The regulation of the Rho GTPases

There are three different classes of regulating proteins for the Rho family of GTPases, Guanosine Exchange Factors (GEF's), GTPases Activating Proteins (GAP's) and Guanosine Disassociation Inhibitors (GDI's). Regulation of these controls the activity of the GTPases, and hence their downstream effects. There is a high degree of

complexity within all these groups of regulating molecules, with a high degree of redundancy and promiscuity. There are over 60 different proteins identified which regulate RhoA, Rac1 and Cdc42, and many of these can act on more than one GTPases. Consequently, through their ability to regulate GAP's, GEF's and GDI's, cells can exert highly specific control over the Rho GTPases, and their effects within the cell.

One of the first characterised GAP's, was found to be one of the genes translocated in Philadelphia leukaemia. In this cancer there is a fusion between the Breakpoint cluster region (BCR) and Abl genes resulting in the production of a functional fusion protein. The full length BCR gene product has been shown to have GAP activity towards Rac1, Rac2 and Cdc42, as well as GEF activity towards Cdc42, RhoA, Rac1 and Rac2 (Chuang et al, 1995). In addition, neutrophils from BCR null mice show an increase in reactive oxygen species production, and an increase in the membrane translocation of Rac2 (Voncken et al, 1995), suggesting BCR is responsible for regulation of Rac-mediated superoxide production via the NADPH-oxidase pathway.

GAP's for the Rho family of GTPases share related GAP domains, and other protein domains can regulate their function. An *in vivo* and *in vitro* comparison of the GAP domains from three different GAP's, BCR, RhoGAP and p190 RhoGAP demonstrated different specificity, with BCR acting on Rac2, RhoGAP acting on Cdc42, and p190RhoGAP acting on RhoA (Ridley et al, 1993).

Even between the GAP's there is evidence of some cross talk. The N-terminal of RasGAP contains two SH2 domains and one SH3 domain. These domains are

responsible for the interaction with β-PDGF receptors, but also with p190RhoGAP. A complex of the RasGAP N-terminal and p190RhoGAP is active, suggesting RasGAP can activate p190RhoGAP, and so regulate RhoA function (McGlade et al, 1993).

GDI's were first identified from bovine brain, and shown to inhibit the release of GDP from the Rho GTPases (Fukumoto et al, 1990; Ueda et al, 1990). In addition they have also been shown to exert a concentration dependant inhibition of GTP hydrolysis, and GAP function (Chuang et al, 1993), as well as solubilising membrane associated Rho proteins (Isomura et al, 1991). RhoGDI was also shown to relocate RhoA, Cdc42, Rac1 and Rac2 but not other Rho proteins such as RhoB or TC10 (Michaelson et al, 2001). Consequently, GDI's have been shown to down regulate Rho GTPases in a number of ways.

Rho GEF's were first identified through the discovery of a novel oncogene, called Dbl (Eva and Aaronson, 1985). Dbl is a truncated protein that contains a region with high homology to a region in the yeast protein Cdc24 (Ron et al, 1991), and this led to the discovery that Dbl was able to facilitate the exchange of GDP for GTP in Cdc42 (Hart et al, 1991). Dbl is an 115kDa cytoskeletal-associated protein, and expression is limited to selective tissues such brain, adrenal glands, testis and ovaries. The region responsible for the GEF activity was termed Dbl homologue domain (DH) (Hart et al, 1994), and was found to be essential for the transforming ability of Dbl (Ron et al 1991). In addition to the DH domain, Dbl also contains a Pleckstrin homology domain (PH), which although poorly conserved, appears to adopt a common 3D structure (Ferguson et al, 1994; Harlan et al, 1994), and is thought to be involved in the cellular localisation of Dbl. All Dbl-like GEF's contain both these domains in close proximity.

Tiam-1, for T lymphoma invasion and metastasis, is a well-studied Dbl-like GEF. It too was discovered due to its involvement in cancer and shown to have two domains with homology to DH domain and two PH domains (Habets et al, 1994). Since then it has been shown to be a Rac1 GEF (Michiels et al, 1995), and has been implicated in neuronal migration and neurite outgrowth in the developing nervous system (Ehler et al, 1997).

1.2.4 The Rho GTPases in cellular migration and the extracellular matrix

The involvement of Rho GTPase activating proteins, such as Dbl, Tiam-1 and BCR in cancers, suggested that GTPases play an important role in cell migration, a pivotal process in cancer metastasis. In fact all three key members of the Rho GTPases play important roles in cell migration. Rac1 is essential for lamellipodia protrusion and forward movement, Cdc42 is important for cell polarisation, and the correct localisation of the lamellipodia to the leading edge (Nobes and Hall, 1999). RhoA and ROK activation are required for monocyte migration (Honing et al, 2003; Worthylake and Burridge, 2003), while RhoA induced phosphorylation of FAK is required for tumour cell invasion (Mukai et al, 2003). Further studies have shown PAK is required in the migration of endothelial cells (Kiosses et al, 1999) and Rac1 is important in the actin reorganisation in response to chemoattractants in chemotaxis (Chung et al, 2000).

An important factor in cell migration is the signalling pathways from the extracellular matrix, through adhesion sites, to the Rho GTPases to regulate the actin cytoskeleton.

The ability of Rac1 and Tiam-1 to induce migration can be inhibited by plating cells on fibronectin, although other collagens have no affect on migration (Sander et al, 1998). There has been shown to be an initial RhoA inhibition followed by a phase of RhoA activation in response to fibronectin adhesion (Ren et al, 1999). The initial inhibition of RhoA appears to be due, at least in part, to the activation of p190RhoGAP. Following integrin activation, there is a c-Src dependant phosphorylation, and hence, activation of p190RhoGAP (Arthur et al, 2000).

The effect of fibronectin on Rho GTPase activity is dependant on substrate concentration. In neutrophils and CHO cells, intermediate fibronectin concentrations, which are optimal for migration, induce activation of both Rac1 and Cdc42. However, higher concentrations result in activation of RhoA, and an inhibition of migration (Cox et al, 2001).

In addition to cell-to-substrate interactions, cell-to-cell interactions have also been shown to regulate the RhoGTPases in MDCK cells. Rac1 is localised to the sites of cell-cell adhesions (Nakagawa et al, 2001), and there is an activation of Rac1 and an inhibition of RhoA, following the formation of cell-cell contacts.

1.2.5 The Rho GTPases in the Nervous System

Due to their ability to drive morphological changes and migration, the Rho family of GTPases play important roles in the development of the nervous system. The growth cones of neurones can be considered similar to migrating cells, but responding to a huge variety of repulsive and attractive signalling cues, utilising the Rho GTPases to effect these morphological changes. Consequently, the role played by the GTPases,

and their regulatory proteins, in the ability of growth cones to correctly guide to their targets, is of great interest.

The complex relationship that exists between the three key members of the Rho GTPases has been demonstrated in the neuroblastoma cell lines, where Cdc42 and Rac1 produce filopodia and lamellipodia respectively, and RhoA causes neurite retraction (Kozma et al, 1997). Both Rac1 and Cdc42 can be activated by acetylcholine via the muscarinic acetylcholine receptor, which acts in competition with LPA activation of RhoA (Kozma et al, 1997). In the same neuroblastoma cell line, Cdc42 and Rac1 have been shown to regulate neurite formation downstream of Ras (Sarner et al, 2000). Rac1 also plays an important role in the differentiation of rat pheochromocytoma PC12. These cells are often used as a model of neuronal differentiation, as they respond to nerve growth factor (NGF) to produce long neurites, and in response to NGF, Rac1 is activated and recruited to protrusion sites (Yasui et al, 2001).

Rho GTPases are important in neuronal and morphological development; RhoA is highly expressed during *Caenorhabditis elegans* larval development (Chen et al, 1994), and Rac1 is important in dorsal closure in embryonic development of *Drosophila* (Harden et al, 1995). Further studies in *Drosophila* have shown that although Cdc42 can regulate the formation of filopodia, this does not affect the pathfinding ability of growth cones (Kim et al, 2002). However, Cdc42, Rac and Rho are all required in the repulsive axon guidance at the midline of *Drosophila* CNS. Midline repulsion requires down-regulation of Cdc42 and Rac and activation of Rho (Fritz et al, 2002). All three key members of the Rho GTPase family play an

important role in *Xenopus laevis* optic nerve development, and dendritic arbor growth (Li et al, 2002), while crosstalk between RhoA and Cdc42 is important for guidance of spinal neurones (Yuan et al, 2002).

Recent work has now placed the Rho GTPases downstream of specific guidance cues in growth cone morphology. In neuroblastoma cells lines, Rac1 and Cdc42 are required for Netrin-1 induced neurite outgrowth, while this is independent of RhoA and ROKα (Li et al, 2002). In *C.elegans* a constitutively active construct of the Netrin-1 receptor, Unc40 (DCC homologue), causes axon guidance defects, which are dependant on the Rac homologue, ced-10 (Gitai et al, 2003).

The ephrins are repulsive guidance cues, causing growth cone collapse. EphrinA-5 has been shown to activate RhoA and down regulate Rac1 to induce growth cone collapse, and inhibition of RhoA blocks ephrinA-5 induced collapse (Wahl et al, 2000). In addition to the role of RhoA in collapse, Rac1 also plays an important role in negative guidance. Although ephrin-A's induce a down regulation of Rac1, there is also a subsequent Rac1 activation stage that is required for growth cone collapse. This activation is required to enable endocytosis of the growth cone membrane, although the role this plays in the collapse pathways is not clear (Jurney et al, 2002).

Another family of repulsive guidance cues, the semaphorins, have also been shown to regulate the Rho GTPases. Collapsin-1, the chick homologue of semaphorin3A, induced collapse in dorsal root ganglia neurones, which is dependant on Rac1. Dominant negative Rac1, Rac1N17, can block the collapse (Jin et al, 1997) and the role of Rac1 in the collapse is dependant on the effector interacting domain, amino

acids 17-32, since deleting this region also blocks the growth cone collapse, (Vastrik et al, 1999)

The semaphorin guidance cues signal through a plexin/neuropilin receptor complex. However, while neuropilins have a short cytoplasmic domain, plexins have large cytoplasmic signalling domains, suggesting that they transduce the signal through the Rho GTPases. The cytoplasmic domain of the plexins, show some sequence similarity to GAPs, and plexin-B1 binds to Rac1 in a GTP dependant manor, while plexin-A1 binds to Rnd1 independent of GTP/GDP state (Rohm et al, 2000). Binding of Rnd1 to plexin-A1 is sufficient to cause growth cone collapse, while RhoD can compete for binding, blocking plexin-A1 activation and sema3A repulsion (Zanata et al, 2002). Plexin-B1 competes with PAK *in vitro* to bind activated Rac1, suggesting a mechanism by which the plexins can downregulate Rac1 signalling, and induce RhoA activation, (Vikis et al, 2000; Driessens et al, 2001; Hu et al, 2001). Furthermore, a different region of plexin-B binds to RhoA in a GTP independent manor (Hu et al, 2001).

In addition to their role in the developing nervous system, the Rho GTPases also play a role in neuronal regeneration following injury. The potent growth inhibitor, myelin-associated glycoprotein (MAG), which is released following nerve damage, activates the p75 receptor resulting in RhoA activation (Yamashita et al, 2002.) This activation could be blocked by neurotrophin binding, resulting in neurite elongation (Yamashita et al, 1999). Another growth inhibitor associated with nerve injury, Nogo-66 has also been shown to activate RhoA (Fournier et al, 2003). Spinal cord injury in rats and mice induces RhoA activation, which is p75 dependant. There is also an upregulation

of p75, which is RhoA-dependant, suggesting some feed back system (Dubreuil et al, 2003).

1.2.6 Rho GTPases regulators and effectors in the nervous system

The Rho GTPases play important roles in the development, and regeneration of the nervous system, and so their regulators and effectors play important roles in transducing the signals to the cytoskeleton, or regulating their activity.

1.2.6.1 GAPs in the nervous system

A large number of RhoGAP's have been identified to date including the Ras GAP's p120GAP, and NF-1, which both play a role in neurofibromatosis (Reviewed in Scheffzek et al, 1998; Dasgupta and Gutmann). However, of these GAP's, only a few have been suggested to play an important role in the control of neuronal differentiation and development of the nervous system.

Chimaerin is a RacGAP that is highly expressed in the nervous system and exists as two splice variants, α1 and α2-chimearin. Both contain a GAP domain and a phorbol ester receptor, but α2-chimearin also contains an N-terminal Src homology (SH2) domain. Both are expressed in the cerebral cortex, hippocampus and thalamus, but α2-chimearin is also expressed in the testis (Hall et al, 1993). α2-Chimearin is expressed much earlier in development than α1-chimearin, and is highly expressed in embryonic stages, including in dorsal root ganglia (Hall et al, 2001). Expression of α1-chimearin in the neuroblastoma cell line N1E-115 induces the formation of lamellipodia and filopodia, which are Rac1 and Cdc42 dependant, respectively. While the GAP activity was not required, activation of the GAP using phorbol ester

abolished these effects, suggesting that some GAPs may have functions in addition to the down regulation of GTPases (Kozma et al, 1996). In the same cell lines, α2-chimaerin forms neurites, but the point mutation, N94H of the SH2 domain activates the GAP resulting in retraction and loss of peripheral structures (Hall et al, 2001). Although a precise physiological function of this Rac GAP has yet to be found in cell signalling, its expression pattern suggests it plays an important role in development.

P190RhoGAP is a potent regulator of RhoA, and is highly expressed throughout the nervous system. Knock out of p190RhoGAP in mice causes wide spread defects in the development of the brain (Brouns et al, 2000), while p190RhoGAP inactivation causes local axon retraction, suggesting a role for p190RhoGAP in the control of structural plasticity of neurones (Billuart et al, 2001). Also, following fear conditioning, p190RhoGAP associates with the adaptor protein GRB2. Inhibition of the p190RhoGAP pathway impaired long-term memory, but had no effect on short-term memory (Lamprecht et al, 2001).

In addition to the well established GAPs, new neurospecific GAPs are being identified and characterised. Grit is a novel GAP that acts on all three key members of the Rho family, and interacts with the NGF receptor, TrkA, suggesting a role in NGF-induced differentiation (Nakamura et al, 2002). SynGAP acts on Ras and interacts with the PDZ domain of PSD-95. It is highly enriched in excitatory synapses, where is forms large complexes with PSD-95 and the NMDA receptor, and may play an important role in modulating synaptic plasticity (Hae Kim et al, 1998).

1.2.6.2 GEFs in the nervous system

The other main group of GTPases regulating proteins, GEF's, have also been implicated in the development of the nervous system. Trio contains two GEF domains, which activate Rac1 and RhoA respectively, and appears to play a role in regulating axonal outgrowth in the developing nervous system (Liebl et al, 2000). From phenotypic studies, it appears that Trio acts in cooperation with the tyrosine kinase Abl (Liebl et al, 2000). In *Drosophila*, Trio knockouts demonstrate defects in both the central and peripheral nervous systems, similar to those observed from GTPase dysfunction. Trio also interacts with the receptor phosphatase LAR, and a reduction in Trio activity potentiates the phenotypes seen from LAR mutants, suggesting these proteins act in synergy during axon development (Bateman et al, 2000). Trio is also important in the NGF-induced differentiation pathway in PC12 cells, and mutants can affect neurite outgrowth (Estrach et al, 2002).

In addition to their role in axonal development, GEF's are also being placed in specific signalling pathways from axonal guidance cues. Activation of the EphB receptor is important in the formation of dendritic spines in the hippocampus, and the Rac1 GEF, kalirin is crucial in this process. Inhibition of the Eph receptor, kalirin, Rac1 or PAK inhibits ephrin induced dendritic spine formation (Penzes et al, 2003). A novel GEF, ephexin acts on RhoA and interacts with the EphA receptor Shamah et al, 2001). Following activation of the receptor, ephexin upregulates RhoA, resulting in down regulation of Rac1 and Cdc42, and growth cone collapse. Mutant ephexin can block the Ephrin-A induced growth cone collapse in cultured primary neurones (Shamah et al, 2001).

The plexin-B family of receptors interact with the RhoAGEFs, PDZ-RhoGEF and LARG. Following activation of the receptor by semaphorin4D this GEF activates RhoA, resulting in growth cone collapse (Perrot et al, 2002; Swiercz et al, 2002). The association of PDZ-RhoGEF with the plexin-B receptor is promoted by the binding of Rnd1 to the plexin, dramatically increasing RhoA activation (Oinuma et al, 2003).

1.2.6.3 Effectors in the nervous system

In order for the GTPases to regulate the actin cytoskeleton, they must activate their effectors. Like the GTPases and their regulators, the role of various Rho family effectors in the nervous system has been studied.

The major effector of RhoA, ROK, is responsible for many RhoA-dependant effects on cell morphology, and activation of ROK can cause neurite retraction in PC12 cells, independently of RhoA (Katoh et al, 1998). In neuroblastoma cell lines, activation of ROK causes neurite retraction, while inhibition causes Rac1 and Cdc42 dependant outgrowth. Therefore ROK is an important component of neurite retraction pathways, but also inhibits the activities of Rac1 and Cdc42 (Hirose et al, 1998).

In cultured neurones inhibition of ROK causes an increase in the size and motility of growth cones produced, while activation of ROK prevents initiation of axon growth (Bito et al, 2000), suggesting that the role of ROK in the developing nervous system mirrors that seen in model cell lines. ROK also plays a role in the morphological changes during *Drosophila* development, acting with the frizzled/dishevelled signalling pathway to control cell polarity (Winter et al, 2001).

Two other RhoA effectors, mDia and citron have been implicated in neuronal development. MDia enters the nucleus and binds to the transcription factor Pax6, resulting in mislocalisation of Pax6 and an increase in neurite branching and length (Tominaga et al, 2003). Therefore it appears that mDia can have an opposite effect to ROK on neuritogenesis and can regulate gene transcription during neuronal development.

Citron associates with PSD-95 at the postsynaptic side hippocampal synapses of GABAergic neurones. This localisation is specific to the hippocampus, although citron is expressed throughout the nervous system, for example in most thalamic neurons. This suggests that citron acts in the inhibitory neurones of the hippocampus, in a signalling complex that is unique to these neurones (Zhang et al, 1999).

The Rac1 effector PAK is expressed in olfactory neurones, and plays an important role in their precise wiring (Ang et al, 2003). While PAK does not affect neuronal differentiation, it does appear to regulate the correct guidance of the axons along the correct trajectories (Ang et al, 2003). Another Rac1 effector, *C.elegans* unc-115, which is similar to human abLIM, a F-actin binding protein contain LIM domains (Roof et al, 1997), is also involved in pathfinding. It can bind directly to actin, and double mutants of unc-115 with Rac1 cause axon pathfinding defects (Struckhoff et al, 2003).

1.3 Axonal guidance in the developing nervous system

During the development of the nervous system, axon growth cones must respond to a huge variety of guidance cues in order to reach their correct targets. These guidance

cues can be either attractive or repulsive, and utilise the ability of the Rho GTPases to regulate the actin cytoskeleton, to control the pathfinding of the growth cones. There are many guidance factors that regulate axonal pathfinding, but the four main families are the netrins, slits, ephrins and semaphorins (See figure 1.7). Each family is broken down into subclasses, some with their own receptors and signalling pathways, while with others there is some redundancy between the receptors and signalling pathways. It is clear from the number of different signalling cues and pathways controlling the growth of axons and dendrites, that the correct development of the nervous system is a very complicated and carefully controlled process. Many of the studies on these guidance cues have been done on simple organisms such as *Drosophila* and *C.elegans*. It has become clear that many of the systems that influence growth guidance are highly conserved across species at the molecular level.

1.3.1 The Netrins

The netrins are a family of highly conserved secreted growth cone guidance cues. To date, one member has been found in *C.elegans*, two in *Drosophila*, and three in vertebrates (Van Raay et al, 1997). Netrins are expressed at the midline of the nervous system and are involved in the attraction of axons to the midline. So far, netrins have been expressed at the midline of every species examined, and netrin knockouts show defects in their guidance to the midline (Serafini et al, 1996). In addition to their role in attracting axons to the midline, netrins also play a role in attracting axons to peripheral targets such as muscle (Mitchell et al, 1996), and retinal axons into the optic nerve (Deiner et al, 1997). Netrins are bifunctional, and have been shown to demonstrate repulsive action on axons (Winberg et al, 1998). The ability of netrins to both repel and attract axons has been attributed to different receptors.

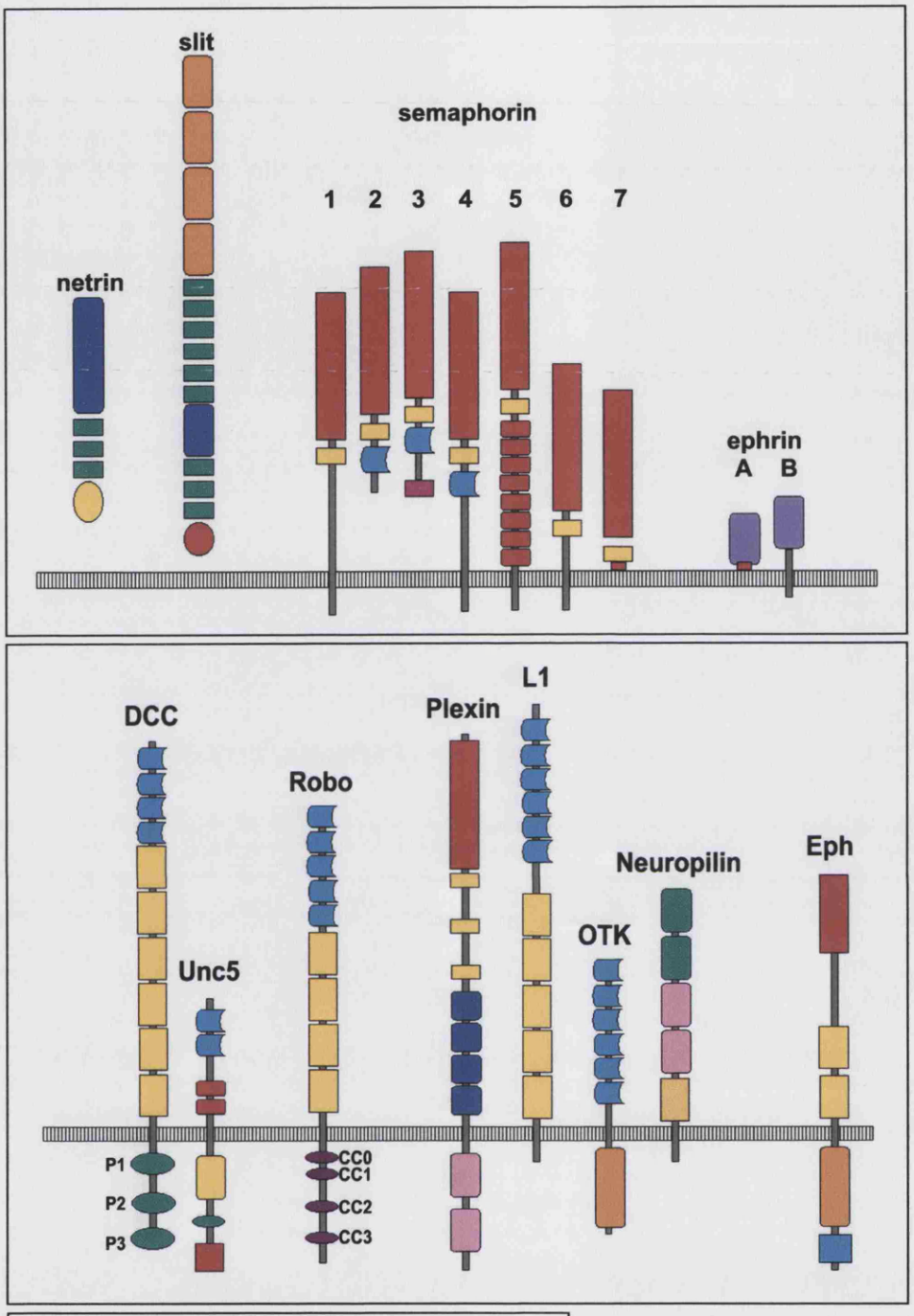

Figure 1.7. Domain structure of the main families of neuronal guidance cues and receptors (adapted from Dickson, 2002)

Attraction from netrins is mediated by the DCC (Deleted in Colorectal Cancer) receptor, while the repulsion is due to an UNC-5 homologue (Fazeli et al, 1997; Leonardo et al, 1997). These two receptors are structurally different, with the DCC receptor consisting of four Ig domains and six fibronectin repeats, and UNC-5 consisting of two Ig domains and two thromobospondin repeats, although it does not appear that there is one receptor for attraction and one for repulsion. DCC is required for both attraction and repulsion, during repulsion the DCC receptor binds to the UNC-5 receptor allowing their intracellular domains to interact and result in the activation of a repulsion pathway (Hong et al, 1999).

Activation of the DCC receptor by netrin-1 leads to activation of Rac1 and Cdc42. Expression of DCC in HEK 293T cells enables netrin-1 to induce filopodia and peripheral actin structures, which can be blocked with dominant negative Rac1 and Cdc42 (Shekarabi et al, 2001). The mechanism by which the netrins can influence the Rho GTPases has not been identified, but the adaptor protein Nck may be involved, as it associates with DCC in neurones, and Nck lacking an SH2 domain can block all DCC induced cytoskeletal changes (Li et al, 2002). Nck also could regulate the actin cytoskeleton by recruiting PAK to the plasma membrane (Bokoch et al, 1996), or by interacting and regulating the dual GEF, Trio (Newsome et al, 2000). How UNC-5 mediates growth cone repulsion is not known.

1.3.2 The slits

The slit family of guidance cues play a role in a number of processes during neuronal development, including neuronal migration, axonal path finding and dendritic branching. Three slits have been identified in vertebrates with overlapping patterns of

expression (Holmes et al, 1998; Itoh et al, 1998), although there appears to be a degree of redundancy amongst them (Plump et al, 2002). Work in *Drosophila* has demonstrated that the slits are important in preventing some axons from crossing the midline, and prevent others from re-crossing (Kidd et al, 1999; Simpson et al, 2000). Although the slits have been shown *in vitro* to act as axonal repellents, an N-terminal cleavage product can promote branching in dorsal root ganglia neurones (Wang et al, 1999). Both these processes require the slit receptor, robo (Nguyen Ba-Charvet et al, 2001).

The robo receptors contain large extracellular domains and an intracellular domain, consisting of domain repeats called CC repeats, which have no apparent enzymatic activity but are required for slit mediated axonal repulsion (Figure 1.7; Bashaw and Goodman, 1999). The intracellular domain has also been shown to inhibit netrin-mediated attraction by binding to the DCC receptor (Stein and Tessier-Lavigne, 2001). The CC repeats of the intracellular domain are important for robo function, and different CC domains mediate different aspects of robo function. For example, the CC1 domain of robo1 is crucial for silencing of the DCC receptor, but is dispensable for repulsion of X*enopus* spinal axons (Stein and Tessier-Lavigne, 2001).

Studies in *Drosophila* suggest a role for Abl tyrosine kinase and one of its substrates, Ena in the downstream signalling pathways mediated by the robo receptor. Association of Ena with the CC1 and CC2 domains positively regulates the robo pathway, while phosphorylation of CC3 by Abl inhibits robo function (Bashaw et al, 2000). The robo receptors also regulate the Rho GTPases. Slit-2 downregulates Cdc42, and dominant positive Cdc42 can block slit-2 mediated repulsion on neuronal

migration (Wong et al, 2001). In addition, a novel family of GAPs, termed srGAPs (slit-robo GAPs), associate with the robo CC3 motiff via their SH2 domains. These GAP's are important for both the downregulation of Cdc42, and the slit-mediated repulsion on neuronal migration (Wong et al, 2001).

1.3.3 The ephrins

The ephrins are another large family of guidance cues, which are involved in the development of the nervous system. There are two classes of ephrins; Ephrin-A, consisting of A1-A5 and ephrin-B, consisting of B1-B3. Class A Ephrins are GPI-linked while class B ephrin's are transmembrane proteins, and so both require cell-to-cell contact in order to mediate their effects. The receptors for the ephrins are the Eph receptors, a large family of receptor tyrosine kinases, which are further divided into two classes, A (EphA1-A8) and B (EphB1-EphB3). As well as their involvement in the axonal guidance, ephrins and Eph receptors are also involved in cell migration, vascular development, tissue-border formation and synaptic plasticity (Knoll and Drescher, 2002).

As a result of the requirement of cell-to-cell contact, the ephrins and Eph receptors are able to mediate both forward and reverse signalling. Forward signalling is the usual direction of signalling pathways, with the ephrin ligand binding to and activating the Eph receptor, which then autophosphorylates. The Eph receptors can influence the Rho GTPases through the RhoA GEF, Eph-interacting exchange factor, ephexin (Shamah et al, 2001). In addition to ephexin, Eph activation has been shown to inactivate the Ras pathway, resulting in neurite retraction, although the mechanism underlying this pathway is yet to be identified (Elowe et al, 2001).

The reverse signalling allows the cell contact to signal from the Eph receptor to the ephrin-bearing cell. Conserved tyrosine residues in the ephrinB cytoplasmic domain are phosphorylated following the formation of the ephrinB/EphB complex (Bruckner et al, 1997), possibly by Src tyrosine kinases, fibroblast growth factor or platelet-derived growth factor receptor tyrosine kinases (Chong et al, 2000; Palmer et al, 2002). A result of the tyrosine phosphorylation of ephrinB is the recruitment of the SH2/SH3 adapter protein Grb4. Grb4 binds via its SH2 and can regulate the activity of focal adhesion kinase (FAK), the distribution of paxillin and the disassembly of actin stress fibres (Cowan and Henkemeyer, 2001). In addition to the tyrosine phosphorylation of ephrinB, reverse signalling can also be mediated through a C-terminal PDZ-binding motif, contained in all ephrinBs. This motif enables the binding of PDZ-domain containing proteins such as PTP-BL tyrosine phosphatase (Palmer et al, 2002), glutamate-receptor-interacting protein GRIP1 and 2 (Bruckner et al, 1999) and PDZ-RGS3 (Lu et al, 2001). The latter contains a regulator-of-heterotrimeric G protein-signalling (RGS) domain, enabling it to regulate the downstream signalling from heterotrimeric G proteins.

Reverse signalling can probably also occur with the ephrinA family, although there are some differences. The recruitment of ephrinBs to lipid rafts is regulated by Eph binding (Bruckner et al, 1999), however ephrinAs are constitutively clustered around these membrane compartments. The binding of EphA to ephrinA5 results in signalling pathways requiring the activation of the lipid raft-associated tyrosine kinase, Fyn (Davy et al, 1999), while activation of EphA2 results in the dephosphorylation of focal adhesion kinase and reduced adhesion (Miao et al, 2000). However the

activation of ephrinAs promote adhesion in the ephrin-bearing cell by an integrin dependant mechanism (Davy and Robbins, 2000).

1.3.4 The semaphorins

The semaphorins are a large family of secreted and membrane anchored guidance cues that can mediate repulsive responses on growth cones, although some attractive responses can occur. Although they have been widely studied in the nervous system, they have also been shown to play a role in the development of the cardiovascular system (Serini et al, 2003), morphogenesis of the lung (Ito et al, 2000) and in invasive growth of epithelial cells (Giordano et al, 2002). Over 30 members of the semaphorin family have been identified so far, all of which contain a N-terminal sema domain.

The functional receptor for class 3 semaphorins is a complex of plexins and neuropilins. The neuropilins are required for ligand binding while plexins, with a large cytoplasmic domain, forms the signalling component (Takahashi et al, 1999).

Neuropilin-1 expression varies during development depending on neurone type and stage of development. NT-3 dependent sensory axons from embryonic chick drg are sensitive to sema3A, although from E7 to E10 there is a progressive decrease in neuropilin-1 expression and a corresponding decrease in the sema3A response (Pond et al, 2002). NGF-dependant drg neurone axons express progressively higher levels of neuropillin-1 and progressively higher response to sema3A during the same stages of development (Pond et al, 2002). Expression of neuropilin-1 is maintained into the adult in dorsal root ganglia neurones, although only nociceptive sensory axons are sensitive to sema3A (Reza et al, 1999). Although neuropilins have only a small

cytoplasmic domain, they may serve some signalling purpose. Neuropilin Interacting Protein (NIP) is a PDZ domain containing protein, which interacts with neuropilin cytoplasmic domain (Cai et al, 1999). It has been shown to interact with RGS-GAIP (a protein located to the membrane of clatherin-coated vesicles), and so may play some role in vesicle transport of the neuropilin receptor (De Vries et al, 1998).

Plexins also contain an N-terminal sema domain, which binds to neuropilin to inhibit signalling. Upon binding of sema3A, this interaction is disrupted and the inhibition is removed (Takahashi and Strittmatter, 2001). Other semaphorins have been shown to bind directly to plexins, such as sema4D, which binds to plexinB1, and sema7A, which binds to plexinC1 (Tamagnone et al, 1999). All plexins and neuropilins found so far are membrane associated. Of the seven classes of semaphorins, only two are soluble, sema2 and sema3. All others are membrane associated and so require cell contact to mediate their effects (Reviewed Dickinson, 2002)

Another component of the semaphorin receptor complex is L1, a cell adhesion molecule of the Ig super family (Reviewed Schachner, 1991). L1 is an important part of the plexinA/neuropilin-1 complex, and is required for the repulsive reaction of cortical and dorsal root ganglia axons to sema3A, but is not required for sema3B, 3C or 3E mediated responses (Castellani et al, 2000).

As with many growth cone guidance cues, the semaphorin receptor complexes signal through to the Rho GTPases, although many of the signalling components are unknown. Sema3A induced growth cone collapse is a Rac1 dependant process, and dominant negative Rac1 inhibits collapse (Jin and Strittmatter, 1997). The

cytoplasmic tail of plexinB1 binds to Rac1 in a GTP-dependant manor, possibly inhibiting Rac1 activation of PAK (Vikis et al, 2000), as well as modulating the binding of sema4D to plexinB1 (Vikis et al, 2002). A different region of plexinB also binds directly to RhoA, although this interaction is independent of the GTP/GDP-bound state of RhoA (Hu et al, 2001). The identification of a novel RhoGEFs presented another way by which the plexins can regulate the RhoGTPases. PDZ-RhoGEF/LARG is crucial for sema4D/plexinB1 induced growth cone collapse in hippocampal neurones (Swiercz et al, 2002), therefore providing mechanisms for plexinB1 to both down regulate Rac1 and up regulate RhoA (Driessens et al, 2002).

PlexinA1 does not bind Rac1, although it does binds to RhoD and Rnd1. RhoD and Rnd1 compete for the same binding site. Recruitment of Rnd1 activates plexinA1 signalling, while RhoD binding inhibits both plexinA1 signalling and Rnd1 activation, consequently blocking sema3A induce growth cone collapse (Zanata et al, 2002). Sema3A induces the phosphorylation of cofilin by LIM kinase (Aizawa et al, 2001), resulting in inactivation of cofilin. Cofilin is required for depolymerisation and turn over of actin, which is an important process in maintaining actin structures (Carlier et al, 1988).

The plexins themselves do not have any kinase activity, although some kinases have been shown to associate with them, providing additional mechanisms for plexin signalling. The tyrosine kinase Fes, interacts with, and phosphorylates plexinA1, although co-expression of neuropilin 1 attenuated this process. Fes appears to be able to activate plexin signalling, and expression of kinase inactive Fes suppresses sema3A-induced growth cone collapse (Mitsui et al, 2002). A member of the Src

family of kinases, Fyn is associated with plexinA2, and phosphorylates the cytoplasmic tail of plexinA2. In addition Fyn phosphorylates Cdk5, which can also associate with the plexin/neuropillin complex, although this appears to be indirect (Sasaki et al, 2002). Tyrosine phosphorylation of Cdk5 by Fyn plays a role in sema3A collapse, and mutation of this site, tyrosine 15, in Cdk5 partially inhibits collapse. Treatment of drg neurones with Cdk5 inhibitors can also block collapse, while drg neurones prepared from either Cdk5 or Fyn knockout mice showed that both kinases are crucial for sema3A signalling (Sasaki et al, 2002).

Another kinase, glycogen synthase kinase (GSK-3), is localised as an inactive pool in the growth cone. Following sema3A treatment, GSK-3 becomes activated (Eickholt et al, 2002), although it is unclear what the consequence of activation is. With the demonstration that 12/15-Lipoxygenase is required, further components of the sema3A signalling pathway are implicated. Inhibiting this enzyme blocks sema3A-mediated collapse, while application of the enzyme/substrate product mimics collapse, causing loss of adhesion at the growth cone (Mikule et al, 2002). Again, the role played by these signalling molecules has yet to be identified.

Another protein, MICAL (molecule interacting with CasL) also plays a role in semaphorin signalling. MICAL, a member of the family of putative flavoprotein monooxygenases, interacts with plexinA and is required for sema1A/plexinA mediated axon repulsion in *Drosophila* neurones (Terman et al, 2002). Mutations in the flavoprotein monooxygenase domain blocks sema1A collapse in *Drosophila* motor neurones, while flavoprotein monooxygenase inhibitors block sema3A induced collapse in vertebrate neurones (Mikule et al, 2002), suggesting redox reactions play

some role in semaphorin signalling, although it remains unclear what this role is. Further searches for novel components of semaphorin signalling identified Off-Track, (OTK), a transmembrane protein that associates with plexinA (Winberg et al, 2001). OTK mutants demonstrate similar phenotypes to plexinA or *Drosophila* sema1A mutants suggesting they act in the same pathway, although no function has yet been assigned to OTK.

Although sema3A has been widely characterised as a repulsive guidance cue, there is some evidence to suggest that, under some circumstances, it can also act as an attractive cue. While sema3A repels cortical axons, it can attract cortical dendrites. This response is dependant on the presence of guanylate cyclase in the growth cone (Polleux et al, 2000), and thereis an involvement of cyclic nucleotide molecules in the modulation of guidance cues (Song et al, 1998).

1.3.5 The role of guidance cues in nervous system development

The role of guidance cues in the development of the nervous system has become an area of intensive research. This has been examined using well-defined processes in the development of both vertebrate and invertebrate nervous systems. One such developmental process is the development and guidance of the commissure neurones. These neurones are born on one side of the nervous system midline, and develop axons that are guided through the midline onto the other side of the nervous system, allowing the two halves to communicate. In the vertebrates these axons cross the spinal cord midline, while in invertebrates they cross the ventral nerve cord.

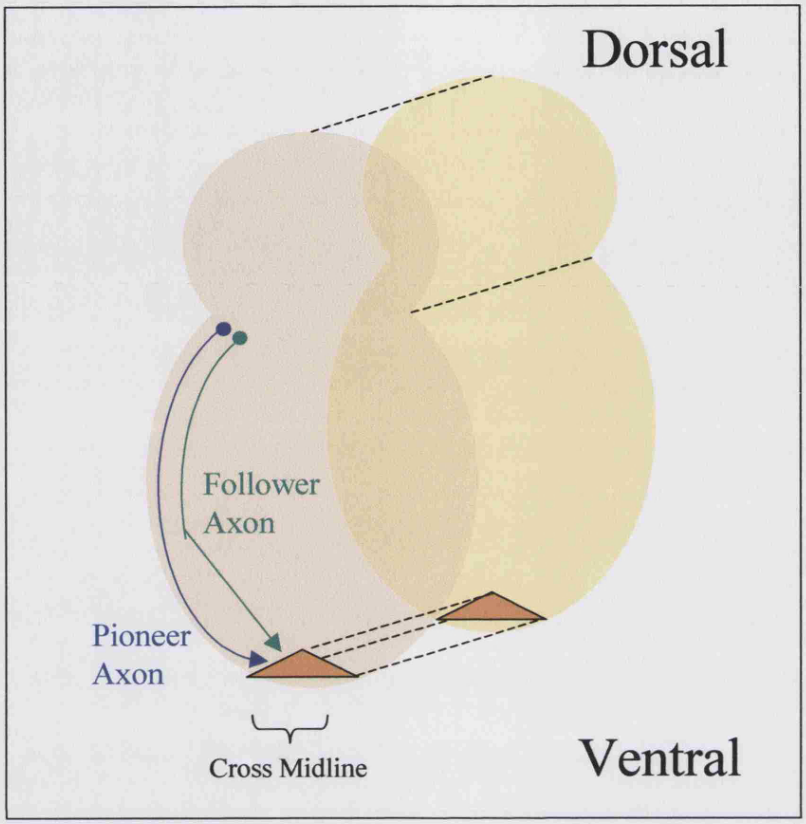

Figure 1.8. Guidance of commissure axons to the spinal cord midline.

The guidance of axons to their targets can be broken down into stages, with the end of each containing a "choice point". These choice points are determined by accessory cells, which provide the guiding axon with information needed to guide to the next choice point (reviewed in Tessier-Lavigne and Goodman, 1996). The midline of the nervous system provides a very important choice point, which some axons cross while others do not. On reaching the midline, axons will turn at right angles to the midline, growing on either the ipsilateral side (same side), or the contralateral side (opposite side) of the midline. Further to the decision whether or not to cross is the decision to

grow either in a rostral (anterior) or caudal (posterior) direction, and the guidance cues required to enable axons to make these decisions are provided by the floor plate cells. The floor plate is a group of cells spanning the width of spinal cord at the ventral midline, and is required for correct guidance of axons along and across the midline.

In the early development of the nervous system, commissure neurones are formed at dorsolateral positions on both sides of the spinal cord. The first axons, pioneer axons, follow the ventral edge of the spinal cord, round until they reach the midline. Subsequent axons, termed follower axons, follow the original path of the pioneer axons, but leave the edge of the spinal cord after a while to take a more direct route to the midline. On reaching the midline, the axons cross the ventral third of the floorplate, and on reaching the contralateral edge of the floor plate turn at right angles and grow in either the rostral or caudal direction. Once they have crossed the midline, these axons do not re-cross.

Another group of neurones, called association interneurones, form axons that originally follow the same path as the commissure neurones, and project to the midline. However these axons do not cross the midline, and instead turn right angles and grow along parallel to the midline, but on the ipsilateral side (reviewed by Colamarino and Tessier-Lavigne, 1995). The floor plate appears to be crucial to enable commissure axons to cross the midline, although is unclear whether the interneurones require the floorplate to run along parallel to the midline.

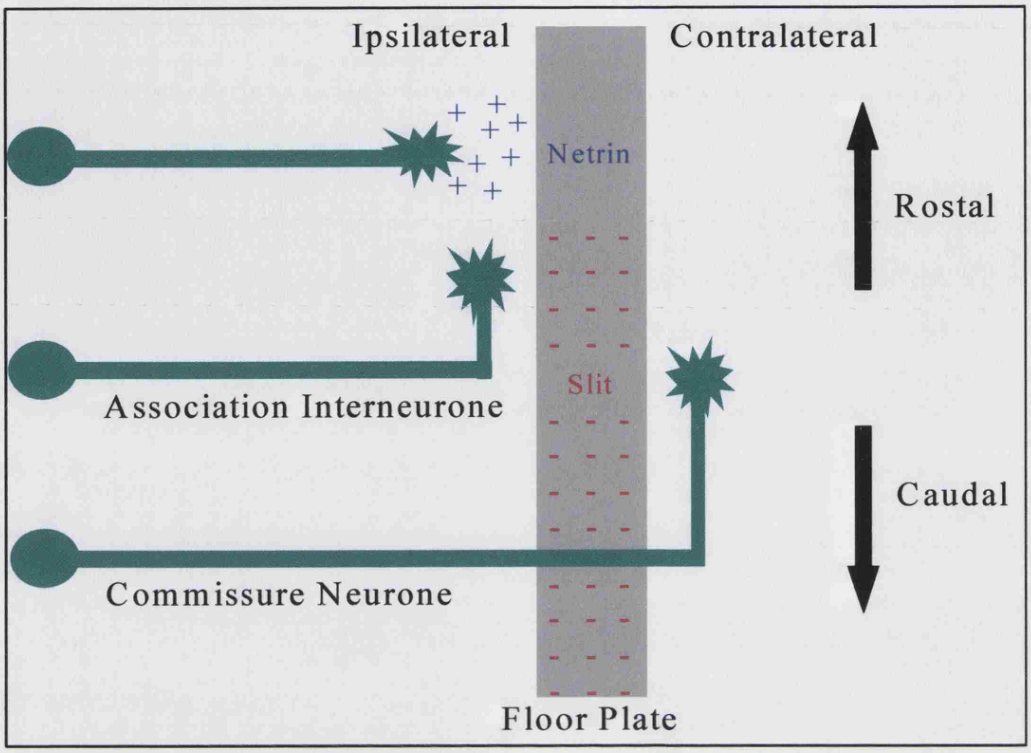

Figure 1.9. The role of the midline in the guidance of commissure axons, (Adapted from Tessier-Lavigne and Goodman, 1996).

The floor plate cells secrete the axonal attractant netrin-1 (Kennedy et al, 1994), which helps guide both the commissure and interneurone axons towards the midline (Serafini et al, 1996). As the netrins can also exhibit repulsive effects in growth cones, it is possible they are also responsible for preventing axons from entering the midline when entering the floor plate is inappropriate.

A further three different axonal repellents also appear to play a role in preventing axons either crossing the midline, or in the case of commissure axons, re-crossing the midline. The slit-robo signalling pathways are a crucial component of the growth inhibition activity of the midline. Knockout studies of robo in *Drosophila* showed that

there is excessive axonal crossing of the midline with ipsilateral axons crossing, and contralateral axons recrossing (Seeger et al, 1993). Expression of robo is very low in axons crossing the midline, while it is high in ipsilateral axons and commissure axons that have reached the contralateral edge of the midline, strongly suggesting a role of the slit/robo pathway in defining the midline guidance. Consequently, axons crossing the midline appear to be insensitive to the slits in order to allow them to cross. However, once they have crossed the midline, they become sensitive to slit, and so do not re-enter the midline (Zou et al, 2000). In the case of slit mutants, the axons enter the midline but do not leave, and instead grow through the spinal cord (Sonnenfield and Jacobs, 1994)

Class B-ephrins also appear to play a role in the guidance of axons through the midline. There are 3 different B-ephrins expressed in the floor plate, and the receptor EphB1 is expressed on many different axons projecting to the midline (Imondi et al, 2000). In addition, B ephrins can collapse commissure growth cones, suggesting the ephrins are involved in preventing axons from inappropriate crossing of the midline. Finally, the semaphorins have also been implicated to play a role in the repulsive guidance from the midline. Several semaphorin proteins are expressed at the midline, as well as other surrounding tissues, and are required to enable correct pathfinding of commissure axons (Zou et al, 2000).

The semaphorins are also important in the development of the peripheral nervous system, and of particular interest is their role in the development of dorsal root ganglia (drg) neurones. In mice drg axons enter the spinal cord by E11, and form branches, which reach the grey matter by E15, and reach their specific targets by E17.

During this time sema3 mRNA is highly expressed in the entire ventral half of the spinal cord, except for the floor plate. By E11, the peripheral sensory axons enter the sclerotome, a region of developing cells that will form the vertebrae and ribs, and sema3 mRNA is expressed throughout these areas, especially regions the axons pass en route to their targets, but do not penetrate (Wright et al, 1995).

Between E12 and E15, the peripheral axons project and branch into smaller fascicles, which then extend into their targets. Many of the tissues surrounding the peripheral nerves express sema3 at this time, before being downregulated, and disappearing by birth (Wright et al, 1995). However, adult sensory drgs retain their ability to respond to sema3 (Tanelian et al, 1997).

The importance of semaphorins in correct neuronal development has been demonstrated in knockout studies in mice, which show abnormal peripheral projections. Homozygous knockouts of sema3D show defects in many nerves such as the trigeminal nerve, which normally projects to the eye (Taniguchi et al, 1997). The nerves still reach the eye in sema3D knockout mutants, although the nerves defasciculate and spread out, resulting in some axons projecting to the wrong targets. In addition, without sema3D, axons project into the lens of the eye, which does not normally occur (Taniguchi et al, 1997).

A sema3D deficiency also causes defects in the structures of the drgs themselves, which are normally exposed to sema3D expression from the surrounding tissues. In the normal environment, the peripheral projections of the sensory neurones leave the drg's at a ventral site before meeting the ventral roots from the spinal cord. However,

in sema3 knockouts, these axons leave the ganglia from a lateral site and innervate the dorsal muscles directly (Taniguchi et al, 1997).

1.3.6 Modulation of guidance cues

Although the predominant effects of many guidance cues have been identified, many can exhibit both attractive and repulsive effects. For example, sema3A attracts cortical dendrites, (Polleux et al, 2000). Conversely, netrin-1 can become repulsive when Unc-5 associates with the DCC receptor (Hong et al, 1999). There are, however intracellular mediators, which can switch the response of neurones to the guidance cues. In *Xenopus* spinal cord neurones, an increase in Ca^{2+} in the growth cone is required for growth cone turning in response to netrin-1 or acetyl choline, and preventing this increase can block growth cone turning (Zheng et al 1994; Hong et al 2000). In addition to Ca^{2+}, cAMP and cGMP can modulate growth cone responses. The response of growth cones to all guidance cues tested can be modulated by either cAMP or cGMP, and so they have been placed into two groups. Group 1, including netrin-1, BDNF, Ach and MAG can all be altered by increased PKA activity; Netrin-1, BDNF and Ach are all converted to repulsive signals, while MAG is converted to an attractive signal. Group 2, including sema3A and NT-3 are converted by PKG activity, with sema3A converting to attraction and NT-3 converting to repulsion (Song et al, 1998). The intracellular targets of PKG or PKA involved in modulating growth cone responses are yet to be identified, but the Ena/VASP proteins may be involved as they are phosphorylated by both PKA and PKG, and play a role in regulation of the actin cytoskeleton (Waldmann et al, 1987; Lambrechts et al, 2000; Reviewed in Krause et al, 2003). Many other proteins may be involved downstream of PKA and PKG during axonal guidance, such as RhoA which is phosphorylated by

PKA (Lang et al, 1996), affecting its interaction with ROK and RhoGDI (Dong et al, 1996).

1.3.7 Collapsin Response Mediator Protein

The Collapsin Response Mediator Proteins (CRMP) are a family of highly conserved neurospecific phosphoproteins, which appear to play a role in axonal guidance. The first member of the CRMP family to be identified was CRMP-62, a 62kDa protein expressed exclusively in the developing chick nervous system (Goshima et al, 1995). It is homologous to unc-33, a nematode protein involved in axonal pathfinding (Minturn et al, 1995), and is important in the sema3A-induced collapse pathway (Goshima et al, 1995), as antibodies against CRMP-2 can block sema3A-induced growth cone collapse. The same protein was independently isolated from rat, and termed Turned On After Division-64, (TOAD-64), due to its high expression during initial neuronal differentiation (Minturn et al, 1995). It was shown to localise to lamellipodia and filopodia of growth cones, and is tightly associated with membranes (Minturn et al, 1995). Three additional members of the family were subsequently identified in rat with distinct expression patterns (Wang et al, 1996). CRMP-2 (same as TOAD-64) is the most widely expressed throughout the nervous system, with the highest expression at postnatal day 1, although can still be detected by postnatal day 30. CRMP-4 and CRMP-1 both show similar expression pattern to CRMP-2, but levels of CRMP-4 expression drop more quickly following birth, and cannot be detected at postnatal day 30. CRMP-1 expression is intermediate between CRMP-2 and CRMP-4. CRMP-3 is quite distinct, with maximum expression in the cerebellum, and persisting with high levels into adulthood (Wang et al, 1996).

A fifth member of the CRMP family, CRMP-5 (also called CRAM), was discovered and shown to be highly expressed in postmitotic neural precursors of the developing nervous system, suggesting an involvement in neuronal migration and differentiation. It is also expressed in some adult neurones, such as oligodendrocytes, and has also been shown to play a role in the sema3A collapse pathway (Fukada et al, 2000; Ricard et al, 2001).

Using CRMP-2 as bait in a yeast two-hybrid screen, CRMP-1 and CRMP-4 were isolated, and shown to form heterotetramers, similar in structure to liver dihydropyrimidinase heterotetramers, although they do not appear to share related enzyamtic functions (Wang and Strittmatter, 1997). The amino acids 8-134 and 281-435 are essential in the ability to form these hetramers (Wang and Strittmatter, 1997). Another study has shown that CRMP-2 forms a membrane-associated complex with glyceraldehydes-3-phosphate dehydrogenase isoform, enolase γ and aldolase C (Bulliard et al, 1997), although there is no indication to the function of this complex.

It has been recently demonstrated that CRMP-1, 2 and 4 all exist as two splice variants, a 64kDa protein, and an N-terminal extended protein of 80kDa (Leung et al, 2002; Quinn et al, 2003). The splice variant of CRMP-4, termed CRMP-4b, appears to play a role in vesicle trafficking in the growth cone (Quinn et al, 2003), while the extended variant of CRMP-1 interacts with ROK inhibiting the kinase activity towards other substrates, although it is not itself a substrate (Leung et al, 2002).

With the exception of other members of the family, very few proteins were found to interact with the CRMP proteins until recently, and there are no identified functional

domains in the sequence. CRMP Associated Molecule (CRAM, also called CRMP-5) is a CRMP-3 interacting protein sharing about 50% homology with other members of the CRMP family. It is brain specific and is highly expressed in the embryonic rat brain, with much lower expression in the adult brain. Although there is no indication of CRAM's function, it does immunoprecipitate from brain with the tyrosine kinase, Fes, and is up regulated during differentiation of P19 and PC12 cells, suggesting some role in neuronal differentiation (Inatome et al, 2000; Mitsui et al, 2002). Fes also associates with, and phosphorylates plexinA1, and expression of kinase inactive Fes suppresses sema3A-mediated collapse in drg neurones (Mitsui et al, 2002), suggesting a role for Fes, CRAM and CRMP-3 in sema3A-mediated growth cone collapse.

CRMP-2 interacts with phopholipase D_2 (PLD_2) via a region between 243 and 300 amino acids, and inhibits PLD_2 activity *in vitro* and *in vivo* in PC12 cells (Lee et al, 2002). In addition, treatment of PC12 cells with sema3A could also inhibit PLD_2 activity. PLD_2 is localised with CRMP-2, in the distal tips of PC12 neurites, and suggests a role for CRMP-2 and PLD_2 in neuronal pathfinding.

CRMP-2 interacts with Numb (Nishimura et al, 2003), a protein involved in regulation of the Notch signalling pathway and associates with α-adapatin, during endocytosis (Reviewed in Jafar-Nejad et al, 2002; Cayouette and Raff, 2002). CRMP-2 associates with Numb during endocytosis of the L1 receptor, and suppression of CRMP-2 expression blocks receptor endocytosis and neurite outgrowth (Nishimura et al, 2003), suggesting a role of CRMP-2 in endocytosis, as well as in the sema3A collapse pathway.

CRMP-4 interacts with chondroitin sulfate, an important component of the extracellular matrix in the nervous system, suggesting CRMP's may also play a role as ligands of the extra cellular matrix, in an unknown function (Franken et al, 2003).

CRMP-2 has been implicated to have some involvement in Alzheimers disease, due to the presence of CRMP-2 in neurofibrillary tangles (Yoshida et al, 1998). Although the role CRMP-2 plays in these tangles is unclear, it is hyperphosphorylated at 3 sites, thr-509, ser-518 and ser-522, suggesting it may be due to the deregulation of a kinase (Gu et al, 2000).

Although the CRMP family of proteins are known to play a role in neuronal development, their function is yet to be ascertained. However there is some evidence to suggest CRMP-2 is involved in microtubule dynamics. CRMP-2 associates with microtubule bundles in the spindles at metaphase, and the midbodies at late telophase in mitotic cells (Gu et al, 2000). In addition, CRMP-2 binds to tubulin monomers via a region stretching from 323-381, and promotes microtubule assembly while deletion of the microtubule-binding domain inhibits axonal growth and branching (Fukata et al, 2002). The ability of CRMP-2 to affect microtubule dynamics is dependent on the splice variant, as the 62kDa CRMP-2 causes organised microtubules, while the 80 kDa splice variant CRMP-2b results in disorganised microtubules (Yuasa-Kawada et al, 2003). These results suggest that the role of CRMP-2, in sema3A-mediated growth cone collapse, could be due to the ability of CRMP-2 to regulate microtubule dynamics.

In addition to its role with microtubules, CRMPs also provide some link to the Rho GTPases. CRMP-2 is a substrate of the RhoA effector, ROK, at site thr-555 (Arimura et al, 2000). This site is phosphorylated in LPA-induced collapse, and its mutation can block LPA collapse. This site is, however, not phosphorylated during sema3A-induced collapse, suggesting the two distinct signalling pathways can converge on CRMP-2 (Arimura et al, 2000). As well as binding to ROK, the N-terminal extended CRMP-1 can also bind to CRMP-2 to block ROK and RhoA induced neurite retraction, suggesting a complex can form which can regulate RhoA signalling in the growth cone (Leung et al, 2002).

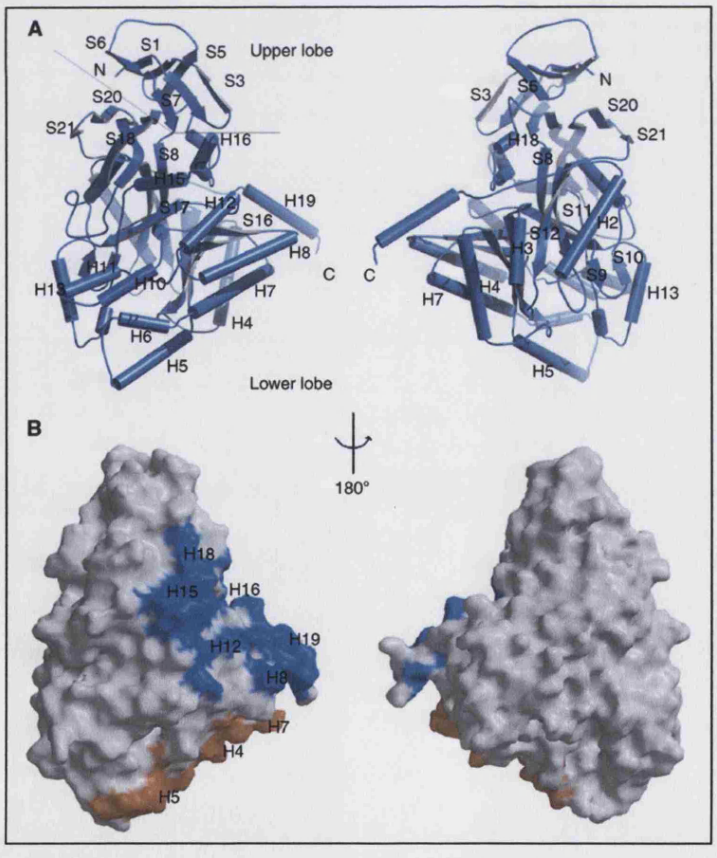

Figure 1.10. 3D structure of CRMP-1. (Taken from Deo et al, 2004.)

A more recent study has resolved the structure of CRMP-1, (Deo et al, 2004; Figure 1.10), and demonstrated that CRMP-2 associates with plexinA1. This interaction is increased in response to sema3A, in Cos7 cells expressing both plexinA1 and neuropilin-1, suggesting a direct interaction between CRMP and the plexins may play a role in sema3A signalling (Deo et al, 2004). In addition, deletion of surface amino acids, enabled the production of CRMP-1 proteins that could delay sema3A collapse (amino acids 487-489, or 367-368), or cause collapse in the absence of sema3A treatment (amino acids, 49-56 or 38-43) (Deo et al, 2004). How these deletions affect the activity of the CRMPs is unclear, but suggests intermolecular interactions are important, although these residues were not involved in the formation of the tetramers (Deo et al, 2004).

Chapter 2

Materials and

Methods

2.1 Materials

2.1.1 General laboratory reagents

General laboratory chemicals were obtained from Sigma or BDH. Water was obtained from an Elga purification system, provided sterile and de-ionised water, which was then autoclaved to sterilise. Ethanol, isopropanol, and acetic acid were obtained from BDH, and glycerol from Gibco Invitrogen. Phosphate Buffered Saline (PBS) tablets were from Oxoid, ampicillin, kanamycin and sodium dodecyl sulphate (SDS) from Sigma. Bovine Albumin was from Jackson Laboratories.

2.1.2 Materials for bacterial work

E.coli, XL1-Blue and BL21 strains were from Stratagene. Bacterial LB medium contained: 1% Tryptone (DIFCO), 1% NaCl (BDH), 0.5% Yeast Extract (DIFCO) in ddH_2O (purified from Elga purification system) previously autoclaved to sterilise. LB agar was made using a 15% Agarose solution (DIFCO) in LB medium. Antibiotics were added to the medium when selection was required. Ampicillin was used at 100μg/ml, and Kanamycin at 30ug/ml.

2.1.3 Reagents for DNA work

Agarose was from Sigma, DNA restriction enzymes, and ligases were obtained from Gibco-Invitrogen, Stratagene, Promega or New Englang Biolabs. DNA markers, HaeIII-digested φx174 and HindIII-digested bacteriophage obtained from Gibco-Invitrogen. Site-directed mutagenesis kit from Stratagene. DNA extraction columns from Amicon. Wizard miniprep DNA kit from Promega. Midi prep DNA kit from Qiagen. Vectors used, pGEX bacterial expression vector, pXJ40, pXJ41 mammalian Flag, HA and GFP

tagged vectors, pEGFP (Clonetech) and pERFP (from Edward Manser) mammalian expression vectors.

2.1.4 Reagents for protein work

Protein markers were from NEB, TEMED, protein quantification assay solution from Bio-Rad, Bis-acrylamide (30%/0.8%) from Scotlab, PVDF membranes from Perkin-Elmer, β-mercaptoethanol, Triton X-100 from BDH, DTT, Sodium Vanadate and Sodium Floride from Sigma, protease inhibitor cocktail tablets from Roche, ECL hyperfilm, and ECL solution from Amersham, ^{32}P GTP from NEN, Glutathione sepharose beads from Pharmacia Biotech, Centriprep Concentrators from Amicon. HRP-tagged secondary antibodies from DAKO.

2.1.5 Reagents for tissue culture

DMEM, Lipofectamine, Lipofectamine 2000, DMSO, Hams:F12 media, 30% BSA, Hanks Buffered Saline Solution and Poly-L-lysine were all from Sigma and Foetal Bovine Serum from Gibco Invitrogen. Collagenase from Worthington Biochemical. Disposable supplies were from Greiner. Laminin from ICN or Gibco Invitrogen. For all cell staining coverslips and slides (BDH), TRITC-labelled phalloidin (Sigma), TRITC, FITC or Cy5 tagged secondary antibodies from DAKO or Jackson laboratories were used. Slide mountant was from ICN. Electroporator and solution from Amaxa.

2.2 Bacterial Work

2.2.1 Transformation of competent bacteria

XL-1Blue E.coli from Stratagene were thawed on ice. 1.7µl of β-Mercaptoethanol was added to 100µl of bacteria, and incubated on ice for 10 minutes. 1µg of plasmid DNA was added to 25µl of bacteria, and incubated on ice for 30 minutes. The bacteria were subsequently heat shocked, by heating them to 40°C for 30 seconds, and then returned to incubate on ice for 2 minutes. 1ml of LB media was added to the bacteria, and incubated at 37°C for 1 hour. 25µl was pipetted onto the agar plates, supplemented with suitable antibiotic, and streaked using a sterile glass pipette, and incubated at 37°C overnight.

2.2.2 Growing bacterial cultures for DNA preparation

A single bacterial colony was selected and placed into 5ml of LB, supplemented with suitable antibiotic, using a sterile toothpick and incubated at 37°C, with agitation, for approximately 7 hours. The 5ml culture was subsequently added to 500ml of LB with appropriate antibiotic, and incubated at 37°C with agitation overnight. The 500ml culture was centrifuged at 3,500 rpm for 15 minutes, and the medium decanted. The bacterial pellets were re-suspended in 10ml PBS, and re-centrifuged in 50ml Falcon tubes. PBS was removed, and the bacterial pellets placed at –20°C until ready for DNA extraction.

2.2.3 Bacterial stocks

If bacterial stocks were to be made, 900µl of the 500ml over night culture was placed into an eppendorf tube with 100µl of glycerol. The solution was vortexed to mix, and stored at –70°C indefinitely.

2.2.4 Isolation of plasmid DNA

The plasmid DNA was extracted from the bacterial pellets using a Midi-kit from Qiagen, as directed by the manufactures instructions. Briefly, bacterial pellets were lysed, and the lysate passed through a filter to remove genomic DNA and cellular debris. The plasmid DNA was then retained in a second filter washed and eluted. DNA of a concentration of approximately 0.3mg/ml was typically obtained using this kit.

2.2.5 Quantification of DNA concentration and quality

5µl of the DNA obtained from the Qiagen kit was added to 1ml of TE buffer. The absorption of this solution was then measured at two different wavelengths, 260nm and 280nm, using a spectrophotometer. The reading at 260nm gave the concentration of DNA, while 280nm gave the quantity of protein in the sample. A ratio of 260/280 provided an indication of the purity of the sample, with a reading of between 1.8 and 2.0 considered good. A blank sample of TE was used to obtain a base reading.

2.3 DNA Work

2.3.1 Polymerase Chain Reaction (PCR)

PCR was carried out to multiply up plasmid DNA inserts that were to be cloned into different vectors, as well as for mutagenesis. The PCR reaction was set up as follows: 0.5µl Taq Polymerase (5u/µl) (stratagene), 10µl Taq Buffer, 2µl 10mM NTP, 30ng template DNA, 250ng Primer 1, 250ng Primer 2, and adjusted to 100µl with ddH_2O.

The thermal profile parameters were:

De-naturation (x1) -94°C – 5 minutes

Cycles (x30)
- -94°C – 30 seconds
- -50°C – 60 seconds
- -72°C – 90 seconds

Final (x1) -72°C – 5 minutes and then 7°C indefinitely.

10µl of the PCR sample was run on a DNA electrophoresis gel to check for the product. If the product was of the correct size, the whole PCR sample was run on a gel, and the band corresponding to the product extracted from the gel.

2.3.2 DNA Electrophoresis

Gels for electrophoresis were made using 1.5% agarose, in 100ml of 1x TBE buffer, (10x TBE buffer stock: 900mM Tris-Base, 900mM Boric Acid, 0.02 M EDTA pH 8.0). The agarose solution was heated and melted in a microwave, allowed to cool and then poured into the prepared electrophoresis tray with comb, and left to set. Once set, the tray and gel were placed into the electrophoresis tank, with 0.5x TBE buffer. DNA samples were prepared by adding 6x loading buffer (30% glycerol, 0.25% bromophenol blue in 1x TBE), and then loaded into the lanes. The gel was run at 140 volts, for approximately 1 hour. Following electrophoresis, the gel was soaked in ethidium bromide for approximately 45 minutes, to allow visualisation of the DNA.

2.3.3 Purification of DNA fragments from the gel

Once the band of interest was located, it was excised from the gel, and placed into a Millipore spin column, and centrifuged at 14,500 rpm for 20 minutes. This forces the gel

through a funnel, reducing it to a liquid. The product was then cleaned using Promega resin and filter columns, to remove salts or impurities, which could interfere with ligation. Once cleaned the DNA was ready to use.

2.3.4 Promega DNA clean up

Promega clean up resin and filter columns were used to clean the DNA following gel extraction. 1ml of resin was added to the DNA, and left to incubate at room temperature for approximately 10 minutes. A syringe was used to force the resin through a filter column, and the flow through discarded. The filter column was cleaned by forcing through 2ml 80% Isopropanol. The filters were centrifuged at 14,500 rpm for 20 minutes to ensure no isopropanol carry over. 50µl of TE buffer heated to 80°C was added to the filters, left for 10 minutes, and then centrifuged at 14,500 rpm, to elute the DNA solution. This could then be used directly in any ligation reactions.

2.3.5 Digestion of DNA using Restriction Enzymes

In order to ligate an insert into a vector, both the insert and vector were digested with two restriction enzymes to produce complimentary overhangs, and allow directional cloning. Typically, when digesting the vector, a 20µl reaction was set up using 10µl vector, 2µl corresponding reaction buffer, 1µl first enzyme, 1µl second enzyme, and 6µl of water. For digestion of insert DNA, a 50µl reaction was set up using 25µl of insert DNA, 5µl of corresponding reaction buffer, 1µl first enzyme, 1µl second enzyme, and 18µl ddH_2O. Both reactions were left from 2 hours to overnight. Following digestion, the DNA was cleaned using the Promega clean-up resin.

2.3.6 5'-Dephosphorylation using Alkaline Phosphatase

When ligations were to be carried out using a blunt ended site, the vector was treated with Alkaline Phosphatase (Shrimp enzyme, Promega), to prevent re-annealing. 4µl of the vector were added to 2µl Phosphatase enzyme, 3µl buffer and 21µl ddH_2O, and incubated at 37°C for 15 minutes. Following this incubation, the enzyme was heat inactivated at 65°C for 15 minutes. The DNA was then used directly in the ligation reaction.

2.3.7 Ligation of insert and vector DNA

Following digestion and cleaning, the insert DNA was ligated into the vector. The reaction was set up by adding, 1µl vector, 5µl insert, 4µl manufacturers ligation buffer, 9µl ddH_2O and 1µl T4 DNA ligase (Promega), and incubated overnight at room temperature. The whole 20µl reaction mix was then used to transform 50µl of competent E.coli.

2.3.8 Selection of clones

All ligations carried out were directional, and the presence of bacterial colonies on the agarose plates indicated either ligation, or empty vector re-annealing had occurred. To check for the presence of the insert, five bacterial colonies were selected from the plates using sterile toothpicks, and incubated overnight at 37°C, with agitation, in 5ml of selective LB media. The following day, the toothpicks were removed, and the cultures centrifuged 3,500rpm for 15minutes, to form a pellet, and then frozen. The plasmid DNA was extracted from the pellets using a Promega Wizard Miniprep kit, following the manufactures instructions. Briefly, the bacterial pellet was re-suspended and then

lysed. The lysate was cleared by centrifugation at 14,500 rpm to remove cellular debris and genomic DNA. The cleared lysate was passed through a filter to capture the plasmid DNA. The filter was washed, and the DNA eluted, in 100µl of nuclease free water. The isolated DNA prep was then digested with the same restriction enzymes used to set up the corresponding ligation reaction, and run on an electrophoresis gel, to confirm the presence of the insert.

2.3.9 Site-Directed mutagenesis

To mutate single phosphorylation sites in the CRMP-2 sequence, the QuikChange XL Site-Directed Mutagenesis Kit from Stratagene was used. Two complimentary mutation primers were made for each site in the FLAG-CRMP-2 vector,

Wild Type: 5'CAGCTAAGACA**TCC**CCTGCCAAGCAG 3'

S522A –1 5'CAGCTAAGACA**GCC**CCTGCCAAGCAG 3'

S522A –2 3' GTCGATTCTGT**CGG**GGACGGTTCGTC 5'

Wild Type: 5'GCCTCATCAGCTAAGACA**TCC**CCTGCCAAGCAGCAGGCG 3'

S522E –1 5'GCCTCATCAGCTAAGACA**GAG**CCTGCCAAGCAGCAGGCG 3'

S522E –2 3' CGGAGTAGTCGATTCTGT**CTC**GGACGGTTCGTCGTCCGC 5'

Wild Type: 5' CCGCCGCACCA**CC**CAGCGCATTGTGG 3'

T555A –1 5' CCGCCGCACC**GCC**CAGCGCATTGTGG 3'

T555A –2 3' GGCGGCGTGG**CGG**GTCGCGTAACACC 5'

Wild Type: 5' CCGCCGCACCA**CC**CAGCGCATTGTGG 3'

T555E –1 5' CCGCCGCACC**GAG**CAGCGCATTGTGG 3'

T555E –2 3' GGCGGCGTGG**CTC**GTCGCGTAACACC 5'

In the first reaction, the serine at position 522 was mutated to an alanine to knock out the phosphorylation site (See Chapter 5, Results 3), and also to a glutamine to mimic phosphorylation. These same mutations were made to the threonine at position 555. The site-directed mutagenesis kit is based on PCR, using the mutant primers to incorporate the mutations. Also included were reagents for a control reaction. In this case, the template plasmid has a mutated B-galactosidase gene, and so bacteria expressing this plasmid would be white when grown on agarose plates containing Isopropyl Thiogalactopyranoside (IPTG) and X-gal. However the control primers in this kit restore expression of this gene, and so following a successful reaction the bacteria would be blue.

The control reaction was set as directed by the manufacturer, and the sample reactions were set up as follows, 5µl 10x reaction buffer, 10ng of template DNA, 125ng primer 1, 125ng primer 2, 1µl of 10mM dNTP mix, 3µl of QuikSolution and ddH_2O to make reaction up to 50lµ. Finally 1µl of *Pfu Turbo* DNA polymerase was added. These samples were then processed through a PCR cycle using the following parameters:

De-naturation (x1) 95°C for 1 minute

Cycles (x18)
- 95°C for 50 seconds
- 60°C for 50 seconds
- 68°C for 8 minutes

Final (x1) 68°C for 7 minutes and then 7°C indefinitely.

Once the PCR cycle was complete, 11µ Dpn1 restriction enzyme was added to each sample, and incubated at 37°C for 1 hour. This restriction enzyme digests the methylated parental DNA template, leaving only the mutated plasmid in the sample. Following digestion, 2µl of the DNA was used to transform XL10-Gold ultracompetent bacteria. Five bacterial colonies were selected, and the DNA isolated following miniprep DNA extraction. The plasmid DNA obtained from these minipreps, were sent for commercial DNA sequencing (Cytomix – Cambridge, UK) to confirm incorporation of the point mutation.

2.3.10 Cloning of CRMP-2 and CRMP-2S522A into GST vector

Following the mutation of S522 to an alanine, both CRMP-2 wild type and the S522A mutant were cloned into the pXJ40 Glutathione-S-transferase (GST) vector.

The GST vector has the same cloning site and sequences at the pXJ40 FLAG vector, therefore the whole insert could be cut out and ligated in. Firstly the FLAG CRMP-2 and FLAG CRMP-2S522A were digested with HindIII and Kpn-1. These sites were used in the original cloning of the CRMP-2 sequence, and produce opposing over hang ends, which would minimise re-annealing.

Following digestion, the samples were run on a DNA gel and the excised insert cut from the gel. The DNA fragment was cleaned and ligated into linearised GST vector also digested with HindIII and Kpn-1. Following ligation, XL-1Blue bacteria were transformed, and positive clones identified as described.

2.3.11 Cloning of CRMP-2 fragments into GST vector

In order to clone fragments of CRMP-2 into a GST vector, the intact FLAG-CRMP-2 construct was digested. Firstly, the construct was digested with HindIII and SmaI, resulting in two fragments, of 336bp and 5700bp. The smaller 336bp fragment was isolated from a gel, and used to clone into an HA vector digested with the same enzymes. SmaI produces a blunt end, which could increase the chances of the vector re-annealing during ligation, and so the linearised vector was treated with alkaline phosphatase. Once the ligation had been completed, and positive clones identified and grown up, the insert was excised from the HA vector using HindIII and Kpn-1. The 336bp insert was then ligated into pXJ40-GST vector that had been digested with HindIII and Kpn-1. This construct allowed the expression of the first 112 amino acids of CRMP-2, fused to a GST tag, which was used for immunoprecipitation studies.

The second fragment was made by digesting the CRMP-2 construct with HindIII and Bgl2. This produced three fragments of 539bp, 1180bp and 4318bp. The 539bp fragment was isolated and ligated into an HA vector, also digested with HindIII and Bgl2. Once complete, the insert was excised from the HA vector, by digesting with HindIII and Bgl2, and then cloned into the pXJ40-GST vector. This construct allowed the expression of the first 180
amino acid residues of CRMP-2 fused to GST. The cloning of this fragment into the vector destroyed a large section of the cloning site.

The third fragment was made by digesting the CRMP-2 construct with HindIII and Oli-1, resulting in four fragments, 760bp, 517bp, 442bp and 4318bp. The 760bp fragment was used to clone into the GST vector. The Oli-1 restriction enzyme is a blunt cutter,

and so the insert was ligated into a GST vector digested with HindIII and Sma-1. The linearised vector was treated with alkaline phosphatase to prevent re-annealing. This construct allowed expression of the first 252 amino acids of CRMP-2.

In addition to the fragments obtained by digesting the construct, further fragments were made by PCR. Two C-terminal deletions were made to remove 22 and 70 amino acids from the C-terminal. The forward primer (provided by C.Monfries) was the standard primer used to PCR the full N-terminal.

Reverse Primer 1 22 amino acid deletion:

5' GACGTCGGTACCTTAATCATACAGGCCACGAGGGAC 3'

Reverse Primer 2 70 amino acid deletion:

5' GACGTCGGTACCTTAGGGAATGTTGTCGTCAATCTGAGCAC 3'

In addition, the N-terminal and C-terminal halves were made by PCR. The N-terminal fragment was made using the standard forward primer, along with a reverse primer designed to anneal halfway along the sequence.

Reverse primer for N-terminal:

5' GACGTCGGTACCTTAGGCAGCGGCCTTGGCCCAGTTC 3'

The C-terminal was made using the standard reverse primer (provided by C.Monfries) along with a forward primer designed to anneal halfway along the sequence.

Forward primer for C-terminal:

5' GACGTCAAGCTTAGCAAGAACTGGGCCAAGGCCGCTGCC 3'

PCR was run as described, and the fragments ligated into FLAG and GST vectors.

2.4 Protein Work

2.4.1 Expression of recombinant protein in E.coli

In order to express, and isolate recombinant protein, XL-1Blue E.coli bacteria were transformed with the pGEX vector containing the required sequence. This vector produces a protein fused to Glutathione-S-Transferase (GST), an enzyme with a very high affinity for its substrate, glutathione. Therefore, using sepharose beads attached to glutathione the fusion protein can be easily purified from the bacterial lysate.

The bacteria were plated out on agarose, and the selected colonies grown up to obtain 50ml cultures. These 50ml cultures were then added to flask containing 500ml of LB medium, and incubated, with agitation, at 37°C, until the culture had reached an optical density of 0.8 - 1.0. This was ascertained by pipetting 1ml of the culture into a visible light wavelength cuvette, and taking a reading at a wavelength of 595nm, using LB medium to take a base reading.

Once the optical density was at the required level, the bacteria were induced into expressing the protein using Isopropyl Thiogalactopyranoside (IPTG), at a working concentration of 200μM. The induction step was usually carried out at 37°C with agitation, however when expressing the GST-PAK CRIB (70-104), the induction was

carried out at 30°C, due to an adverse effect of the protein on the bacteria. The cultures were then left to express the protein for 1-2 hours, before being centrifuged and frozen.

2.4.2 Purification of GST fusion proteins.

The bacterial pellets were thawed on ice, and re-suspended in 20ml of lysis buffer, containing 1% Triton, 1mM PhenylMethylSulfonylFluoride (PMSF), 1mM Dithiothrentol (DTT) and supplemented with protease inhibitor cocktail tablets (Roche). Following re-suspension, the mixture was sonicated for 5 minutes, and centrifuged at 15,000 rpm for 30 minutes. The supernatant was removed and glutathione sepharose beads prepared. The beads are stored in an ethanol-based buffer, and so were washed three times in ddH_2O prior to use. 1ml of beads was added to each 500ml bacterial culture lysate, and incubated at 4°C, with rotation, for 2 hours. Following the incubation, the beads were spun down, the supernatant removed, and the beads re-suspended in 20ml of fresh lysis buffer. They were then incubated again at 4°C for 45 minutes. This wash was repeated, before the protein was eluted off the glutathione beads. The GST fusion protein was eluted off with 10ml of 10mM glutathione/50mM Tris HCl pH7.5, incubated at room temperature for 10 minutes. Sepharose beads were removed by passing the mixture through filter columns. Any excess glutathione was removed by concentrating the protein in Amincon concentrating filters, and adding PBS back up to 10ml. This step was repeated three times, although no PBS was added at the final step so the protein was in a smaller volume, and so more concentrated.

When the Rho GTPases were being made a p21 buffer (50mM TrisHCl pH 7.5, 2.5mM $MgCl_2$) was used as PBS has an adverse effect on GTPase function.

2.4.3 Measuring concentration of GST fusion proteins

Following recombinant protein preparation, concentrations was determined using a Bio-Rad protein assay. 2µl of the protein sample was added to 800µl of water and 200µl of Biorad protein assay reagent. A blank sample was also used, which contained no protein. These were left at room temperature for five minutes, and the absorbance at 595nm measured, using the blank sample as a base reading. The absorbance readings were calibrated using a Bovine Serum Albumin (BSA) standard curve in order to determine the protein concentrations for each of the samples. The BSA standard curve was obtained using 1, 2, 5 and 10mg of protein in the protein assay, and a graph of absorbance against protein concentration was plotted.

2.4.4 Purification of MBP fusion proteins

An alternative to GST fusion proteins is the Maltose Binding Protein (MBP) fusion protein. MBP binds to maltose with high affinity and maltose conjugated to sepharose beads are used to purify the protein from the bacterial lysate. Once the protein had been extracted bound to the column and washed in lysis buffer, it was eluted off with 10mM maltose, and then concentrated as before. All proteins to be stored long term were kept at -70°C otherwise they were kept at –20°C.

2.4.5 Protein Dot Blot Assay

Dot blot assays were carried out to test the ability of the Rho family of GTPases to bind directly to CRMP-2. 5µg of the target protein was blotted onto a $1cm^2$ square of nitrocellulose. The target proteins used were, GST, GST-CRMP-2, cleaved CRMP-2, PAK CRIB and ROK Rho-binding domain. The nitrocellulose was allowed to dry, and soaked in re-naturation buffer (3% BSA, 0.1% Triton, 0.5mM $MgCl_2$, 5mM DTT) for 1

hour at 4°C. The GTPase probes were then prepared by adding 25µl of NEB buffer (50mM NaCl, 25mM Mes pH6.5, 25mM Tris HCl pH 7.5, 1.25mM EDTA, 1.25mg/ml BSA, 1.25mM DTT), 5µg of RhoAV14, Rac1V12 or Cdc42V12, 1ul of GTP $\alpha^{32}P$ to 19µl of ddH_2O. This was then incubated for ten minutes at room temperature. After the ten minute period, 25µl of cold GTP was added to 4ml of binding buffer (50mM NaCl, 25mM Mes pH6.5, 25mM TrisHCl pH7.5, 1.25mM $MgCl_2$ 1.25mg/ml BSA, 1.25mM DTT). The GTPase probes were then added to the binding buffer, and poured over the blots. After five minutes, the nitrocellulose filters were removed from the probes and washed five times in wash buffer (50mM NaCl, 25mM Mes pH6.0, 5mM $MgCl_2$, 0.25% Triton). The filters were allowed to dry, wrapped in cling film, placed into a cassette with a sheet of radiofilm and left at –70°C overnight. The film was exposed the following day.

2.4.6 Analysis of proteins by SDS Polyacrylamide Gel Electrophoresis (PAGE)

Protein samples were separated by SDS PAGE in order to verify their molecular weight. The percentage of the polyacrylamide varied depending on the size of proteins needed to be resolved, but typically a gel of 12% polyacrylamide suited most cases. The gel mix was made (12% polyacrylamide, 0.4M TrisHCl pH 8.8, 0.1% SDS, 10% Glycerol, 0.02% TEMED, 0.05% Ammonium Persulphate), poured into the prepared cassettes and allowed to set, typically 45 minutes to 1 hour. Once set, the stacker was prepared and poured on top of the gel, and the comb added to make the lanes. The stacker was made by adding to water, 25% stacking buffer (0.5M TrisHCl pH 6.8, 0.4% SDS), 4% polyacrlyamide, 0.05% Ammonium Persulphate and 0.2% TEMED. This was also allowed to set, the combs removed, and the cassette fixed into the electrophoresis

equipment. The electrophoresis tank was filled with 1x running buffer (made from 10x stock, 250mM TrisBase, 1.92M Glycine, 1% SDS), and then to each sample, a 5x solution of Lammeli sample buffer (62mM TrisHCl pH 7.8, 10% Glycerol, 2% SDS, 0.5% β-mercaptoethanol, 0.05% bromophenol blue) was added. Samples were heated to 80°C for ten minutes to ensure complete de-naturation of the proteins before being loaded into the lanes. Protein markers (New England Biolabs) were also run to allow the sizes of the sample proteins to be identified. The samples were electrophoresed at 170 volts for 1 hour or until the dye front has reached the edge of the gel.

2.4.7 Coomassie stain of proteins

Following PAGE, the proteins in the gel were visualised by staining with coomassie blue dye. The gel was soaked in a 0.1% coomasie dye dissolved in destain solution, for at 1 hour, and then soaked in destain (40% methanol, 10% glacial acetic acid, 50% water) overnight to remove free dye. If the gel was to be kept, it was dried in a vacuum drier.

2.4.8 Transferring protein to membranes

In order to perform a Western blot on samples, proteins were transferred from the gel and immobilised on a membrane, Polyscreen PVDF membrane (PerkinElmer), which was cut into the correct size pieces, and soaked in methanol for 45 minutes prior to transfer. The gels were removed from the electrophoresis equipment, and soaked in 1x Transfer Buffer (10x stock 25mM TrisBase, 192mM Glycine, made up to 1x with water and 20% methanol). Extra thick filter paper was also soaked in the transfer buffer, and applied to the Bio-Rad semidry transfer blotter, followed by standard filter paper, also soaked in the transfer buffer. The PVDF membrane was laid on top, and the gel on top

of the PVDF. The edges of the gel were marked on the PVDF to indicate the size of the gel. Another layer of standard filter paper was applied on top of the gel, and then finally a second layer of the extra thick filter paper. Care was taken to ensure no air remained between any of the layers. Transfer was carried out at 4°C, for either 1 hour at 15 volts, or overnight at 9 volts.

2.4.9 Immuno-detection of proteins immobilised on PVDF membrane

Once transfer had been completed, the PVDF was removed from the blotter, and stained in 0.15% coomasie stain for 2 minutes. The membrane was then soaked in destain for 20-30 minutes, changing destain in between. This would allow visualisation of the proteins on the membrane, and also reduces background detection with the antibodies. The PVDF was washed in water, and then blocked in 5% marvel/0.1% Tween PBS, for 1 hour at room temperature, after which the membranes were added to 50ml flacon tubes and placed on to a spiralmix and rotated. Primary antibodies were diluted in to 5ml 1% marvel/0.1% Tween-20 PBS, at the optimal dilution, typically 1:1000 – 1:2000, then added to the PVDF, and incubated for 1 hour at room temperature. Following incubation with the primary antibody, the PVDF was washed five times in 0.1% Tween PBS. The secondary antibody was conjugated to Horse Radish Peroxidase to allow proteins to be visualised by chemiluminescence. This was also diluted in 5ml 1% marvel/0.1% Tween PBS before being incubated with the PVDF, and incubated at room temperature for 1 hour. After the final incubation the PVDF was removed from the falcon tubes and placed into a dish, and washed with excess 0.1% Tween PBS. This would ensure a harsher washing step, and so reduce the background. Following the wash, the PVDF was dried, soaked in ECL solution (Amersham), and placed into a cassette. Under safe lighting, a single sheet of ECL film was added to the cassette and

exposed for 2 minutes, after which the film was removed, and developed in 1x developer solution (Kodak). Once developed, the film was fixed (1x fixer solution - Kodak) and washed in water, before being left to dry. Typically two further exposures were taken, at 5 minutes and 20 minutes, depending on the strength of signal. Once dry, the film was placed in the cassette and lined up with the PVDF to allow the protein markers to be indicated.

2.5 Cell Work

2.5.1 Tissue Culture

Four different types of cell line were used in this study. All cell lines were maintained in incubators at 37°C with 5% CO_2.

The cell line N1E-115, a mouse neuroblastoma cell line, was used for morphological studies on the Rho family of GTPases. Cells were cultured in Dulbecco's Modified Eagle Medium (DMEM) (Gibco), with 10% Foetal Calf Serum (FCS) and 1% antibiotic/antimitotic (Ab/Am) (Gibco), and plated out on Nunc coated petri dishes (Gibco). To passage the cells, one plate was taken, and the media removed. 10ml of fresh, pre-warmed media was added to the dish, and the cells removed by pipetting. The cell suspension was then transfered into a 50ml falcon tube, and centrifuged at 750 rpm for 8 minutes, after which the media was removed. The cells were re-suspended in fresh media and plated out at the required density.

The second cell line used was the α2-chimaerin permanent expression cell line α2.13. These cells are a permanent N1E-115 cell line previously transfected with a α2-chimaerin vector encoding a neomycin selection gene. These cells were cultured in the

antibiotic G418 (Calbiochem) to ensure the transfected vector was maintained in all the cells. G418 was made up into a 100mg/ml stock, and used at 800μg/ml. To passage these cells it was necessary to trypsinise them, due to their increased adhesion to the dishes. The media was removed, and the cells washed once in PBS to remove any residual FCS, a potent inhibitor of trypsin. Subsequently, 1ml of 10x trypsin (Gibco) was added to the dish, and incubated at 37°C for 2 minutes. The dishes were placed under a microscope to check for loss of adhesion, and then passaged as for the standard N1E-115 cell line.

Cos-7 cells derived from monkey kidney cells, were used for interaction studies, and to verify protein expression, due to their ability to express very high levels of a transfected cDNA construct. Culturing was the same as described for the N1E-115 cells line, except like the α2.13 cells, they required trypsin in order to detach from the dish.
Swiss 3T3 cells, a fibroblast cell line, were cultured following the same protocol for the Cos-7 cells.

Cell stocks were made for all cell lines used. One confluent plate was taken and the cells centrifuged to pellet them. They were then re-suspended in a filter sterilised solution of 90% FCS/10% Dimethyl Sulphoxide (DMSO). This suspension was then pipetted into cryotubes (Gibco), which were labelled and placed in –70°C overnight. The following day the tubes were placed in liquid nitrogen.

To resuscitate cell stocks from liquid nitrogen, they were thawed quickly at 37°C in the water bath, and the cell suspension was added to 10ml of fresh media. This was then

centrifuged to pellet the cells, and so remove DMSO. The cell pellet was re-suspended in media, and plated out.

2.5.2 Preparation of coverslips

Glass coverslips were placed into a 10cm dish, and 10ml of 60% ethanol/40% HCl was added. The coverslips were left for 10 minutes, and then rinsed three times in ddH_2O. They were dried on filter paper, wrapped in polyfoil and baked in an oven to sterilise. Before use, the coverslips were coated with laminin (Gibco/ICN) (10μg/ml) or Poly-L-lysine (Invitrogen) (5μg/ml). The substrate was added to the coverslip and left 1 hour for laminin or 10 minutes for Poly-L-lysine, after which they were washed 3 times in PBS and left to dry. Once coated, the coverslips could be kept at 4°C for up to a week before use. Chamber slides were coated using the same protocol.

2.5.3 Transfection of the cell lines

In order to express the required constructs, N1E-115, α2.13 and Cos-7 cells were transfected with the required vectors, typically pXJ40. For morphology studies, N1E-115 or α2.13 were plated on acid washed, substrate coated coverslips, or chamber slides, and left to plate down over night. The following day, the media was removed from the dishes and replaced with plain DMEM, with no FCS or Am/Ab. The DNA was prepared by adding 1μg of DNA, along with 5μl of Lipofectamine, or Lipofectamine 2000 (Invitrogen) to 200μl of DMEM. This mixture was pipetted up and down to form liposomes with the DNA, and then left for 45 minutes at room temperature before being added to the cells. The cells were left in serum-free media for 5 hours. It was then

replaced with fresh DMEM with FCS and Am/Ab, and the cells left to express overnight.

2.5.4 Cell Immunostaining

Cultures and cells to be assessed by immunostaining were washed with PBS and fixed with 3% paraformaldehyde (PF) for 20 minutes at room temperature. The PF was removed, and cells washed with PBS for 10 minutes, and then 100mM Glycine/PBS was added for 10 minutes to quench any residual PF. Cells were permeabilised in 0.2% triton/PBS for 10 minutes, rinsed in PBS, and blocked in 3% BSA/PBS for 10 minutes. The primary antibody was diluted in 1% BSA/PBS and added to the coverslip at a typical dilution of 1:100. If chamber slides were used, the volume of primary antibody/1% BSA solution added was 500µl, while if coverslips were used, only 100µl was added, parafilm was laid on top to spread the solution over the coverslip. The coverslips were incubated with the primary antibody for 1 hour at 37°C, making sure the cells did not dry out. Following the primary antibody, the coverslips were washed three times in PBS, and then the secondary antibody conjugated to a fluorescent label (FITC-Fluorescein Isothiocyanate, TRITC-Tetramethyl Rhodamine Isothiocyanate or Cy5) diluted in 1% BSA/PBS, was added. The FITC label has an excitation wavelength of 488nm, while TRITC is excited at 545nm, and Cy5 at 633nm. The secondary antibody was also typically at a dilution of 1:100. In addition to the secondary antibody, TRITC conjugated phalloidin was often added at a concentration 1:100. This compound has a very high affinity for actin, and so was used to stain for actin, without having to use an antibody. When more than one antibody was used, care was taken to ensure there was no risk of any cross reactivity. The coverslips were incubated with the secondary antibodies, and phalloidin for 1 hour at 37°C, and washed three times in PBS and

allowed to dry. Coverslips were then mounted onto slides using immunofluor mountant (ICN). When using chamber slides, the chamber was removed from the slides, and the gasket cut off using a razor. Once the slide was smooth, a coverslip was mounted onto the slide using immunofluor mountant. The mountant was allowed to dry over night, and the slides were examined the following day.

If cells were to be stained with phalliodin, but no antibodies, they were fixed as described, and queched with 100mM glycine. They were washed with PBS, and the phalliodin added without permeabilising.

2.5.5 Transfection of Cos-7 cells

Cos-7 cells were usually used for interaction studies and to check expression of constructs. As such 10cm dishes of Cos-7 cells were transfected. The cells were serum-starved in 5ml of DMEM, and 5μg DNA prepared in 1ml of DMEM with 20μl of Lipofectamine. As for the neuroblastoma cells, the DNA was left for 45 minutes and then added to the dishes. After 5 hours the media was replaced with FCS media and the cells left overnight.

2.5.6 Immunoprecipitation

One of the main experiments undertaken in Cos-7 cells was immunoprecipitations (IP). Two proteins were expressed in the Cos-7 cells using the transfection protocol described, both were tagged, one was usually FLAG and GST due to the availability of both anti-FLAG antibodies and glutathione conjugated to sepharose beads. The following day the cells were washed with PBS, and lysed in 600μl of lysis buffer (25mM Hepes (pH 7.5), 0.3M NaCl, 1mM $MgCl_2$ 1mM EGTA, 20mM β-

glycerophosphate, 5% Glycerol, 0.5% Triton X-100) and supplemented with freshly added, 1mM Sodium Vanadate, 10mM Sodium Floride, 5mM DTT, 1mM PMSF and 1x complete protease inhibitor cocktail (Roche). The cells were scraped off, and pipetted into tubes, before being sonicated in a reservoir sonicator for 5 minutes. The lysates were centrifuged at 14,500 rpm for 10 minutes in a cooled centrifuge, and the supernatant pipetted off. 50µl were kept for expression analysis, and the remainder was incubated with 20µl of anti-FLAG beads (or prepared glutathione beads), on a rotor for 3 hours at 4°C. Following incubation, the beads were pelleted in a cooled centrifuge, and washed three times in lysis buffer. After the final wash, the beads were left in approximately 30µl of buffer, and 10µl of 5x sample buffer was added. 10µl of cell lysate was also taken, and 2µl of 5x sample buffer was added. Both the bead samples, and the lysate samples were boiled for 10 minutes and resolved by PAGE, before being transferred onto PVDF. The PVDF's were tested for the presence of the secondary protein by immuno analysis, and hence demonstrate an interaction. Probing for the immunoprecipitated protein, i.e. FLAG or GST tagged, was also performed to confirm successful immunoprecipitation.

2.5.7 Expression in Swiss 3T3 fibroblasts

Swiss 3T3 fibroblasts are not suitable for transfection, and consequently all work involving Swiss 3T3 fibroblasts was performed using microinjection. The cells were plated onto poly-L-lysine coated coverslips, and left overnight to plate down. They were then placed onto a Zeiss Axiovert 135 microscope with a heated stage and CO_2 box, to maintain temperature and CO_2 levels. Using a microinjector, DNA, at a concentration of 50µg/ml was microinjected directly into the nucleus. Approximately 100 cells were

injected in a marked area, and left for 5 hours to express the construct. Cells were then fixed and stained as described.

2.5.8 Time Lapse Microscopy

In order to observe the changes in cell morphology over time, time-lapse microscopy was used. N1E-115 or α2.13 cells were plated out on coverslips, and left to plate down over night. For some experiments, the cells were transfected, otherwise they were used the following day. They were placed on the microscope, in the CO_2 chamber, and in some instances were injected with DNA as described. Movies were then made using a monitor and a video recorder, with 30 second movies being made approximately every 10 minutes or so, depending on requirement. Once completed, the movies were converted to digital images using frame capture software on a confocal microscope. Later, movies were made using a digital camera connected to a computer, and using Metamorph software, which also enabled fluorescent movies to be made.

2.5.9 Microscopy

Once the slides had been fixed and stained, they were observed on a Zeiss 135 Axiovert microscope using fluorescent filters to observe staining. This microscope was used for general examination, and all cell counting. For more detailed pictures with higher resolution, a Zeiss LSM 410 confocal microscope was used.

2.5.10 Preparation of rat dorsal root ganglia (drg)

Drg cultures were isolated and maintained according to G. Michaels (Queen Mary Westfield College, London). Growth media was prepared by supplementing Hams:F12 media with 1% 100x N2 supplement (100x N2 supplement: 10ml Hams:F12

supplemented with 5mg insulin, 100mg transferring, 6.3μg progesterone, 16mg putrecine, and 5.2ug selenium (all from Sigma)), 0.3% fatty acid free BSA (Sigma), 10nM AraC (Sigma) and 500μl antibiotic solution (Gibco). The solution was filter sterilised and stored at –20°C. This media was then filter sterilised, and stored at 4°C for no longer than 1 month.

Prior to drg extraction, all coverslips and dishes to be used, were coated with 10μg/ml laminin (Gibco). Drg's were isolated from day 1 postnatal Wistar rats. The rats were culled in accordance with the Scientific Procedures Act, and the spines removed. Under a microscope, the vertebrae were cut open, exposing the spinal cord. The drg's were removed from the vertebrae using tweezers, and placed into Hams:F12. As many drg's were removed as possible, before being incubated, at 37°C/5% CO2, in 0.125% collagenase in 5%FCS/F12, for 30 minutes. Following three washes in calcium chloride/ magnesium sulphate-free Hank's buffered saline solution (HBSS) (Sigma), the drg's were incubated in 1x trypsin/HBSS (Sigma) for ten minutes. Enzymatic treatment was needed to break down the ganglia capsule and tissue, as well as break the cells apart. Trypsin treatment was carefully limited to ten minutes to ensure minimal damage to the cells. Following trypsin treatment, the ganglia were washed three times in 5% FCS/F12, and a further three times in F12. After these washes, the ganglia were triturated in 1ml Hams:F12, using a pipette and P1000 tip with the end 0.5cm cut off. Once a suspension had been formed, trituration was repeated using a standard P1000 tip. The cell suspension was centrifuged through a 15% BSA/F12 gradient, at 1000rpm for 10 minutes, to remove debris. The cell pellet was re-suspended in F12, and centrifuged again, before being plated out in growth media supplemented with 100ng/ml NGF.

2.5.11 Electroporation of drg's

If the cells were to be electroporated, the cell pellet was re-suspended in room temperature nucelofector reagent (Amaxa), using 100µl for each DNA construct to be used. 100µl of the cell suspension was pipetted into the provided cuvettes, along with 1-3ug DNA. The cuvettes were placed into the electroporator (Amaxa), and the cells processed, using programme 0-03. Following electroporation, 500µl of growth media was added to each cuvette, and the cells either plated out immediately, or incubated at 37°C/5%CO2 until ready to be used. Drg's were plated out in growth media supplemented with 100ng/ml NGF. If Sema3A collapse assay were to be performed on the cells, the media was replaced the following day, with growth media supplemented with 20ng/ml NGF.

2.6 Statistical Analysis

Where stated error bars indicated represent Standard Error of the Mean (SEM), or Standard Deviation (SD). Following transfection or treatment, cell morphology was quantified accordingly with percentages calculated, and three different fields of view were averaged. Each experiment was repeating three times, to allow SEM's over three averages to be used. For drg neurone growth cone collapse assays, certain experiments were carried out in triplicate, allowing SEM's to be calculated over three experiments, while others were carried out individually over three experiments, and consequently SD's were used.

Significant values were obtained using a two-tailed students t-test, using all the original values before averages were taken. Stars used to indicate significance, relate to standard format, * = 0.05, ** = 0.01, *** = 0.001.

Chapter 3

Results 1

3.1 The effect of CRMP-2 of Rho GTPase morphologies in N1E-115 neuroblastoma cells.

The role of the Rho family of GTPases in cell morphology has been widely studied in a variety of cell lines (Ridley and Hall, 1992; Ridley et al, 1992; Kozma et al, 1995). Of the three key members, RhoA causes cell retraction and formation of stress fibres, while both Rac1 and Cdc42 form peripheral actin structures, such as lamellipodia and filopodia, respectively. Although there can be an antagonistic relationship between RhoA and Rac1 (Kozma et al, 1997; Sander et al, 1998), as well as between RhoA and Cdc42, in Swiss 3T3 fibroblasts (Kozma et al, 1995), there can also be a hierarchal relationship, with Cdc42 activating Rac1 (Nobes et al, 1995), and with Rac1 activating RhoA (Ridley and Hall, 1992).

The neuroblastoma cell line, N1E-115, is one of the best characterised neuronal cell lines. In these cells, the GTPases display similar effects on cell morphology as in other cells described previously, with both Rac1 and Cdc42 inducing the formation of peripheral actin structures, and RhoA causing neurite retraction (Kozma et al, 1997). However, because the N1E-115 cell line is of neuronal origin, it can be used to investigate the possible role of the GTPases in neurite formation, and this provides information on morphological differentiation and development in the nervous system (Leeuwen et al, 1997; Sarner et al, 2000). Therefore these cells were selected as a model system to examine possible interplay between the Rho GTPases and CRMP-2 in neurite outgrowth.

Collapsin Response Mediator Protein-2 (CRMP-2), is a neurospecific phosphoprotein, which is homologous to the *C.elegans* protein, Unc33 (Goshima et al, 1995; Minturn et al, 1995). It is a component of the semaphorin3A signalling pathway (Goshima et al, 1995) and is involved in axonal outgrowth (Inagaki et al, 2001; Fukata et al, 2002), although its involvement in these functions is not well established. The effect of CRMP-2 and its possible relationship with the Rho GTPases was investigated in N1E-115 cells. An involvement of CRMP-2 with the Rho GTPases had been suggested by the finding that it might interact with the RacGAP, α2-chimaerin (PhD Thesis, M. Teo) and by studies showing that CRMP-2 is a substrate of ROK, a major RhoA effector (Arimura et al, 2000).

3.1.1 The role of the Rho family of GTPases on cell morphology

In order to investigate the role played by Rho GTPases in neuronal morphology, and the effect of CRMP-2 on GTPase function, cDNA constructs coding for mutated Rho GTPases were used. These were dominant positive mutants, which result in a loss of GTPase enzymatic function and causes the GTPase to be constitutively active, and dominant negative mutants, which sequester guanosine exchange factors (GEF's), and so reduce the proportion of active GTPase in the cells (Reviewed in Feig, 1999). These two mutants of RhoA, Rac1 and Cdc42 are commonly used to respectively mimic or block the effects of the GTPases (Ridley et al, 1992; Kozma et al, 1997; Sarner et al, 2000).

N1E-115 cells demonstrate heterogeneous morphologies, but when cultured in media containing 10% FCS are generally round, with few small filopodia (Figure 3.1g). This is due to the presence of LPA (lysophosphatidic acid) in the media, which activates RhoA and ROK (Ridley and Hall, 1992; Kranenburg et al, 1999), hence resulting in contraction of peripheral actin structures (Ridley and Hall, 1992).

Mutant	Examples	Description
Dominant Positive	RhoAV14 Rac1V12 Cdc42V12	Mutants have a defective GTPase enzymatic activity, and so are unable to hydrolyse GTP. Consequently, they remain GTP bound, and strongly activate downstream effectors.
Dominant Negative	RhoAN19 Rac1N17 Cdc24N17	Mutants sequester endogenous GEF's, and so are able to interfere with normal signalling pathways of endogenous GTPases.

Table 3.1. Description of the dominant positive and dominant negative Rho GTPase mutants used in this study.

The neuroblastoma cells were transfected with different GTPase constructs and plated on poly-L-lysine in 10% FCS media. Poly-L-lysine provides an adhesion substrate for the cells, thought to be due to the anionic cell surface, and the cationic polylysine (Mazia et al, 1975) but unlike laminin does not signal through integrins (Rodriguez et al, 1989; Guan et al, 1991; Burridge et al, 1992), which activate GTPases (Reviewed in Arthur et al, 2002). Therefore, poly-L-lysine was chosen as a substrate to assess the effect of the Rho GTPases on the morphology of N1E-115 cells.

After transfection and fixation, the cells were stained for actin using TRITC-conjugated phalloidin, and with antibodies to detect protein expression from transfected cDNA. Examples of some of the morphologies generated by the GTPases obtained using confocal microscopy are shown (Figure 3.1). The dominant positive Rac1 mutant, Rac1V12 produced cells that were large, flat and had large lamellipodia around the whole periphery (Figure 3.1a), as has been described previously (Leeuwen et al, 1997; Sarner et al, 2000). This morphology is characteristic of Rac activation in N1E-115 neuroblastomas cells (Leeuwen et al, 1997; Sarner et al, 2000). Cdc42V12 also resulted in a proportion of cells exhibiting this Rac phenotype, presumably because of the hierarchal relationship between Cdc42 and Rac1, with Cdc42 signalling through to Rac1 (Nobes and Hall, 1995).

The dominant negative Rac1, Rac1N17, expressing cells, demonstrated a very different phenotype to that seen with the Rac1V12. Cells did not form the Rac

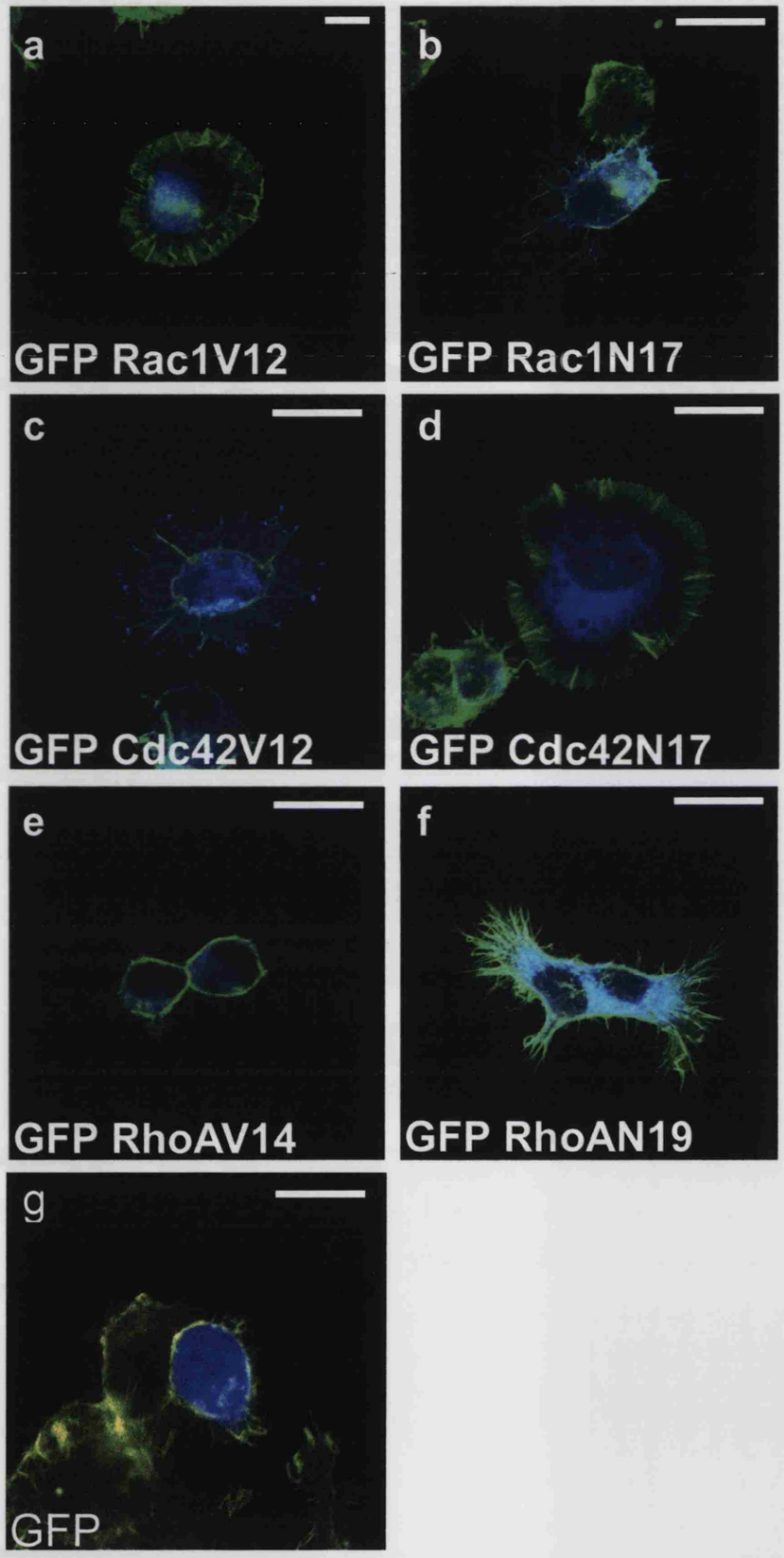

Figure 3.1. Examples of morphologies observed from N1E-115 cultured in 10% FCS media.

Cells were transfected with GFP tagged dominant positive (active) and dominant negative (inactive) mutants of the Rho GTPases (see Table 3.1). Images show TRITC labelled phalloidin (green), and GFP expression (blue). Scale bar equals 25μm.

phenotypes, and had very few lamellae. Many cells produced short filopodia, (Figure 3.1b) which are thought to be of sensory rather than structural function (Davenport et al, 1993), and exhibited features normally associated with Cdc42 activity. Cdc42V12, in addition to the Rac phenotypes formed, also produced cells with many filopodia (Figure 3.1c), as previously described (Sarner et al, 2000). This phenotype was very similar to that seen with Rac1N17 (Figure 3.1b). It is possible that Rac1 and Cdc42 can be activated simultaneously, as well as in a hierarchal relationship, and so blocking Rac1 signalling could result in Cdc42 activation, and filopodia formation.

The dominant negative Cdc42 construct, Cdc42N17, formed cells exhibiting the Rac phenotype (Figure 3.1d). The morphologies generated by dominant positive Cdc42 and dominant negative Rac1 suggest some interplay between Rac1 and Cdc42, with Cdc42 being activated when Rac1 is inhibited. In addition some cells expressing the dominant negative Cdc42 construct exhibited typical Rac phenotypes.

In contrast to Rac1V12 and Cdc42V12, the RhoA dominant positive mutant, RhoAV14 expressing cells produced very little outgrowth (Figure 3.1e), as previously shown (Tigyi et al, 1996; Kozma et al, 1997). Most cells expressing RhoAV14 were round with few or no filopodia or lamellipodia. The dominant negative RhoA mutant, RhoAN19, demonstrated a very different effect from RhoAV14. Cells had many more filopodia (Figure 3.1f). This could possibly be attributed to activation of Cdc42 and Rac1 following RhoA inhibition, since RhoA and Cdc42/Rac1 have an antagonistic relationship in neurite outgrowth (Kozma et al, 1997). It is unclear why expression of dominant negative RhoA (Figure 3.1f) does not induce the formation of round Rac

phenotypes similar to those observed (Figure 3.1a), especially considering both Cdc42V12 and Rac1V12 can produce these phenotypes.

The various morphologies of these cells were quantified using the following four categories, (i) Rac phenotype, (ii) spiky Rac phenotype, which are similar to Rac phenotype with large spread cells, but having filopodia or microspikes around the edge instead of ruffles, (iii) cells with processes equal to 1 cell diameter and (iv) cells with processes greater than one cell diameter (Figure 3.2).

Morphologies of cells expressing GFP alone were similar to non-transfected cells, cultured in 10% serum; they had very few peripheral structures, lamellae or processes, although most did produce some small filopodia.

The proportion of cells expressing Rac1V12 adopted the characteristic full Rac phenotype (Figure 3.1a), was 7% (Figure 3.2a), whilst cells expressing GFP or Rac1N17 did not produce any of this phenotype. Rac1N17 expressing cells instead formed a variety of phenotypes, such as the formation of filopodia and processes, but in conditions of 10% serum, showed no significant morphological changes from the GFP control in the categories counted. Although some cells expressing Rac1V12 also formed morphologies of the other categories, these were not significantly different from the GFP control values.

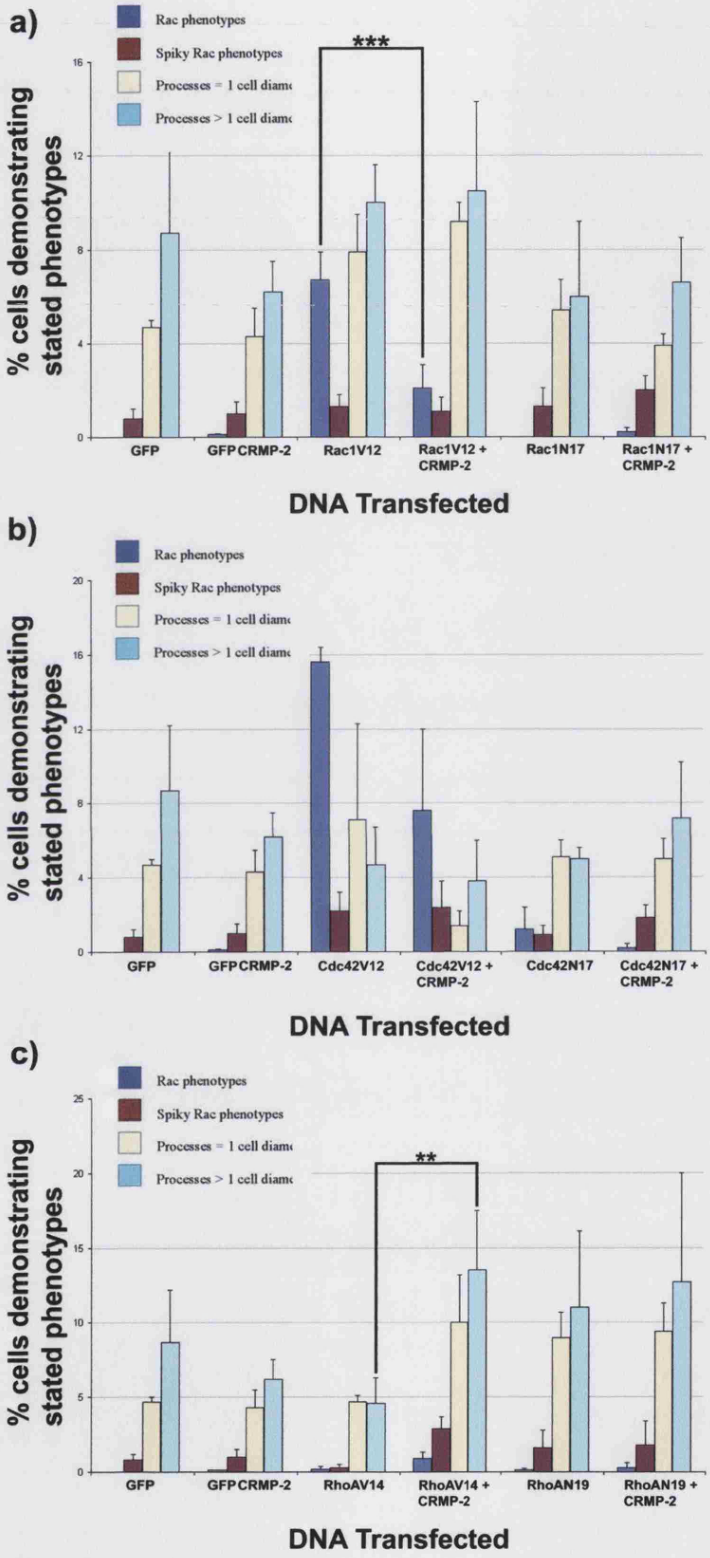

Figure 3.2. Graphical representation of morphologies observed in N1E-115 cultured in 10% serum.

Cells were plated on Poly-L-lysine and transfected with GFP Rac1 constructs (a), GFP Cdc42 constructs (b) and GFP RhoA constructs (c), with HA CRMP-2. Data taken from single experiment performed in triplicate. GFP and GFP CRMP-2 data shown in each graph for comparison. Error bars indicate SEM.

In the N1E-115 cells plated on poly-L-lysine, Cdc42V12 produced a larger number of round Rac phenotypes (16%), than Rac1V12 (Figure 3.2a). This could be due to the hierarchal relationship of the Rho family GTPases, with Cdc42 rapidly signalling to Rac1 (Kozma et al, 1995). It is possible that activation of endogenous Rac1 under these conditions is more effective in the production of the round Rac phenotypes than the constitutively active Rac1 mutant. This may be due to the time of expression. Cdc42V12 may induce up regulation of Rac1GTP after 16 hours. Rac1V12 may generate a larger number of these phenotypes at an earlier time point. This may also be due to the ability of wild type Rac1 to cycle between GTP and GDP binding, which may be important in the signalling from the GTPases. Cdc42 is usually associated with the production of filopodia, and sensory structures, however this was not observed after 16 hours in N1E-115 cells plated on poly-L-lysine in 10% serum, possibly because of the signalling to Rac1. Although expression of Cdc42V12 also produced cells with filopodia and short processes, the counts for these categories proved to be variable. Cdc42N17 produced a few Rac phenotypes but which was less than Cdc42V12, (only 1%), although the presence of these Rac phenotypes suggests that Rac1 can be activated independently of Cdc42.

Finally, quantification of these peripheral structures in RhoAV14 transfected cells, showed RhoAV14 generated round cells with very little peripheral structures and values were low for all categories counted (Figure 3.2c). RhoAN19, however, elicated more processes equal to, (9%), and longer than, (12%), 1 cell diameter in length, although results showed variability. However there was a significant increase ($P < 0.03$), in processes equal to 1 cell diameter, when compared to the GFP control.

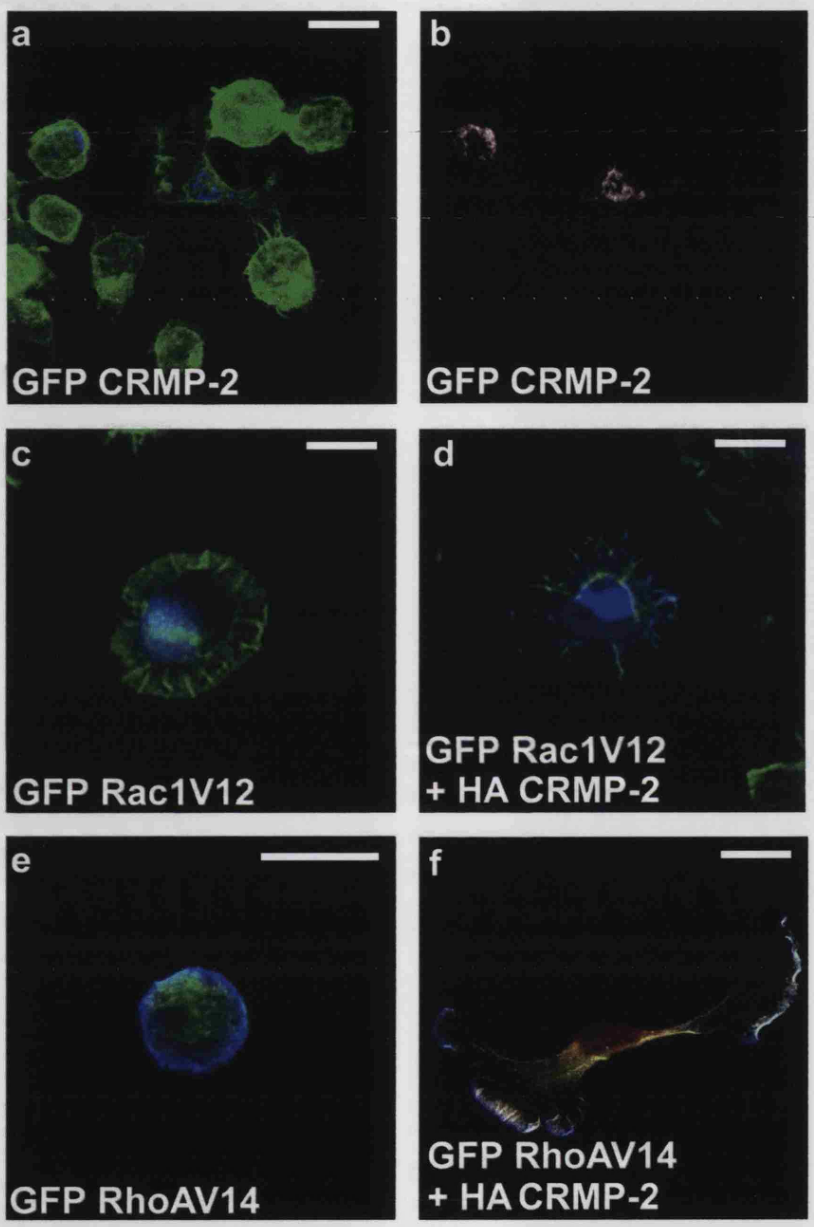

Figure 3.3. Representative morphologies of N1E-115 co-expressing HA CRMP-2 with either Rac1V12 or RhoAV14.

HA CRMP-2 was co-expressed with dominant positive mutants, GFP Rac1V12 and GFP RhoAV14 in N1E-115. These mutants, are constuituvely active, and so result in strong signalling from the relavent GTPase. TRITC labelled phalloidin is shown (green), along with GFP expression (blue). HA-staining confirmed expression of CRMP-2 (not shown in Fig.3.3d). Scale bar equals 25μm.

3.1.2 The effect of CRMP-2 on GTPase function

CRMP-2 has been implicated in axon elongation (Inagaki et al, 2002) and its effects on neurite outgrowth and associated Rho GTPase morphology were therefore investigated. CRMP-2 was expressed alone, and in combination with the dominant positive and dominant negative GTPases, to assess whether it exerted any effect on cell morphology and GTPase function. When expressed alone in N1E-115 cells, in 10% serum, GFP CRMP-2 had very little affect on morphology, and all morphology categories were very similar to the GFP control (Figure 3.2,a,b,c). GFP CRMP-2 had a punctate localisation (Figure 3.3a,b) suggesting that CRMP-2 may localise to vesicles or internal membranes. However, it is also possible that this localisation may not be physiological, and may be an artefact of overexpression. This was investigated further in section 5.6.1.

CRMP-2 had a significant effect when co-expressed with the dominant positive mutants, Rac1V12 and RhoAV14. When co-expressed with Rac1V12, CRMP-2 significantly reduced ($P < 0.00026$) the number of round Rac phenotypes from 7% to 2% (Figure 3.2a), although there was no increase in the number of processes produced. Some of the cells co-expressing CRMP-2 with Rac1V12 appear to show a broken outline of the typical Rac phenotype, but instead have filopodia or retraction fibres (Figure 3.3d). It appeared that the Rac phenotypes might have been formed, but subsequently collapsed, and this was further investigated using time-lapse analysis in section 3.5. Not every cell demonstrated this phenotype, and this could well depend on the relative expression levels or some cell variability on the time scale at which the two constructs are expressed.

When co-expressed with RhoAV14, CRMP-2 resulted in a significant increase ($P < 0.001$) in the number of cells with processes > 1 cell diameter from 5% to 13% (Figure 3.2c). Typical phenotypes formed from co-expression of CRMP-2 with dominant positive RhoA are shown (Figure 3.3). Cells expressing both RhoAV14 and CRMP-2 demonstrated more processes and more lamellipodia (Figure 3.3f), both of which are not usually associated with RhoA activation.

CRMP-2 did not significantly affect the percentage of Rac phenotypes generated by Cdc42V12, although there was a trend towards its reduction (Figure 3.2b). Unlike co-expression with Rac1V12, CRMP-2 did not significantly alter the number of cells exhibiting the Rac phenotype. This could be because CRMP-2 inhibits the response to endogenous Rac1, but does not affect Cdc42V12, which could continue to signal through to Rac1. However, overexpressed CRMP-2 may be expected to inhibit signalling through to endogenous Rac1 eventually. CRMP-2 also had little effect when co-expressed with any of the three dominant negative RhoGTPases, (Figure 3.2,a,b,c), resulting in no significant differences in morphologies, when compared with expression of the dominant negative constructs alone.

3.1.3 Laminin enhances Rac1 morphology

To investigate whether the substrate affected the morphologies produced, transfections were repeated with cells plated on laminin. The preceding experiments were carried out on poly-L-lysine, which provides little substrate signalling. Therefore, in order to investigate whether the substrate exerts any effect on the morphology, the experiment was repeated using mouse laminin, which activates αβ integrins and enhances adhesion (Buck and Horwitz, 1987).

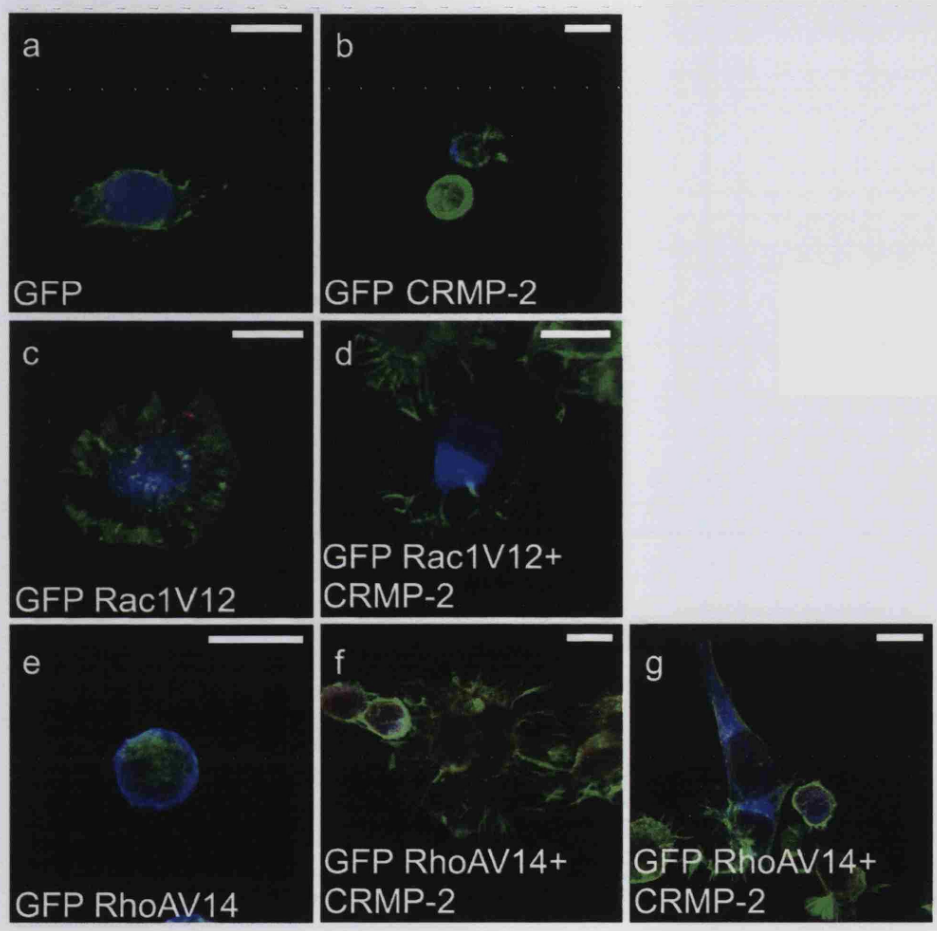

Figure 3.4. Examples of morphologies observed in N1E-115, expressing dominant positive RhoA or Rac1, with and without CRMP-2, plated on laminin.

HA CRMP-2 was co-expressed with GFP RhoAV14 or GFP Rac1V12 in N1E-115 plated on laminin, and cultured in 10% serum. Cells were stained for actin using TRITC labelled phalliodin (green), anti HA (red), while GFP expression (blue) acted as a marker of GTPases expression. HA stain was used to confirm CRMP-2 expression (not shown in Fig3.4d). Scale bar equals 25μm.

Morphologies of N1E-115 cells cultured on laminin were similar to those on poly-L-lysine (Figure 3.4). Cells expressing GFP CRMP-2 were very similar in appearance to those expressing GFP alone (Figure 3.4a,b). On laminin, GFP and GFP CRMP-2 produced 1-2% cells with processes longer than 1 cell diameter. GFP CRMP-2 produced a small but significant increase ($P < 0.02$) in the number of cells with processes equal to 1 cell diameter, 5% for GFP and 8% for GFP CRMP-2 (Figure 3.5, c). There were fewer cells with processes longer than 1 cell diameter when expressing GFP or GFP CRMP-2, and cultured on laminin (Figure 3.5a-d) when compared with those cultured on poly-L-lysine (Figure 3.2).

On laminin, cells expressing GFP Rac1V12 were typically large, flat with lamellipodia (Figure 3.4c), similar to those seen with cells cultured on poly-L-lysine but a higher proportion of these phenotypes were formed (10%). On laminin, Rac1V12 expression also resulted in more round flat Rac phenotypes (10%) than Cdc42V12 expression (5%) unlike results with cells cultured on poly-L-lysine (Figure 3.5a). Thus, the laminin substrate enabled expression of Rac1V12 to produce more cell exhibiting spread phenotypes and lamellipodia. Laminin enhances adhesion to the substrate, and adhesion may be an important component of the Rac phenotype.

Co-expression of HA CRMP-2 with GFP Rac1V12 gave rise to cells that did not form the usual Rac phenotype, but which did form some filopodia and lamellipodia (Figure 3.4d). There was a larger effect of CRMP-2 co-expression with Rac1V12 on N1E-115 cells plated on laminin, compared to poly-L-lysine. Expressed alone, Rac1V12 produced 10% round flat Rac phenotypes (Figure 3.5a). However co-expression with

CRMP-2 resulted in only 2% flat round Rac phenotypes (Figure 3.5a), and this difference was significant ($P < 0.001$).

Although there was a trend towards an increase in spiky Rac phenotypes when CRMP-2 was co-expressed with Rac1V12, this was variable and not significant (Figure 3.5b). There was however, a significant increase ($P < 0.0003$) in the numbers of cells with processes equal to one cell diameter (Figure 3.5c). This increase was not maintained in the processes longer than 1 cell diameter (Figure 3.5d). This may be due to the time scale of the experiment, which was 16 hours. However, these short processes, equal to 1 cell diameter, maybe a result of the collapse of the round flat Rac phenotypes, leaving short retraction fibres.

Cdc42V12 expressing cells cultured on laminin demonstrated a reduction in the number of Rac phenotypes when compared to poly-L-lysine, with 5% as opposed to 10% on poly-L-lysine (Figure 3.5a). Values for the other categories remained similar to the N1E-115 cells cultured in poly-L-lysine. This would suggest that Cdc42V12 is able to active endogenous Rac1 more effectively in cells plated on poly-L-lysine, compared with cells plated on laminin.

Co-expression of CRMP-2 with Cdc42V12 did not produce any large morphological differences, compared with expression of Cdc42V12 alone. There was a small but significant decrease ($P < 0.02$) in the number of flat round Rac phenotypes when Cdc42V12 was co-expressed with CRMP-2 (Figure 3.5a), which had not been observed when cells were cultured on poly-L-lysine. When co-expressed with Cdc42V12, CRMP-2 also produced a significant increase ($P < 0.008$)

Figure 3.5. Quantification of morphologies in N1E-115, plated on laminin and expressing dominant positive Rho GTPases, with or without HA CRMP-2.

HA CRMP-2 alone or co-expressed with either GFP Rac1V12, GFP Cdc42V12 or GFP RhoAV14. Counts for Rac phenotypes (a), spikey Rac phenotypes (b), processes 1 cell diameter in length (c) or processes longer than 1 cell diameter in length (d) were quantified from the same study and plotted on different graphs. Data is from three separate experiments. Error bars represent SEM.

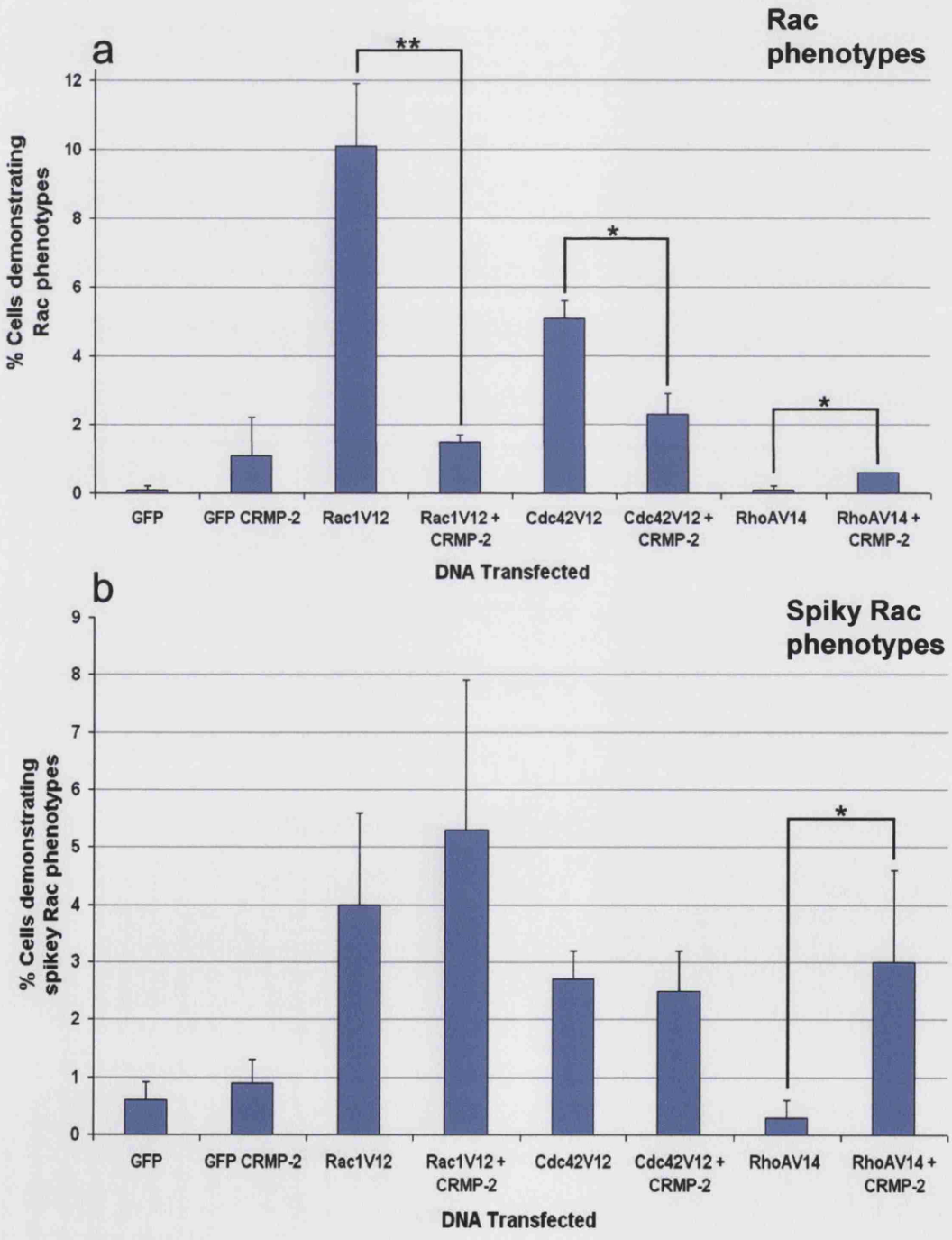

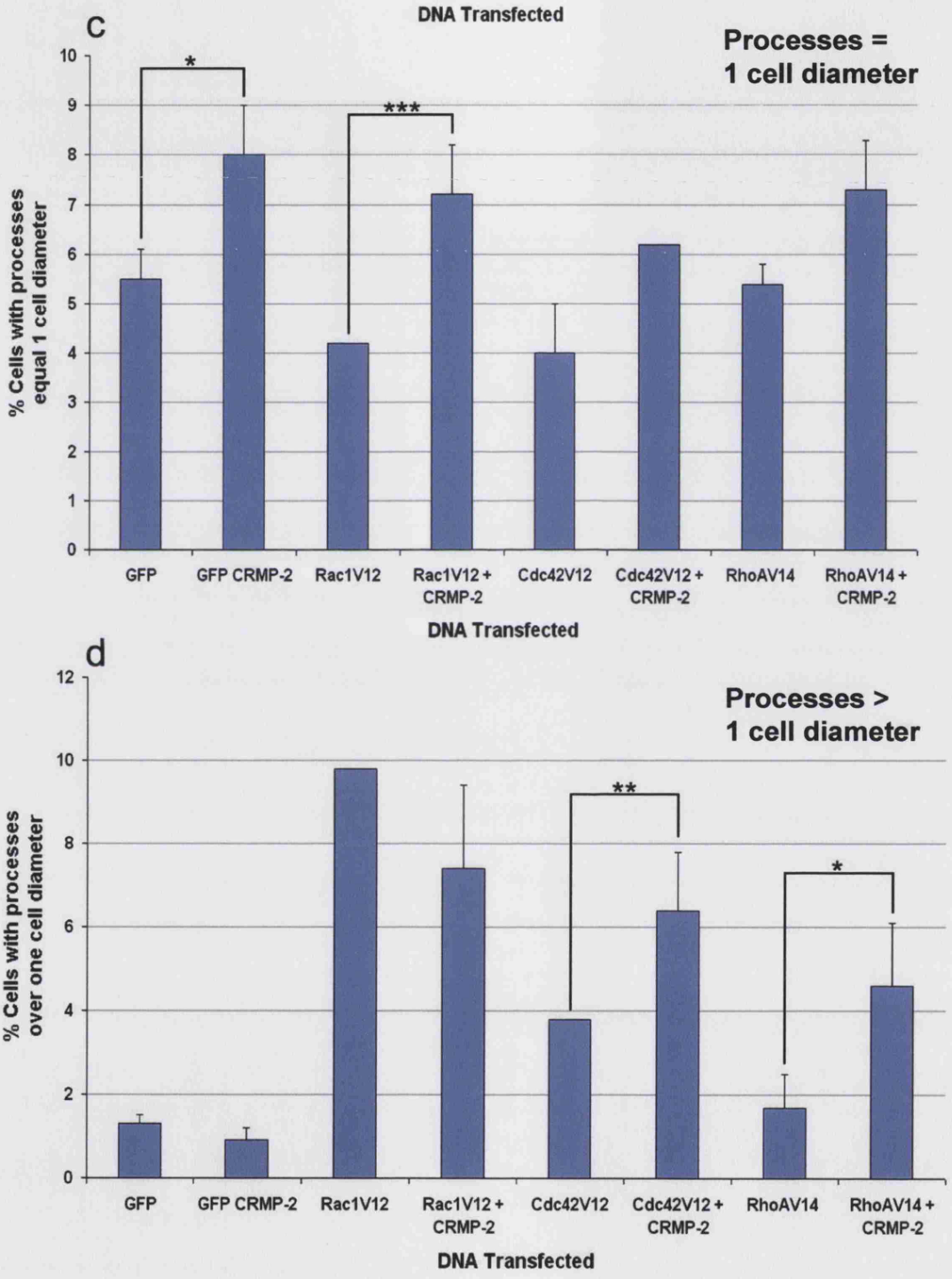
c
DNA Transfected
Processes =
1 cell diameter
% Cells with processes
equal 1 cell diameter
10
9
8
7
6
5
4
3
2
1
0
*
***
GFP
GFP CRMP-2
Rac1V12
Rac1V12 +
CRMP-2
Cdc42V12
Cdc42V12 +
CRMP-2
RhoAV14
RhoAV14 +
CRMP-2
DNA Transfected
d
Processes >
1 cell diameter
% Cells with processes
over one cell diameter
12
10
8
6
4
2
0
**
*
GFP
GFP CRMP-2
Rac1V12
Rac1V12 +
CRMP-2
Cdc42V12
Cdc42V12 +
CRMP-2
RhoAV14
RhoAV14 +
CRMP-2
DNA Transfected

in the percentage of cells bearing processes longer than 1 cell diameter, when compared with Cdc42V12 alone. These results are similar to those observed with Rac1V12 and CRMP-2, although there was an increase in cells bearing processes equal to 1 cell diameter with Rac1V12 and CRMP-2, and an increase in cells bearing processes longer than 1 cell diameter with Cdc42V12 and CRMP-2, suggesting some involvement of Cdc42 in neurite elongation.

Cells expressing GFP RhoAV14 were small and round with no peripheral structures (Figure 3.4e), on laminin as well as on poly-L-lysine. Counts were very similar to the GFP control in cells in 10% serum (Figure 3.5a-d).

Co-expression of HA CRMP-2 with GFP RhoAV14 produced different phenotypes. Some cells produced filopodia and lamellae, and some cells exhibited elongated cell bodies (Figure 3.4f,g). There was a small but significant increase ($P < 0.02$) in the number of round Rac phenotypes when CRMP-2 was co-expressed with RhoAV14, compared with expression of RhoAV14 alone (Figure 3.5a). In addition to this increase, there was an increase ($P < 0.01$) in the number of spiky Rac phenotypes when CRMP-2 was co-expressed with RhoAV14 (Figure 3.5b). There was a small but significant increase ($P < 0.01$) in the number of cell processes longer than 1 cell diameter (Figure 3.5c) but this difference was not as great as the effect observed on poly-L-lysine (Figure 3.2c). The number of cells with shorter processes remained the same (Figure 3.5c).

The substrate on which N1E-115 cells were cultured was an important factor in determining cell morphologies, with laminin and poly-L-lysine having different

Figure 3.6. Comparason of Rac morphologies observed in N1E-115 on different laminin sources.

Cells were plated on laminin from ICN or Gibco-Invitrogen, and the number of Rac morphologies observed was quantified. Error bars represent SEM.

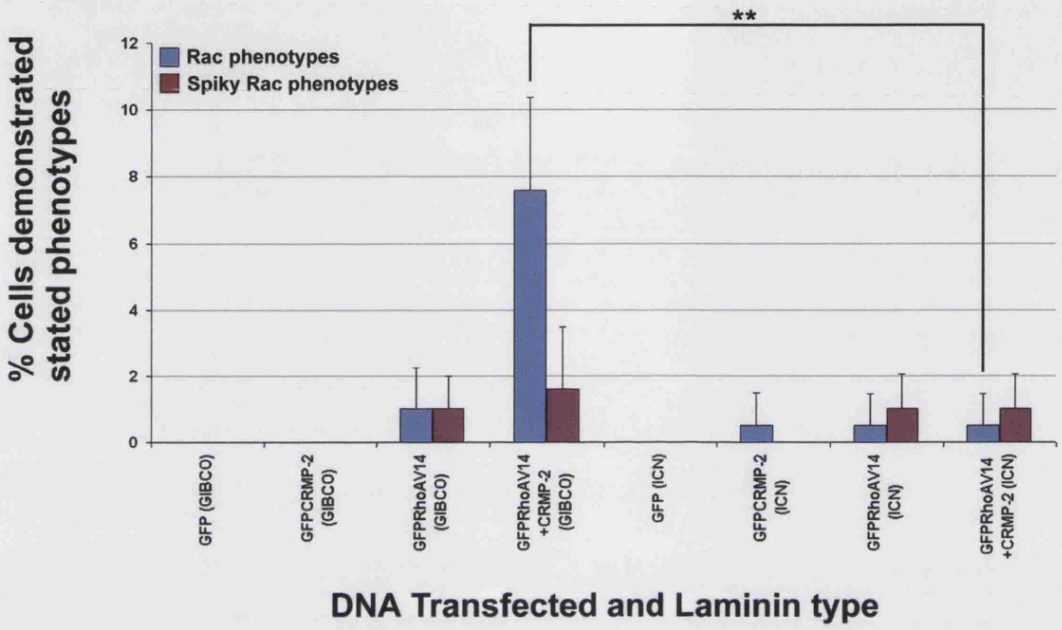

effects on the morphologies produced with the Rho GTPases and CRMP-2. It was also found that laminin from different sources showed quantitatively different effects when CRMP-2 was co-expressed with RhoAV14. On previous experiments, laminin was obtained from ICN, and an alternative laminin source was obtained from Gibco-Invitrogen. N1E-115 cells were transfected with RhoAV14 alone, or co-expressed with CRMP-2, and generated significantly more Rac phenotypes when plated on laminin from Gibco-Invitrogen ($P < 0.006$) (Figure 3.6). RhoAV14 and CRMP-2 co-expression produced approximately 1% Rac phenotypes on ICN laminin, and 8% Rac phenotypes on Gibco-Invitrogen laminin. Subsequent experiments were performed using laminin from Gibco-Invitrogen.

3.1.4 CRMP-2 alters Rac1 and RhoA morphologies

On Gibco-Invitrogen laminin substrate, Rac1V12 alone had a greater effect on N1E-115 cell morphology. The number of Rac phenotypes was > 20% of cells expressing Rac1V12 (Figure 3.7a), compared with 6% on poly-L-lysine (Figure 3.2a), and 10% on ICN laminin (Figure 3.5A). When CRMP-2 was co-expressed with Rac1V12 in cells on Gibco-invitrogen laminin, there was a highly significant decrease ($P < 3.6 \times 10^{-6}$) in the number of round Rac phenotypes, from > 20% to around 3% (Figure 3.7a). In these experiments, cells bearing processes equal to, and longer than 1 cell diameter, were quantified. The number of cells with processes remained the same for both cells expressing Rac1V12, and those co-expressing Rac1V12 and CRMP-2, suggesting that the decrease in round Rac phenotypes was not a consequence of the production of processes (Figure 3.7a).

The effects of RhoAV14 and CRMP-2 co-expression in the generation of Rac phenotypes were enhanced on Gibo-invitrogen laminin, (Figure 3.7b). Alone, RhoAV14 had very little effect on the morphology of cells in 10% serum, when compared with the GFP control. There were no Rac phenotypes and very few cells with processes (Figure 3.7b). However, when CRMP-2 was co-expressed with RhoAV14, there was a highly significant increase ($P < 3.9 \times 10^{-5}$) in the number of Rac phenotypes from 0% with RhoAV14 alone to 8% when RhoAV14 was co-expressed with CRMP-2. The number of Rac phenotypes in cells co-expressing CRMP-2 and RhoAV14 was 8%, although this represents a major effect since dominant positive RhoA would normally be expected to have an opposite effect on outgrowth.

Figure 3.7a.

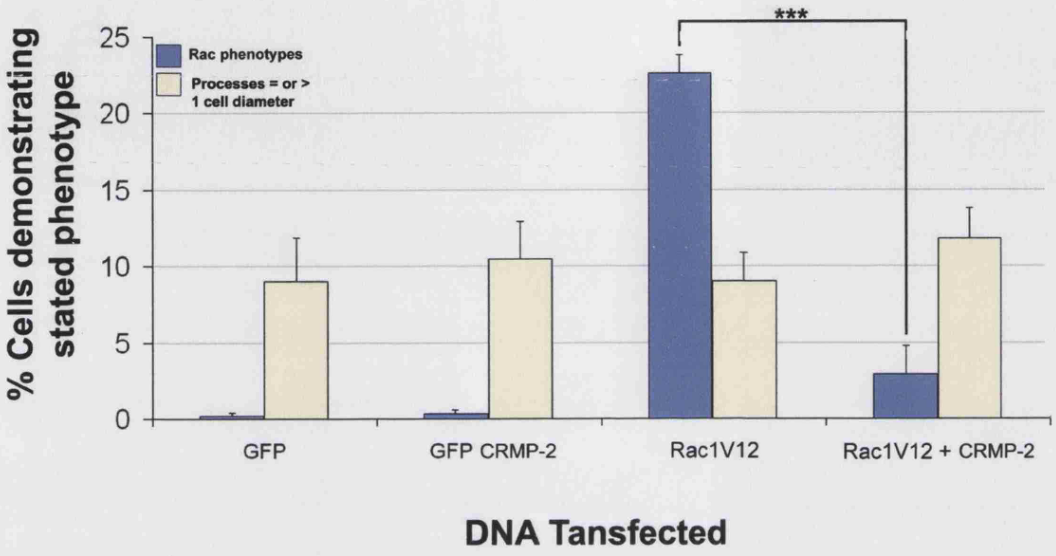

Figure 3.7b.

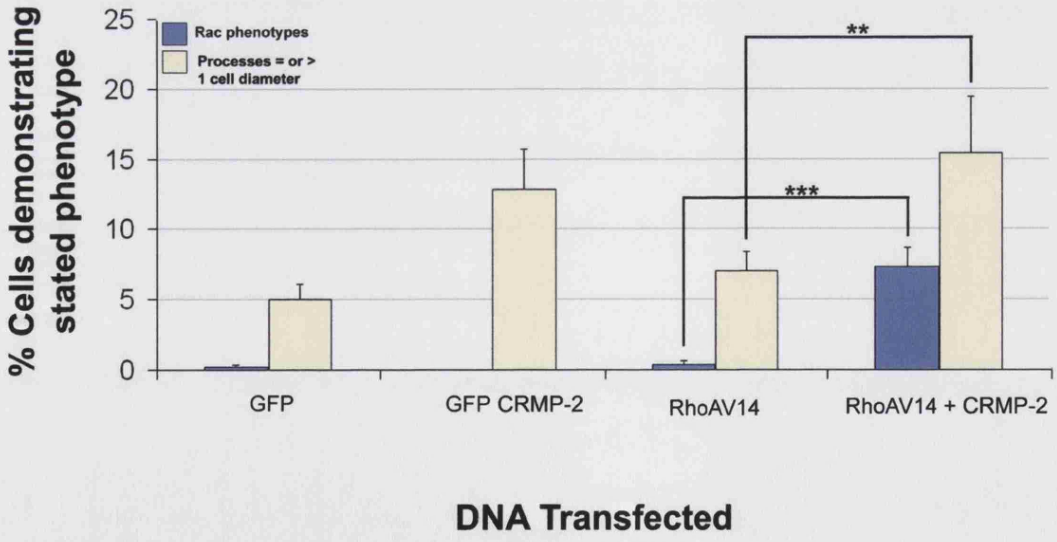

Figure 3.7. Graphical representation of the effect of HA CRMP-2 on morphologies observed with GFP Rac1V12 (a) or GFP RhoAV14 (b).

N1E-115 were transfected with dominant positive Rac1 or RhoA alone, or with HA CRMP-2. Cells were plated on Gibco-Invitrogen laminin, and cultured in 10% serum. Counts were obtained from three separate experiments, and error bars represent SEM.

Coupled to this increase in the number of Rac phenotypes, was a significant increase ($P < 0.001$) in the number of cells bearing processes, from 6% in cells expressing RhoAV14 alone, to 15% with cells expressing RhoAV14 and CRMP-2. This effect is unusual as RhoA is usually associated with contraction and the inhibition of outgrowth, and dominant active RhoA is a strong inhibitor of outgrowth (Kozma et al 1997).

These results further suggested that the expression of CRMP-2 alone could increase the number of process bearing cells. When CRMP-2 alone was expressed in cells in 10% serum, there was a significant increase ($P < 0.03$) in the number of cells with processes (Figure 3.7b), although this increase has not been consistent, and suggests that under certain conditions, CRMP-2 alone can induce the formation of processes. CRMP-2 has been shown to play a role in axonal development of cultured hippocampal neurones (Inagaki et al, 2001), and in other studies has been shown to induce neurite outgrowth in N1E-115 cells (Fukata et al, 2002). In this study all experiments were performed in 10% serum-containing media. However, Fukata et al, (2002) expressed CRMP-2 in cells cultured in 5% serum-containing media. N1E-115 cells undergo differentiation when deprived of serum (Reagan et al, 1990) and so the serum content of the media could have a large effect on the morphologies of these cells expressing Rho GTPases and CRMP-2, as well as the substrate. It is also possible in these experiments there was some variability in the serum, with some serum batches activating RhoA more strongly, and so result in some variability in cell morphologies, especially in the absence of a strong signalling pathway, such as the expression of dominant positive GTPases.

3.2 Time-lapse analysis of CRMP-2 and the Rho GTPases in N1E-115 cells

The transfection experiments, analysed at a fixed time point, demonstrated that expression of CRMP-2 with RhoAV14 and Rac1V12 could affect cell morphology after 16 hours. However these experiments do not provide an indication of how these changes occur over time. This was investigated using time-lapse microscopy to observe N1E-115 cells on laminin, and either transfected or microinjected with GTPase cDNA and CRMP-2 cDNA mammalian expression vectors.

3.2.1 Time-lapse analysis of CRMP-2 and Rac1V12 co-injection in N1E-115 neuroblastomas.

Cells plated on laminin-coated coverslips were injected with both GFP Rac1V12 DNA and GFP CRMP-2 DNA. The cells were monitored from the time of injection, and images were taken at set time points in order to observe any changes over time (Figure 3.8a,b). When injected alone, GFP Rac1V12 caused the cells to flatten and spread after 1 hour, and then induced the formation of lamellipodia and membrane ruffles (Figure 3.8a). However, injection of GFP CRMP-2 had no effect on cell morphology (Figure 3.8a). Following co-injection of GFP CRMP-2 and GFP Rac1V12, only minimal morphological changes occurred during the 6 ½ hour time period investigated. The initial round cell, with no peripheral structures, became slightly flattened with few filopodia at points around the edge, approximately 4 hours post-injection. Despite the filopodia becoming more pronounced after the 6 ½ hour period, the cell did not resemble the flat round Rac phenotype shown in earlier experiments (See Figure 3.1), in response to Rac1V12.

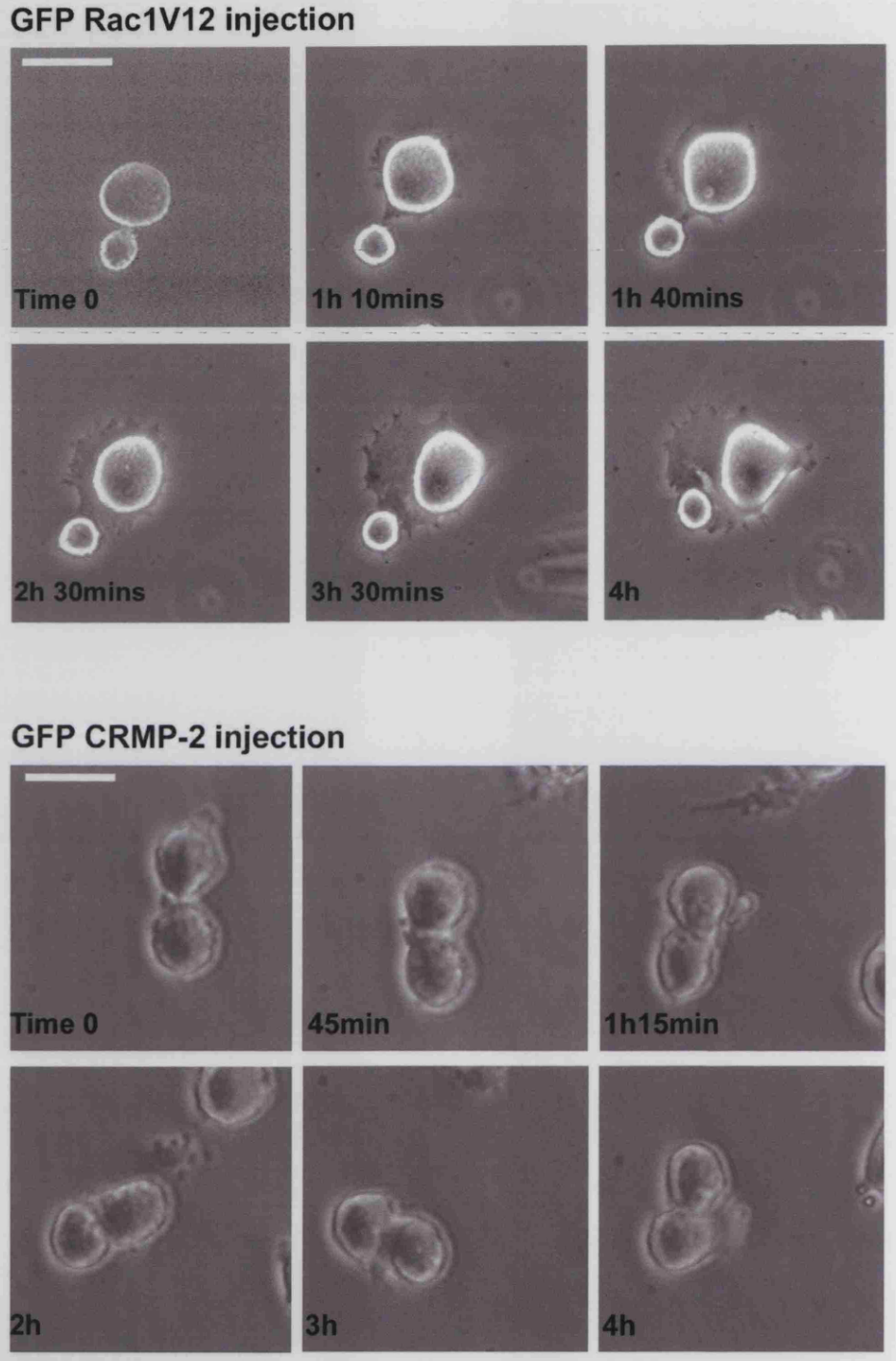

Figure 3.8a. Phase contrast time-lapse analysis of N1E-115 injected with GFP CRMP-2 or GFP Rac1V12.

Cells were plated on laminin over night. DNA was injected at 1μg/ml at time point 0. Cells were analysed over the time points indicated. Scale bar equals 25μm.

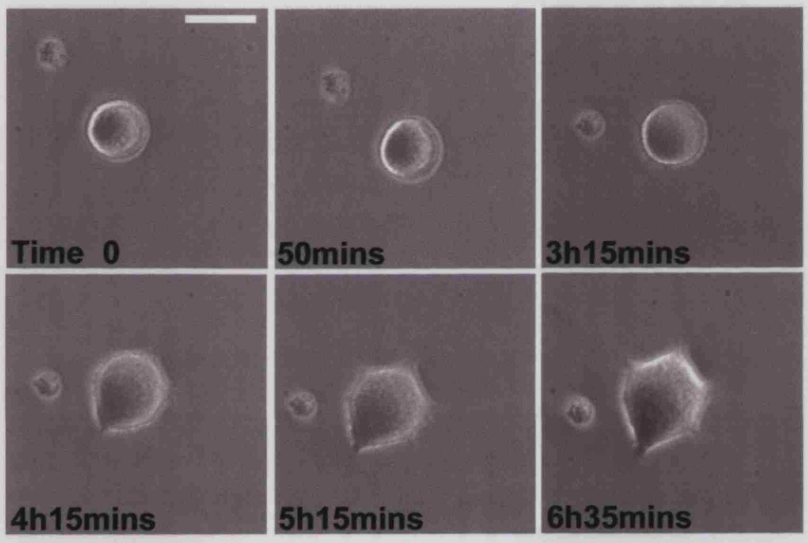

Figure 3.8b. Phase contrast time-lapse analysis of N1E-115 injected with GFP CRMP-2 and GFP Rac1V12.

Cells were plated on laminin over night. DNA was injected at 1μg/ml at time point 0. Cells were analysed over the time points indicated. Scale bar equals 25μm.

3.2.2 Time-lapse analysis of Rac1V12 DNA injection, followed by CRMP-2 DNA injection.

When GFP Rac1V12 cDNA was injected alone, cells spread extensively and produced lamellipodia and a recognisable Rac phenotype (Figure 3.9). GFP CRMP-2 cDNA was subsequently injected into the same cell, at time point 2hours 40mins. Over the following 4 hours, a dramatic change in morphology was observed (Figure 3.9). Within 35 minutes the cell began to collapse around the edge and the main cell body became thin and retracted back, leaving thin processes. Over the next 3 hours the cell periphery became thinner, and retracted back into the cell. By the final time point, 6 hours 40 minutes, the cell had changed considerably.

These time-lapse studies suggest that CRMP-2 is able to inhibit Rac1 signalling when both cDNA's are injected into cells together. Furthermore, if CRMP-2 cDNA is injected following Rac1 activation and stabilisation of a Rac morphology, it is able to cause cell collapse reversing the effects of Rac1. It is unclear how CRMP-2 was preventing the formation of Rac phenotypes, although this effect could be due to direct inhibition of Rac1, activation of RhoA or some other mechanism.

3.2.3 Time-lapse analysis of the role of RhoA and Cdc42 in CRMP-2-induced collapse of Rac morphologies in Rac1V12 expressing N1E-115.

To investigate the mechanism involved, and whether other members of the Rho family of GTPases participated in generating the morphological response to CRMP-2 and Rac1V12, dominant negative GTPases were used to determine whether they

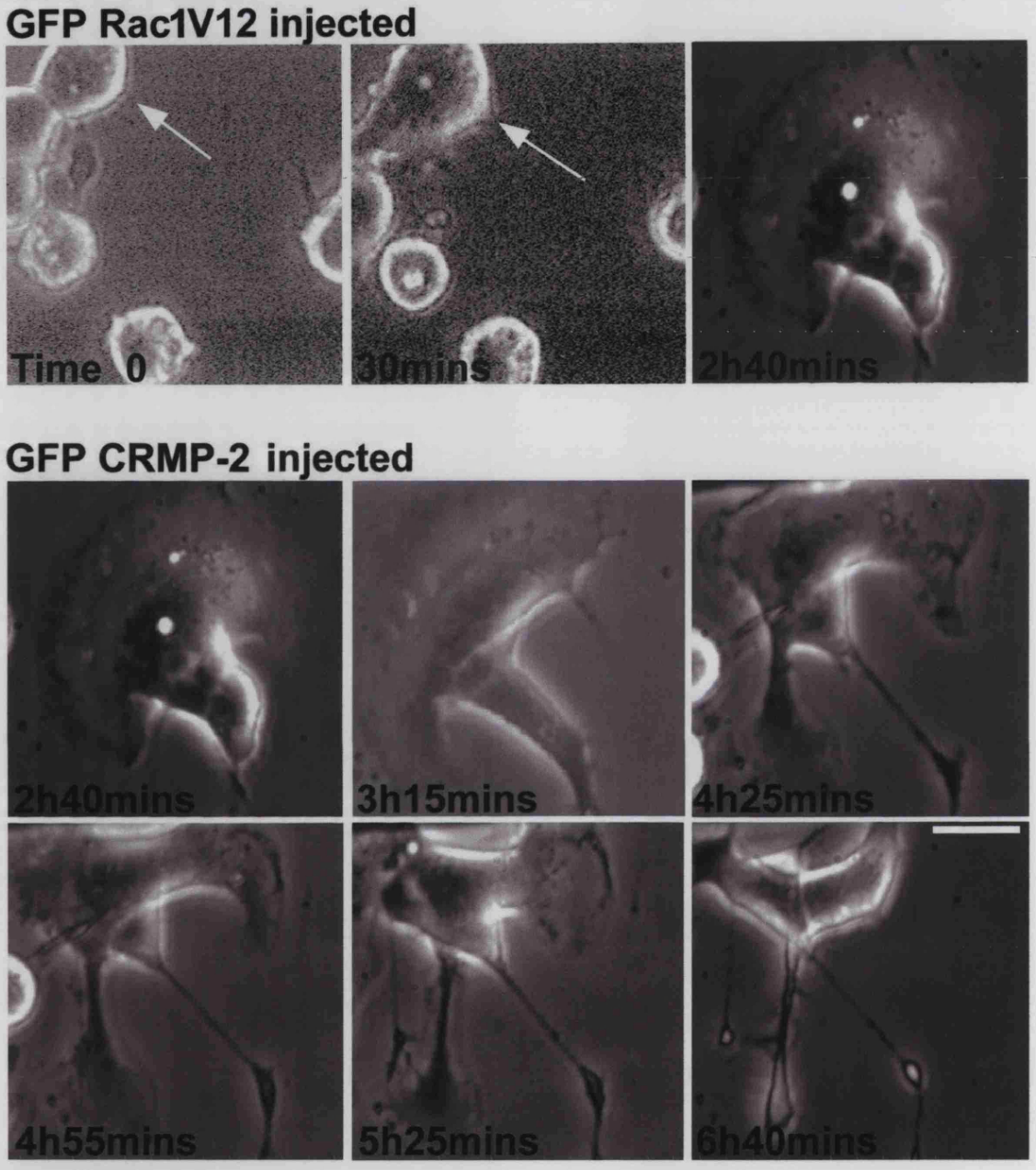

Figure 3.9. Phase contrast time-lapse analysis of N1E-115 injected with GFP Rac1V12, and subsequently injected with GFP CRMP-2.

Cells were plated over night on laminin, and injected with GFP Rac1V12 DNA at 1μg/ml. After 2h 40mins, GFP CRMP-2 DNA was injected into the same cell at 1μg/ml. A typical cell is shown, and recorded at the time points indicated. Scale bar equals 25μm.

blocked the response. Cells were first transfected with Rac1V12 and allowed to form the Rac phenotype over night. The following day, cells exhibiting Rac phenotypes were injected with either CRMP-2 cDNA alone or CRMP-2 cDNA in combination with dominant negative GTPases cDNA (Figure 3.10). Each injection was repeated three times, and a typical result of each injection is shown (Figure 3.10).

The injection with CRMP-2 alone in a Rac1V12 expressing cell, (Figure 3.10a) resulted a very similar effect as with previous microinjection experiments (see Figure 3.9), with cell periphery collapsing. The collapse was not complete however, with some retraction fibres remaining at the original cell edge, and perhaps even extending further (Figure 3.10a, see arrow). This collapse occurred over a much shorter time course than the previous time-lapse at 2 ½ hours, possibly because the cells had been expressing Rac1V12 overnight, expressing higher levels of Rac1V12, and so exhibited stronger Rac1 signalling, and had formed a full Rac phenotype initially.

In order to determine whether the collapse involved activation of RhoA signalling, dominant negative RhoAN19 was used to block RhoA signalling. Rac1V12 expressing cells, with established Rac phenotype, were co-injected with RhoAN19 with CRMP-2 cDNAs (Figure 3.10b). In this case there was no elaborate collapse of the periphery, however the lamellipodia around the edge did collapse slightly and appeared to form dense retraction fibres. The cells were monitored for over 4 hours, but the phenotype formed by 3 hours appeared to be stable (Figure 3.10b).

When CRMP-2 cDNA was injected into Rac1V12 expressing cells, some areas of the periphery did not collapse, but appeared to form filopodia (Figure 3.10a), structures

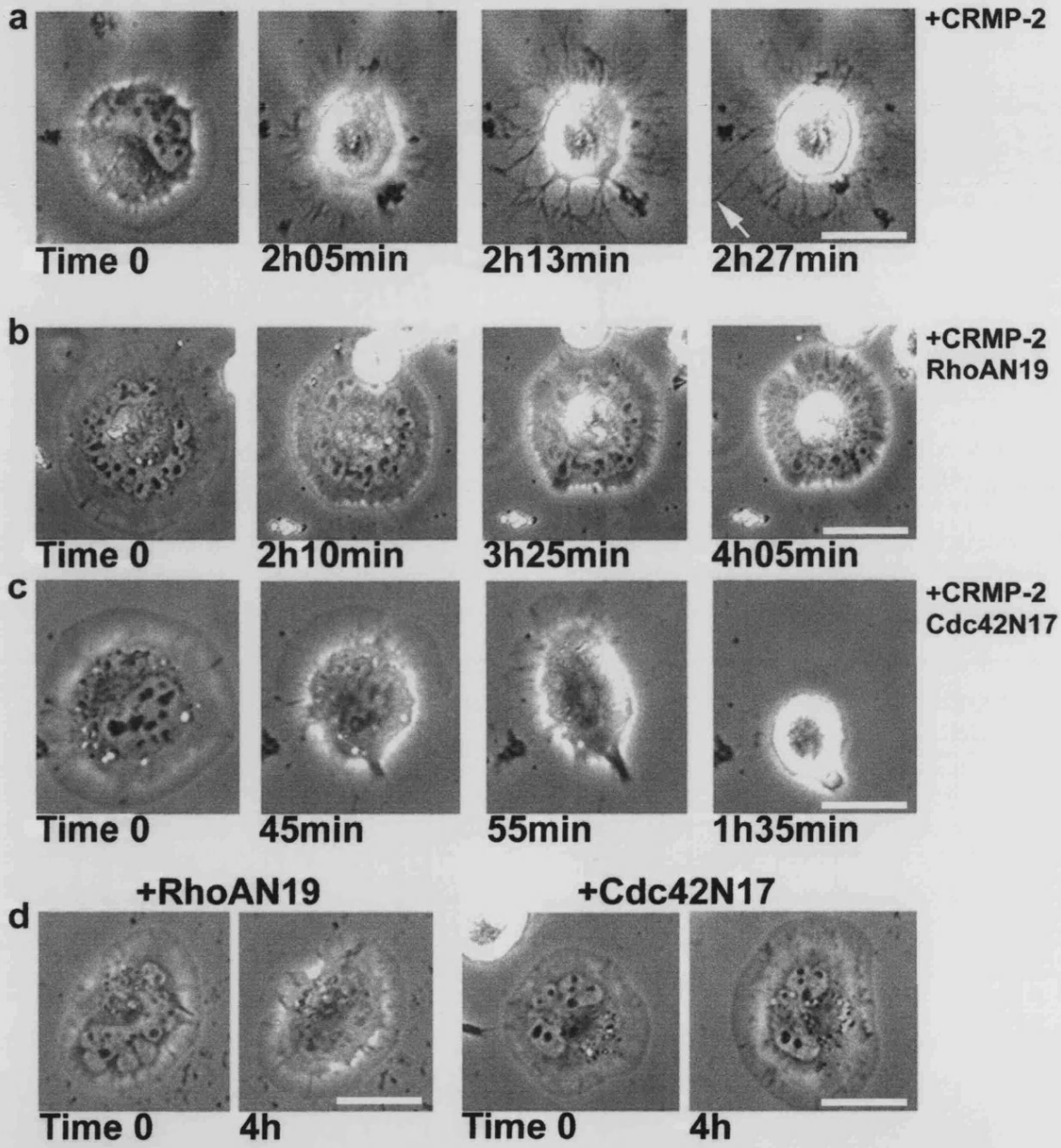

Figure 3.10. Phase contrast analysis of N1E-115 expressing GFP Rac1V12, injected with GFP CRMP-2, alone or with dominant negative RhoA or Cdc42.
Cells plated on laminin and cultured in 10% serum, were transfected with GFP Rac1V12, and left overnight to express. Following morning, CRMP-2 was injected alone (a), with GFP RhoAN19 (b) or with Cdc42N17 (c), at time point 0. Injection of GFP RhoAN19 or GFP Cdc42N17 alone is shown (d). All DNA's were injected at 1μg/ml. Scale bar equals 25μm.

usually associated with Cdc42. Therefore, in order to test for any Cdc42 involvement in the maintenance of the filopodia, CRMP-2 and Cdc42N17 cDNA's were co-injected into a Rac1V12 expressing cell. This resulted in a very different morphology, with cells collapsing completely, typically within 2 hours (Figure 3.10c). There were no filopodia remaining, and by the end, there were no peripheral structures visible. Control Rac1V12 cells injected with either Cdc42N17 or RhoAN19 cDNAs in the absence of CRMP-2 showed that these constructs alone had no effect on pre-established Rac morphology (Figure 3.10d).

These time-lapse studies indicate that both Cdc42 and RhoA are both involved in the cellular collapse response to CRMP-2 with active Rac. A single experiment is shown for each condition. The experiment was performed on three separate occasions, producing the same response.

3.2.4 CRMP-2 and RhoAV14 in time-lapse

In order to observe the changes occurring when CRMP-2 and RhoAV14 are co-expressed, GFP CRMP-2 and GFP RhoAV14 cDNA's were co-injected into N1E-115 neuroblastomas cells. The cells started round, with no peripheral structures, typical of the N1E-115 cell line cultured in 10% serum, (Figure 3.11). However, after 2 hours there were changes in cell morphology. Typically filopodia started to form, and then the cells began to spread. By 5 hours, cells had a very flat, and spread phenotype, with small filopodia around the edge. This morphology appears to be a Rac-like phenotype, although the presence of filopodia would suggest some Cdc42 involvement. This experiment was repeated on three occasions, and a typical response is shown in Figure 3.11.

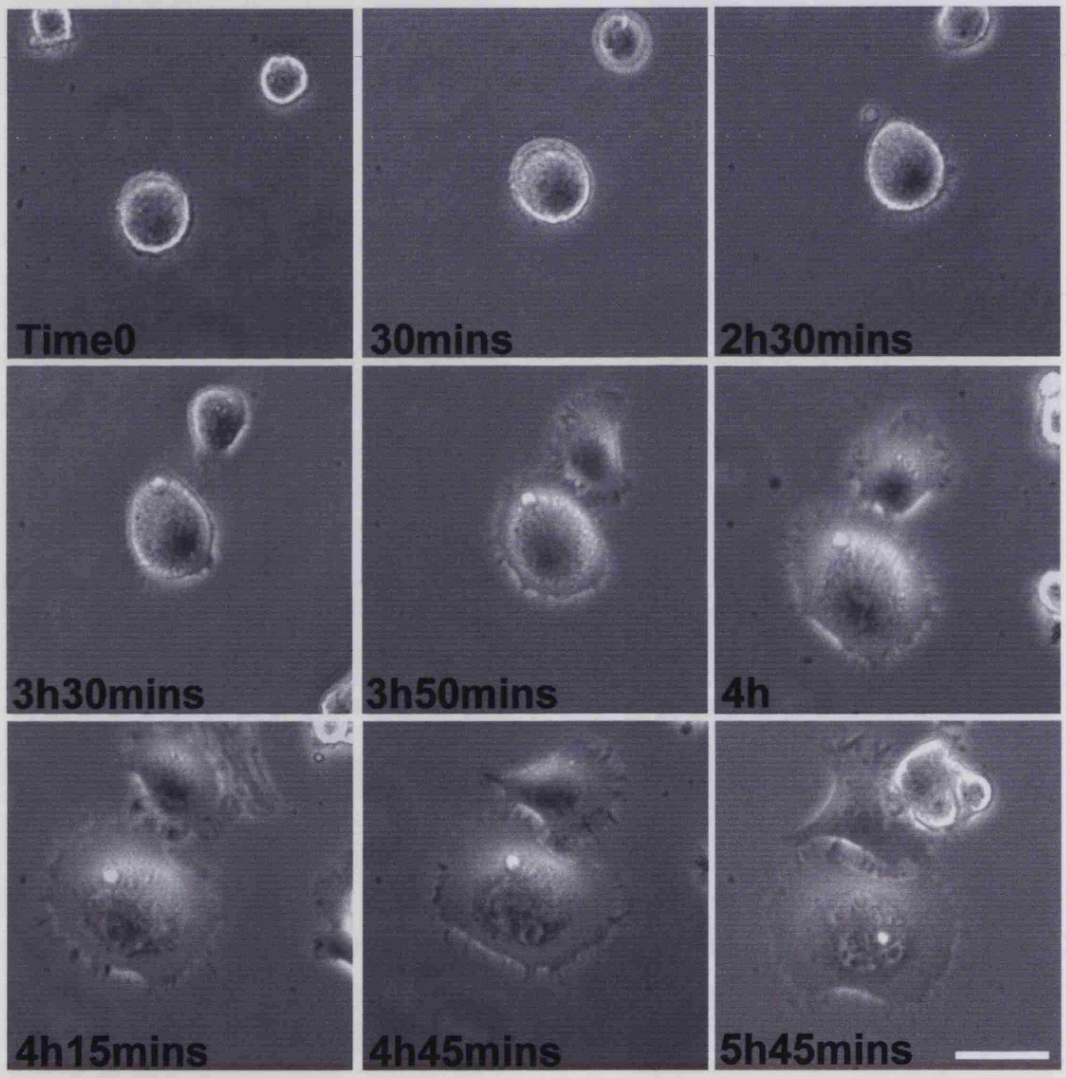

Figure 3.11. Phase contrast time-lapse analysis of N1E-115 co-injected with GFP RhoAV14 and GFP CRMP-2.

Cells were plated overnight on laminin, in 10%serum. GFP RhoAN19 and GFP CRMP-2 were co-injected at time point 0. DNA's were injected at1μg/ml, and images taken at the time points indicated. Scale bar equals 25μm.

3.2.5 The role of Rac1 and Cdc42 on the effect of CRMP-2 with RhoAV14

The time-lapse study of CRMP-2 and RhoAV14 suggested that both Rac1 and Cdc42 might be involved, since cells produced both filopodia and cell spreading (Figure 3.11), effects associated with Cdc42 and Rac1, respectively. To investigate the role Rac1 and Cdc42 play in the effect of CRMP-2 with RhoAV14, dominant negative GTPases were used. Transfections were carried out with RhoAV14 alone, RhoAV14 co-expressed with CRMP-2, or RhoAV14 and CRMP-2 together with either Rac1N17 or Cdc42N17, to block the effects of Rac1 and Cdc42 respectively.

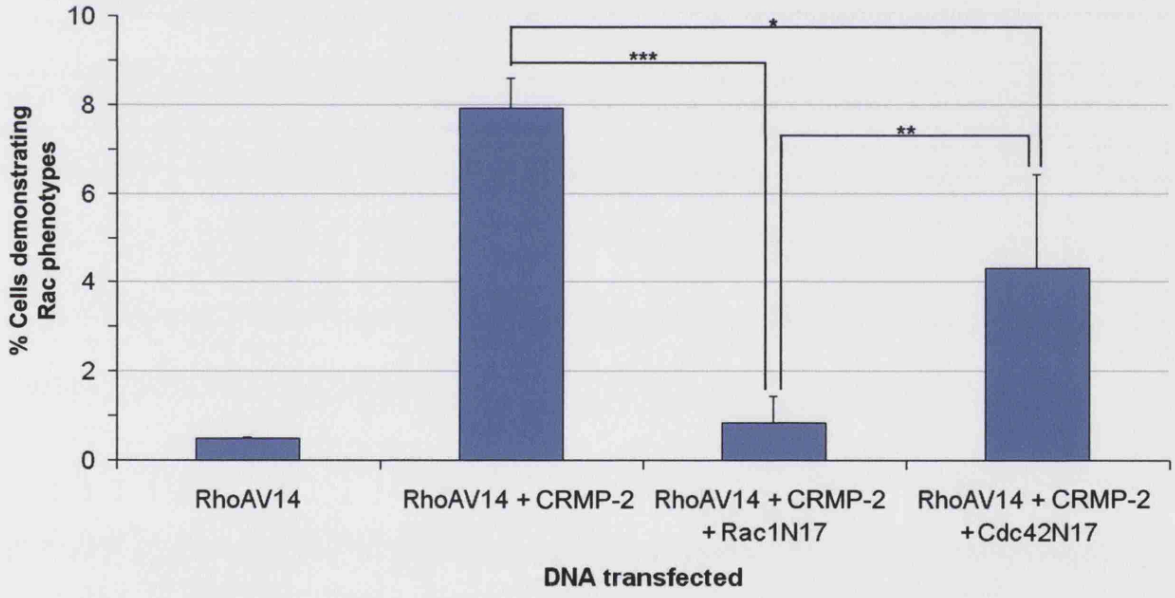

Figure 3.12. CRMP-2 and RhoAV14 induced Rac phenotypes involve both Rac1 and Cdc42.

N1E-115 were transfected with the DNA constructs shown. Three different fields of view, of at least 50 cells, were counted per experiment, over three separate experiments. Error bars represent SEM.

Results showed that Rac1N17 strongly inhibited the effect of CRMP-2 with RhoAV14 (Figure 3.12). The percentage of Rac phenotypes, produced with RhoAV14 and CRMP-2, was reduced from 8% to 1% in the presence of Rac1N17 ($P < 0.0004$). Cdc42N17 exerted a lesser effect, reducing the number of Rac phenotypes from 8% down to 4% ($P < 0.04$). This suggests that, although both Rac1 and Cdc42 are both involved in the phenotype seen with CRMP-2 and RhoAV14, Rac1 is the major contributor to the morphologies counted, and suggests that Rac1 is activated independently of Cdc42. However, Cdc42N17 did reduce the number of cells demonstrating the Rac phenotype, and so is involved. Rac1 may be activated downstream of Cdc42, as well as by a separate, Cdc42-independent mechanism.

3.3 The effect of CRMP-2 phosphorylation on Rho GTPase induced morphologies

CRMP-2 has been shown to be a substrate for the RhoA effector ROK, which phosphorylates CRMP-2 at threonine 555 (Arimura et al, 2000). To examine whether this phosphorylation site contributed to the ability of CRMP-2 to alter Rac1 and RhoA signalling, it was mutated to alanine (See Methods). The effect of this mutant, CRMP-2T555A, was investigated in combination with either Rac1V12 or RhoAV14.

3.3.1 CRMP-2T555A with Rac1V12 and RhoAV14

The T555A mutation completely blocked the ability of CRMP-2 to inhibit the Rac phenotype with Rac1V12 (Figure 3.13a). The number of Rac phenotypes when Rac1V12 was co-expressed with the CRMP-2T555A mutant, was the same as for the Rac1V12 control, with 25% Rac phenotypes. Both were significantly different ($P <$

Figure 3.13a.

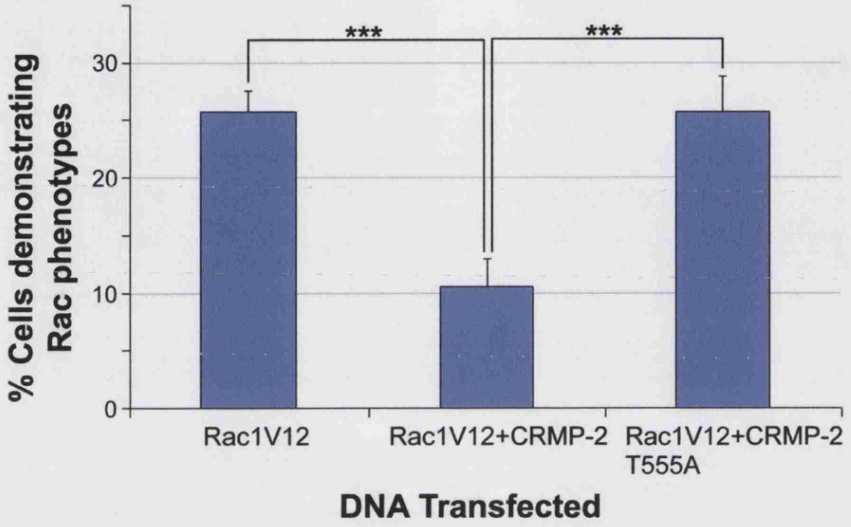

Figure 3.13b.

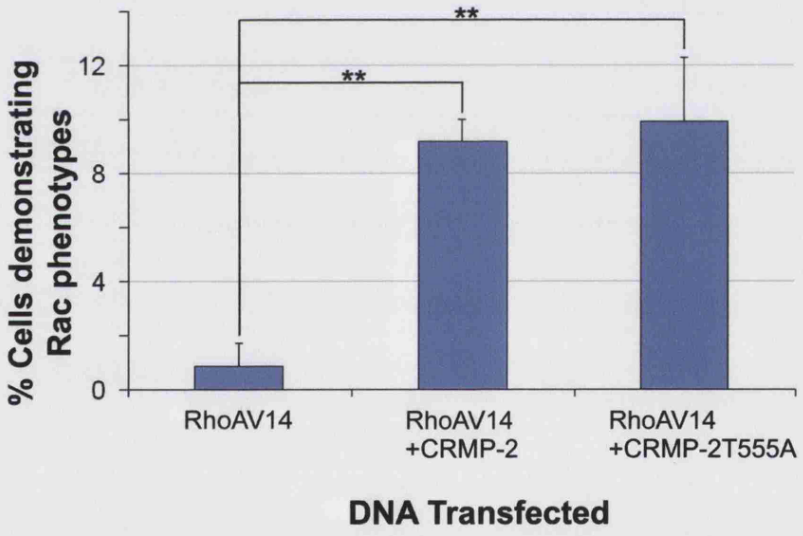

Figure 3.13. The effect of the T555A mutation of CRMP-2 function.

N1E-115 were transfected with GFP Rac1V12 alone, or in combination with FLAG CRMP-2 or FLAG CRMP-2T555A (a). Cells were also transfected with GFP RhoAV14 alone or in combination with FLAG CRMP-2 or FLAG CRMP-2T555A (b). Cells demonstrating Rac phenotypes were counted. Three experiments were performed with three different fields of view counted. Error bars represent SEM.

$P<2.5 \times 10^{-5}$ and $P<0.004$) from the Rac1V12 and CRMP-2 wild type transfection. However elimination of the phosphorylation site had no effect in combination with RhoAV14 (Figure 3.13b). RhoAV14 co-expressed with either CRMP-2T555A or CRMP-2 wild type produced around 9% Rac phenotypes. The difference from the RhoAV14 control was equally significant for both CRMP-2 ($P < 0.002$) and CRMP-2T555A ($P < 0.003$) co-expressed with RhoAV14. This result was unexpected as CRMP-2 is phosphorylated at T555 by ROK, and therefore might have been expected that phosphorylation at this site would have been downstream of RhoAV14 and required for this activity. CRMP-2 has been shown to be phosphorylated at T555 downstream of LPA (Arimura et al, 2001), and so is phosphorylated downstream of RhoA in some pathways. While CRMP-2 may indeed be phosphorylated downstream of RhoAV14 when both are co-expressed in N1E-115 cells, it appears that is not required for the ability of CRMP-2 to activate Rac1 when co-expressed with RhoAV14. However, CRMP-2 is phosphorylated by ROK during the collapse produced by Rac1V12 and CRMP-2. The collapse process does appear to involve RhoA signalling as RhoAN19 blocked CRMP-2-induced collapse of Rac1 phenotypes (Figure 3.10b).

3.3.2 CRMP-2 induced inhibition of Rac1V12 morphologies, involves ROK

To determine whether it was indeed ROK that phosphorylated CRMP-2 at T555 during the collapse of Rac phenotypes, Rac1V12 was co-expressed with CRMP-2, in the presence of either kinase dead ROK, or RhoAN19 (Figure 3.14). In the presence of kinase dead ROK, the effect of CRMP-2 with Rac1V12 was eliminated. Co-expression of Rac1V12 with CRMP-2 significantly reduced the number of round Rac

phenotypes from the Rac1V12 control value ($P < 0.0003$) and from that of Rac1V12/CRMP-2/kinase dead ROK transfection ($P < 9 \times 10^{-5}$). The transfection of Rac1V12/CRMP-2/kinase dead ROK was also significantly different from the Rac1V12/CRMP-2/RhoAN19 ($P < 0.0002$).

RhoAN19 had a lesser, and intermediate effect, than kdROK on Rac phenotypes, ($P < 0.001$), but in combination with Rac1V12 and CRMP-2 the production of rac phenotypes was still significantly reduced and there was no significant difference from Rac1V12/CRMP-2 in the absence of RhoAN19.

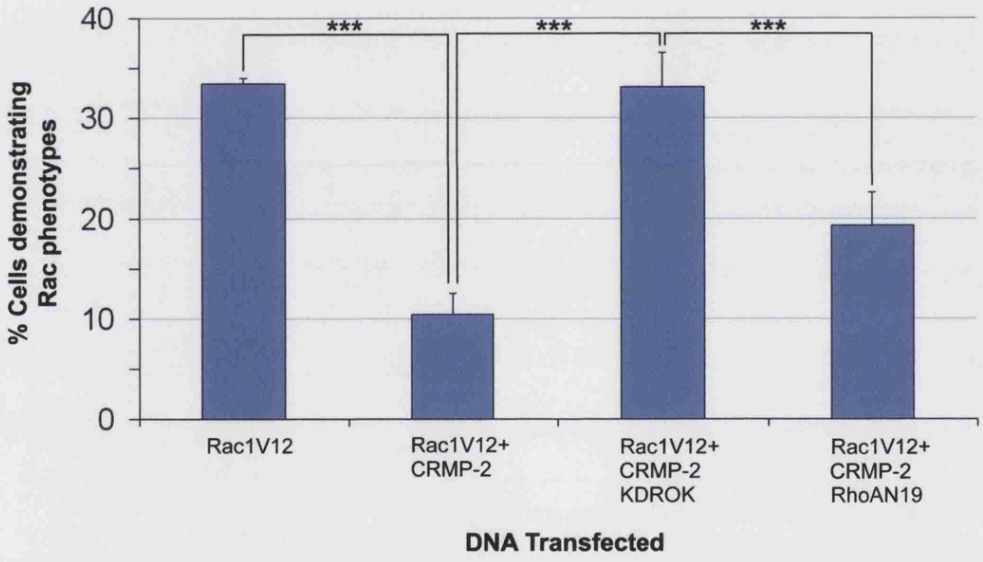

Figure 3.14. The effect of ROK and RhoA on morphologies produced by CRMP-2 and Rac1V12.

N1E-115 cells were transfected with GFP Rac1V12 alone, or in combination with FLAG CRMP-2, FLAG CRMP-2 and kinase dead ROK, or FLAG CRMP-2 and GFP RhoAN19. Cells with Rac phenotypes were counted. Three separate experiments were performed, with three different fields of view counted for each. Error bars represent SEM.

The transfections involving kinase dead ROK correlate well with the inability of the CRMP-2T555A to inhibit the production of round Rac phenotypes (Figure 3.13b). It also suggests that ROK is responsible for phosphorylation of CRMP-2 at T555, to inhibit Rac1 signalling.

The expression of RhoAN19 had a slight effect on the number of Rac phenotypes, but this was not statistically different from those produced by co-expression of Rac1V12 with CRMP-2. In time-lapse experiments, RhoAN19 was able to block CRMP-2-induced collapse with Rac1V12, and so this result appears to be in contradiction to that result. This may be due to the time scale of the experiment. The time-lapse experiments were performed over a few hours, whereas these transfection studies were performed over 16 hours. Possibly by this time point, RhoAN19 has much less of an effect. This result might indicate that kinase inactive ROK is a far more effective inhibitor of function, than RhoAN19. Alternatively, the ability of ROK to phosphorylate CRMP-2, when co-expressed with Rac1V12 could be independent of RhoA. Other GTPases have been shown to bind to ROK, such as RhoE (Riento et al, 2003), Gem and Rad (Ward et al, 2002), but these all inhibit ROK function. It is possible another GTPase, other than RhoA binds to, and activates ROK. Kinase inactive ROK would interact with ROK substrates and prevent the kinase active endogenous form from phosphorylating them. However RhoAN19 sequesters GEF's, and so should prevent endogenous GEF's from activating endogenous RhoA, but may affect others GEFs such as Trio.

3.3.3 Morphological studies in Swiss 3T3 fibroblasts

The N1E-115 neuroblastoma cells provided some insights into the effect of CRMP-2 with the Rho GTPases. However, the Swiss 3T3 fibroblast cell line is a model commonly used for studying RhoA and Rac1 signalling and their effects on the actin cytoskeleton. They show clear and well defined RhoGTPases morphology, with RhoA forming stress fibres and focal adhesions, and Rac1 forming lamellipodia, ruffles, and dissolution of stress fibres and focal adhesions (Ridley and Hall, 1992; Ridley et al, 1992). RhoAV14 expression in N1E-115 cells produces rounded phenotypes similar to those cultured in 10% FCS media alone, and N1E-115 cells do not form stress fibres. Swiss 3T3 fibroblasts were therefore used to further investigate effects of CRMP-2 on Rho signalling.

When cultured in 10% serum, Swiss 3T3 fibroblasts form actin stress fibres, and focal adhesions, (Figure 3.15b,v,x) in a RhoA dependent manner (Ridley et al, 1992). Swiss3T3 cells cultured in 1% serum produce filopodia, and have few stress fibres, while expression of RhoAV14 results in the formation of dense stress fibres and causes the cells to round up (Figure 3.15a,i).

Swiss 3T3 fibroblasts were injected with the relevant cDNAs, and allowed to express for four hours, before fixing and staining. RhoAV14 expression produced very clear and characteristic phenotypes (Figure 3.15a,i), small rounded cells with very dense and thick stress fibres. RhoA activation is known to cause the formation of focal adhesions (Ridley and Hall, 1992), which anchor the stress fibres to the membrane allowing them to span the width of the cell. When CRMP-2 was co-injected with RhoAV14, the cells did not form these dense stress fibres, and instead formed

Figure 3.15a.

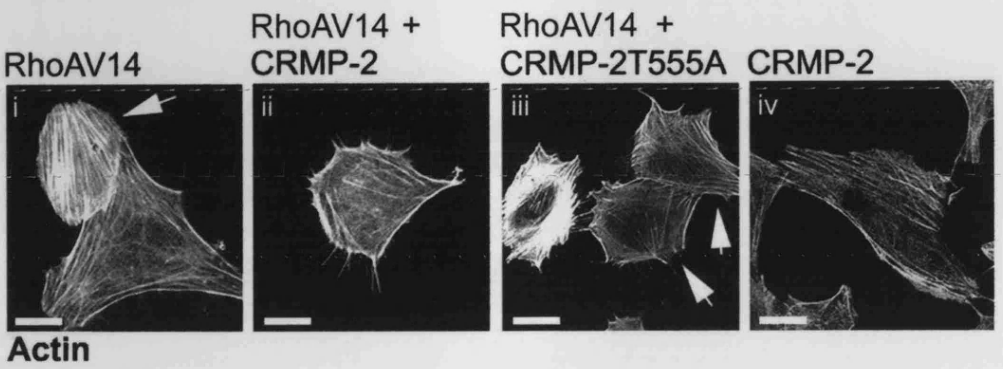

Figure 3.15b.

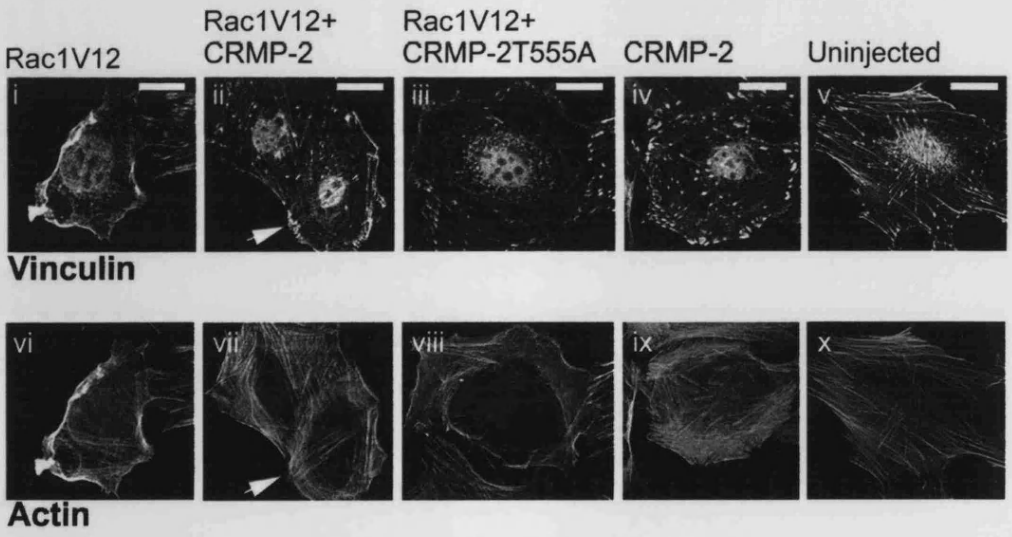

Figure 3.15. The effect of CRMP-2 and CRMP-2T555A on RhoA and Rac1-induced morphologies in Swiss 3T3 fibroblasts.

Cells were injected with GFP RhoAV14 (a) or GFP Rac1V12 (b), along with FLAG CRMP-2 or FLAG CRMP-2T555A. Cells were stained with TRITC conjugated phalliodin to label actin, and anti-vinculin antibody (Sigma) was used in the Rac1V12 experiments to label focal adhesions, while GFP fluorescence indicated GTPase expression. All DNA's were injected at 50μg/ml. Where necessary arrows indicate injected cells. Scale bar equals 25μm.

filopodia, with actin structures around the cell periphery (Figure 3.15a(ii)). This demonstrated a difference between the two different cell lines; in the N1E-115 cells, co-expression of RhoAV14 with CRMP-2 produced Rac phenotypes, but in Swiss 3T3 cells, they produced a Cdc42 phenotype. This suggests the two cell types have a predisposition to either Rac1 or Cdc42 signalling when RhoA signalling is inhibited. As with the N1E-115 transfections, the T555A mutation had no effect on the ability of CRMP-2 to alter RhoAV14 morphologies (Figure 3.15a, iii).

When expressed in Swiss 3T3 cells, cultured in 10% serum, Rac1V12 also produced a very characteristic phenotype (Figure 3.15b, vi). There were few stress fibres crossing the cell, but the actin formed dense structures around the cell periphery forming lamellipodia. The cells did not have the typical angular shape of fibroblasts, but instead form rounded ruffles around the edge. Staining for vinculin, a protein present in focal adhesions, showed that although there were no large focal adhesions, as seen in control cells, there were many smaller focal adhesions around the cell periphery, which have been previously reported in response to Rac1 activation (Nobes et al, 1995) demonstrating that adhesion is an important component of lamellipodia formation. Expression of CRMP-2 alone had little effect compared to the uninjected cells (Figure 3.15b,iv-v).

When CRMP-2 and Rac1V12 were co-expressed, the cell formed a more angular shape (Figure 3.15b,ii,vii). The vinculin staining showed that some dense focal adhesions have been formed. Also some stress fibres had formed, crossing between the focal adhesions. This suggests that there is RhoA signalling in these cells, resulting in these structural changes. Expression of the CRMP-2T555A mutant

abolished this effect, and very few stress fibres or focal adhesions were observed further suggesting that phosphorylation at threonine 555 is required for CRMP-2 to be able to inhibit Rac1V12-induce phenotypes. However, cells expressing CRMP-2T555A and Rac1V12 did not appear to form as many ruffles as Rac1V12 alone, suggesting the T555A phosphorylation mutation did not completely block the effect of CRMP-2 on Rac1V12 morphologies.

Chapter 3 summary

The Rho family of GTPases have a well established role in the regulation of the actin cytoskeleton (Ridley and Hall, 1992; Ridley et al, 1992), and their effects in the neuroblastoma cell line N1E-115 have been well characterised (Kozma et al, 1995). The data here suggest that CRMP-2, a neurospecific protein involved in the sema3A pathway, can alter the effects of the GTPases.

The transfection experiments showed that when co-expressed with Rac1V12, CRMP-2 reduced the production of Rac phenotypes, and when co-expressed with RhoAV14, CRMP-2 induced the production of neurites and Rac phenotypes. CRMP-2 had a ,uch lesser effect when co-expressed with Cdc42V12.

When CRMP-2 and Rac1V12 were co-injected, and subject to time-lapse analysis there was no production of lamellipodia or processes. When cells already expressing Rac1V12 were microinjected with CRMP-2, the cell collapsed in localised regions, leaving microspikes/retraction fibres and promoting filopodia in others. The microspikes and collapse appear to be due to different members of the Rho GTPases as RhoAN19 blocked the collapse, while the filopodia were blocked with Cdc42N17. The time-lapse analysis of N1E-115 cells expressing both RhoAV14 and CRMP-2 showed that the cells flatten and spread out, before producing filopodia around the edge.

CRMP-2T555A, a non-phosphorylatable ROK mutant had the same effect as CRMP-2 with RhoAV14, and resulted in generation of Rac phenotypes. When expressed with Rac1V12, CRMP-2T555A was not able to inhibit the formation of Rac phenotypes.

Expression of kinase inactive Rho kinase confirmed that Rho kinase was responsible for phosphorylating CRMP-2 in this pathway.

The use of Swiss 3T3 fibroblast cells enabled the investigation of positive RhoA signalling. Expression of RhoAV14 in Swiss 3T3 cells cultured in low serum, results in formation of very dense stress fibres and focal adhesions. In these cells, CRMP-2 expressed with RhoAV14, produces a Cdc42 like phenotype with filopodia. When CRMP-2 was co-expressed with Rac1V12, there was a loss of lamellipodia and some focal adhesions were formed and also some stress. This appeared to be dependent on the T555 site.

These results indicate that CRMP-2 is able to switch Rac1 and RhoA morphologies, in two different cell lines, and this switch is, at least in part, regulated by phosphorylation at threonine 555 by ROK.

Chapter 4

Results 2

4.1 Interactions between CRMP-2 and Rho GTPases

4.1.1 Binding of CRMP-2 and the Rho GTPases.

The ability of CRMP-2 to alter GTPase function suggested CRMP-2 might interact directly with the Rho GTPases, and so inhibit activation of their effectors. In order to test this, dotblots were performed using recombinant CRMP-2, probed with labelled recombinant Rho GTPases (Figure 4.1a). Recombinant GST control, GST CRMP-2, and cleaved CRMP-2 were pipetted into a nitrocellulose membrane. PAK CRIB, which binds Rac1V12 and Cdc42V12, and ROK RhoA Binding Domain (RBD), which binds RhoAV14, were used as positive controls. GST was also included to ensure any interaction was not due to the GST tag. The dotblots were incubated with recombinant Rac1V12, RhoAV14 or Cdc42V12 loaded with α^{32}P GTP (Figure 4.1a).

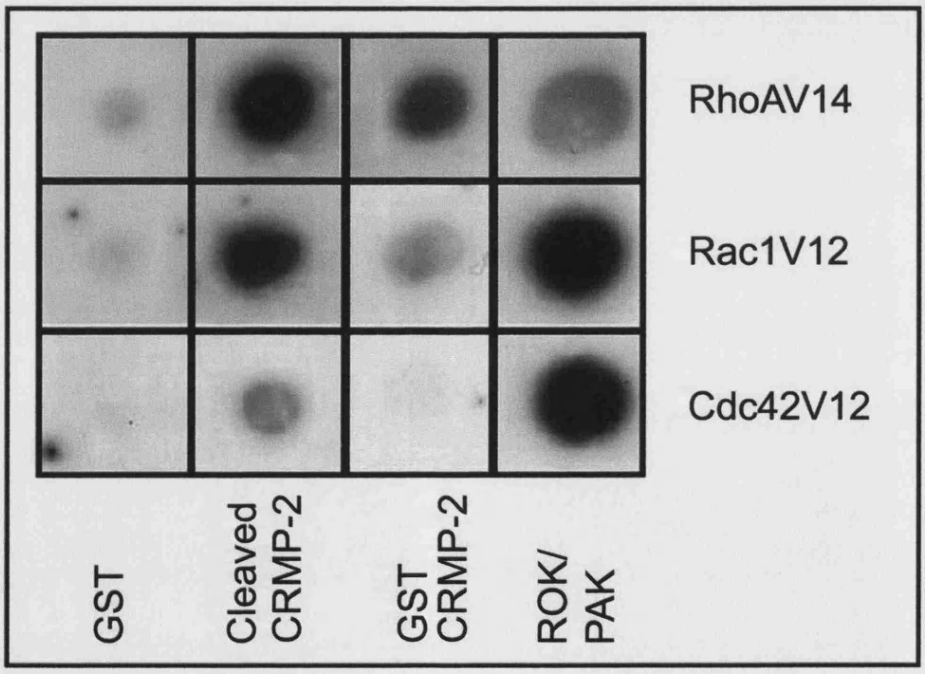

Figure 4.1a. Dot blot showing the binding of CRMP-2 with the Rho GTPases.
GSTCRMP-2, cleaved CRMP-2, GST, ROK RB or PAK CRIB (5μg) on nitrocellulose were incubated with 5μg of ^{32}P-GTP loaded GSTRhoAV14, GSTRac1V12 or GSTCdc42V12 for 10 minutes, and washed before being exposed to hyperfilm for 24 hours (see Materials and Methods, Chapter 2).

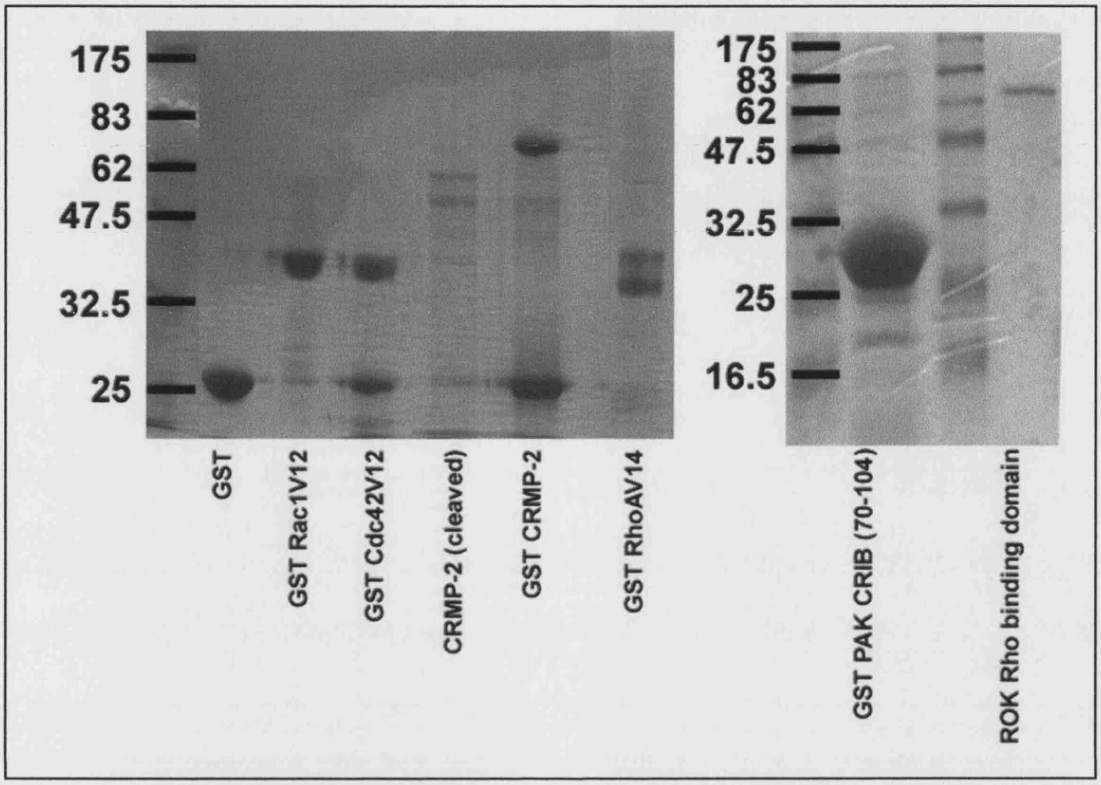

Figure 4.1b. Coomasie stain of proteins used for dotblot.

Indicated proteins were subject to PAGE to check purity. 5μg of proteins were loaded, and the gel incubated with coomase stain for 2 hours, before incubating in destain overnight. Most proteins appeared to be intact with little breakdown. However cleaved CRMP-2 showed some degradation, although appeared to be fairly pure.

Both Rac1V12 and Cdc42V12 bound very strongly to the PAK CRIB control, although RhoAV14 did not bind as strongly to RBD. This could be due to the preparation of the RBD protein sample. The dotblots demonstrated that both Rac1V12 and RhoAV14 bound strongly to CRMP-2. Cdc42V12, however, demonstrated a much weaker interaction. The cleaved CRMP-2 showed a much stronger interaction with RhoA and Rac1 than the GST CRMP-2 construct suggesting the GST tag may

interfere with the interaction. This experiment was repeated three times indicating that CRMP-2 can interact directly with both RhoA and Rac1, because there were no other proteins present. All proteins were subject to PAGE, and stained with coomasie to ensure they were pure, and had not degraded (Figure 4.1b).

However, subsequent CRMP-2 protein samples showed inconsistency in results on the dotblot assay, and it would appear that the ability of RhoGTPases to bind recombinant CRMP-2 protein is variable, and may depend on some unidentified factor in preparation of this protein. CRMP-2 did not bind on western blots, indicating that the native confirmation of the protein might be important.

4.1.2 CRMP-2 Immunoprecipitates with the Rho GTPases in Cos-7 cells

Immunoprecipitation experiments were performed in Cos-7 cells, to test whether CRMP-2 can interact with the GTPases *in vivo*. Cos-7 cells were co-transfected with FLAG tagged dominant positive GTPases, and HA tagged CRMP-2. The Cos-7 cells were left to express for 16 hours, and then lysed. The GTPases were immunoprecipitated by incubating the lysate with anti-FLAG antibody conjugated to sepharose beads for 3 hours at 4°C. After incubation, the beads were washed three times in lysis buffer before adding SDS loading buffer and running them on a SDS gel. Probing a western blot with HA antibody demonstrated CRMP-2 co-precipitation.

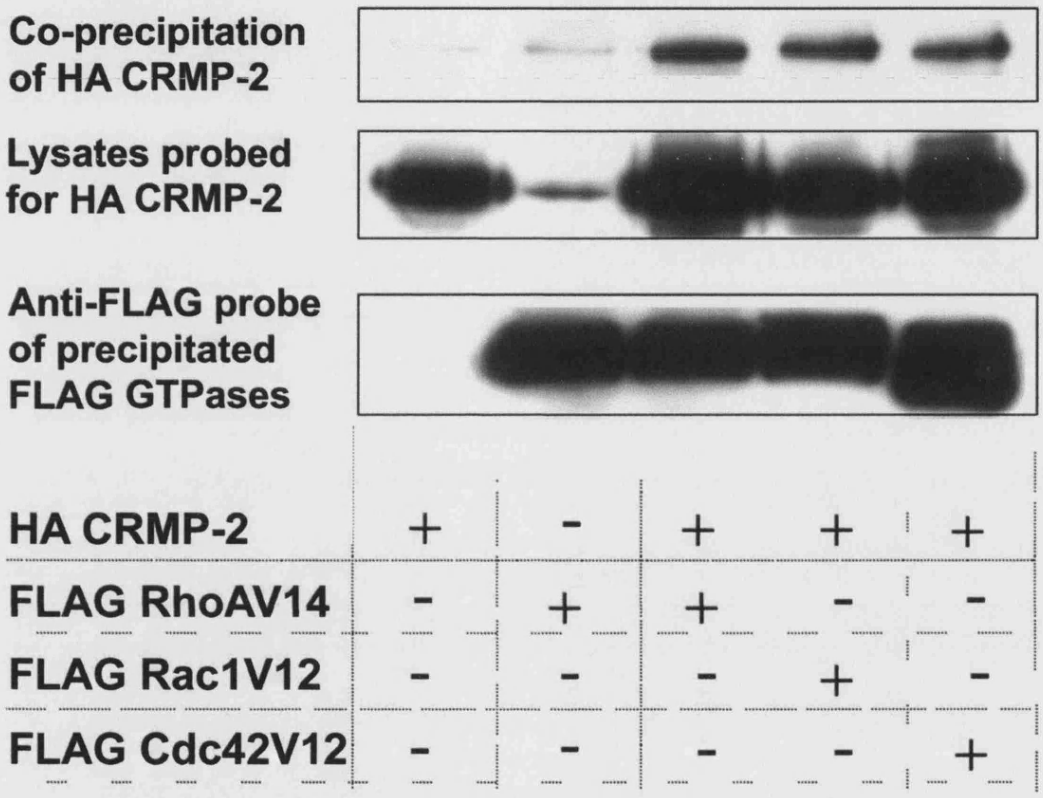

Figure 4.2. Immunoprecipitation of CRMP-2 with the Rho GTPases

FLAG tagged RhoAV14, Rac1V12 or Cdc42V12 were immunoprecipitated from Cos7 cells coexpressing HA CRMP-2. Probing a western blot with anti-HA antibodies was performed to test for the presence of CRMP-2.

Immunoprecipitations with all three GTPases showed the presence of CRMP-2 (Figure 4.2), demonstrating that in Cos-7 cells, CRMP-2 associates with all three key members of the Rho family of GTPases. The immunoprecipitations were equally strong with all three GTPases, which is in contrast with the dot blot, where Cdc42V12 demonstrated a weaker interaction than RhoA and Rac1. However the difference observed between the dotblot and the immunoprecipitation could be due other proteins involved in the interaction. Although CRMP-2 co-precipitates with Rac1V12, RhoAV14 and Cdc42V12, these interactions may not be direct. Alternatively, CRMP-2 may be able to interact with Cdc42 *in vivo* because of structural differences between the proteins synthesised in the Cos7 cells, and those synthesised in bacterial cells.

4.1.3 CRMP-2 may be a RhoA effector, but not a Rac1 effector

Since CRMP-2 was found to associate with RhoA, Rac1 and Cdc42, further immunoprecipitatons were performed to test whether CRMP-2 only interacted with the GTP-bound form of the GTPases, and so was a putative effector. Only Rac1 and RhoA were used in these experiments because of their stronger interactions on the dotblot, and their effects on cell morphologies. RhoAV14 or RhoAN19 were immunoprecipitated from Cos7 cells co-expressing CRMP-2. Following immunoprecipitation of FLAG tagged GTPases, the presence of HA CRMP-2 was tested using anti-HA mouse monoclonal antibody on western blots (Figure 4.3). CRMP-2 could be co-precipitated with FLAG RhoAV14, but not FLAG RhoAN19, immunoprecipitates (Figure 4.3a). However, when HA CRMP-2 was expressed with either Rac1V12 or Rac1N17, CRMP-2 could be co-precipitated with either constitutively active, or dominant negative Rac1, (Figure 4.3b).

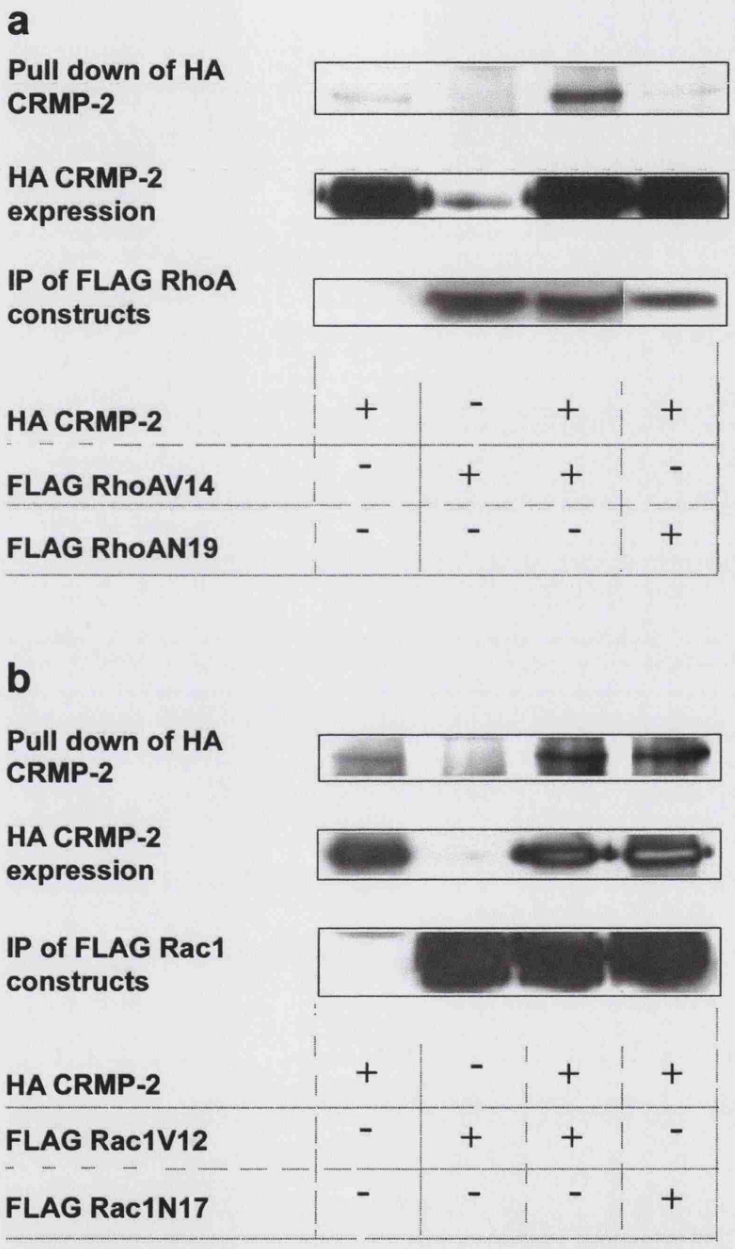

Figure 4.3. Immunoprecipitation of dominant positive RhoA and Rac1 with CRMP-2.

FLAG RhoA (a) and Rac1 (b) dominant positive and dominant negative constructs were immunoprecipitated from Cos7 cells co-expressing HA CRMP-2. Probing a western blot with anti-HA antibody was performed to test for the presence of CRMP-2.

The dominant positive GTPase mutants have defective GTPase activity, and remain bound to GTP. Therefore these mutants can represent GTP bound RhoA or Rac1. However, the method of action of the dominant negative mutants is not as well understood. They are believed to sequester GEF's, (Reviewed in Feig, 1999) and so they may not be GDP bound. However, they do not activate effectors, and so can represent the inactive state of RhoA or Rac1. Therefore the use of dominant negative GTPases can provide an indication as to whether or not a protein is an effector for RhoA or Rac1, and were used to show that Cdk5 was a novel Rac1 effector (Nikolic et al, 1998).

An alternative approach to determining whether a protein is an effector, involves the use of GTPases that are capable of hydrolysing GTP, which are then used in the dotblot, to ascertain whether the target protein binds to GTP bound or/and GDP bound GTPase.

4.2 Co-localisation of CRMP-2 with the GTPases

4.2.1 Co-localisation of CRMP-2 and the RhoGTPases in cerebellum granule neurones

To examine whether CRMP-2 and the GTPases were likely to interact *in vivo*, co-localisation studies of endogenous proteins were performed. Cerebellum granule neurones (CGC) isolated from day 3 postnatal rats (obtained from J.Pocock) were stained for CRMP-2 (mouse monoclonal from Ihara, Japan; Gu et al, 2000) and

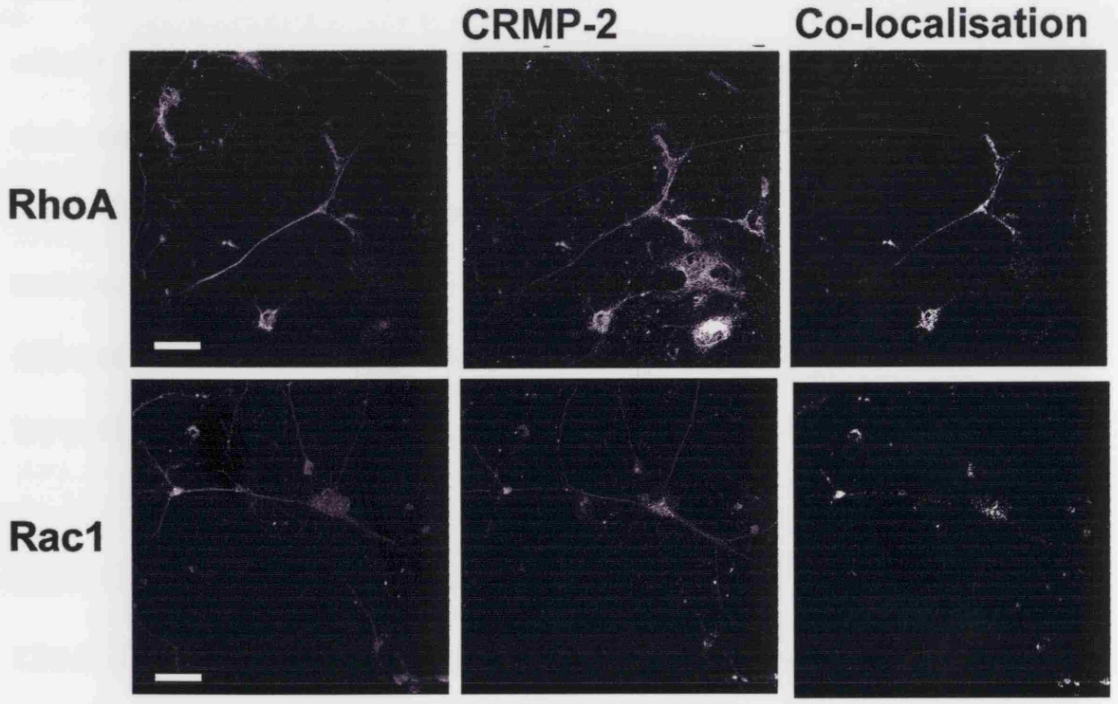

Figure 4.4. Colocalisation studies using cerebellum granule neurones from postnatal day 3 rats.

Cells were fixed and stained with anti-CRMP-2 rabbit polyclonal (in house) and either anti-Rac1 mouse monoclonal (Transduction labs) or anti-RhoA mouse monoclonal (Santa Cruz) antibodies. Colocalisation was performed using a confocal microscope and Zeiss LSM software. Scale bar equals 50μm.

either RhoA (rabbit Santa Cruz) or Rac1 (rabbit Santa Cruz). Co-localisation between the FITC labelled RhoA or Rac1, and the Cy5 labelled CRMP-2 was analysed using confocal microscopy.

Both Rac1 and RhoA co-localised with CRMP-2 (Figure 4.4), although in different cellular compartments. CRMP-2 and RhoA appeared to co-localise in the neurite shafts and down to the growth cones, and neurite branch points. However, Rac1 and CRMP-2 both localised to the cell body, neurite branch points and the base of neurites. This slight difference in colocalisation may indicate that CRMP-2 plays a different role with RhoA than with Rac1, in neurite morphology. However this result has not been quantified, and so must be further examined before drawing conclusions.

4.2.2 Co-localisation of CRMP-2 and the Rho GTPases in drg's

CRMP-2 has been shown to play an important role in the sema3A collapse pathway (Goshima et al, 1995). Dorsal root ganglia (drg) neurones, which respond to sema3A by collapse of growth cones (Eickholt et al, 1997) and are repulsed by sema3A *in vivo* (Wright et al, 1995), are widely studied. Drg neurones were removed from day 1 postnatal Wistar rats and cultured for 24 hours before fixing and staining with CRMP-2 polyclonal antibody (in house) and mouse monoclonal Rac1 (Transduction Labs) or RhoA (Santa Cruz) antibodies. Slides were then analysed on fluorescent microscope using digital camera and Provision software (Figure 4.5a). Strong CRMP-2 staining was observed in drg neurones, and appeared to co-localise with staining of both Rac1 and RhoA. From merged images, and co-localisation software (indicated white), co-localisation appeared to be down neurites and in the cell body (Figure 4.5a).

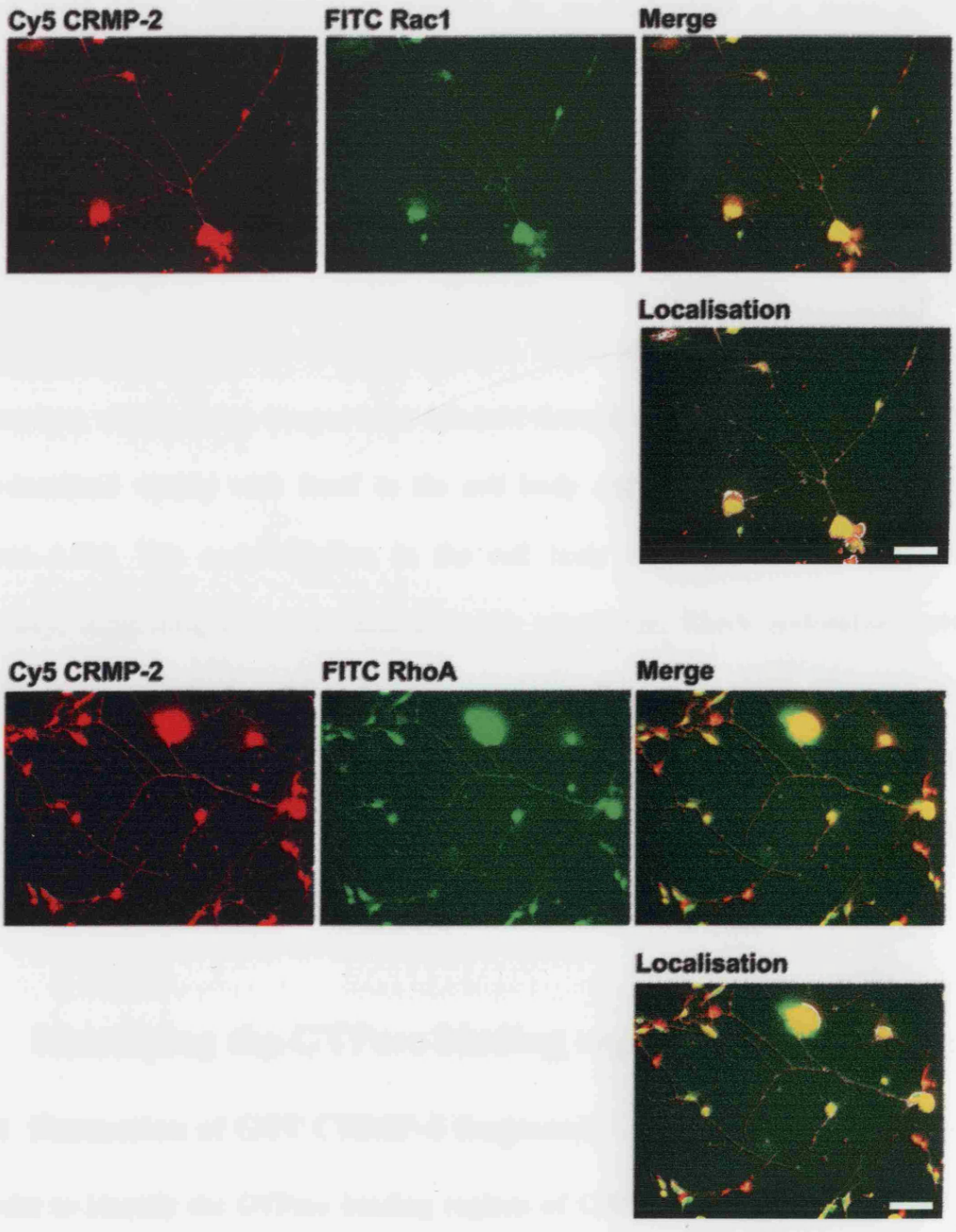

Figure 4.5a. Staining of drg neurones for endogenous CRMP-2, and either Rac1 or RhoA.

Cells were prepared from day 1 postnatal rats and stained with anti-CRMP-2 rabbit polyclonal (in house) and either anti-Rac1 mouse monoclonal (Transduction labs) or anti-RhoA mouse monoclonal (Santa Cruz) antibodies. Images were obtained using a digital camera and Provision software. Merged images are a composite of Cy5 and FITC images, and areas of colocalisation are indicated in white. Scale bar equals 50μm.

These images were obtained from a fluorescent microscope, and so do not represent a single focal plane. Therefore it is possible the co-localisation is a result of the antibodies staining different depths through the cells. However, this does provide some evidence for endogenous CRMP-2 existing in similar cellular locations to Rac1 and RhoA.

To provide further evidence for colocalisation, slides were analysed on a confocal microscope, which allows images to be obtained through a single focal plane. CRMP-2 co-localised weakly with Rac1 in the cell body and down some neurite shafts (Figure 4.5b). The co-localisation in the cell body appeared to be around the periphery, suggesting they may interact at the membrane. RhoA co-localised with CRMP-2 in the cell body, with very little detected in the neurite shafts (Figure 4.5b). The RhoA staining was strong in the cell body but very little was detected in the shafts or growth cones, although CRMP-2 staining was throughout the cell. There appeared to be very little RhoA in the neurites to co-localise with CRMP-2.

4.3 Identifying the GTPase binding region in CRMP-2

4.3.1 Formation of GST CRMP-2 fragments

In order to identify the GTPase binding regions of CRMP-2, a number of CRMP-2 fragments were made, and cloned into the mammalian GST vector. Use of the GST vector would allow the constructs to be expressed in Cos-7 cells, and isolated from the cell lysate using glutathione- conjugated sepharose beads. The N-terminal and C-terminal fragments were made using PCR, producing two halves of approximately 300 residues each. Cutting the full-length sequence with restriction enzymes, and

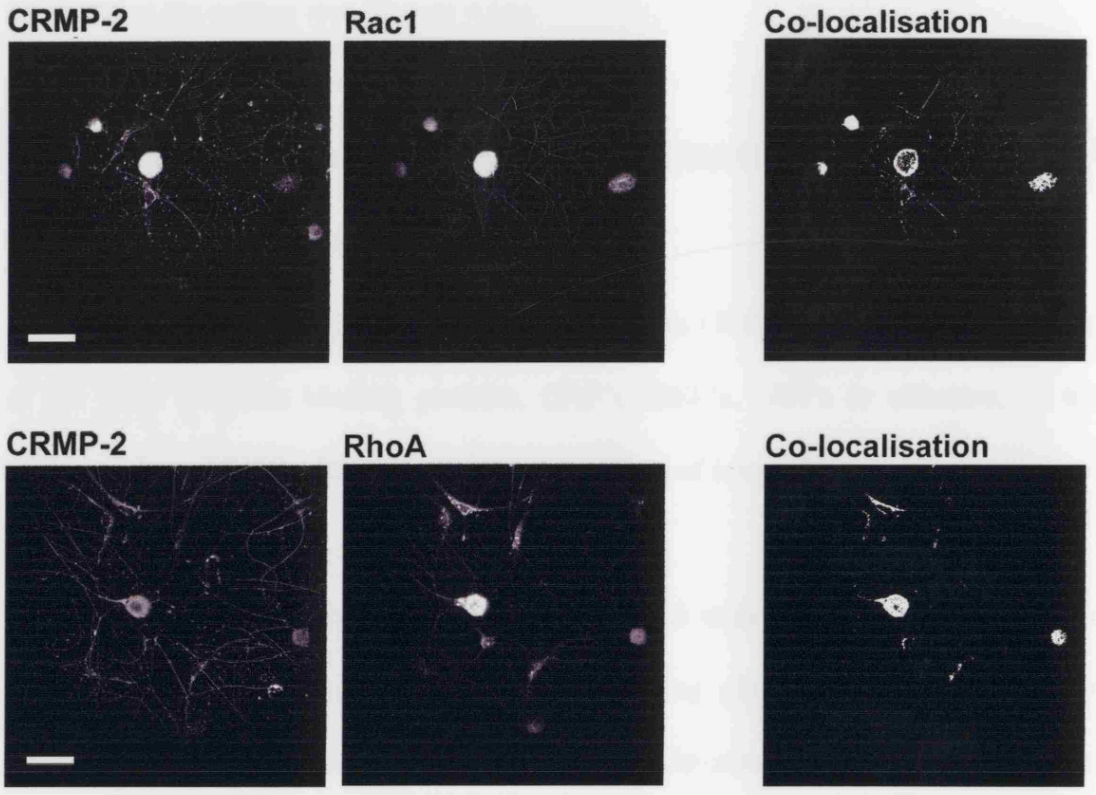

Figure 4.5b. Colocalisation of endogenous CRMP-2 and either RhoA or Rac1 in in drg neurones.

Cells were prepared from day 1 postnatal rats and stained with anti-CRMP-2 rabbit polyclonal (in house) and either anti-Rac1 mouse monoclonal (Transduction labs) or anti-RhoA mouse monoclonal (Santa Cruz) antibodies. Colocalisation was performed using a confocal microscope and LSM software. Scale bar equals 50μm.

cloning the fragments into the vector made three additional fragments. All three were N-terminal fragments, consisting of 1-112, 1-180 and 1-253 amino acid residues (Figure 4.6a). All fragments were expressed in Cos7 cells to ensure proteins were produced at the correct size (Figure 4.6b).

4.3.2 Immunoprecipitation studies using CRMP-2 fragments with Rac1 and RhoA

CRMP-2 does not contain any sequence similarity to GTPase binding regions of any of the main GTPases binding proteins, GAP's, GEF's, GDI's or effectors, so the sequence does not provide any indication of the area of interaction.

CRMP-2 protein fragments were then co-expressed with GTPases to test for their interaction. CRMP-2 fragments were purified using glutathione beads while HA tagged RhoA or Rac1 were used to indicate co-precipitation of the GTPases. Neither RhoA nor Rac1 interacted with the CRMP-2 1-112 fragment. However, both interacted with all the other fragments (Figure 4.7). While Rac1V12 appeared to interact equally well with all fragments, RhoAV14 demonstrated a stronger interaction with the 291-573 and 1-180 fragments, than with the 1-297 and 1-253 fragments. There was no pull down with GST alone, indicating the GST tag did not associate with the GTPases. RhoA and Rac1 associated with all but one of the fragments. This could be due to a single large domain required for interaction, running from residues 113 to over 300. Alternatively, more than one region of CRMP-2 contributed to RhoAV14 and Rac1V12 binding. To answer this question, and isolate the region, or regions of CRMP-2 that bind to the GTPases, a more comprehensive set of CRMP-2 fragments would be needed.

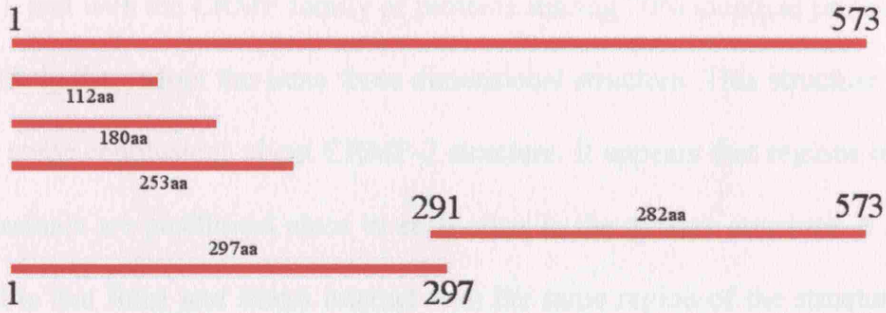

Figure 4.6(a). Representation of CRMP-2 fragments

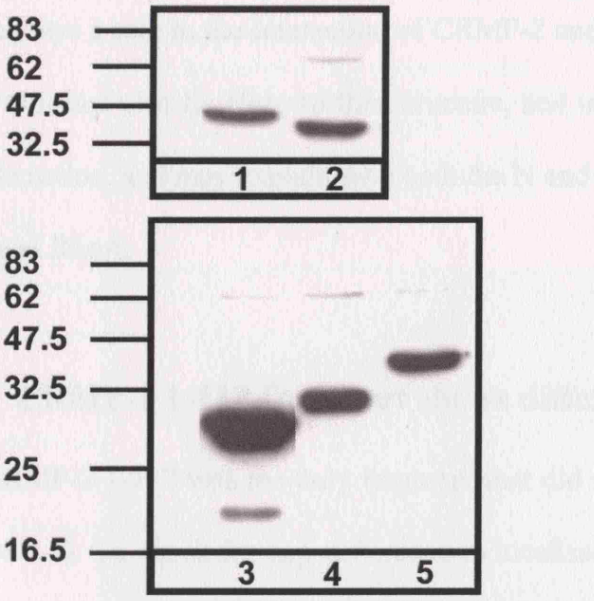

1 = GST CRMP-2 N-Terminal
2 = GST CRMP-2 C-Terminal
3 = GST CRMP-2 1-112
4 = GST CRMP-2 1-180
5 = GST CRMP-2 1-253

Figure 4.6(b). Western blot showing expression of GST tagged CRMP-2 fragments in Cos7 cells.

Lysates from Cos7 cells were subjected to western blot analysis using anti-GST mouse monoclonal antibody (Sigma).

The three dimensional structure of CRMP-1 has been recently resolved (Deo et al, 2004), and with the CRMP family of proteins sharing 70% identical protein sequence, it is likely they adopt the same three dimensional structure. This structure can used to draw some conclusions about CRMP-2 structure. It appears that regions of the N and C terminals are positioned close to each other in the tertiary structure. It is therefore possible that Rac1 and RhoA interact with the same region of the structure, which is composed of sequences from the N and C terminals. Two α-helices and a β-sheet, formed from the region of protein between 112 and 180. It is therefore possible this region plays a role in the interaction of CRMP-2 and Rac1 or RhoA. Other regions in the C terminal also lie close to this structure, and may form an accessory region for the interaction, and may explain why both the N and C terminal sequences can bind to Rac1 and RhoA.

4.3.3 CRMP-2 1-112 fragment shows different cellular localisation

The CRMP-2 1-112 was the only fragment that did not associate with RhoA or Rac1 (Figure 4.7). To check for any difference in localisation, all the GST fragments were expressed in Cos-7 cells. These were then fixed and stained using an anti-GST antibody (mouse monoclonal, Santa Cruz) (Figure 4.8a). All the fragments except, CRMP-2 1-112, demonstrated the same localisation seen with full length CRMP-2 in N1E-115 (see Chapter 1). They were very punctate and localised to particulate structures. However, CRMP-2 1-112 had a very diffuse cytoplasmic localisation, which was the same as seen with GST alone.

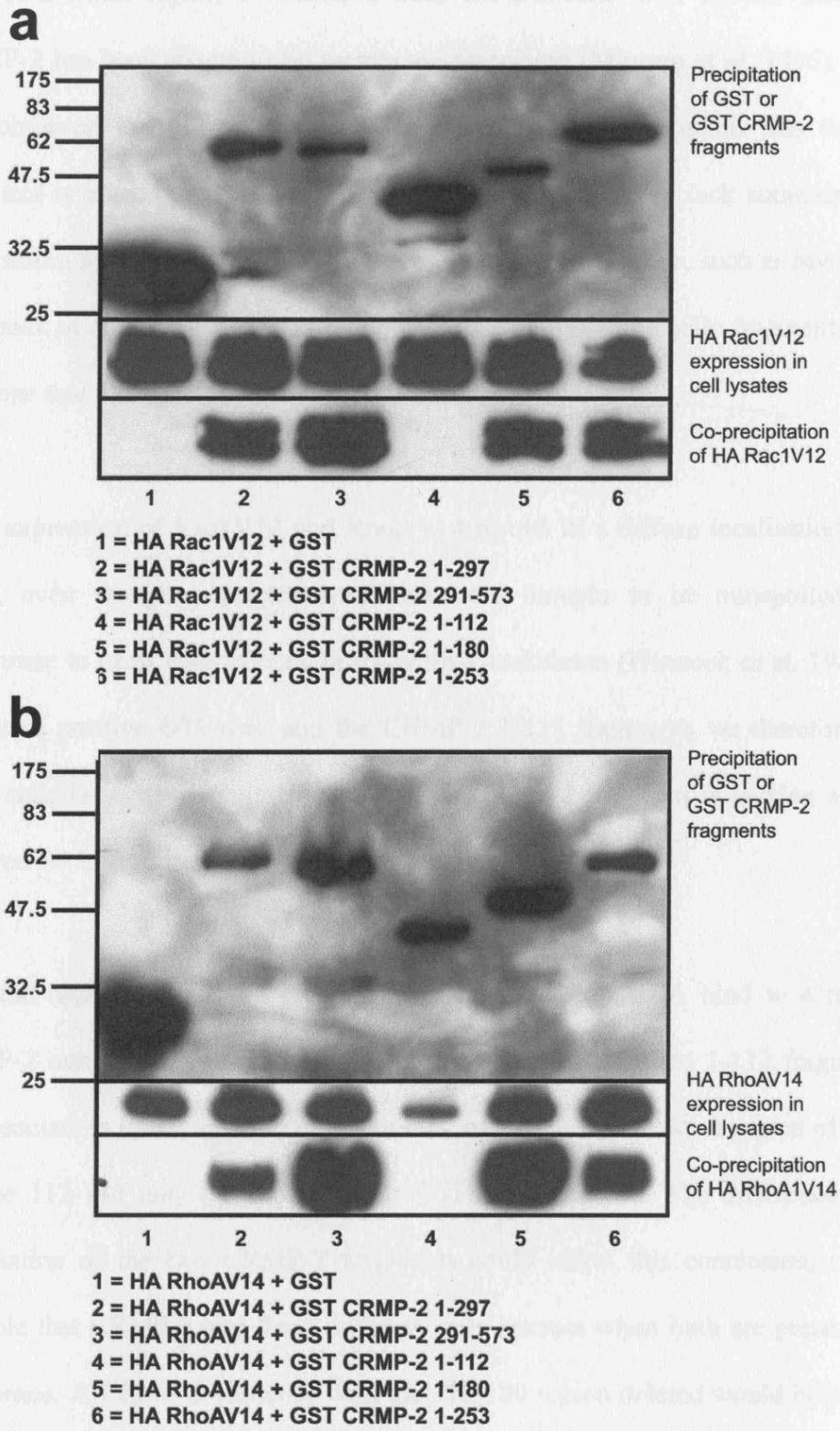

Figure 4.7. Western blot showing co-precipitation with GST CRMP-2 fragments and either Rac1V12 (a) or RhoAV14 (b).

GST constructs and HA GTPases were expressed in Cos7 cells before isolation using glutathione beads. Cell lysates and glutathione beads were subjected to western blot analysis and the presence of GTPases determined using anti-HA antibodies (Babco).

This N-terminal region of CRMP-2 does not associate with cellular membranes. CRMP-2 has been shown to be membrane-associated (Minturn et al, 1995), and this was observed with all the other CRMP-2 fragments. It is possible that this 1-112 fragment is not involved with membrane anchoring, and may lack some membrane localisation sequence required to send proteins to the membrane, such as myristilation (Hancock et al, 1990). The 1-112 fragment was the only cytosolic fragment, and the only one that did not associate with RhoA or Rac1.

Over expression of Rac1V12 and RhoAV14 results in a diffuse localisation (Figure 4.8b), even though endogenous GTPases are thought to be transported to the membrane to exert their effects on the actin cytoskeleton (Hancock et al, 1989). The dominant positive GTPases, and the CRMP-2 1-112 fragments we therefore in the same cellular compartments, suggesting this CRMP-2 fragment is lacking a domain required for interaction.

It would appear from these results that both Rac1 and RhoA bind to a region in CRMP-2 outside the first 112 amino acid residues, because the 1-112 fragment did not associate in immunoprecipitation studies, while the 1-180 did. A region of CRMP-2 from 112-180 may be important for GTPase interaction. The differences in the localisation of the two CRMP-2 fragments could affect this conclusion, and it is possible that CRMP-2 and Rac1 or RhoA only interact when both are present at the membrane. A CRMP-2 sequence with the 112-180 region deleted would help answer this.

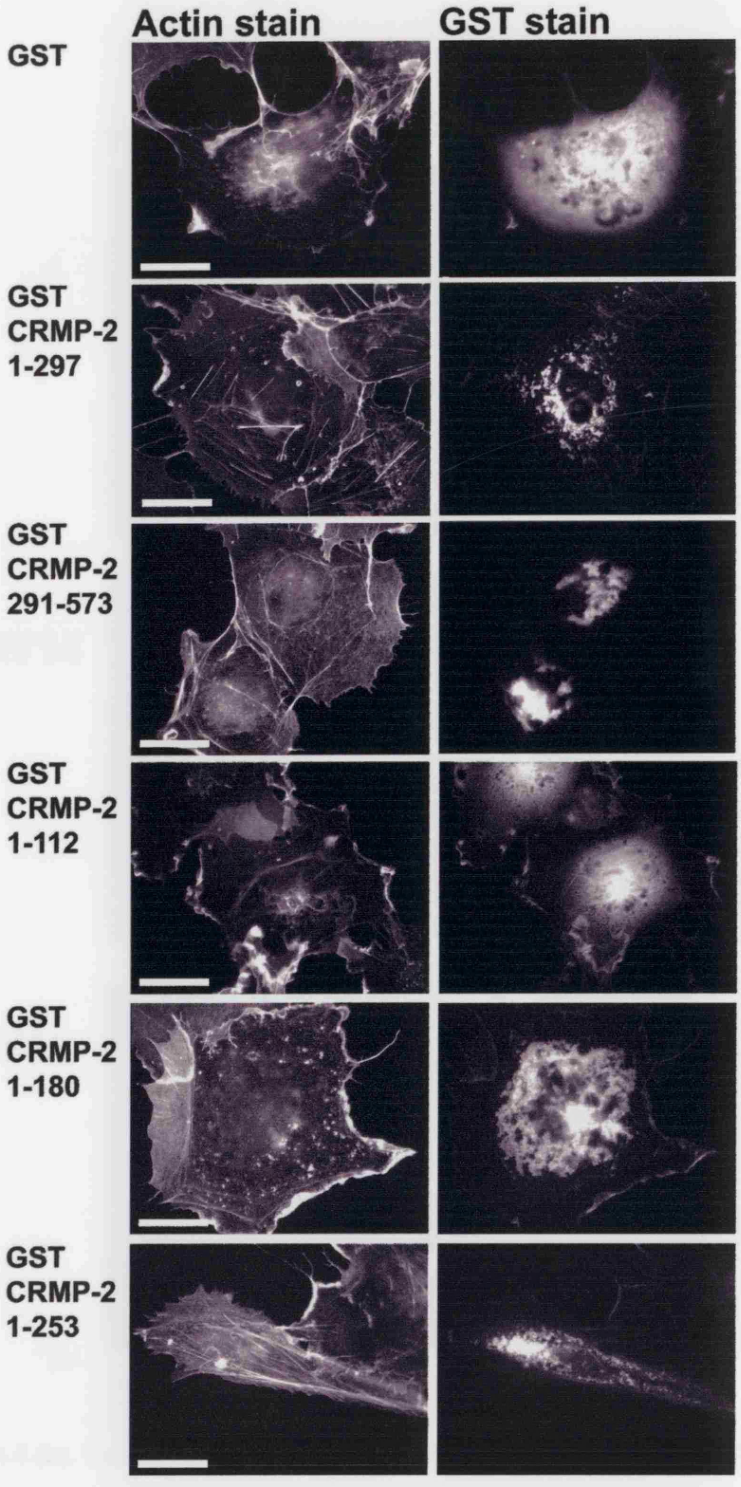

Figure 4.8 (a). Cos7 cells transfected with GST CRMP-2 fragments.
Cells were fixed and stained using anti-GST mouse monoclonal antibody (Sigma), and TRITC conjugated phalloidin. Imaging was performed using axiovert microscope with digital camera and Metamorph software. Scale bars equal 25μm.

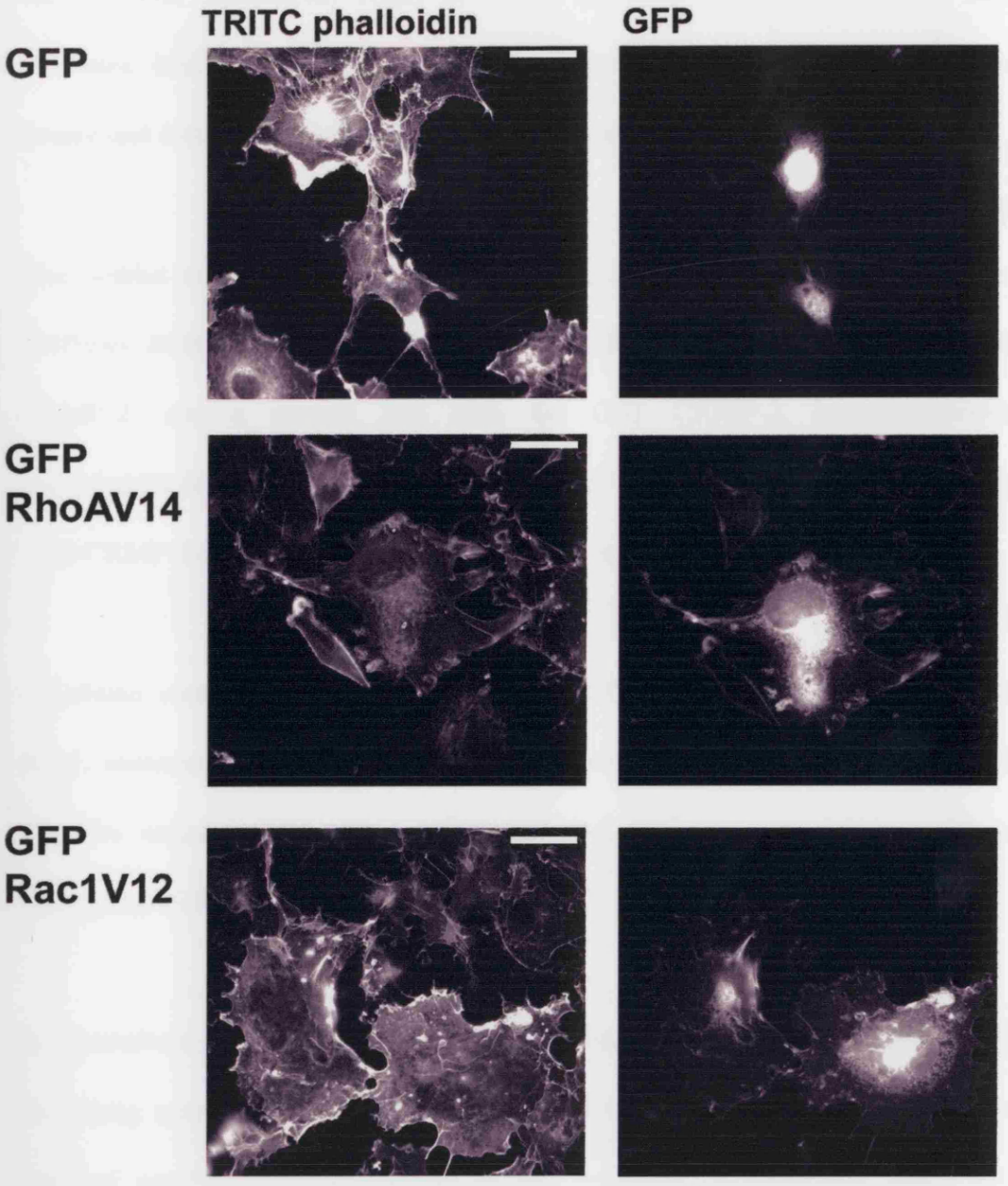

Figure 4.8 (b). Cos7 cells transfected with GFP. GFP Rac1V12 or GFP RhoAV14.
Cells were fixed and stained using TRITC conjugated phalloidin. Imaging was performed using axiovert microscope with digital camera and Provision software. Scale bar equals 25µm.

Chapter 4 summary

Morphologies from Chapter 3 suggested CRMP-2 can alter GTPase function, and so one possible mechanism could be direct interaction of CRMP-2 with the Rho GTPases, inhibiting activation of their effectors. To answer this question, dotblot assays and immunoprecipitation experiments were performed.

The dotblot assay demonstrated that CRMP-2 could interact directly with the Rho GTPases. Both RhoAV14 and Rac1V12 showed a strong interaction with the cleaved CRMP-2, and a weaker one with the GST CRMP-2. Immunoprecipitation experiments demonstrated that RhoAV14, Rac1V12 and Cdc42V12 could all interact with CRMP-2 equally well when co-expressed in Cos7 cells.

To obtain some information as to whether CRMP-2 was an effector for RhoA or Rac1, immunoprecipitations were performed using dominant positive and dominant negative mutants. This showed that CRMP-2 co-immunoprecipitates with active RhoA, but with both active and inactive Rac1.

In cerebellum granular neurones CRMP-2 colocalised with RhoA in the cell body, and along some neuritis. CRMP-2 colocalised with Rac1 in the cell body and at the base of neurites. Immunostaining of drg neurones demonstrated much stronger CRMP-2 staining, and Rac1 colocalised to the cell body and down the neurites, whereas RhoA colocalisation was mainly in the cell body, with very little in the neurites.

In an attempt to determine the GTPase binding region of CRMP-2, several fragments were made and cloned into a GST vector. Both RhoA and Rac1 interacted with all CRMP-2 fragments, except the 1-112 fragment. In addition, all CRMP-2 fragments were membrane associated except the 1-112 fragment.

Chapter 5

Results 3

5.1 Sema3A collapse in neuroblastoma N1E-115 cells permanently expressing α2-chimaerin

Results from Chapters 3 and 4 suggested that CRMP-2 could regulate Rac1 and RhoA, possibly through a direct interaction. CRMP-2 is a crucial component of the sema3A collapse pathway (Goshima et al, 1995), but its function in sema3A signalling is unknown. Therefore, the role of CRMP-2 in sema3A collapse was investigated. CRMP-2 was isolated from a screen for novel interactors of α2-chimaerin (PhD Thesis, G.Ferrari), and so the role of this GAP in sema3A collapse was also investigated.

5.1.1 Time-lapse analysis of sema3A retraction

Experiments were performed to investigate the role of CRMP-2 in sema3A-mediated neurite retraction. The N1E-115 cell line permanently expressing α2-chimaerin, α2.13, was used in sema3A collapse phase time-lapse analysis. These are N1E-115 neuroblastoma cells that have been previously transfected with vectors encoding α2-chimaerin and also a neomycin resistance gene (Hall et al, 2001). This clonal cell line is cultured in G418 (Calbiochem) to maintain the vector in the population. These were used in preference to parental N1E-115 cells because of their ability to produce large neurites and growth cones when cultured in media containing 10% FCS (Figure 5.1a). N1E-115 cells have previously been shown to respond to sema3A, inducing neurite retraction (van Horck et al, 2002). Growth cone collapse and neurite retraction were first investigated using time-lapse analysis. N1E-115 α2.13 cells were plated in 10% FCS, onto laminin-coated glass coverslip bottom dishes to ensure optimum microscope imaging. A microscope with a CO_2 box and heated stage was used to

maintain the cells for the duration of the experiment. Neurites with growth cones were selected, and monitored for 30 minutes, to ensure they did not collapse in the absence of sema3A (Figure 5.1a). Neurites and growth cones appeared to be stable for the duration of the time-lapse. For sema3A collapse studies, neurites were selected and monitored for 10 minutes prior to treatment with sema3A, with images taken every 30 seconds. A microinjection needle containing purified sema3A (50μg/ml, obtained from B. Eickholt; see Materials and Methods) was placed near the neurites, ensuring a free stream of fluid from the needle. The neurites were monitored for 30 minutes. All time-lapse experiments were repeated 10 times. The nature of collapse of the growth cones was variable, with some growth cones collapsing although the neurites did not retract. Only complete neurite retraction was quantified as a sema3A-induced response.

Out of 10 neurites examined, 6 showed a rapid response to sema3A, (Figure 5.1b). In the sample shown, the neurite began to retract at around 20 minutes, and by the end of the 30 minute period the neurite had retracted back from the needle. To examine the actin dynamics in the growth cone during collapse, α2.13 cells were transfected with GFP-actin to allow fluorescent imaging of the actin in the growth cone. Prior to sema3A treatment, the actin in the growth cone was rich in polymerised actin, with clear actin filaments extending to the edge of the growth cone from the centre (Figure 5.1c). There were also dense actin structures at the base of the growth cone. Following addition of sema3A from the needle, the actin filaments in the middle of the growth cone appeared to dissolve, along with the dense actin structures at the base of the growth cone. This dissolution of the actin appeared to happen almost immediately, and the actin at the base of the growth cone had dissolved by 4 minutes.

Figure 5.1a. Time-lapse of untreated neurite in N1E-115 cell line expressing α2-chimaerin.

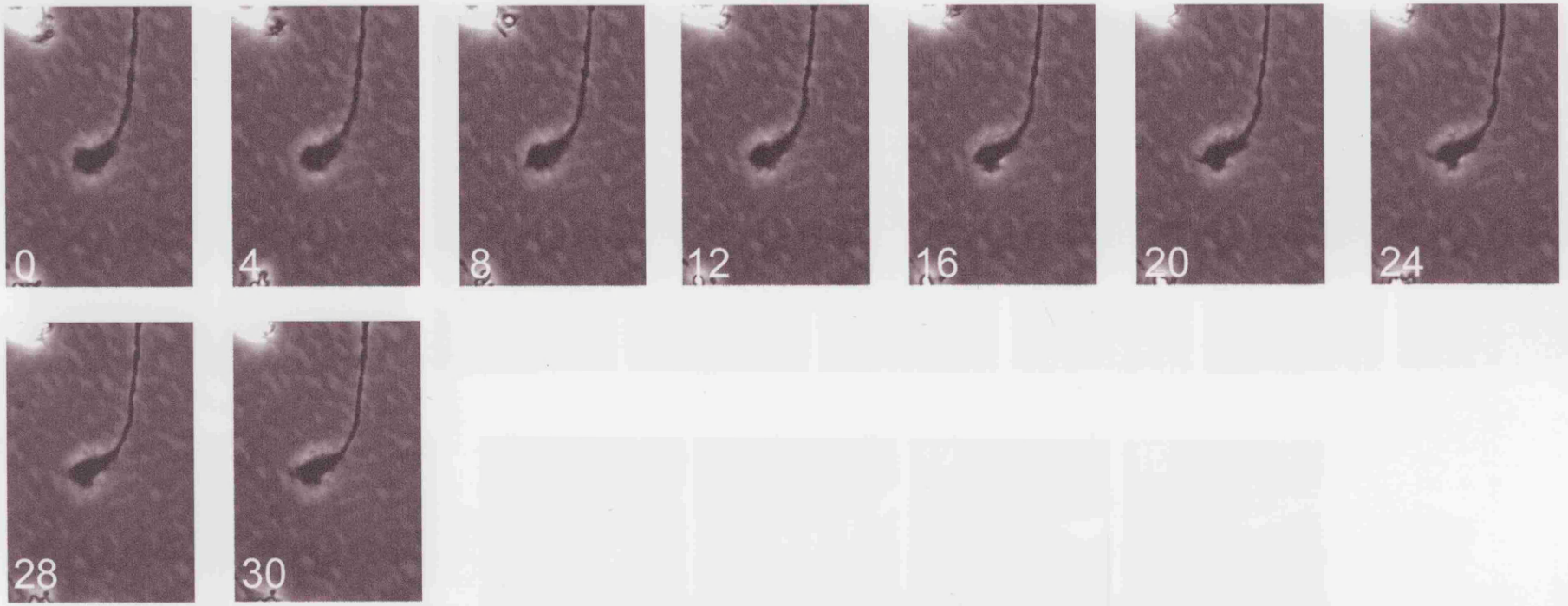

Phase contrast images time-lapse microscopy of neurites from α2.13 cells. Neurites were monitored for 30 minutes to ensure they were stable, and did not collapse. Images were taken at the time points indicated.

Figure 5.1b.c. Growth cone collapse and neurite retraction in N1E-115 cell line expressing α2-chimaerin.

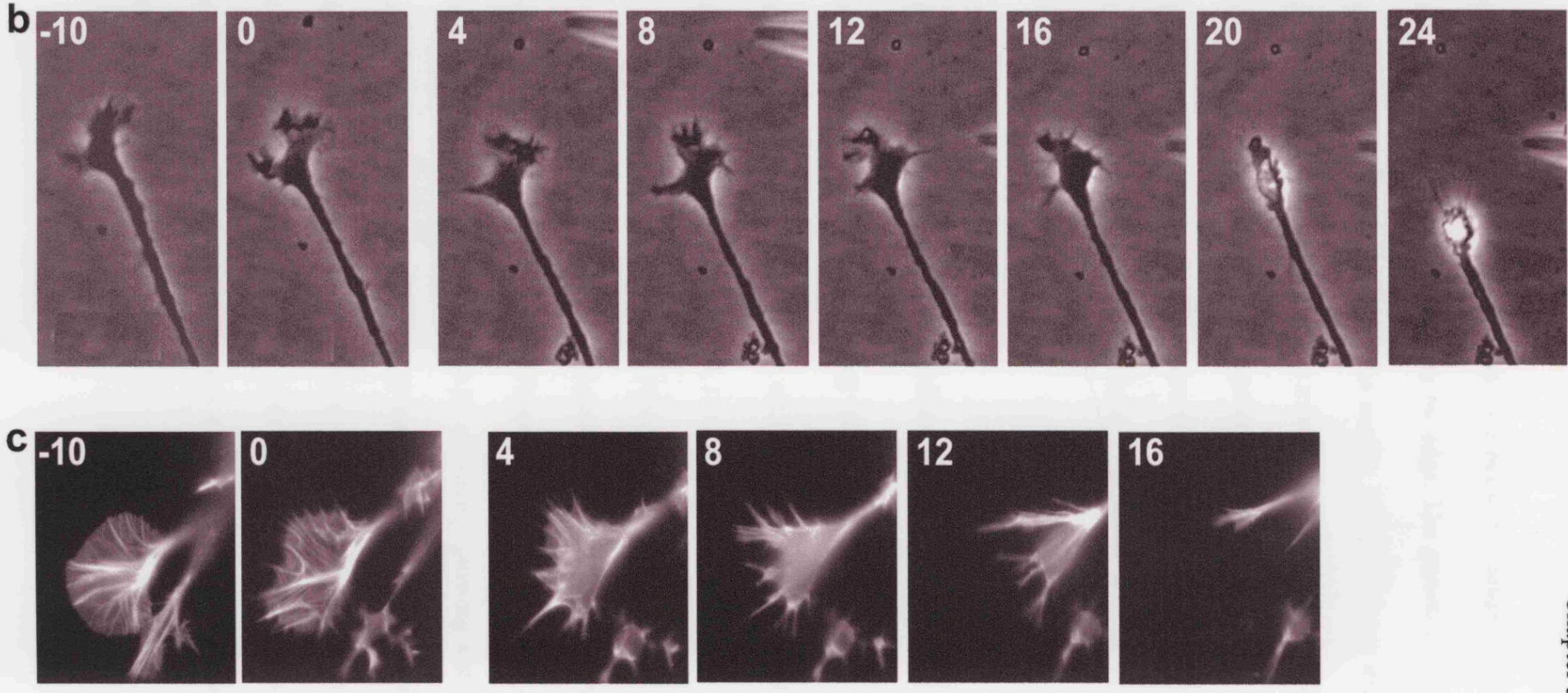

Phase contrast images (b) and flourescent GFP actin (c) time-lapse microscopy of neurites from α2.13 cells. A microinjection needle containing sema3A was placed near the growth cone at time point 0. Time in minutes, -10 to +24 as indicated.

Once the filaments had broken down, the growth cone began to collapse at around 10 minutes, leaving retraction fibres protruding from the edge. The growth cone then collapsed completely and retracted back from the needle. This time-lapse experiment suggests that the collapse of the growth cone is a consequence of act reorganisation, and dissolution of actin structures, as actin dissolution preceded retraction. Growth cone collapse does not appear to be an actin contraction driven process, which would involve RhoA and ROK, signalling to form dense contractile actin filaments that could contract the growth cone.

5.1.2 Roscovitine blocks sema3A retraction in neuroblastoma N1E -115 cells permanently expressing α2-chimaerin

The time-lapse experiments were repeated with α2.13 cells treated with roscovitine, a Cdk5 inhibitor (De Azevedo et al, 1997). α2.13 cells were treated with the Cdk5 inhibitor, roscovitine over night prior to sema3A treatment. In the presence of 10μM roscovitine, the neurites did not collapse (Figure 5.2a), but instead appeared to produce filopodia at approximately 8 minutes. These filopodia remained for the whole 30 minutes, but were not static and appeared to be constantly growing and retracting. There was no neurite retraction in 7 of the 10 neurites examined. This time-lapse experiment suggests Cdk5 is a crucial component of the sema3A collapse/retraction pathway. Recently Saski et al (2002) have shown that roscovitine can inhibit sema3A-induced collapse, and that drg neurones isolated from Cdk5 knockout mice do not respond to sema3A (Sasaki et al, 2002).

Figure 5.2. Time-lapse analysis of the role of ROK and Cdk5 in sema3A-mediated collapse of neurites from α2.13 cells.

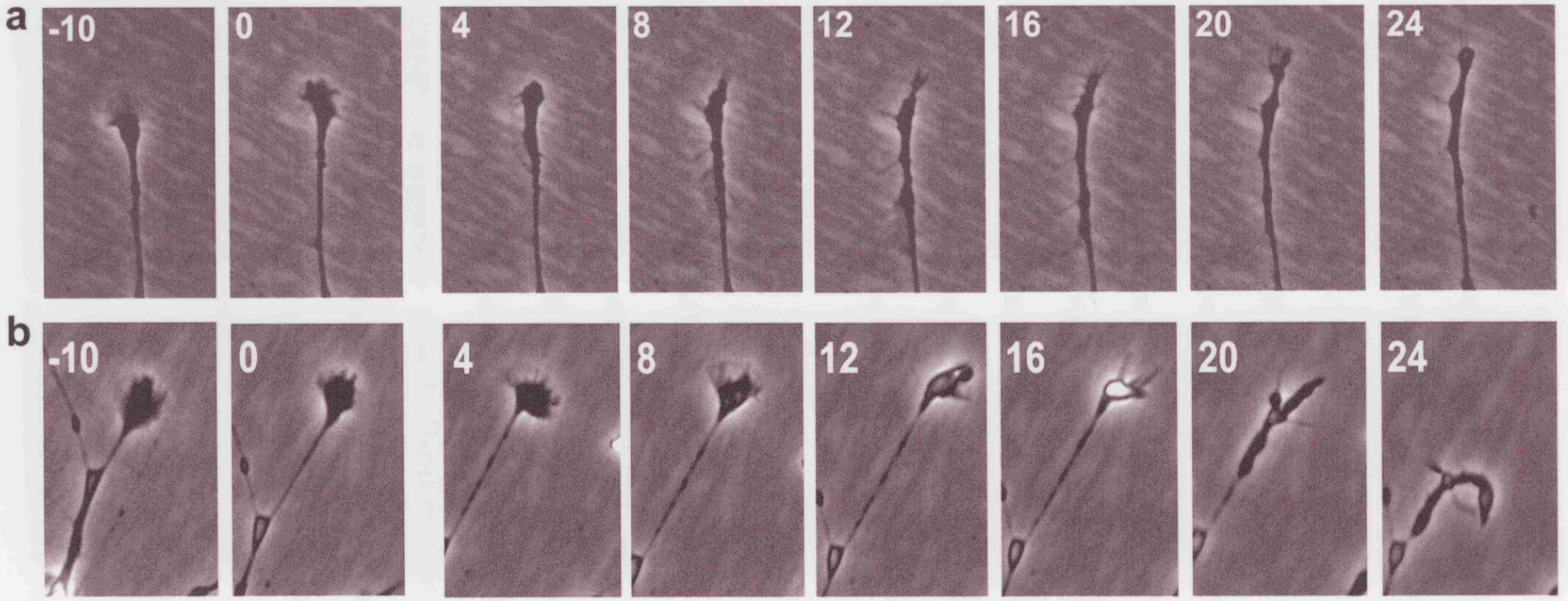

Cells were treated with roscovitine (a) (10μM) or Y-27632 (b) (10μM) overnight to inhibit Cdk5 and ROK respectively. A microinjection needle containing sema3A was placed near the growth cones at time point 0. Time points are in minutes, as indicated.

5.1.3 Sema3A-mediated retraction is independent of ROK

ROK is an important component of many collapse pathways, following RhoA activation (Katoh et al, 1998; Hirose et al, 1998; Bito et al, 2000). To test the role of the RhoA/ROK pathway in the collapse, α2.13 cells were cultured in the specific ROK inhibitor Y-27632 (10μM) over night prior to sema3A treatment (Uehata et al, 1997). However, Y-27632 did not block the collapse (Figure 5.2b), and even appeared to enhance the collapse affect. In the example shown, the neurites started to retract after about 20 minutes, and had retracted away from the needle by 30 minutes. In this experiment 9 out of 10 neurites collapsed, producing the highest count for collapse out of all conditions examined. These time-lapse experiments indicate the sema3A collapse pathway is independent of ROK, while Cdk5 is a crucial component of this signalling pathway.

5.1.4 CRMP-2S522A blocks sema3A collapse

CRMP-2 has been shown to be a substrate for p35/Cdk5, and the site of phosphorylation was mapped to serine 522 (PhD Thesis, T. Jacobs). The ability of the roscovitine to inhibit sema3A-mediated retraction, suggested the possibility that Cdk5 phosphorylates CRMP-2 in response to sema3A. Therefore, to examine the role of CRMP-2 in the sema3A-collapse pathway, the α2.13 cells were transfected with constructs encoding either CRMP-2, or a phosphorylation mutant, CRMP-2S522A, in combination with GFP as a fluorescent marker.

Transfected CRMP-2 appeared to have no affect on the Sema3A collapse (Figure 5.3a). In the example shown, the lamellipodia at the growth cones appeared to migrate down the neurite after 8 minutes, and by 16 minutes the neurite followed, retracting

Figure 5.3. Time-lapse analysis of CRMP-2(a) and CRMP-2S522A (b) on sema3A-induced neurite retraction.

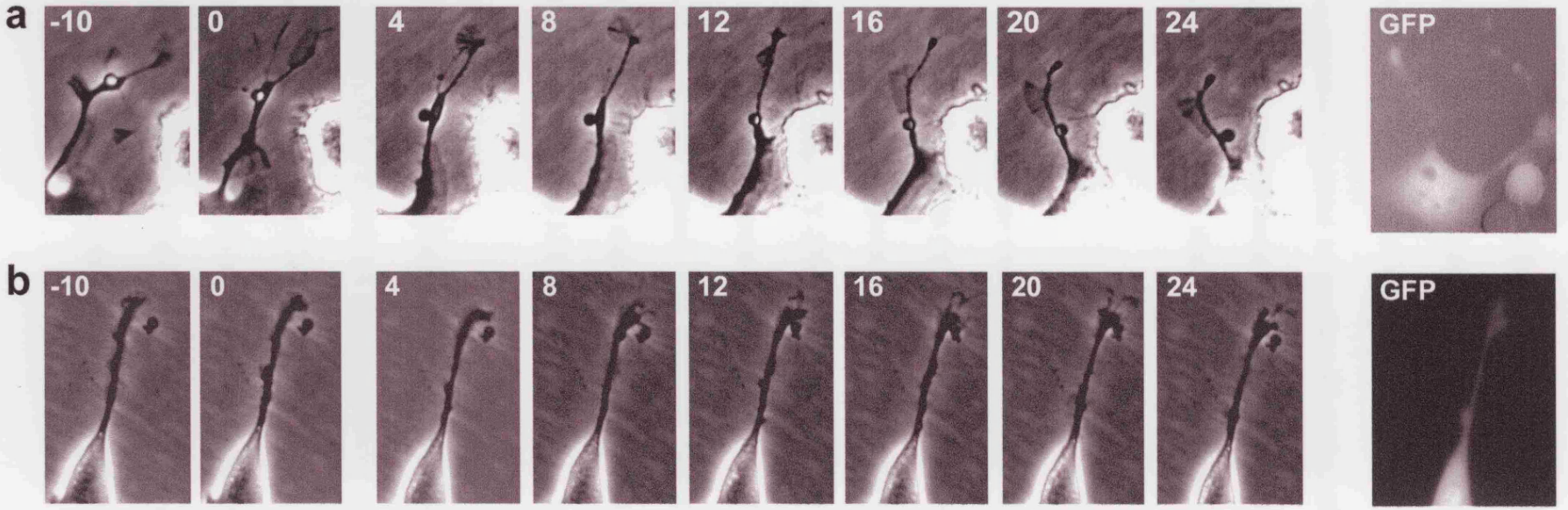

Cells were transfected with CRMP-2 (a) or CRMP-2S522A with GFP, and allowed to express overnight. Flourescence analysis was used to indentify GFP expression which was used as a maker of CRMP-2 or CRMP-2S522A expression. A microinjection needle was placed near the neurites at time point 0. Time indicated is is minutes.

from the needle. At the 30 minute time point, the neurite had retracted back to the lamellipodia, which were still intact. In other experiments, the growth cones collapsed with neurites retraction. 8 out of 10 neurites retracted. When expressed in the α2.13 cell line, CRMP-2S522A inhibited the sema3A collapse (Figure 5.3b). As with roscovitine, the neurites appeared to produce filopodia, which were not stable, but continuously grew and retracted back. By the 30 minute time point, there was no sign of neurite retraction. Counts for these cells showed that only 3 out of 10 neurites collapsed.

Each sema3A collapse time-lapse experiment was repeated ten times, and for each condition the number of neurites that retracted is summarised in Figure 5.4. With sema3A alone, 6 out of 10 neurites retracted. The clearest effect of sema3A was with α2.13 cells treated with 10μM Y-27632, where 9 out of 10 neurites retracted, which represents an increase over the control experiment. Both CRMP-2S522A expressing cells and 10μM roscovitine treated cells produced similar results with 3 out of 10 neurites retracting. This suggests that Cdk5 activity is crucial to sema3A collapse, as well as phosphorylation at serine 522 in CRMP-2.

Studies on the specificity of the roscovitine have shown that roscovitine has a IC_{50} of 17μM for CK1δ, 3.1μM for DYRK1A (Dual-specificity tyrosine-phosphorylated and regulated kinase), and 0.25μM for Cdk2, and so at the concentration used, roscovitine is fairly specific for CDK's (Bain et al, 2003). Similarly, Y-27632 has a IC_{50} of 800nM for ROK-2, 600nM for PRK-2, 8.3μM for MSK-2 and 44μM for PHK, and so again, Y-27632 is fairly specific at the concentrations used in this study, (Davies et al, 2000)

5.1.5 Quantification of sema3A collapse assay

To analyse the effects seen using time-lapse analysis in larger numbers of cells, sema-induced retraction was quantified after fixation of the cells. Cells were plated on poly-L-lysine coverslips in 1% serum media, and following transfection or inhibitor

Cell Treatment	Number Retracted
None	0/10
Sema3A	6/10
Sema3A + Rosocovitine	3/10
Sema3A + Y-27632	9/10
Sema3A + CRMP-2 expression	8/10
Sema3A + CRMP-2S522A expression	4/10

Figure 5.4. Table showing total counts from time-lapse analysis of sema3A-induced neurite retraction.
Each experiments was repeated 10 times, with a needle placed near the neurite, delivering sema3A. Each neurite was categorised to whether or not it retracted in the 30 minutes time period. Cells were treated with 10μM of each kinase inhibitor

treatment, sema3A-containing cell media was added to half the coverslips. The sema3A media (obtained from B.Eickholt) was added at a 1/50 dilution, (working concentration of 1μg/ml) and cells were then left for 30 minutes. Cells were fixed and stained (with TRITC-labelled phalloidin) following 30 minutes sema3A treatment. All transfections were performed using GFP in addition to the relevant cDNA to identify transfected cells. The absence of any peripheral structures, with the exception of

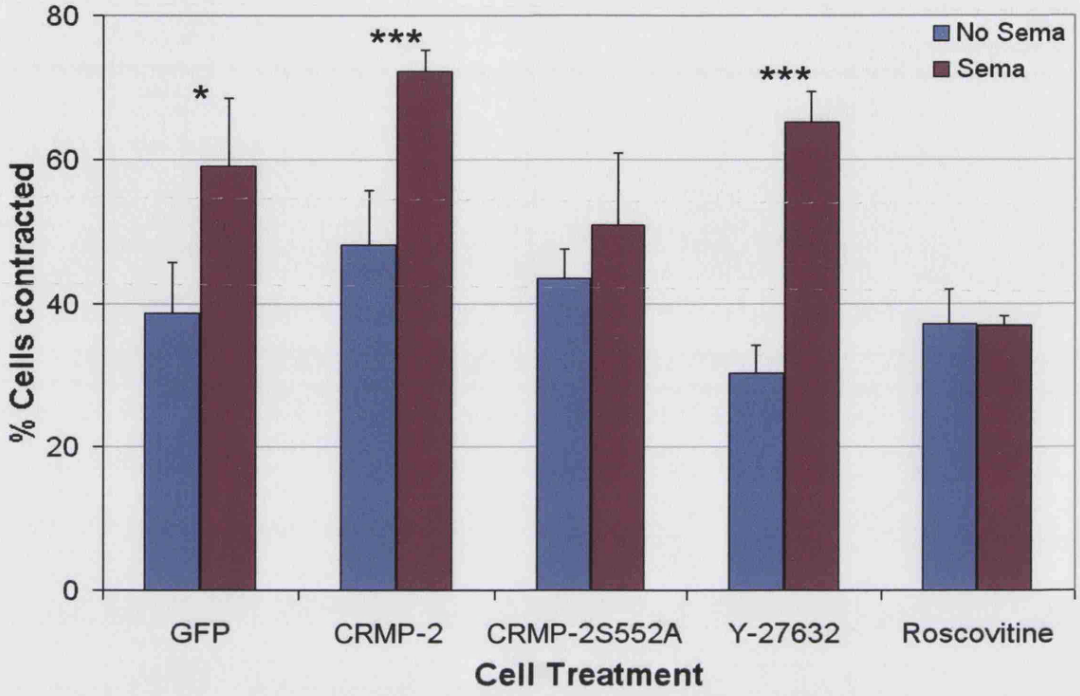

Figure 5.5. The role of CRMP-2, Cdk5 and ROK in sema3A-induced neurite retraction in α2.13 cell lines.

Cells were transfected with the constructs, or treated with the kinase inhibitors (10μM for roscovitine and Y-27632), and treated with control or sema3A media (1μg/ml). Cells were then categorised as to whether they were contracted or not. The absence of any peripheral structures was considered contracted. The number of cells counted for each treatment with/without sema3A treatment were, 469/448 for GFP, 441/368 for CRMP-2, 254/348 for CRMP-2S522A, 457/401 for Y-27632 and 437/475 for Roscovitine. Each experiment was performed in triplicate over three separate occasions. Error bars represent SEM.

microspikes, was scored as contracted. Counts for three coverslips were averaged, over three different experiments performed. Graphs show averages and SEMs.

Sema3A caused significant retraction in the GFP control experiment (Figure 5.5). There were a high percentage of contracted cells in the absence of sema3A, approximately 40%, which this rose to approximately 60% with sema3A treatment. The increase in collapsed cells following sema3A treatment was larger in cells

expressing wild type CRMP-2, where there were more contracted cells in the absence of sema3A treatment. Following the addition of sema3A there with over 70% contracted cells, suggesting that over expression of CRMP-2 may increase the collapse effect of sema3A. CRMP-2S522A blocked sema3A retraction, supporting the effects observed with the time-lapse experiments. Although there was a slight trend towards an increase in the number of contracted cells with the sema3A, this was not statistically significant.

Results in the case of sema3A treatment in the presence of roscovitine and Y-27632 confirm those of the time-lapse experiments, where Y-27632 did not inhibit neurite retraction. When cells were fixed and stained without sema3A, there were fewer contracted cells due to the inhibition of endogenous ROK, allowing activation of Rac1 and Cdc42 signalling pathways and resulting in a stimulation of more outgrowth. Against this lower background, the sema3A resulted in approximately 65% contracted cells. This difference proved to be highly significant, and shows that ROK is not required for the sema3A retraction pathway in these cells.

When α2.13 cells were treated with roscovitine, sema3A collapse was completely blocked. The number of contracted cells with the sema3A was almost identical to that of the control cells. Cdk5 is, thus, a crucial component of the sema3A collapse pathway, without which, retraction is completely inhibited.

Taken together, these results, and those indicated by the time-lapse analysis, show both roscovitine and the Cdk5 phosphorylation mutant, CRMP-2S522A, block

sema3A collapse. Y-27632 enhanced the effect of sema3A collapse, and so ROK does not appear to be required in this collapse pathway.

5.2 The role of CRMP-2 and Cdk5 in drg neurone growth cone collapse

In the nervous system, drg neurones are responsive to sema3A (Wright et al, 1995) and are frequently used for studying growth cone collapse in the sema3A pathway. These peripheral neurones respond well to sema3A *in vitro* (Fan et al, 1995; Messersmith et al, 1995) and therefore were used to determine whether effects of CRMP-2 and the kinase inhibitors observed in the α2.13 cells were relevant to sema3A signalling in primary neurones.

5.2.1 drg neurones express CRMP-2 and α2-chimaerin

CRMP-2 was isolated as a novel α2-chimaerin interactor (PhD Thesis, G.Ferrari), and so drg neurones were prepared (see Materials and Methods) and stained for endogenous CRMP-2 and α2-chimaerin. CRMP-2 distribution was punctate and membrane-associated, as observed when CRMP-2 was over expressed in N1E-115 cells, (see Chapter 3, Figure 3.3) suggesting the punctate localisation of transfected CRMP-2 is not an artefact of over-expression. The particulate CRMP-2 appeared to localise in the cell body and along the neurites, (Figure 5.6a).

Rat drg neurones appeared to express high levels of α2-chimaerin, (Figure 5.6b) throughout the cell body, and down neurites. Expression appeared to be diffuse throughout the cell.

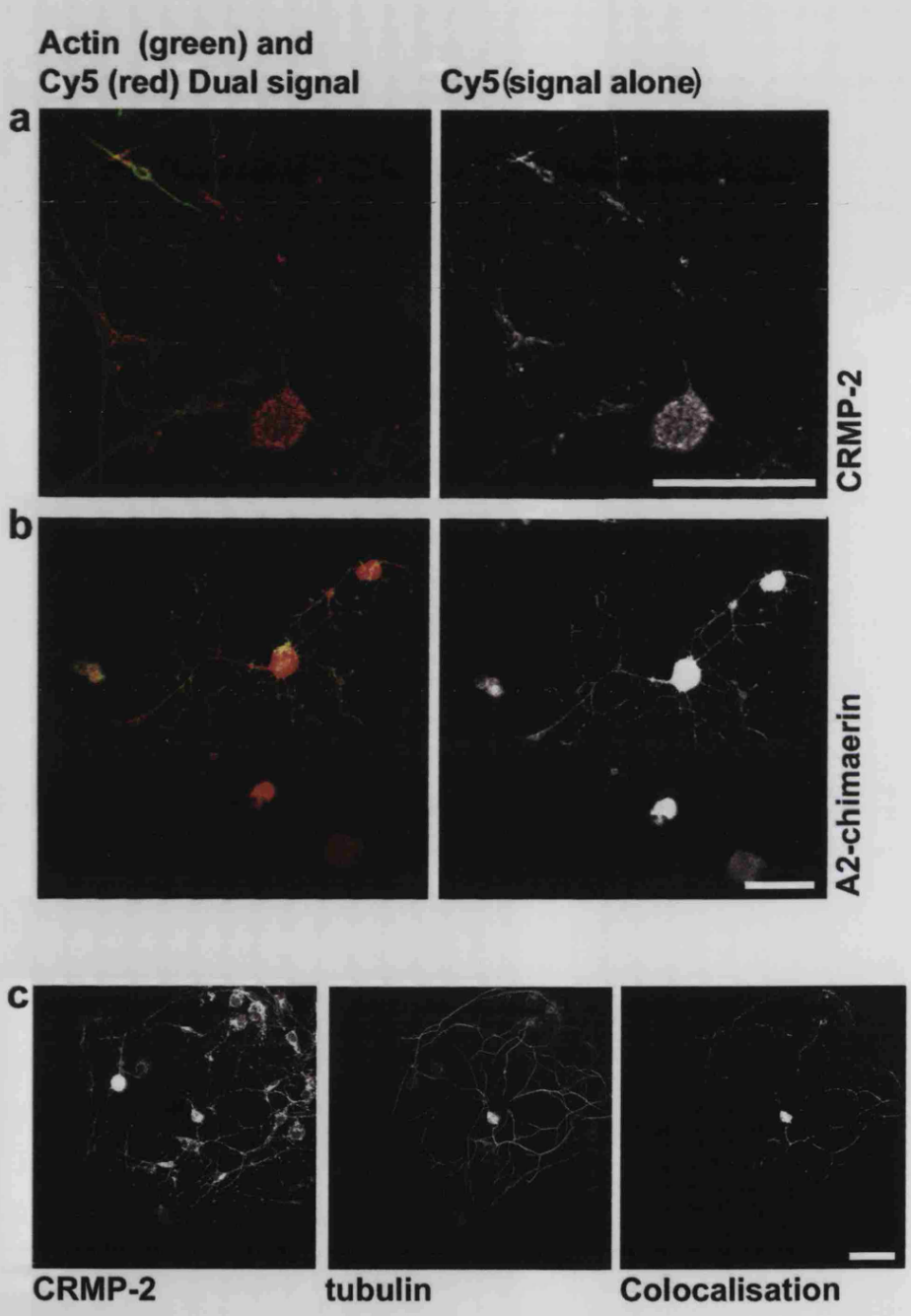

Figure 5.6. Endogenous staining of dorsal root ganglia neurones.

Neurones were fixed and stained for endogenous CRMP-2 (a) using anti CRMP-2 rabbit polyclonal (in house), and for α2-chimaerin (b), using anti-α2chimaerin rabbit polyclonal (in house). Neurones were also stained for CRMP-2 and tubulin, using anti-βtubulin mouse monoclonal (Sigma). Co-localisation of CRMP-2 and tubulin was performed using confocal microscopy and LSM software. Scale bars equal 50μm.

5.2.2 CRMP-2 co-localises with β-tubulin in rat drg neurones

CRMP-2 has been shown to bind to tubulin and regulate microtubule dynamics (Fukata et al, 2002). To investigate this association, drg neurones were stained for both CRMP-2 (rabbit polyclonals, in house) and β-tubulin (Sigma, mouse monoclonal). β-tubulin staining was intense in the neurites with some staining in the cell body, while CRMP-2 appear to stain the cell body, and some of the neurites. CRMP-2 co-localised with β-tubulin in the cell body and along parts of the neurites, suggesting they associate in some cellular compartments (Figure 5.6c).

5.2.3 Growth cone collapse in drg neurones

Sema3A-induced collapse was investigated in drg neurones to examine the signalling pathways downstream of sema3A, and CRMP-2 involvement in a well-established neuronal pathway. Time-lapse analysis of sema3A collapse in rat drg neurones growth cones was first undertaken to test the conditions and time of collapse (Figure 5.7). The drg neurones growth cones were morphologically quite different from those in α2.13 cells, which consisted of large lamellipodia with fan-like actin structures. In the drg neurones, growth cones had many more filopodia with small lamellipodia between them. The growth cones began to collapse after around 10 minutes following exposure to sema3A, and had completely retracted by 24 minutes.

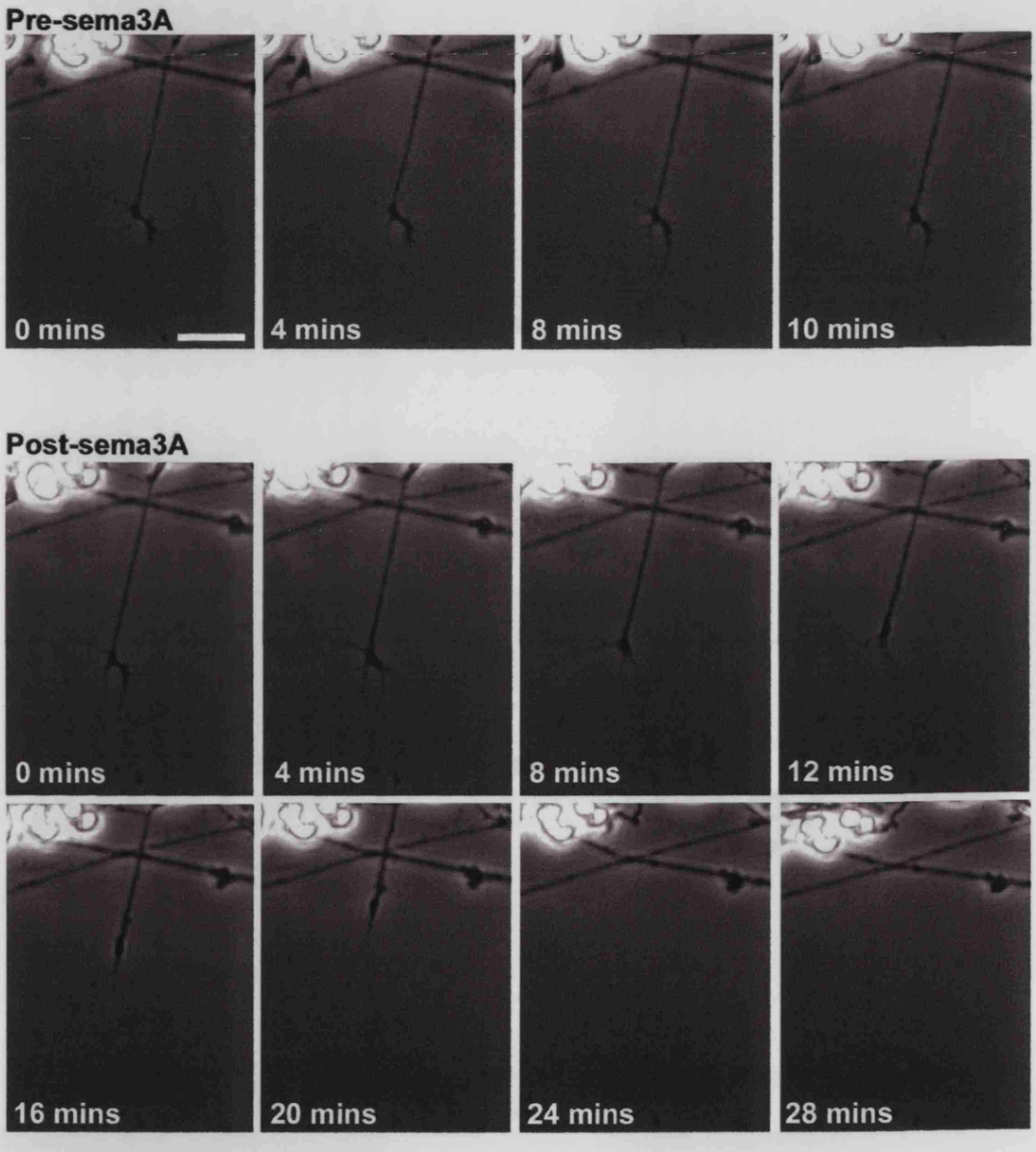

Figure 5.7. Time-lapse analysis showing collapse and retraction of rat dorsal root ganglia neurones in response to sema3A.

Growth cones were recorded for 10 minutes prior to sema3A treatment to ensure it was stable. A microinjection needle containing sema3A was placed near the growth cone, ensuring a constant flow of sema3A. Images were taken every 30 seconds for 30 minutes. Scale bar equals 20μm.

5.2.4 The role of kinases and CRMP-2 in drg growth cone collapse

To establish the role of CRMP-2 in sema3A growth cone collapse, cells were first electroporated with mammalian expression vectors encoding selected cDNAs and GFP, as a fluorescent label (see Materials and Methods), or treated with inhibitors and cultured for 16 hours. Cultures were fixed and growth cones quantified as collapsed, or not collapsed (Figure 5.8).

To test the role of Cdk5 and ROK in sema3A collapse, drg neurones were prepared as previously described (Materials and Methods, Chapter 2). Frequently, sema3A collapse assays utilise embryonic drg neurones, however it has been shown that postnatal, and even adult drg neurones are still highly responsive to sema3A (Tanelian et al, 1997). During the course of this study, in the absence of sema3A drg neurones typically had 20-30% collapsed growth cones. However when treated with sema3A this value rose significantly to 60% (Figure 5.9). Other investigators, using embryonic chick drg neurones have reported 80-90% collapse with sema3A (Eickholt et al, 1997) suggesting that whilst embryonic drg neurones may have a heightened level of sensitivity to sema3A, the use of postnatally derived cells is valid.

Roscovitine (10μM) completely inhibited the sema3A-induced collapse and in these neurones actually demonstrated a significant decrease in the number of collapsed growth cones compared with the untreated control. Treatment of drg neurones with 10μM Y-27632 had no effect on sema3A collapse, when compared with sema3A alone; 65% growth cones collapsed with sema3A treatment in the presence of ROK inhibitor.

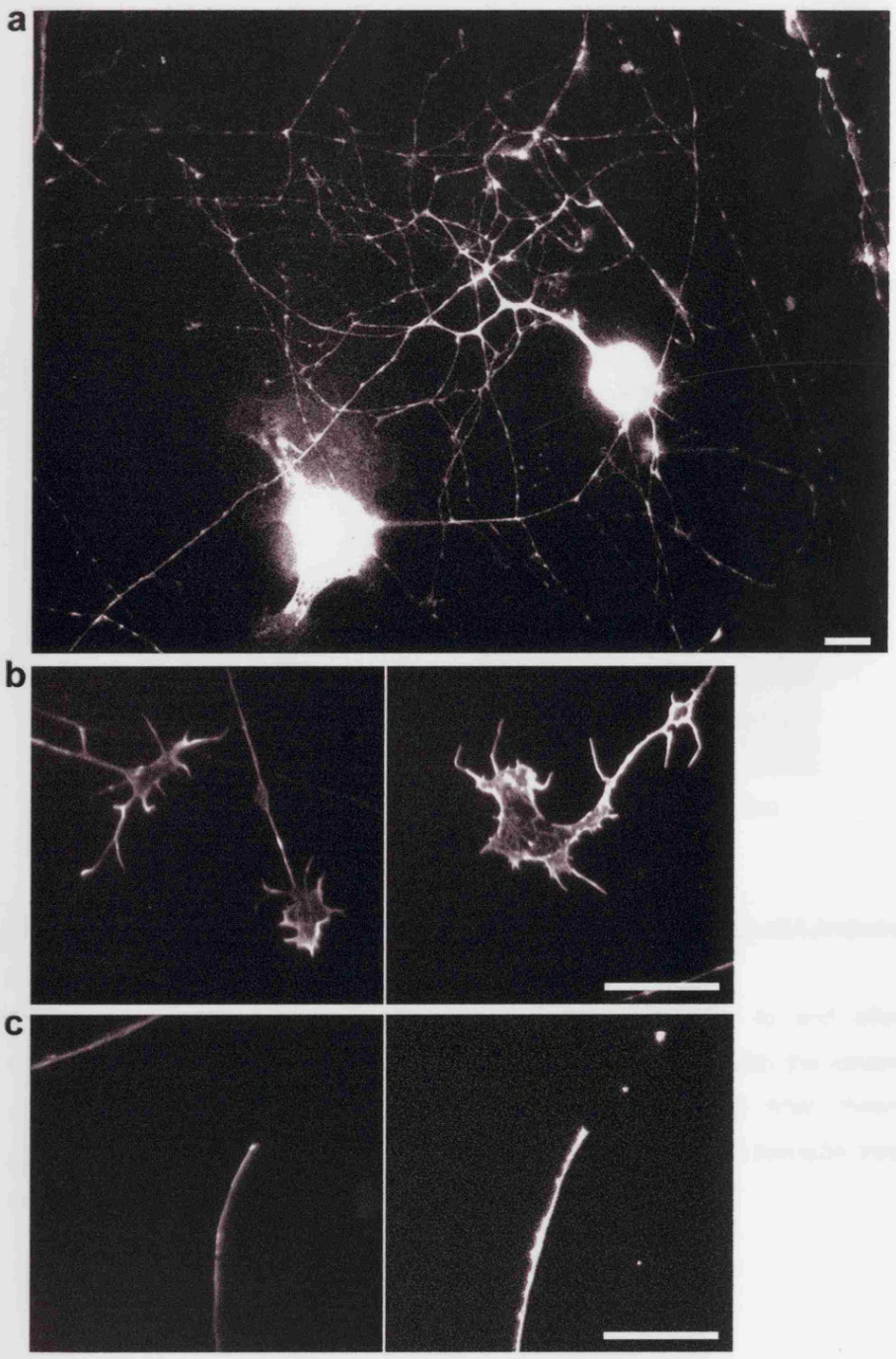

Figure 5.8. Images showing dorsal root ganglia neurones in culture.
Images show drg neurones in culture (a), drg growth cones (b) and sema3A collapsed growth cones (c). Cells were fixed following sema3A or control treatment, and then stained with TRITC-labelled phalloidin. Images were taken using axiovert microscope and digital camera, using Metamorph software. Scale bars equal 10μm.

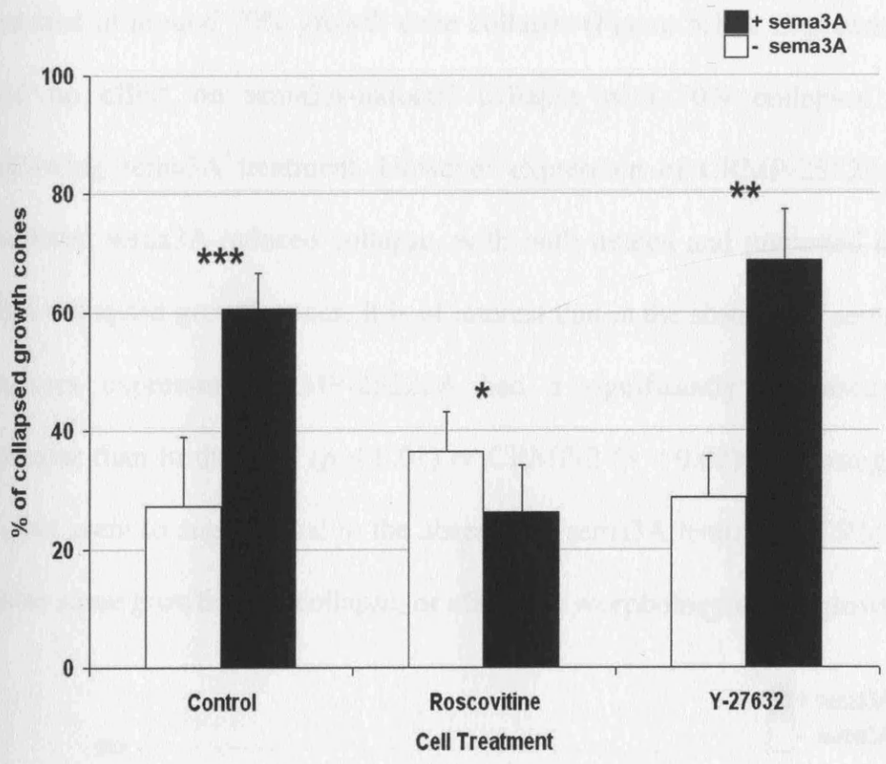

Figure 5.9. The effect of Roscovitine and Y-27632 on sema3A-induced growth cone collapse in rat drg neurones.

The percentage of collapsed growth cones is shown prior to and after sema3A treatment (1µg/ml) for cultures in control conditions or treated with the kinase inhibitors (10µM roscovitine and Y-27632). Error bars represent SD from three separate experiments. Total number of growth cones counted with/without sema3A treatment are, control 147/194, roscovitine 163/143, Y-27632 206/176.

Primary neurones show very low transfection rates by conventional methods, however with the use of Amaxa electroporator equipment, drg neurones could be successfully electroporated with cDNAs cloned in mammalian expression vectors. This equipment

was used to introduce cDNA constructs of CRMP-2 and GFP in the drg neurones to examine their effect in sema3A mediated growth cone collapse (Figure 5.10).

In control cultures were cells were electroporated with GFP alone, sema3A treatment resulted in around 70% growth cone collapse (Figure 5.10). Expression of CRMP-2 had no effect on sema3A-induced collapse with 70% collapsed growth cones following sema3A treatment. However expression of CRMP-2S522A significantly inhibited sema3A-induced collapse, with both treated and untreated cultures having 40% collapsed growth cones. It is of interest that in the absence of sema3A treatment, cultures expressing CRMP-2S522A had a significantly increased growth cone collapse than in the GFP ($p < 0.01$) or CRMP-2 ($p < 0.02$) expressing cultures. This would seem to suggest that in the absence of sema3A teratment, CRMP-2S522A can cause some growth cone collapse, or affect the morphology of the growth cones.

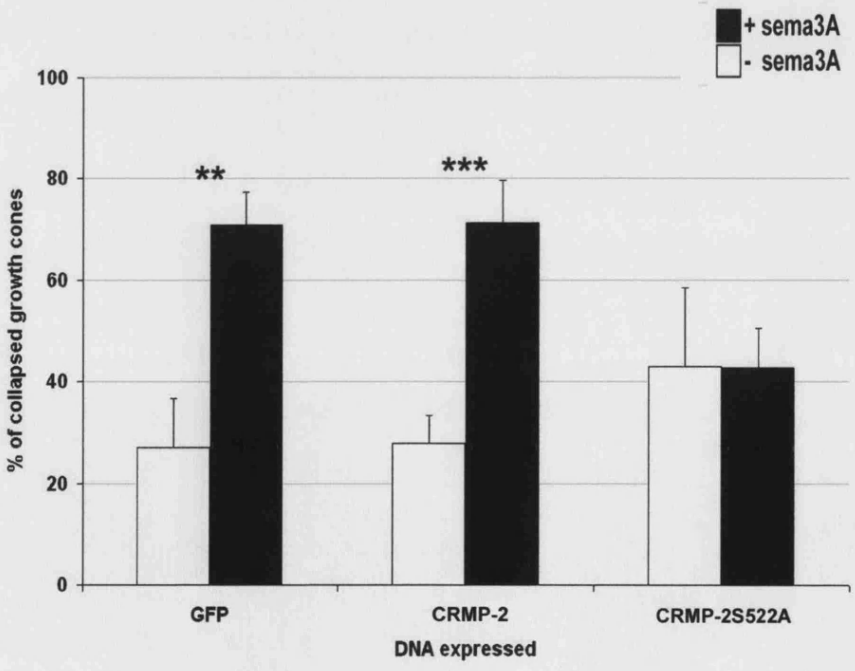

Figure 5.10. The role of CRMP-2 and S522A on sema3A-mediated growth cone collapse in rat drg neurones.

The percentage of collapsed growth cones is shown for control and sema3A treatment (1µg/ml), for cultures expressing CRMP-2 constructs. Error bars represent SD from three separate experiments. Total number of growth cones counted with/without sema3A treatment are GFP 174/148, CRMP-2 161/142, CRMP-2S522A 95/106.

Serine 522 has been shown to be a phosphorylation site for Cdk5 (PhD thesis, T. Jacobs), and the CRMP-2S522A mutation prevents phosphorylation by Cdk5 at this site. Cdk5 is crucial for sema3A-mediated collapse in drg neurones (Sasaki et al, 2002), and so the ability of CRMP-2S522A to inhibit collapse suggests CRMP-2 maybe a downstream substrate of Cdk5 in the sema3A pathway.

5.3 The role of α2-chimaerin in sema3A and PMA-induced growth cone collapse

The neuronal RacGAP, α2-chimaerin, has been shown to interact with CRMP-2 (PhD Thesis, G. Ferrari; PhD Thesis, T. Jacobs), as well as with p35, the neuronal regulator of Cdk5 (Qi et al, 2004). Therefore, it was possible that it is involved with sema3A-mediated collapse, as well as CRMP-2. This GAP contains three domains, an SH2 domain, a GAP domain and a C1 domain, which acts as a phorbol ester receptor. Binding of the artificial phorbol ester compound, PMA, to the C1 domain, changes the conformation of the protein, thereby activating the GAP activity (Ahmed et al, 1990; Ahmed et al, 1993; PhD thesis, T. Jacobs). PMA, a strong activator of PKC (Kikkawa et al, 1983), has been shown to cause collapse in drg neurones (Fournier et al, 2000).

5.3.1 α2-chimaerin in PMA-induced growth cone collapse

To examine whether α2-chimaerin plays a role in growth cones response to PMA, or whether collapse was attributable to PKC, collapse assays were performed using drg

neurones, treated with PKC inhibitor Bisindolylmaleimide (10μM) or expressing the α2-chimaerin GAP-inactive mutant, R304G.

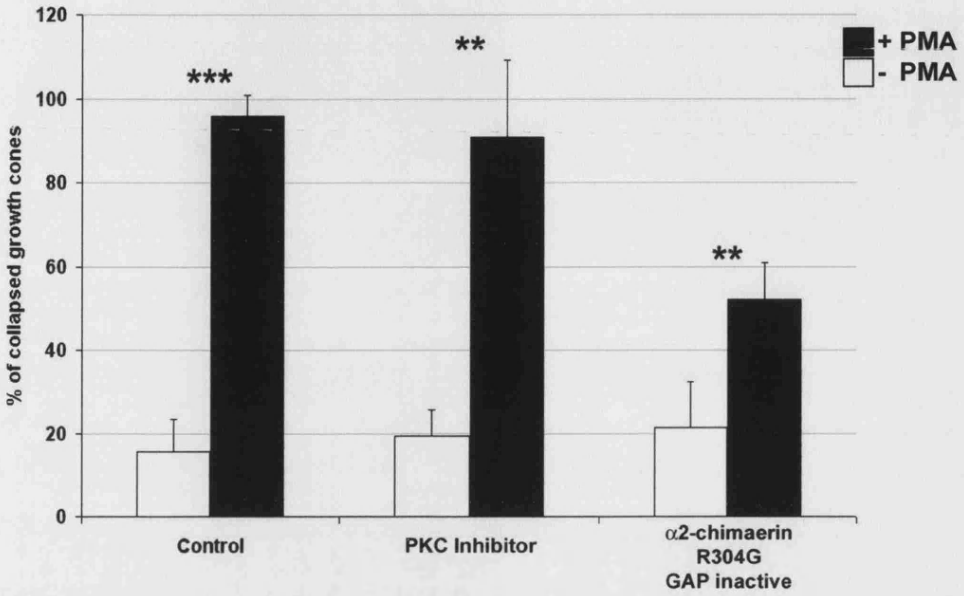

Figure 5.11. The effect of PKC inhibitor and α2-chimaerin in PMA-induced growth cone collapse in drg neurones.

The percentage of collapsed growth cones is shown with sema3A and control treatment. Error bars represent SD from three separate experiments. Total number of growth cones counted with/without sema3A treatment were control 67/49, PKC inhibitor – bisindolymaleimide (10μM) 76/53, α2chimaerin R304G 97/84.

PMA in DMSO, or DMSO control, was added to the cultures, which were left for 30 minutes before fixing and staining. PMA was used at 100nM, a final concentration that has been shown to cause growth cone collapse (Fournier et al, 2000).

PMA caused nearly 100% growth cone collapse, compared with the basal value of approximately 20% collapsed growth cones (Figure 5.11). This was a larger response

than previously observed with sema3A, where about 70% collapsed growth cones was observed. The PKC inhibitor (10μM) was added four hours prior to sema3A treatment, but had little effect on the PMA-induced collapse (Figure 5.11). Expression of the GAP inactive α2-chimaerin R304G mutant reduced the response to PMA, showing approximately 50% collapsed growth cones, which is much lower than that of PMA-treated growth cones in the presence or absence of the PKC inhibitor. These results suggest that the PMA collapse response of drg neurones is not due to activation of PKC, but to activation of α2-chimaerin. In addition, this suggests that activation of α2-chimaerin GAP activity by PMA may be sufficient to cause growth cone collapse.

5.3.2 The role of α2-chimaerin in sema3A-mediated collapse

To test if α2-chimaerin played a role in sema3A collapse, three different GFP tagged α2-chimaerin constructs were expressed in drg neurones, which were then subject to the sema3A collapse assay. The effects of α2-chimaerin, GAP inactive mutant, R304G, and an SH2 mutant, R73L, which inhibits phosphotyrosine interactions with the SH2 domain (Hall et al, 2001), were quantified (Figure 5.12).

In drg neurones expressing GFP, sema3A produced around 45% collapsed growth cones ($P < 0.0001$) (Figure 5.12), which was a lower proportion than in previous results (Figure 5.10), where sema3A typically induced 70% growth cone collapse. It is unclear why there was a difference in the proportion of collapsed growth cones.

Transfected α2-chimaerin produced a slightly larger effect with nearly 60% of growth cones collapsed following sema3A treatment ($P < 0.00001$) (Figure 5.12). However, both the α2-chimaerin GAP mutant and SH2 domain mutants totally blocked the

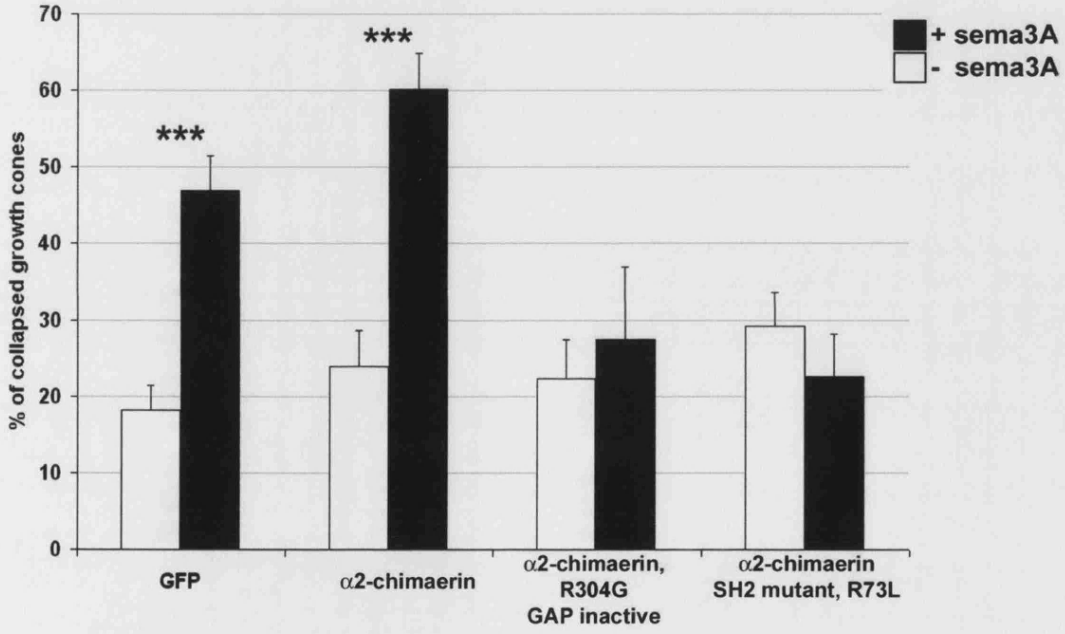

Figure 5.12. The role of α2-chimaerin in sema3A-induced growth cone collapsed in drg neurones.

The percentage of collapsed growth cones is shown with control and sema3A treatment (1μg/ml). Error bars represent SEM from three separate experiments performed in triplicate. Total number of growth cones counted with/without sema3A treatment are GFP 242/299, α2-chimaerin 214/331, α2-chimaerin R304G 239/412, α2-chimaerin R73L 223/298.

sema3A-induced collapse. Sema3A produced very little difference in the number of collapsed growth cones in cells expressing the R304G GAP inactive α2-chimaerin. Expression of the R73L SH2 mutant, caused a slight decrease in the number of collapsed growth cones following sema3A treatment, although this was not significant.

These results suggest that the GAP domain of α2-Chimaerin is crucial to the sema3A collapse pathway. In addition, a functional SH2 domain is required, implying α2-Chimaerin must interact with some other component of the pathway for collapse to occur. CRMP-2 interacts with the SH2 domain of α2-Chimaerin *in vitro*, (PhDThesis, T. Jacobs) and so CRMP-2 could be the *in vivo* target of the SH2 during sema3A collapse, but this has yet to be determined.

A

Comparison of:	With:	P Value	
GFP Control	Roscovitine Treatment	0.0001	***
GFP Control	Y-27632 Treatment	0.08	NS
Roscovitine Treatment	Y-27632 Treatment	0.0003	***
GFP Control	CRMP-2 Expression	0.5	NS
GFP Control	CRMP-2S522A Expression	0.005	**
CRMP-2 Expression	CRMP-2S522A Expression	0.0008	***

B

Comparison of:	With:	P Value	
Control	PKC Inhibitor Treatment	0.3	NS
Control	α2-chimaerin R304G Expression	0.003	**
PKC Inhibitor Treatment	α2-chimaerin R304G Expression	0.008	**
GFP Control	α2-chimaerin Expression	0.01	*
GFP Control	α2-chimaerin R304G Expression	0.009	**
GFP Control	α2-chimaerin R73L Expression	0.0003	***
α2-chimaerin Expression	α2-chimaerin R304G Expression	0.0007	***
α2-chimaerin Expression	α2-chimaerin R73L Expression	1.4×10^{-6}	***
α2-chimaerin R304G Expression	α2-chimaerin R73L Expression	0.2	NS

Figure 5.13. Table showing significance values for data from figures 5.9, 5.10, 5.11 and 5.12.

Values were obtained using students t-test, from original data.

Chapter 5 summary

To examine the role of CRMP-2 in sema3A-mediated collapse, collapse assays were performed in N1E-115 cells permanently expressing α2-chimaerin. Under control conditions, a proportion of these growth cones collapsed in response to sema3A within about 30 minutes. The ROK inhibitor Y-27632 had no effect on the sema3A-induced collapse of growth cones, while the Cdk5 inhibitor, roscovitine, blocked the sema3A collapse. Wildtype CRMP-2 did not affect the collapse, but mutation of the CRMP-2S522A, mutated at the Cdk5 phosphorylation site, blocked collapse.

Drg neurones were prepared from postnatal day 1 rats and cultured before performing growth cone collapse assays. The results from the collapse assays of drg neurones were comparable with those obtained from the cell lines. Both roscovitine and CRMP-2S522A inhibited sema3A collapse. The ROK inhibitor, Y-27632 did not inhibit the collapse, and appeared to enhance the effect, while CRMP-2 wildtype did not have an effect on collapse. Drg neurones have been shown to collapse in response to the phorbol ester, PMA, a powerful activator of PKC. In the drg neurones, treatment with a PKC inhibitor did not inhibit PMA-induced growth cone collapse, while a GAP inactive α2-chimaerin mutant reduced the percentage of collapsed growth cones by half. When studied in the sema3A collapse assay in drg neurones, wild type α2-chimaerin slightly and significantly increased the collapse effect of sema3A, while both the GAP inactive and SH2 phosphotyrosine binding inactive mutants strongly inhibited collapse.

Chapter 6

Discussion

6.1 Discussion

The Rho family of GTPases have a well established role in the regulation of the actin cytoskeleton (Ridley and Hall, 1992; Ridley et al, 1992), and their effects in the neuroblastoma cell line N1E-115 have been previously characterised (Kozma et al, 1995). In addition, the Rho GTPases are involved in growth cone remodelling, axonal guidance and neuritogenesis. CRMP-2 is homologous to the *C.elegans* protein, Unc33, which plays an important role in the development of the nervous system (Goshima et al, 1995; Minturn et al, 1995; Byk et al, 1996). CRMP-2 is also crucial for sema3A-induced growth cone collapse (Goshima et al, 1995), although no specific function has been assigned to it. The purpose of this study was to examine effects of CRMP-2 on the morphologies induced by the Rho family of GTPases. A link between CRMP-2 and the Rho GTPases had been suggested by work showing that CRMP-2 is a ROK substrate (Arimura et al, 2000), and that CRMP-2 interacts with the RacGAP α2-chimaerin (PhD thesis G. Ferrari, 2000; PhD thesis T. Jacobs.)

6.1.1 CRMP-2 switches RhoA and Rac1 morphologies

Results obtained from this study demonstrate that CRMP-2 can regulate Rho GTPase function. CRMP-2 was able to switch between RhoA and Rac1 signalling in N1E-115 neuroblastomas and Swiss 3T3 fibroblasts (Chapter 3). Co-expression of CRMP-2 with RhoAV14 produced Rac phenotypes and neurites (Figure 3.2; 3.3; 3.5), which were dependent on both Rac1 and Cdc42 (Figure 3.12). Co-expression of CRMP-2 with Rac1V12 caused localised collapse, which was dependent on RhoA (Figure 3.10)

In growth cone guidance, the local regulation of the Rho GTPases, and the ability to switch between Rac1 and RhoA signalling pathways could be very important, for example, during path finding of neuronal growth cones, which have to respond to both attractive and repulsive guidance cues as they develop (Dickson, 2002). Under these circumstances, CRMP-2 may play an important role in the regulation of the Rho GTPases in neuronal growth cones during their development.

The mechanism by which CRMP-2 was able to effect these changes remains unclear. Rac1 and RhoA have been shown to have opposing effects on neuronal cell morphology (Kozma et al, 1997; Luo, 2001), with Rac1 causing outgrowth and peripheral structures, and RhoA causing retraction. However activation of Rac1 can also lead to the activation of RhoA when expressed in fibroblasts (Ridley and Hall, 1992), although this occurs after a time delay. Therefore in these experiments, it is possible that, when co-expressed with CRMP-2, Rac1V12 was capable of signalling through to activate endogenous RhoA, causing retraction and cell rounding. This signalling does not usually occur in N1E-115 neuroblastoma cells, where Rac1 and RhoA usually act antagonistically (Kozma et al, 1997). CRMP-2 may activate an endogenous signalling mechanism from Rac1V12 to endogenous RhoA.

There is no previous evidence to indicate that RhoA can signal through to activate Rac1. In other cell types, Rac1 activation is upstream of RhoA in a hierachal relationship (Ridley et al, 1992). The morphological effects observed in this study indicate there is Rac1 activity downstream of RhoAV14 co-expressed with CRMP-2. These effects were relatively small, compared with dominant active Rac1, suggesting that there is not a strong activation of Rac1 when CRMP-2 and RhoAV14 are co-

expressed. This could be explained by activation of endogenous Rac1, which would not produce such a dramatic phenotype as the expression of Rac1V12, a strong activator of Rac1 signalling.

A possible explanation for these results would be the activation of an endogenous GAP or GEF. The experiments were carried out with dominant positive GTPases. While it is unlikely that GAPs can still exert some effect on these mutants, the endogenous GTPases could be affected by down regulation of a GAP or by up regulation of a GEF. CRMP-2 has been shown to interact with the RacGAP α2-chimaerin *in vitro* (PhD Thesis, G. Ferrari) and *in vivo* (PhD Thesis, T. Jacobs), so CRMP-2 may be able to active endogenous GAPs, to down regulate endogenous Rac1. There is so far no evidence that CRMP-2 is able to regulate α2-chimaerin GAP activities, but it may form a component of a regulatory complex, which can influence the GAP activity of α2-chimaerin, such as sequestering the Rac GAP, and allowing activation of endogenous Rac1.

Alternatively, CRMP-2 may activate endogenous GEFs, which could then activate alternative RhoGTPase members. CRMP-2 has not been shown to interact with any GEFs, although GEFs have been shown to play a role in some sema-mediated signalling. The Rho GEF, PDZ-RhoGEF binds to plexin B and is involved in semaphorin4D/plexin-B signalling pathways (Perrot et al, 2002; Swiercz et al, 2002) to activate RhoA. At present GEFs have not been identified in sema3A-mediated growth cone collapse, but it could well be that GEFs are also involved, and so may interact with CRMP-2 to influence the activity of the Rho GTPases.

The effects observed when CRMP-2 and RhoAV14 were co-expressed were small, and so rather than activating a Rac GEF, a more probable explanation may be that CRMP-2 is able to block RhoAV14 signalling, by either inhibiting RhoAV14 itself, or the downstream effector Rho-kinase (ROK), a serine/threonine kinase. CRMP-2 was found to bind directly to RhoAV14 (Chapter 4, Results 2), and so may compete with ROK for RhoA binding.

6.1.2 The enzymatic function of CRMP-2

Some clues to the function of CRMP-2 are suggested by its high degree of sequence similarity to liver dihydropyrimidinase (Wang and Strittmatter, 1997). These enzymes are involved in the breakdown of guanosine-based molecules, although at present there is no evidence to suggest CRMP-2 exhibits any enzymatic function, and some key residues are not conserved in CRMP-2 (Wang and Strittmatter, 1996). However, an interesting notion is that CRMP-2 is involved in the regulation of cGMP in the neurones. All guidance cues discovered to date can be modulated by either cGMP or cAMP, and the sema3A repulsive pathway can be reversed to an attractive pathway by increasing cGMP concentration leading to an increase in PKG activity (Song et al, 1998). CRMP-2 appears to play a role in both outgrowth (Inagaki et al, 2001; Fukata et al, 2002) and in repulsion (Goshima et al, 1995), and so regulation of intracellular cGMP levels could enable cells to regulate CRMP-2 and so control both processes. Since CRMP-2 is able to switch Rac1 and RhoA induced morphologies, it is possible that CRMP-2 acts downstream of cGMP to regulate RhoA and Rac1, and so enable growth cones to respond to sema3A in different ways.

Guanine is a purine, which consists of pyrimidine ring fused to a imidazole ring, and while dihydropyrimidinases catalyse the breakdown of pyrimidine rings. However it is still possible that the homology CRMP-2 shows with these enzymes, would still enable it to breakdown purines, possibly by catalysing the pyrimidine ring.

6.1.3 CRMP-2 interacts with RhoA and Rac1

One possible mechanism, by which CRMP-2 could alter Rho GTPases-induced morphologies, would be to bind to the GTPases altering their effector binding or upstream signalling. Binding assays were performed between CRMP-2 and the Rho GTPases, and preliminary results using dotblot assays showed that recombinant CRMP-2 bound directly to RhoA and Rac1 (Figure 4.1). Due to problems obtaining purified recombinant full length and fragments of CRMP-2 protein, it was not possible to repeat the dotblot assay with subsequent protein preparations. This suggests this interaction is variable, and is not of as high affinity as the interaction between the GTPases and their effectors, such as the Rac1/PAK interaction. Dotblots have been used to show whether interacting proteins are effectors, i.e. bind selectively to active, GTP-bound GTPases, (Manser et al, 1992, Govind et al, 2001), however due to the variability of CRMP-2 protein preparations, these could not be performed. The reason behind this difference in protein samples is not clear. It is possible that the E.coli strain used to grow the recombinant protein exhibited some differences in processing the protein, such as phosphorylation or protein folding. CRMP-2 may undergo conformational changes during bacterial expression, which could influence binding, or may need some other modification to bind to the GTPases. Although CRMP-2 interactions were detected on dotblots, they could not detected on western blots, suggesting the conformation of CRMP-2 is important for interactions. All

proteins expressed were subject to PAGE to ensure they were of the correct size and there was little breakdown, and so it is unlikely that degradation of protein affected the binding assay.

CRMP-2 is synthesised more effectively in mammalian cells, such as Cos-7 cells, and so immunoprecipitation studies with dominant negative and dominant positive GTPase constructs were performed to investigate their interaction *in vivo*. Rac1V12, RhoAV14 and Cdc42V12 could all be co-precipitated with CRMP-2 when co-expressed in Cos7 cells. The possibility that the interaction is indirect cannot be ruled out, but this result shows the proteins are capable of associating *in vivo*.

Dominant negative GTPase constructs were used in immunoprecipitation experiments to test if CRMP-2 was an effector of RhoA or Rac1V12. This procedure has been used previously to show that Cdk5 is a Rac1 effector (Nikolic et al, 1998). While CRMP-2 could be co-precipitated with RacN17, it could not with RhoAN19, suggesting that CRMP-2 is a RhoA effector. However, CRMP-2 bound to both Rac1N17 and Rac1V12, suggesting that Rac1 in a GTP-bound state was not required. However, dominant negative GTPases exert their effects by titrating out GEF activity, and so further studies would need to be performed to confirm these observations.

In an attempt to isolate the region in CRMP-2 responsible for GTPase binding, a number of protein fragments were made (Chapter 4), and used for immunoprecipitation studies in Cos7 cells. As the 1-112 CRMP-2 fragment was the only one which did not associate with either Rac1V12 or RhoAV14 in Cos cells, there may be a large interacting domain stretching from just after 112 to around 300, just

after the start of the C-terminal fragment. This would need to be confirmed with C-terminal deletions. The 3D structure of CRMP-1 has shown that the N and C-terminal halves of the protein are very closely associated, and so regions from both fragments could be involved in the interaction with the GTPases.

It is possible that CRMP-2 1-112 did not interact with Rac1 or RhoA because of its localisation. CRMP-2 and Rac1/RhoA may only interact when both are present at the membrane. Full-length CRMP-2 is membrane-associated (Minturn et al, 1995, Chapter 3), while active RhoA and Rac1 would both be transported to the membrane to exert their effects on the actin cytoskeleton (Hancock et al, 1989). However overexpression of dominant positive Rac1 or RhoA results in a diffuse localisation, so CRMP-2 1-112 would be in the same cellular compartments as Rac1 and RhoA, and so the GTPases would be available to interact with this CRMP-2 fragment.

6.1.4 CRMP-2 and ROK

RhoA is activated in response to lysophosphatidic acid (LPA), which signals through G-protein G13 (Gohla et al, 1998), to activate p115RhoGEF (Hart et al, 1998; Kranenburg et al, 1999). Once active, RhoA is able to activate its downstream effector, ROK. One of the key substrates of ROK is the myosin binding subunit (MBS) of myosin phosphatase. Myosin phosphatase binds to myosin light chain (MLC) to dephosphorylate and inactivate it. Phosphorylation of MBS by ROK inactivates it, so it can no longer downregulate MLC and hence enables formation of actin stress fibres, and myosin contraction. ROK can also directly phosphorylate MLC, enabling it to regulate MLC activity through direct and indirect mechanisms (reviewed in Amano, 2000).

One possible mechanism, by which CRMP-2 could inhibit RhoA-induced morphologies, would be to bind to and inhibit ROK, and there is evidence to link CRMP-2 to ROK. Firstly, CRMP-2 is a substrate of ROK, and mutation of the phosphorylation site, T555, can inhibit LPA-induced collapse in neurones (Arimura et al, 2000). This not only demonstrates that CRMP-2 could play a role in ROK signalling pathways, but also indicates a role of CRMP-2 in response to LPA. Secondly, CRMP-2 interacts with an N-terminal extended CRMP-1 isoform, which binds to the ROK kinase domain and blocks the kinase function (Leung et al, 2002). Therefore CRMP-2 could affect ROK function by direct association, or through association of other CRMP members.

The Rho kinase site in CRMP-2, threonine 555, was mutated to alanine to see if it played any role in the ability of CRMP-2 to affect Rho GTPase function. While wildtype CRMP-2 was able to inhibit the formation of Rac phenotypes when co-expressed with Rac1V12, CRMP-2T555A had no effect on the Rac1V12 morphologies (Chapter 3). Further experiments using kinase-inactive ROK confirmed that ROK was responsible for phosphorylating CRMP-2 at this site, and not another kinase phosphorylating the same site. Therefore CRMP-2, when expressed with Rac1V12, needs to be phosphorylated by ROK, to be able to block the formation of Rac phenotypes. This result was unexpected, as it was thought that phosphorylation of CRMP-2 by ROK would occur downstream of RhoA, when RhoAV14 and CRMP-2 were co-expressed. However, CRMP-2T555A was still able to induce the formation of Rac phenotypes when co-expressed with RhoAV14, indicating that phosphorylation of CRMP-2 by ROK is not required for this function of CRMP-2. RhoA and its effector ROK are both involved in the formation of focal adhesions

(Ridley and Hall, 1992; Leung et al, 1995), and it is possible that they will play an active role in the formation of the Rac phenotypes, allowing the peripheral membrane to adhere to the substrate and maintain the cell morphology. Therefore, cells expressing Rac1V12 may still contain active ROK available to phosphorylate CRMP-2, which appears to be required to down regulate Rac1 signalling (Chapter 3). Due to the antagonistic relationship of Rac1 and RhoA, this could lead in more RhoA/ROK signalling, potentially causing a positive feed back loop resulting in more CRMP-2 phosphorylation by ROK, and hence a greater downregulation of Rac1. The consequence of CRMP-2 phosphorylation at T555 is unknown, but this could alter its conformation or interactions with other CRMP family members. CRMP proteins form heterotetramers, similar to dihydropyrimidinases (Wang and Strittmatter, 1997), which may be functionally important. Therefore regulation of tetramer formation could alter CRMP-2 function.

6.1.5 C-terminal of CRMP-2

The C-terminal of CRMP-2 appears to be important to CRMP-2 function in the formation of axons. Overexpression of CRMP-2 in hippocampal neurones promotes the formation of multiple axons, which become long and thin (Inagaki et al, 2001). However truncation of the C-terminal 24 amino acid residues resulted in the formation of a single axon, while the truncation of the C-terminal 191 amino acid residues resulted in either a single axon or no axons at all (Inagaki et al, 2001). Furthermore, CRMP-2 is localised to neurofibrillary tangles in Alzheimer's disease (Yoshida et al, 1998), and three C-terminal phosphorylation sites, threonine 509, serine 518 and serine 522, were all hyper-phosphorylated in neurofibrillary tangles (Gu et al, 2000). These findings suggest that the C-terminal is important in the

regulation of CRMP-2 activity in neuronal morphology.

6.1.6 CRMP-2 and microtubule dynamics

CRMP-2 has been shown to bind to tubulin heterodimers (Fukata et al, 2002) and promote tubulin assembly, while deletion of the CRMP-2 tubulin-binding region can block axonal growth and branching (Fukata et al, 2002). CRMP-1, 2 and 4 all exist as two splice forms, a 64kDa isoform and an 80kDa variant isoform (Leung et al, 2002; Quinn et al, 2003). The 62kDa CRMP-2 promotes organised microtubules, while the N-terminal extended variant CRMP-2b causes disorganisation of microtubules (Yuasa-Kawada et al, 2003). Taken together these studies show that CRMP-2 plays an important role in the regulation of microtubules in the cell. Staining of drg neurones showed that CRMP-2 and tubulin colocalise in drg neurones (Chapter 5). Whether this plays any role in the ability of CRMP-2 to regulate Rho GTPases function is not clear, although microtubule dynamics affect Rho GTPase activity (see section 6.1.6).

CRMP-2 overexpression can induce neurite formation when expressed in N1E-115 cells cultured in 5% serum (Fukata et al, 2002). Although the ability to induce neurites was dependent on the presence of the tubulin-binding region, this region alone was not sufficient to promote neurite formation, indicating that other regions of CRMP-2 are needed along with the tubulin binding region to form neurites (Fukata et al, 2002). This latter observation contradicts observations in this study, where alone CRMP-2 had little effect on morphology, and those of Gu et al, 2000, where CRMP-2 over expression in Neuro2a cells caused membrane blebbing. This difference could be due to the conditions in which the N1E-115 cells were cultured. In this study cells were cultured in 10% serum, while the experiments showing CRMP-2 induces

neurites (Fukata et al, 2002) were carried out in 5% serum. N1E-115 cells undergo differentiation when deprived of serum (Reagan et al, 1990), and so the serum content of the media has a major effect on the morphology of the cells. In addition, results in this study have shown cell morphology is influenced by the substrate, which also contributes to neurite outgrowth (Sarner et al, 2000). The apparent differences in the ability of CRMP-2 to promote neurite outgrowth may be substrate dependent.

6.1.7 Microtubules and the actin cytoskeleton

There is considerable interplay between the actin cytoskeleton and the microtubule cytoskeleton, and CRMP-2 could regulate microtubule dynamics, leading to regulation of the Rho GTPases. Rac1 binds directly to tubulin (Best et al, 1996), while the downstream effector of both Rac1 and Cdc42, PAK, phosphorylates the microtubule destabilising protein, stathmin at serine 16, down regulating its effects on microtubules (Daub et al, 2001). Microtubules appear to be required for cell migration (Ballestren et al, 2000), and a number of GEF's have been found to associate with them, such as the Rac1/RhoA GEF, GEF-H1 (Ren et al, 1998) and its mouse homologue, Lfc (Glaven et al, 1999). There is a direct interaction between microtubules and actin, as well as cross-linking proteins such as MIP-90 and calponin. The growth of microtubules induces the activation of Rac1, while microtubules also enable RhoG to activate Rac1 and Cdc42 (reviewed in Waterman-Storer, 1999). The shortening of microtubules induces myosin activation and an increase in contractility, raising the possibility that RhoAGEF, GEF H1, is released and activated as microtubules depolymerise (Kolodney and Elson, 1995). Therefore, if CRMP-2 is able to regulate the assembly and disassembly of microtubules, it could have a profound affect on the RhoGTPases, and hence the actin cytoskeleton.

6.1.8 The role of actin and ROK in sema3A-mediated growth cone collapse

To examine the role on CRMP-2 in the sema3A pathway, neurite retraction assays were performed in N1E-115 cells permanently expressing α2-chimaerin. The parental N1E-115 cells have been shown to respond to sema3A (Van Horck et al, 2002), and permanent expression of α2-chimaerin induces longer neurites (Hall et al, 2001). Observations from fluorescent imaging of GTP-actin in growth cones suggest that sema3A induced growth cone collapse involves actin dissolution (Chapter 5, Figure 5.1), rather than contraction of actin filaments, which is in agreement with previous findings (Fan et al, 1993). It has been suggested that sema3A and sema3F collapse in drg neurones is independent of ROK (Arimura et al, 2000; Sahay et al, 2003). Arimura et al, (2000), indicated that sema3A collapse is independent of ROK-induced contraction, and this is in agreement with data from this study showing that sema3A induced growth cone collapse is not affected by the ROK inhibitor Y-27632 (Chapter 5, Results 3), although elsewhere the involvement of ROK in sema3A-mediated growth cone collapse has also been inferred (Dontchev et al, 2002). The lack of involvement of ROK in sema3A-mediated growth cone collapse is interesting, as several neuronal guidance cues involved in neurite retraction and inhibition of neurite growth involve RhoA and ROK. Several substrates such as Nogo, Myelin Associated Protein (MAG) and Chondroitin Sulphate Proteoglycans (CSPG), which are inhibitory to neuronal regeneration, have all been shown to activate RhoA, leading to inhibition of neuronal growth (Niederost et al, 2002; Fournier et al, 2003; Monnier et al, 2003). In addition, ephrins have been shown to activate RhoA (Wahl et al, 2000) and RhoA is also activated downstream of plexinB, (Driessens et al, 2001).

While the time-lapse analysis of sema3A-induced collapse demonstrated that ROK does not play a role in the collapse pathway (Chapter 5, Results 3, Figure 5.1), some involvement of RhoA cannot be ruled out, since RhoA activates effectors other than ROK, e.g. mDia, citron, and CRMP-2 may itself prove to function as a RhoA effector, as suggested by results in Chapter 4, Results 2. The RhoA effector, Citron contains no kinase domain (Maduale et al, 1995), although it appears to play a role in the regulation of RhoA and ROK in controlling actin assembly around cell organelles such as the Golgi (Camera et al, 2003). An alternative splice variant, Citron-kinase, which does contain a kinase domain, inhibits neurite outgrowth in N1E-115 cells (Di Cunto et al, 2003), and phosphorylates the regulatory light chain of myosin II (Yamashiro et al, 2003). Unlike ROK, it does not phosphorylate the myosin binding subunit of myosin phosphotase, and is thought to play a role in cytokinesis (Yamashiro et al, 2003). Therefore, RhoA could still be active in the collapse pathway, but signalling through an effector other than ROK. To demonstrate any involvement of RhoA, collapse assays would need to be repeated using the dominant negative RhoA, RhoAN19, or C3 toxin, which is a potent inhibitor of RhoA (Aktories et al, 1989).

6.1.9 The role of p35/Cdk5 in sema3A-mediated growth cone collapse

CRMP-2 is a substrate of p35/Cdk5, (PhD Thesis, T.Jacobs), and so considering the role CRMP-2 in sema3A collapse, any potential involvement of Cdk5 in sema3A collapse was examined using kinase inhibitors. P35/Cdk5 had been suggested to play a role in growth cone collapse (Nakayama et al, 1999) and recent results showed an

involvement in EphA2 guidance signalling (Cheng et al, 2003) and sema3A signalling (Sasaki et al, 2002). Treatment of the cells with the Cdk5 inhibitor, roscovitine (De Azevedo et al, 1997), completely blocked sema3A retraction in both the α2.13 cells and in rat drg neurones, showing that Cdk5 is an important component of the sema3A collapse pathway. During the course of this project, it was shown that drg neurones obtained from Cdk5 knockout mice did not respond appropriately to sema3A, and treatment with roscovitine blocked sema3A collapse (Sasaki et al, 2002).

The p35/Cdk5 phosphorylation site in CRMP-2 was mapped to serine522 (PhD Thesis, T.Jacobs), and this site was mutated to allow the effect of this site to be studied. While wildtype CRMP-2 did not affect neurite retraction in the α2.13 cells, or growth cone collapse in drg neurones, expression of CRMP-2S522A was able to block both sema3A-induced collapse in both cell types. The inhibition of collapse by roscovitine implicates Cdk5 phosphorylation of CRMP-2 in the sema3A-mediated collapse pathway, although phosphorylation of CRMP-2 by Cdk5 following sema3A treatment has not been shown directly. In the absence of direct evidence for the phosphorylation of CRMP-2 by Cdk5, it is possible that this site in CRMP-2 is phosphorylated by another kinase. However the phosphorylation of CRMP-2 by Cdk5, downstream of sema3A would fit with CRMP-2 playing a role in microtubule dynamics (Fukata et al, 2002). Staining of drg neurones for CRMP-2 showed that it is present throughout the length of neurites of drg neurones (Chapter 5), and not only in the growth cone. CRMP-2 has been shown to bind to and regulate tubulin assembly (Fukata et al, 2002), and co-localises with tubulin in cell staining (Chapter 5, Results 2, Figure 5.6). Consequently, Cdk5 phosphorylation of CRMP-2 may regulate CRMP-2 function in microtubule assembly. An effect on microtubules could cause neurite

retraction. P35/Cdk5, and its phosphorylation of tau, play an important role in microtubule dynamics (Baumann et al, 1993), although the consequence of CRMP-2 phosphorylation, and its downstream signalling cascade is unknown.

The involvement of Cdk5 in the sema3A pathway may be associated with phosphorylation and inactivation of PAK (Nikolic et al, 1998). This would reduce Rac1 and Cdc42 signalling to the actin cytoskeleton, which could affect the maintenance of the actin structures in the growth cone. However, there is so far no evidence that inhibition of PAK can cause growth cone collapse, although PAK has been shown to play an important role in guidance (Ang et al, 2003).

LIM kinase is transiently phosphorylated in the sema3A collapse pathway, and then phosphorylates the actin severing protein cofilin (Aizawa et al, 2001). Inhibiting either of these phosphorylation sites suppresses sema3A collapse (Aizawa et al, 2001). LIM kinase can be phosphorylated by either ROK or PAK, at the same site (Edwards et al, 1999; Maekawa et al, 1999; Ohashi et al, 2000). LIM kinase could be phosphorylated by PAK, downstream of sema3A, because ROK does not appear to be involved in sema3A-induced neurite retraction (Chapter 5, Arimura et al, 2000). However kinases related to ROK, such as MRCK, may show similar substrate specificity (Leung et al, 1998).

Although PAK, along with Dock, are required for photoreceptor guidance in *Drosophila* (Hing et al, 1999), there is presently no evidence to suggest the involvement of PAK in the sema3A collapse pathway and this would be interesting to focus on during future research.

If growth cone collapse and neurite retraction were regulated by microtubule dynamics, this may explain the lack of involvement of ROK, which has a major role in actin dynamics. However actin changes are important in sema3A growth cone collapse (Fan et al, 1993), possibly through the involvement of LIM kinase and cofilin (Aizawa et al, 2001). The breakdown of microtubules may lead to the release of the tubulin-associated RhoA GEF, GEF H1 (Kolodney and Elson, 1995), and so may activate RhoA. This raises the possibility that sema3A results in breakdown of microtubules, resulting in RhoA activation. Although this collapse pathway appears to be independent of ROK, it is possible that RhoA could cause neurite retraction though another effector. The involvement of CRMP-2 and p53/Cdk5, which have been shown to influence microtubule dynamics, in the sema3A signalling pathway strongly suggests some role in microtubule regulation during this collapse pathway.

6.1.10 Signalling pathways upstream of CRMP-2 in sema3A-mediated growth cone collapse

Information on the upstream components of sema3A signalling has come from work showing Cdk5 associates with plexinA2 via the tyrosine kinase Fyn (Sasaki et al, 2002), which phosphorylates tyr15 in Cdk5 activating it. Cdk5 and Fyn are crucial to sema3A growth cone collapse. Fyn itself phosphorylates plexinA2, although its activity does not affect the interaction with plexinA2. Therefore, it would appear activation of Fyn results in phosphorylation of both plexinA2 and Cdk5, possibly resulting in a Cdk5/plexinA2/Fyn complex. How this signals through to CRMP-2 is unclear. There may be recruitment of CRMP-2 to the complex, leading to its phosphorylation, as CRMP-2 is membrane associated (Minturn et al, 1995; Chapter 3,4). Recently, CRMP-2 has been shown to be capable of associating with plexinA,

when overexpressed in Cos-7 cells (Deo et al, 2004).

Another protein thought to play a role in CRMP function, is CRMP-3 Associated Molecule (CRAM)(or CRMP-5), which contains 563 amino acid residues and shows 50% homology with the other CRMP family proteins (Inatome et al, 2000). Although the function of CRAM is unknown, its expression is upregulated during PC12 differentiation. Associated with both CRAM and CRMP-3 is the tyrosine kinase Fes (Mitsui et al, 2002). This tyrosine kinase associates with and phosphorylates plexinA1. Kinase-inactive Fes suppresses sema3A-mediated collapse, suggesting that Fes, CRAM and CRMP-3 all play a role in the sema3A pathway (Mitsui et al, 2002). Although it is unknown whether CRMP-2 is involved in this complex, the CRMP proteins form tetrahetramers (Wang and Strittmatter, 1997), so CRMP-2 could associate with CRMP-3. Sema3A can interact with NP-1 and either plexinA1 or plexinA2. Both plexinA1 and plexinA2 can transduce sema3 signalling equally well, (Takahashi et al, 2001), so it is possible two distinct signalling pathway exists, with plexinA1 signalling through Fes, CRAM and CRMP-3, while plexinA2 signals through Fyn, Cdk5 and CRMP-2. There may be some redundancy in signalling, or these two pathways may converge downstream, perhaps at the level of the CRMP family of proteins.

6.1.11 PMA-induced growth cone collapse

Drg neurones have been shown to collapse in response to the phorbol ester, PMA (Fournier et al, 2000), which is a powerful activator of PKC (Orr et al, 1992). In this study, PKC kinase inhibitor did not block PMA-induced growth collapse. PMA is also a strong activator of α2-chimaerin (Ahmed et al, 1993), and GAP inactive α2-

chimaerin mutants reduce the percentage of collapsed growth cones by 50% (Chapter 5). These data suggest that growth cone collapse in response to PMA is due to activation of α2-chimaerin GAP activity. This implies that activation of α2-chimaerin is sufficient to cause growth cone collapse. In the sema3A pathway, α2-chimaerin appears to be required for growth cone collapse (Chpater 5, Results 3), although the signalling mechanisms that activate α2-chimaerin in response to sema3A are unknown. There is no evidence to date to show there is involvement of any phospholipids in sema3A pathway, which could activate α2-chimaerin *in vivo*. The production of diaclyglycerol (DAG) could potentially activate α2-chimaerin in this pathway, but whether DAG plays a role in collapse pathways has not been determined. DAG can be produced by PLC, activated by heterotrimeric G proteins or by PLCγ activated by tyrosine kinase (Reviewed in Liu et al, 2004), although PLC inhibition causes growth cone collapse, and it would be difficult to determine the role of PLC in growth cone guidance (Ming et al, 1999).

Under some conditions, PMA has been shown to cause phosphorylation of α-adducin by ROK (Fukata et al, 1999). α-adducin is involved in the association of spectrin and F-actin under ruffling membranes, and accumulates around the membranes of PMA stimulated Madin-Darby canine kidney (MDCK) cells. Knockout of this phosphorylation site or inhibition of either RhoA or ROK, prevents PMA induced ruffling or cell migration in these cells (Fukata et al, 1999). These observations may be cell specific, however this could suggest a role for ROK in the formation of membrane ruffles and in cell migration, processes that are involved in the guidance of neuronal growth cones. ROK does not appear to play a role in sema3A-mediated collapse, and results seemed to suggest that inhibition of ROK enhanced the effect of

sema3A (Chapter 5). This could be due to a requirement for ROK to maintain membrane ruffles, and inhibition of ROK could make the growth cones less stable, and so more susceptible to collapse.

Results show PMA treatment caused a high degree of growth cone collapse (Chapter 5, Results 3), which appears to be independent of PKC, while requiring, at least in part, the GAP activity of α2-chimaerin. However, ROK may play a role in the collapse of these growth cones if, in response to a strong activator such as phorbol ester, it is able to phosphorylate substrates other than α-adducin, like MBS, resulting in contraction rather than maintenance of the growth cone. In order to test this idea, the PMA collapse experiments would need to be repeated with the ROK inhibitor.

The effects of PMA on growth cones collapse in the presence of PKC inhibitor, and its inhibition by GAP inactive α2-chimaerin, suggest that activation of α2-chimaerin GAP activity can cause growth cone collapse. It is therefore possible that downregulation of Rac1 signalling is sufficient to collapse neuronal growth cones. Inhibition of Rac1 signalling may prevent the maintenance of the actin structures required to form the growth cone. However, activation of α2-chimaerin also enables its interaction with target proteins (PhD thesis, T. Jacobs), and these could be responsible for generating collapse

In response to sema4D, plexinB1 has been shown to bind to Rac1GTP, and prevent it from recruiting PAK (Vikis et al, 2002), and the binding of Rac1GTP to plexinB1 results in RhoA activation (Driessens et al, 2001). Thus, the prevention of signalling from Rac1GTP to PAK can, under some circumstances, ultimately result in growth

cone collapse. There are, however, some important differences between the sema4D/plexinB signalling pathway and the sema3A/plexinA1-signalling pathway. Firstly, unlike plexinB/sema4D, no RhoA GEF has been identified in sema3A-mediated guidance, and so there is no clear way of activating RhoA in response to plexinA. Although the sema3A collapse was found to be ROK-independent (Chapter 5, Results 3), the involvement of RhoA itself has not been studied. CRMP-2 and Rac1 leads to RhoA activity (Chapter 3, Results 1), and so may provide a mechanism of RhoA activation downstream of the plexins.

Secondly, Rac1 does not bind to plexin-A1 (Driessens et al, 2001; Vikis et al, 2002), and so alone this receptor has no direct way of regulating Rac1 activity. This raises the interesting possibility of CRMP-2 binding to and regulating, or being regulated by, Rac1 or RhoA, providing a link between plexinA1 and the GTPases. CRMP-2 appears to bind to Rac1 in either the active or inactive state, while only binding to active RhoA (Chapter 4), suggesting CRMP-2 could have more influence on positive RhoA signalling than positive Rac1 signalling. By analogy with the sema4D pathway, where plexinB binds to a RhoGEF and signals through RhoA, plexinA could be predicted to bind to a RacGEF and signal through active Rac1.

Although Rac1 does not bind to plexinA1, other GTPases do bind. Both Rnd1 and RhoD bind plexinA1, and compete for the same binding site. The binding of Rnd1 results in activation of plexinA1 signalling, while binding of RhoD prevents binding Rnd1 and so prevents plexinA1 signalling (Zanata et al, 2002). RhoD appears to act antagonistically to RhoA, and promotes the disassembly of stress fibres and focal adhesions (Tsubakimoto et al, 1999), as well as possibly playing a role in the

regulation of endosomes (Gasman et al, 2003). The Rnd proteins are unusual GTPases, as they have a very low intrinsic GTPase activity, and so are GTP bound. Rnd1 binds to and activates p190RhoGAP (Wennerberg et al, 2003), as well as playing a role in the development and regulation of dendritic spines (Ishikawa et al, 2003).

Sema3A collapse requires active Rac1, and expression of the dominant negative Rac1, Rac1N17 can block collapse (Jin and Strittmatter, 1997). Rac1 is usually involved in outgrowth and the production of peripheral actin structures (Ridley et al, 1992; Kozma et al, 1997). In response to the repulsive guidance receptor, EphA2, there is a transient downregulation of Rac1 activity followed by up regulation (Jurney et al, 2002). In response to both EphA2 and sema3A, Rac1 activity is required for actin reorganisation and endocytosis of the membrane (Jurney et al, 2002), which are important components of drg neurone growth cone collapse. This may explain the requirement for active Rac1 in the growth cone, and the down regulation of Rac1 may involve the GAP activity of α2-chimaerin.

6.1.12 α2-Chimaerin in sema3A-medited growth cone collapse

The RacGAP, α2-chimaerin, contains an SH2 domain and a regulating phorbol ester receptor, C1 domain, and is expressed in brain tissue and the testis (Hall et al, 1993). It is involved in neuritogenesis in N1E-115 cells (Hall et al, 2001), and interacts with CRMP-2 *in vitro* (PhD Thesis, G. Ferrari) and *in vivo* (PhD Thesis, T.Jacobs). When activated, this powerful GAP causes collapse in Cos7 cells and neurite retraction in N1E-115 neuroblastoma cells (PhD thesis, T. Jacobs). While α2-chimaerin slightly and significantly increased the collapse effect of sema3A (Chapter 5), two specific

domain mutants, the GAP inactive and SH2 phosphotyrosine binding inactive mutants, both blocked the collapse. This strongly suggests α2-chimaerin is a crucial component of the sema3A collapse pathway.

It is unclear whether α2-chimaerin can be activated by phosphorylation, or through phosphotyrosine interaction with the SH2 domain. However, its involvement in the sema3A collapse pathway requires a functional phosphotyrosine/SH2 binding. Whatever the activation mechanism is *in vivo*, it is clear from the sema3A collapse assays, that α2-chimaerin is an important component of the sema3A-mediated collapse. Sema3A-mediated collapse requires both the GAP activity and also the ability of the SH2 domain to bind phosphotyrosine. CRMP-2 is an *in vitro* target of the α2-chimearin SH2 domain, although this is not phosphotyrosine dependant (PhD thesis, T. Jacobs), suggesting the SH2 domain interacts with another target *in vivo*.

From the time-lapse analysis of GFP-actin, it was observed that the collapse involved actin reorganisation and dissolution, but not the formation of dense contracting actin structures, which is in agreement with previous observations (Fan et al, 1993). An active GAP in the growth cone could downregulate Rac1, preventing maintenance of the growth cone. That the SH2 mutant also blocked the collapse, even more efficiently than the GAP mutant, suggests that the SH2 domain of α2-chimaerin must interact with a phosphotyrosine target for α2-chimaerin to be able to exert its effects. Whether the interaction of the SH2 with its target is necessary for GAP activation or for correct localisation, is not clear, but the tyrosine kinases Fyn and Fes have both been shown to play a role in sema3A collapse, and both phosphorylate the cytoplasmic domains of plexin-As (Mitsui et al, 2002; Sasaki et al, 2003).

There is some evidence to suggest that the α2-chimaerin SH2 domain may bind to its own GAP domain to maintain an auto-inhibited state (PhD Thesis, T. Jacobs). The cytoplasmic domains of plexins have some GAP homology but no GAP function, (Rohm et al, 2000) as well as being tyrosine phosphorylated, so α2-chimaerin SH2 could bind to this region of plexins, and so localise α2-chimaerin to the area of collapse. CRMP-2 also binds to the α2-chimaerin SH2 domain when co-expressed in Cos7 and N1E-115 cells (PhD Thesis, T.Jacobs), although it is not known whether this interaction occurs in neurones, or in response to sema3A. To test these ideas, further interaction must be performed to try and identify whether CRMP-2 and α2-chimaerin interact in response to sema3A stimulation, and if not, what the *in vivo* α2-chimaerin SH2 targets are in this pathway.

6.2 Conclusion

These results have demonstrated that CRMP-2 is able to affect Rho GTPase function, and switch Rac1 and RhoA signalling. When co-expressed with RhoAV14, CRMP-2 resulted in the formation of Rac-like phenotypes and outgrowth, morphologies more usually associated with Rac1 and Cdc42 activation. Both Rac1 and Cdc42 appeared to play a role in the phenotypes, although Rac1 was the main contributor. When co-expressed with Rac1V12, CRMP-2 resulted in the activation of both Cdc42 and RhoA, resulting in collapsed phenotypes. This effect was dependant on CRMP-2 phosphorylation at T555 by ROK. These functions may involve the direct association of CRMP-2 with either Rac1 or RhoA, although further experiments must be performed to confirm whether CRMP-2 is a RhoA effector.

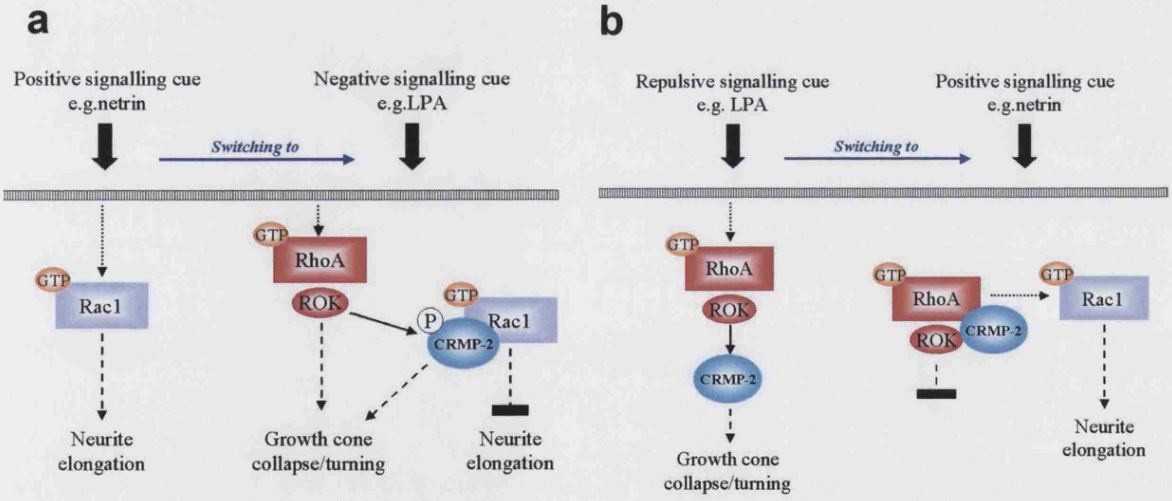

Figure 6.1. Model of CRMP-2 regulation of RhoA and Rac1 in response to guidance cues. If the guidance cue is switched from attractive to negative, CRMP-2 is phophorylated down stream of negative guidance cues, such as LPA, to inhibit Rac1 and promote growth cone collapse or growth cone turning (a). When the guidance is switched from negative to positive, CRMP-2 does not inhibit Rac1, but remains associated to the RhoA/ROK complex, to prevent further downstream signalling (b).

Over expression of Rac1V12 in the neuroblastomas could be homologous to the situation in a neuronal growth cone, where Rac1 and Cdc42 are active to enable the growth cone to advance. N1E-115 cells overexpressing Rac1V12 look similar to some neuronal growth cones. Therefore, the fact that CRMP-2 is phosphorylated at T555A when collapsing Rac1V2 dependant morphologies, suggests that CRMP-2 could be phosphorylated at this site during growth cone collapse, downstream of RhoA and ROK. In the situation of stimulation with a negative signalling cue, the Rac1 and Cdc42 activity must be reduce to allow collapse. In N1E-115 cells, the collapse of Rac1 active cells by CRMP-2 is dependant on ROK activity, and it's ability to phosphorylate CRMP-2. Therefore, CRMP-2 may be phosphorylated by ROK downstream of inhibitory signalling, such as LPA, to downregulate Rac1, and so induce collapse.

N1E-115 cells over-expressing RhoAV14 would be more analogous to a neurone which has not began to differentiate, and so under these conditions, it appears CRMP-2 may play a role to promote differentiation, although phosphorylation at T555A does not appear to be required. Alternatively, a growth cone, which is switching from a negative growth environment to a positive environment, would need to downregulate RhoA, while increasing Rac1 activity. CRMP-2 could potentially mediate this effect, by blocking RhoA signalling, although it is in this situation that CRMP-2 does not appear to be phosphorylated at T555 by ROK.

Furthermore, phosphorylation of CRMP-2 at serine 522 is crucial to sema3A-induced collapse. Cdk5 phosphorylates this site, and Cdk5 is essential to sema3A-induced collapse. It is possible that Cdk5 phosphorylates this site in CRMP-2 in response to

sema3A, but this remains to be established. α2-chimaerin was found to be another crucial component of sema3A collapse, requiring both the SH2 and the GAP domains indicating that a phosphotyrosine interaction links it to the pathway and its regulation of Rac1 is essential. Although α2-chimaerin interacts with CRMP-2, it is not known whether this interaction occurs, or is required, during sema3A-induced growth cone collapse.

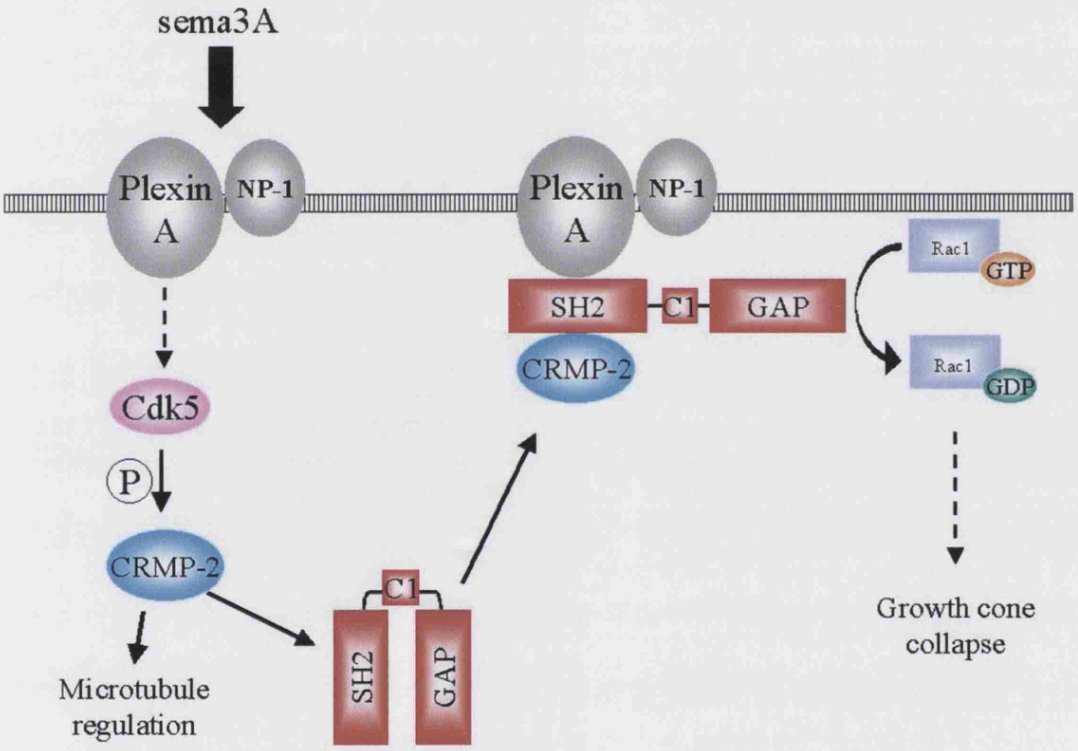

Figure 6.2. Model of CRMP-2 and α2-chimaerin downstream of sema3A.
CRMP-2 is phosphorylated by Cdk5 resulting in CRMP-2 interaction with α2-chimaerin SH2 domain. α2-chimaerin becomes activated and transported to the membrane where it interacts with plexinA. The active GAP domain down regulates Rac1 causing growth cone collapse. Alternatively, activation of α2-chimaerin by tyrosine phosphorylation or DAG, in response to sema3A, enables it to bind plexinA and downregulate Rac1, while promoting association with Cdk5 phosphorylated CRMP-2, potentially leading to regulation of microtubules

References

Ahmed,S., Kozma,R., Monfries,C., Hall,C., Lim,H.H., Smith,P., and Lim,L. (1990). Human brain n-chimaerin cDNA encodes a novel phorbol ester receptor. Biochem.J. *272*, 767-773.

Ahmed,S., Lee,J., Kozma,R., Best,A., Monfries,C., and Lim,L. (1993). A novel functional target for tumor-promoting phorbol esters and lysophosphatidic acid. The p21rac-GTPase activating protein n-chimaerin. J.Biol.Chem. *268*, 10709-10712.

Ahmed,S., Kozma,R., Hall,C., and Lim,L. (1995). GTPase-activating protein activity of n(alpha 1)-Chimaerin and effect of lipids. Methods Enzymol. *256*, 114-125.

Aizawa,H., Wakatsuki,S., Ishii,A., Moriyama,K., Sasaki,Y., Ohashi,K., Sekine-Aizawa,Y., Sehara-Fujisawa,A., Mizuno,K., Goshima,Y., and Yahara,I. (2001). Phosphorylation of cofilin by LIM-kinase is necessary for semaphorin 3A-induced growth cone collapse. Nat.Neurosci. *4*, 367-373.

Aktories,K. and Hall,A. (1989). Botulinum ADP-ribosyltransferase C3: a new tool to study low molecular weight GTP-binding proteins. Trends Pharmacol.Sci. *10*, 415-418.

Allen,W.E., Zicha,D., Ridley,A.J., and Jones,G.E. (1998). A role for Cdc42 in macrophage chemotaxis. J.Cell Biol. *141*, 1147-1157.

Amano,M., Chihara,K., Kimura,K., Fukata,Y., Nakamura,N., Matsuura,Y., and Kaibuchi,K. (1997). Formation of actin stress fibers and focal adhesions enhanced by Rho-kinase. Science *275*, 1308-1311.

Amano,M., Fukata,Y., and Kaibuchi,K. (2000). Regulation and functions of Rho-associated kinase. Exp.Cell Res. *261*, 44-51.

Ang,L.H., Kim,J., Stepensky,V., and Hing,H. (2003). Dock and Pak regulate olfactory axon pathfinding in Drosophila. Development *130*, 1307-1316.

Arimura,N., Inagaki,N., Chihara,K., Menager,C., Nakamura,N., Amano,M., Iwamatsu,A., Goshima,Y., and Kaibuchi,K. (2000). Phosphorylation of collapsin response mediator protein-2 by Rho-kinase. Evidence for two separate signaling pathways for growth cone collapse. J.Biol.Chem. *275*, 23973-23980.

Arthur,W.T., Petch,L.A., and Burridge,K. (2000). Integrin engagement suppresses RhoA activity via a c-Src-dependent mechanism. Curr.Biol. *10*, 719-722.

Arthur,W.T., Noren,N.K., and Burridge,K. (2002). Regulation of Rho family GTPases by cell-cell and cell-matrix adhesion. Biol.Res. *35*, 239-246.

Aspenstrom,P., Lindberg,U., and Hall,A. (1996). Two GTPases, Cdc42 and Rac, bind directly to a protein implicated in the immunodeficiency disorder Wiskott-Aldrich syndrome. Curr.Biol. *6*, 70-75.

Bain,J., Mclauchlan,H., Elliot,M., Cohen,P. (2003) The specificities of protein inhibitors: an update. J.Biochem. *371*, 199-204.

Ballestrem,C., Wehrle-Haller,B., and Imhof,B.A. (1998). Actin dynamics in living mammalian cells. J.Cell Sci. *111 (Pt 12)*, 1649-1658.

Bamburg,J.R., Harris,H.E., and Weeds,A.G. (1980). Partial purification and characterization of an actin depolymerizing factor from brain. FEBS Lett. *121*, 178-182.

Banzai,Y., Miki,H., Yamaguchi,H., and Takenawa,T. (2000). Essential role of neural Wiskott-Aldrich syndrome protein in neurite extension in PC12 cells and rat hippocampal primary culture cells. J.Biol.Chem. *275*, 11987-11992.

Bashaw,G.J. and Goodman,C.S. (1999). Chimeric axon guidance receptors: the cytoplasmic domains of slit and netrin receptors specify attraction versus repulsion. Cell *97*, 917-926.

Bashaw,G.J., Kidd,T., Murray,D., Pawson,T., and Goodman,C.S. (2000). Repulsive axon guidance: Abelson and Enabled play opposing roles downstream of the roundabout receptor. Cell *101*, 703-715.

Bateman,J., Shu,H., and Van Vactor,D. (2000). The guanine nucleotide exchange factor trio mediates axonal development in the Drosophila embryo. Neuron *26*, 93-106.

Baumann,K., Mandelkow,E.M., Biernat,J., Piwnica-Worms,H., and Mandelkow,E. (1993). Abnormal Alzheimer-like phosphorylation of tau-protein by cyclin-dependent kinases cdk2 and cdk5. FEBS Lett. *336*, 417-424.

Ben Yaacov,S., Le Borgne,R., Abramson,I., Schweisguth,F., and Schejter,E.D. (2001). Wasp, the Drosophila Wiskott-Aldrich syndrome gene homologue, is required for cell fate decisions mediated by Notch signaling. J.Cell Biol. *152*, 1-13.

Best,A., Ahmed,S., Kozma,R., and Lim,L. (1996). The Ras-related GTPase Rac1 binds tubulin. J.Biol.Chem. *271*, 3756-3762.

Billuart,P., Winter,C.G., Maresh,A., Zhao,X., and Luo,L. (2001). Regulating axon branch stability: the role of p190 RhoGAP in repressing a retraction signaling pathway. Cell *107*, 195-207.

Bito,H., Furuyashiki,T., Ishihara,H., Shibasaki,Y., Ohashi,K., Mizuno,K., Maekawa,M., Ishizaki,T., and Narumiya,S. (2000). A critical role for a Rho-associated kinase, p160ROCK, in determining axon outgrowth in mammalian CNS neurons. Neuron *26*, 431-441.

Blanchoin,L., Pollard,T.D., and Mullins,R.D. (2000). Interactions of ADF/cofilin, Arp2/3 complex, capping protein and profilin in remodeling of branched actin filament networks. Curr.Biol. *10*, 1273-1282.

Blanchoin,L., Amann,K.J., Higgs,H.N., Marchand,J.B., Kaiser,D.A., and Pollard,T.D. (2000). Direct observation of dendritic actin filament networks nucleated by Arp2/3 complex and WASP/Scar proteins. Nature *404*, 1007-1011.

Bokoch,G.M., Wang,Y., Bohl,B.P., Sells,M.A., Quilliam,L.A., and Knaus,U.G. (1996). Interaction of the Nck adapter protein with p21-activated kinase (PAK1). J.Biol.Chem. *271*, 25746-25749.

Borowsky,M.L. and Hynes,R.O. (1998). Layilin, a novel talin-binding transmembrane protein homologous with C-type lectins, is localized in membrane ruffles. J.Cell Biol. *143*, 429-442.

Bray,J.J., Fernyhough,P., Bamburg,J.R., and Bray,D. (1992). Actin depolymerizing factor is a component of slow axonal transport. J.Neurochem. *58*, 2081-2087.

Bridgman,P.C. (2004). Myosin-dependent transport in neurons. J.Neurobiol. *58*, 164-174.

Brouns,M.R., Matheson,S.F., Hu,K.Q., Delalle,I., Caviness,V.S., Silver,J., Bronson,R.T., and Settleman,J. (2000). The adhesion signaling molecule p190 RhoGAP is required for morphogenetic processes in neural development. Development *127*, 4891-4903.

Bruckner,K., Pasquale,E.B., and Klein,R. (1997). Tyrosine phosphorylation of transmembrane ligands for Eph receptors. Science *275*, 1640-1643.

Bruckner,K., Pablo,L.J., Scheiffele,P., Herb,A., Seeburg,P.H., and Klein,R. (1999). EphrinB ligands recruit GRIP family PDZ adaptor proteins into raft membrane microdomains. Neuron *22*, 511-524.

Bubeck,P., Pistor,S., Wehland,J., and Jockusch,B.M. (1997). Ligand recruitment by vinculin domains in transfected cells. J.Cell Sci. *110 (Pt 12)*, 1361-1371.

Buck,C.A. and Horwitz,A.F. (1987). Integrin, a transmembrane glycoprotein complex mediating cell-substratum adhesion. J.Cell Sci.Suppl *8*, 231-250.

Bulliard,C., Zurbriggen,R., Tornare,J., Faty,M., Dastoor,Z., and Dreyer,J.L. (1997). Purification of a dichlorophenol-indophenol oxidoreductase from rat and bovine synaptic membranes: tight complex association of a glyceraldehyde-3-phosphate dehydrogenase isoform, TOAD64, enolase-gamma and aldolase C. Biochem.J. *324 (Pt 2)*, 555-563.

Burbelo,P.D., Drechsel,D., and Hall,A. (1995). A conserved binding motif defines numerous candidate target proteins for both Cdc42 and Rac GTPases. J.Biol.Chem. *270*, 29071-29074.

Burridge,K. and Chrzanowska-Wodnicka,M. (1996). Focal adhesions, contractility, and signaling. Annu.Rev.Cell Dev.Biol. *12*, 463-518.

Byk,T., Dobransky,T., Cifuentes-Diaz,C., and Sobel,A. (1996). Identification and molecular characterization of Unc-33-like phosphoprotein (Ulip), a putative mammalian homolog of the axonal guidance-associated unc-33 gene product. J.Neurosci. *16*, 688-701.

Cabrera-Vera,T.M., Vanhauwe,J., Thomas,T.O., Medkova,M., Preininger,A., Mazzoni,M.R., and Hamm,H.E. (2003). Insights into G protein structure, function, and regulation. Endocr.Rev. *24*, 765-781.

Cai,H. and Reed,R.R. (1999). Cloning and characterization of neuropilin-1-interacting protein: a PSD-95/Dlg/ZO-1 domain-containing protein that interacts with the cytoplasmic domain of neuropilin-1. J.Neurosci. *19*, 6519-6527.

Camera,P., da Silva,J.S., Griffiths,G., Giuffrida,M.G., Ferrara,L., Schubert,V., Imarisio,S., Silengo,L., Dotti,C.G., and Di Cunto,F. (2003). Citron-N is a neuronal Rho-associated protein involved in Golgi organization through actin cytoskeleton regulation. Nat.Cell Biol. *5*, 1071-1078.

Carlier,M.F. and Pantaloni,D. (1982). Assembly of microtubule protein: role of guanosine di- and triphosphate nucleotides. Biochemistry *21*, 1215-1224.

Carlier,M.F., Pantaloni,D., Evans,J.A., Lambooy,P.K., Korn,E.D., and Webb,M.R. (1988). The hydrolysis of ATP that accompanies actin polymerization is essentially irreversible. FEBS Lett. *235*, 211-214.

Carlier,M.F., Jean,C., Rieger,K.J., Lenfant,M., and Pantaloni,D. (1993). Modulation of the interaction between G-actin and thymosin beta 4 by the ATP/ADP ratio: possible implication in the regulation of actin dynamics. Proc.Natl.Acad.Sci.U.S.A *90*, 5034-5038.

Castellani,V., Chedotal,A., Schachner,M., Faivre-Sarrailh,C., and Rougon,G. (2000). Analysis of the L1-deficient mouse phenotype reveals cross-talk between Sema3A and L1 signaling pathways in axonal guidance. Neuron *27*, 237-249.

Castrillon,D.H. and Wasserman,S.A. (1994). Diaphanous is required for cytokinesis in Drosophila and shares domains of similarity with the products of the limb deformity gene. Development *120*, 3367-3377.

Cattelino,A., Albertinazzi,C., Bossi,M., Critchley,D.R., and de,C., I (1999). A cell-free system to study regulation of focal adhesions and of the connected actin cytoskeleton. Mol.Biol.Cell *10*, 373-391.

Cayouette,M. and Raff,M. (2002). Asymmetric segregation of Numb: a mechanism for neural specification from Drosophila to mammals. Nat.Neurosci. *5*, 1265-1269.

Chalasani,S.H., Sabelko,K.A., Sunshine,M.J., Littman,D.R., and Raper,J.A. (2003). A chemokine, SDF-1, reduces the effectiveness of multiple axonal repellents and is required for normal axon pathfinding. J.Neurosci. *23*, 1360-1371.

Chen,W. and Lim,L. (1994). The Caenorhabditis elegans small GTP-binding protein RhoA is enriched in the nerve ring and sensory neurons during larval development. J.Biol.Chem. *269*, 32394-32404.

Cheng,Q., Sasaki,Y., Shoji,M., Sugiyama,Y., Tanaka,H., Nakayama,T., Mizuki,N., Nakamura,F., Takei,K., and Goshima,Y. (2003). Cdk5/p35 and Rho-kinase mediate ephrin-A5-induced signaling in retinal ganglion cells. Mol.Cell Neurosci. *24*, 632-645.

Chong,L.D., Park,E.K., Latimer,E., Friesel,R., and Daar,I.O. (2000). Fibroblast growth factor receptor-mediated rescue of x-ephrin B1-induced cell dissociation in Xenopus embryos. Mol.Cell Biol. *20*, 724-734.

Choquet,D., Felsenfeld,D.P., and Sheetz,M.P. (1997). Extracellular matrix rigidity causes strengthening of integrin-cytoskeleton linkages. Cell *88*, 39-48.

Chuang,T.H., Xu,X., Knaus,U.G., Hart,M.J., and Bokoch,G.M. (1993). GDP dissociation inhibitor prevents intrinsic and GTPase activating protein-stimulated GTP hydrolysis by the Rac GTP-binding protein. J.Biol.Chem. *268*, 775-778.

Chuang,T.H., Xu,X., Kaartinen,V., Heisterkamp,N., Groffen,J., and Bokoch,G.M. (1995). Abr and Bcr are multifunctional regulators of the Rho GTP-binding protein family. Proc.Natl.Acad.Sci.U.S.A *92*, 10282-10286.

Chung,C.Y., Lee,S., Briscoe,C., Ellsworth,C., and Firtel,R.A. (2000). Role of Rac in controlling the actin cytoskeleton and chemotaxis in motile cells. Proc.Natl.Acad.Sci.U.S.A *97*, 5225-5230.

Colamarino,S.A. and Tessier-Lavigne,M. (1995). The role of the floor plate in axon guidance. Annu.Rev.Neurosci. *18*, 497-529.

Cowan,C.A. and Henkemeyer,M. (2001). The SH2/SH3 adaptor Grb4 transduces B-ephrin reverse signals. Nature *413*, 174-179.

Cox,E.A., Sastry,S.K., and Huttenlocher,A. (2001). Integrin-mediated adhesion regulates cell polarity and membrane protrusion through the Rho family of GTPases. Mol.Biol.Cell *12*, 265-277.

Dasgupta,B. and Gutmann,D.H. (2003). Neurofibromatosis 1: closing the GAP between mice and men. Curr.Opin.Genet.Dev. *13*, 20-27.

Daub,H., Gevaert,K., Vandekerckhove,J., Sobel,A., and Hall,A. (2001). Rac/Cdc42 and p65PAK regulate the microtubule-destabilizing protein stathmin through phosphorylation at serine 16. J.Biol.Chem. *276*, 1677-1680.

Davenport,R.W., Dou,P., Rehder,V., and Kater,S.B. (1993). A sensory role for neuronal growth cone filopodia. Nature *361*, 721-724.

David-Pfeuty,T., Erickson,H.P., and Pantaloni,D. (1977). Guanosinetriphosphatase activity of tubulin associated with microtubule assembly. Proc.Natl.Acad.Sci.U.S.A *74*, 5372-5376.

Davies,S., Reddy,H., Caivano,M., Cohen,P. (2000). Specificity and mechanism of action of some commonly used protein kinase inhibitors. J.Biochem, *351*, 95-105.

Davy,A., Gale,N.W., Murray,E.W., Klinghoffer,R.A., Soriano,P., Feuerstein,C., and Robbins,S.M. (1999). Compartmentalized signaling by GPI-anchored ephrin-A5 requires the Fyn tyrosine kinase to regulate cellular adhesion. Genes Dev. *13*, 3125-3135.

Davy,A. and Robbins,S.M. (2000). Ephrin-A5 modulates cell adhesion and morphology in an integrin-dependent manner. EMBO J. *19*, 5396-5405.

De Azevedo,W.F., Leclerc,S., Meijer,L., Havlicek,L., Strnad,M., and Kim,S.H. (1997). Inhibition of cyclin-dependent kinases by purine analogues: crystal structure of human cdk2 complexed with roscovitine. Eur.J.Biochem. *243*, 518-526.

De Vries,L., Lou,X., Zhao,G., Zheng,B., and Farquhar,M.G. (1998). GIPC, a PDZ domain containing protein, interacts specifically with the C terminus of RGS-GAIP. Proc.Natl.Acad.Sci.U.S.A *95*, 12340-12345.

Deiner,M.S., Kennedy,T.E., Fazeli,A., Serafini,T., Tessier-Lavigne,M., and Sretavan,D.W. (1997). Netrin-1 and DCC mediate axon guidance locally at the optic disc: loss of function leads to optic nerve hypoplasia. Neuron *19*, 575-589.

Dent,E.W. and Kalil,K. (2001). Axon branching requires interactions between dynamic microtubules and actin filaments. J.Neurosci. *21*, 9757-9769.

Deo,R.C., Schmidt,E.F., Elhabazi,A., Togashi,H., Burley,S.K., and Strittmatter,S.M. (2004). Structural bases for CRMP function in plexin-dependent semaphorin3A signaling. EMBO J. *23*, 9-22.

Di Cunto,F., Calautti,E., Hsiao,J., Ong,L., Topley,G., Turco,E., and Dotto,G.P. (1998). Citron rho-interacting kinase, a novel tissue-specific ser/thr kinase encompassing the Rho-Rac-binding protein Citron. J.Biol.Chem. *273*, 29706-29711.

Di Cunto,F., Ferrara,L., Curtetti,R., Imarisio,S., Guazzone,S., Broccoli,V., Bulfone,A., Altruda,F., Vercelli,A., and Silengo,L. (2003). Role of citron kinase in dendritic morphogenesis of cortical neurons. Brain Res.Bull. *60*, 319-327.

Dickson,B.J. (2002). Molecular mechanisms of axon guidance. Science *298*, 1959-1964.

Donnai,D. and Karmiloff-Smith,A. (2000). Williams syndrome: from genotype through to the cognitive phenotype. Am.J.Med.Genet. *97*, 164-171.

Dontchev,V.D. and Letourneau,P.C. (2002). Nerve growth factor and semaphorin 3A signaling pathways interact in regulating sensory neuronal growth cone motility. J.Neurosci. *22*, 6659-6669.

Dontchev,V.D. and Letourneau,P.C. (2003). Growth cones integrate signaling from multiple guidance cues. J.Histochem.Cytochem. *51*, 435-444.

Driessens,M.H., Hu,H., Nobes,C.D., Self,A., Jordens,I., Goodman,C.S., and Hall,A. (2001). Plexin-B semaphorin receptors interact directly with active Rac and regulate the actin cytoskeleton by activating Rho. Curr.Biol. *11*, 339-344.

Dubreuil,C.I., Winton,M.J., and McKerracher,L. (2003). Rho activation patterns after spinal cord injury and the role of activated Rho in apoptosis in the central nervous system. J.Cell Biol. *162*, 233-243.

Edwards,D.C. and Gill,G.N. (1999). Structural features of LIM kinase that control effects on the actin cytoskeleton. J.Biol.Chem. *274*, 11352-11361.

Edwards,D.C., Sanders,L.C., Bokoch,G.M., and Gill,G.N. (1999). Activation of LIM-kinase by Pak1 couples Rac/Cdc42 GTPase signalling to actin cytoskeletal dynamics. Nat.Cell Biol. *1*, 253-259.

Ehler,E., van Leeuwen,F., Collard,J.G., and Salinas,P.C. (1997). Expression of Tiam-1 in the developing brain suggests a role for the Tiam-1-Rac signaling pathway in cell migration and neurite outgrowth. Mol.Cell Neurosci. *9*, 1-12.

Eickholt,B.J., Walsh,F.S., and Doherty,P. (2002). An inactive pool of GSK-3 at the leading edge of growth cones is implicated in Semaphorin 3A signaling. J.Cell Biol. *157*, 211-217.

Elowe,S., Holland,S.J., Kulkarni,S., and Pawson,T. (2001). Downregulation of the Ras-mitogen-activated protein kinase pathway by the EphB2 receptor tyrosine kinase is required for ephrin-induced neurite retraction. Mol.Cell Biol. *21*, 7429-7441.

Estrach,S., Schmidt,S., Diriong,S., Penna,A., Blangy,A., Fort,P., and Debant,A. (2002). The Human Rho-GEF trio and its target GTPase RhoG are involved in the NGF pathway, leading to neurite outgrowth. Curr.Biol. *12*, 307-312.

Eva,A. and Aaronson,S.A. (1985). Isolation of a new human oncogene from a diffuse B-cell lymphoma. Nature *316*, 273-275.

Fan,J., Mansfield,S.G., Redmond,T., Gordon-Weeks,P.R., and Raper,J.A. (1993). The organization of F-actin and microtubules in growth cones exposed to a brain-derived collapsing factor. J.Cell Biol. *121*, 867-878.

Fan,J. and Raper,J.A. (1995). Localized collapsing cues can steer growth cones without inducing their full collapse. Neuron *14*, 263-274.

Fazeli,A., Dickinson,S.L., Hermiston,M.L., Tighe,R.V., Steen,R.G., Small,C.G., Stoeckli,E.T., Keino-Masu,K., Masu,M., Rayburn,H., Simons,J., Bronson,R.T., Gordon,J.I., Tessier-Lavigne,M., and Weinberg,R.A. (1997). Phenotype of mice lacking functional Deleted in colorectal cancer (Dcc) gene. Nature *386*, 796-804.

Ferguson,K.M., Lemmon,M.A., Schlessinger,J., and Sigler,P.B. (1994). Crystal structure at 2.2 A resolution of the pleckstrin homology domain from human dynamin. Cell *79*, 199-209.

Ferrari,G.H. The interaction of the A2 chimaerin SH2 domain with target proteins. Ph.D.thesis . 1999. Ref Type: Thesis/Dissertation

Forscher,P. and Smith,S.J. (1988). Actions of cytochalasins on the organization of actin filaments and microtubules in a neuronal growth cone. J.Cell Biol. *107*, 1505-1516.

Fournier,A.E., Nakamura,F., Kawamoto,S., Goshima,Y., Kalb,R.G., and Strittmatter,S.M. (2000). Semaphorin3A enhances endocytosis at sites of receptor-F-actin colocalization during growth cone collapse. J.Cell Biol. *149*, 411-422.

Fournier,A.E., Takizawa,B.T., and Strittmatter,S.M. (2003). Rho kinase inhibition enhances axonal regeneration in the injured CNS. J.Neurosci. *23*, 1416-1423.

Franken,S., Junghans,U., Rosslenbroich,V., Baader,S.L., Hoffmann,R., Gieselmann,V., Viebahn,C., and Kappler,J. (2003). Collapsin response mediator proteins of neonatal rat brain interact with chondroitin sulfate. J.Biol.Chem. *278*, 3241-3250.

Fritz,J.L. and VanBerkum,M.F. (2002). Regulation of rho family GTPases is required to prevent axons from crossing the midline. Dev.Biol. *252*, 46-58.

Fukada,M., Watakabe,I., Yuasa-Kawada,J., Kawachi,H., Kuroiwa,A., Matsuda,Y., and Noda,M. (2000). Molecular characterization of CRMP5, a novel member of the collapsin response mediator protein family. J.Biol.Chem. *275*, 37957-37965.

Fukata,Y., Oshiro,N., Kinoshita,N., Kawano,Y., Matsuoka,Y., Bennett,V., Matsuura,Y., and Kaibuchi,K. (1999). Phosphorylation of adducin by Rho-kinase plays a crucial role in cell motility. J.Cell Biol. *145*, 347-361.

Fukata,Y., Itoh,T.J., Kimura,T., Menager,C., Nishimura,T., Shiromizu,T., Watanabe,H., Inagaki,N., Iwamatsu,A., Hotani,H., and Kaibuchi,K. (2002). CRMP-2 binds to tubulin heterodimers to promote microtubule assembly. Nat.Cell Biol. *4*, 583-591.

Fukumoto,Y., Kaibuchi,K., Hori,Y., Fujioka,H., Araki,S., Ueda,T., Kikuchi,A., and Takai,Y. (1990). Molecular cloning and characterization of a novel type of regulatory protein (GDI) for the rho proteins, ras p21-like small GTP-binding proteins. Oncogene *5*, 1321-1328.

Fukuoka,M., Miki,H., and Takenawa,T. (1997). Identification of N-WASP homologs in human and rat brain. Gene *196*, 43-48.

Gasman,S., Kalaidzidis,Y., and Zerial,M. (2003). RhoD regulates endosome dynamics through Diaphanous-related Formin and Src tyrosine kinase. Nat.Cell Biol. *5*, 195-204.

Giordano,S., Corso,S., Conrotto,P., Artigiani,S., Gilestro,G., Barberis,D., Tamagnone,L., and Comoglio,P.M. (2002). The semaphorin 4D receptor controls invasive growth by coupling with Met. Nat.Cell Biol. *4*, 720-724.

Gitai,Z., Yu,T.W., Lundquist,E.A., Tessier-Lavigne,M., and Bargmann,C.I. (2003). The netrin receptor UNC-40/DCC stimulates axon attraction and outgrowth through enabled and, in parallel, Rac and UNC-115/AbLIM. Neuron *37*, 53-65.

Glaven,J.A., Whitehead,I., Bagrodia,S., Kay,R., and Cerione,R.A. (1999). The Dbl-related protein, Lfc, localizes to microtubules and mediates the activation of Rac signaling pathways in cells. J.Biol.Chem. *274*, 2279-2285.

Goh,K.L., Cai,L., Cepko,C.L., and Gertler,F.B. (2002). Ena/VASP proteins regulate cortical neuronal positioning. Curr.Biol. *12*, 565-569.

Gohla,A., Harhammer,R., and Schultz,G. (1998). The G-protein G13 but not G12 mediates signaling from lysophosphatidic acid receptor via epidermal growth factor receptor to Rho. J.Biol.Chem. *273*, 4653-4659.

Goldberg,D.J., Foley,M.S., Tang,D., and Grabham,P.W. (2000). Recruitment of the Arp2/3 complex and mena for the stimulation of actin polymerization in growth cones by nerve growth factor. J.Neurosci.Res. *60*, 458-467.

Goshima,Y., Nakamura,F., Strittmatter,P., and Strittmatter,S.M. (1995). Collapsin-induced growth cone collapse mediated by an intracellular protein related to UNC-33. Nature *376*, 509-514.

Goshima,Y., Kawakami,T., Hori,H., Sugiyama,Y., Takasawa,S., Hashimoto,Y., Kagoshima-Maezono,M., Takenaka,T., Misu,Y., and Strittmatter,S.M. (1997). A novel action of collapsin: collapsin-1 increases antero- and retrograde axoplasmic transport independently of growth cone collapse. J.Neurobiol. *33*, 316-328.

Govind,S., Kozma,R., Monfries,C., Lim,L., and Ahmed,S. (2001). Cdc42Hs facilitates cytoskeletal reorganization and neurite outgrowth by localizing the 58-kD insulin receptor substrate to filamentous actin. J.Cell Biol. *152*, 579-594.

Gu,Y., Hamajima,N., and Ihara,Y. (2000). Neurofibrillary tangle-associated collapsin response mediator protein-2 (CRMP-2) is highly phosphorylated on Thr-509, Ser-518, and Ser-522. Biochemistry *39*, 4267-4275.

Gu,Y. and Ihara,Y. (2000). Evidence that collapsin response mediator protein-2 is involved in the dynamics of microtubules. J.Biol.Chem. *275*, 17917-17920.

Guan,J.L., Trevithick,J.E., and Hynes,R.O. (1991). Fibronectin/integrin interaction induces tyrosine phosphorylation of a 120-kDa protein. Cell Regul. *2*, 951-964.

Haas,T.A. and Plow,E.F. (1996). The cytoplasmic domain of alphaIIb beta3. A ternary complex of the integrin alpha and beta subunits and a divalent cation. J.Biol.Chem. *271*, 6017-6026.

Habets,G.G., Scholtes,E.H., Zuydgeest,D., van der Kammen,R.A., Stam,J.C., Berns,A., and Collard,J.G. (1994). Identification of an invasion-inducing gene, Tiam-1, that encodes a protein with homology to GDP-GTP exchangers for Rho-like proteins. Cell *77*, 537-549.

Hall,A. (1998). Rho GTPases and the actin cytoskeleton. Science *279*, 509-514.

Hall,C., Sin,W.C., Teo,M., Michael,G.J., Smith,P., Dong,J.M., Lim,H.H., Manser,E., Spurr,N.K., Jones,T.A., and . (1993). Alpha 2-chimerin, an SH2-containing GTPase-activating protein for the ras-related protein p21rac derived by alternate splicing of the human n-chimerin gene, is selectively expressed in brain regions and testes. Mol.Cell Biol. *13*, 4986-4998.

Hall,C., Michael,G.J., Cann,N., Ferrari,G., Teo,M., Jacobs,T., Monfries,C., and Lim,L. (2001). alpha2-chimaerin, a Cdc42/Rac1 regulator, is selectively expressed in the rat embryonic nervous system and is involved in neuritogenesis in N1E-115 neuroblastoma cells. J.Neurosci. *21*, 5191-5202.

Hancock,J.F., Magee,A.I., Childs,J.E., and Marshall,C.J. (1989). All ras proteins are polyisoprenylated but only some are palmitoylated. Cell *57*, 1167-1177.

Hancock,J.F., Paterson,H., and Marshall,C.J. (1990). A polybasic domain or palmitoylation is required in addition to the CAAX motif to localize p21ras to the plasma membrane. Cell *63*, 133-139.

Harden,N., Loh,H.Y., Chia,W., and Lim,L. (1995). A dominant inhibitory version of the small GTP-binding protein Rac disrupts cytoskeletal structures and inhibits developmental cell shape changes in Drosophila. Development *121*, 903-914.

Harlan,J.E., Hajduk,P.J., Yoon,H.S., and Fesik,S.W. (1994). Pleckstrin homology domains bind to phosphatidylinositol-4,5-bisphosphate. Nature *371*, 168-170.

Hart,M.J., Eva,A., Evans,T., Aaronson,S.A., and Cerione,R.A. (1991). Catalysis of guanine nucleotide exchange on the CDC42Hs protein by the dbl oncogene product. Nature *354*, 311-314.

Hart,M.J., Eva,A., Zangrilli,D., Aaronson,S.A., Evans,T., Cerione,R.A., and Zheng,Y. (1994). Cellular transformation and guanine nucleotide exchange activity are catalyzed by a common domain on the dbl oncogene product. J.Biol.Chem. *269*, 62-65.

Hart,M.J., Jiang,X., Kozasa,T., Roscoe,W., Singer,W.D., Gilman,A.G., Sternweis,P.C., and Bollag,G. (1998). Direct stimulation of the guanine nucleotide exchange activity of p115 RhoGEF by Galpha13. Science *280*, 2112-2114.

Higgs,H.N., Blanchoin,L., and Pollard,T.D. (1999). Influence of the C terminus of Wiskott-Aldrich syndrome protein (WASp) and the Arp2/3 complex on actin polymerization. Biochemistry *38*, 15212-15222.

Hing,H., Xiao,J., Harden,N., Lim,L., and Zipursky,S.L. (1999). Pak functions downstream of Dock to regulate photoreceptor axon guidance in Drosophila. Cell *97*, 853-863.

Hirose,M., Ishizaki,T., Watanabe,N., Uehata,M., Kranenburg,O., Moolenaar,W.H., Matsumura,F., Maekawa,M., Bito,H., and Narumiya,S. (1998). Molecular dissection of the Rho-associated protein kinase (p160ROCK)-regulated neurite remodeling in neuroblastoma N1E-115 cells. J.Cell Biol. *141* , 1625-1636.

Holmes,G.P., Negus,K., Burridge,L., Raman,S., Algar,E., Yamada,T., and Little,M.H. (1998). Distinct but overlapping expression patterns of two vertebrate slit homologs implies functional roles in CNS development and organogenesis. Mech.Dev. *79*, 57-72.

Hong,K., Hinck,L., Nishiyama,M., Poo,M.M., Tessier-Lavigne,M., and Stein,E. (1999). A ligand-gated association between cytoplasmic domains of UNC5 and DCC family receptors converts netrin-induced growth cone attraction to repulsion. Cell *97*, 927-941.

Hong,K., Nishiyama,M., Henley,J., Tessier-Lavigne,M., and Poo,M. (2000). Calcium signalling in the guidance of nerve growth by netrin-1. Nature *403*, 93-98.

Honing,H., Van Den Berg,T.K., Van Der Pol,S.M., Dijkstra,C.D., van der Kammen,R.A., Collard,J.G., and De Vries,H.E. (2003). RhoA activation promotes transendothelial migration of monocytes via ROCK. J.Leukoc.Biol.

Howard,J. and Hyman,A.A. (2003). Dynamics and mechanics of the microtubule plus end. Nature *422*, 753-758.

Hu,H., Marton,T.F., and Goodman,C.S. (2001). Plexin B mediates axon guidance in Drosophila by simultaneously inhibiting active Rac and enhancing RhoA signaling. Neuron *32*, 39-51.

Hughes,P.E. and Pfaff,M. (1998). Integrin affinity modulation. Trends Cell Biol. *8*, 359-364.

Igarashi,M., Strittmatter,S.M., Vartanian,T., and Fishman,M.C. (1993). Mediation by G proteins of signals that cause collapse of growth cones. Science *259*, 77-79.

Imondi,R., Wideman,C., and Kaprielian,Z. (2000). Complementary expression of transmembrane ephrins and their receptors in the mouse spinal cord: a possible role in constraining the orientation of longitudinally projecting axons. Development *127*, 1397-1410.

Inagaki,N., Chihara,K., Arimura,N., Menager,C., Kawano,Y., Matsuo,N., Nishimura,T., Amano,M., and Kaibuchi,K. (2001). CRMP-2 induces axons in cultured hippocampal neurons. Nat.Neurosci. *4*, 781-782.

Inatome,R., Tsujimura,T., Hitomi,T., Mitsui,N., Hermann,P., Kuroda,S., Yamamura,H., and Yanagi,S. (2000). Identification of CRAM, a novel unc-33 gene family protein that associates with CRMP3 and protein-tyrosine kinase(s) in the developing rat brain. J.Biol.Chem. *275*, 27291-27302.

Ishikawa,Y., Katoh,H., and Negishi,M. (2003). A role of Rnd1 GTPase in dendritic spine formation in hippocampal neurons. J.Neurosci. *23*, 11065-11072.

Isomura,M., Kikuchi,A., Ohga,N., and Takai,Y. (1991). Regulation of binding of rhoB p20 to membranes by its specific regulatory protein, GDP dissociation inhibitor. Oncogene *6*, 119-124.

Ito,T., Kagoshima,M., Sasaki,Y., Li,C., Udaka,N., Kitsukawa,T., Fujisawa,H., Taniguchi,M., Yagi,T., Kitamura,H., and Goshima,Y. (2000). Repulsive axon guidance molecule Sema3A inhibits branching morphogenesis of fetal mouse lung. Mech.Dev. *97*, 35-45.

Itoh,A., Miyabayashi,T., Ohno,M., and Sakano,S. (1998). Cloning and expressions of three mammalian homologues of Drosophila slit suggest possible roles for Slit in the formation and maintenance of the nervous system. Brain Res.Mol.Brain Res. *62*, 175-186.

Jacobs,T. Regulation of A2 chimaerin and associated phosphorylation pathways in neuronal signalling and morphogenesis. Ph.D.thesis . 2004.
Ref Type: Thesis/Dissertation

Jafar-Nejad,H., Norga,K., and Bellen,H. (2002). Numb: "Adapting" notch for endocytosis. Dev.Cell *3*, 155-156.

Jin,Z. and Strittmatter,S.M. (1997). Rac1 mediates collapsin-1-induced growth cone collapse. J.Neurosci. *17*, 6256-6263.

Jockusch,B.M., Bubeck,P., Giehl,K., Kroemker,M., Moschner,J., Rothkegel,M., Rudiger,M., Schluter,K., Stanke,G., and Winkler,J. (1995). The molecular architecture of focal adhesions. Annu.Rev.Cell Dev.Biol. *11*, 379-416.

Jurney,W.M., Gallo,G., Letourneau,P.C., and McLoon,S.C. (2002). Rac1-mediated endocytosis during ephrin-A2- and semaphorin 3A-induced growth cone collapse. J.Neurosci. *22*, 6019-6028.

Katoh,H., Aoki,J., Ichikawa,A., and Negishi,M. (1998). p160 RhoA-binding kinase ROKalpha induces neurite retraction. J.Biol.Chem. *273*, 2489-2492.

Kelleher,J.F., Atkinson,S.J., and Pollard,T.D. (1995). Sequences, structural models, and cellular localization of the actin-related proteins Arp2 and Arp3 from Acanthamoeba. J.Cell Biol. *131*, 385-397.

Kennedy,T.E., Serafini,T., de,l.T., Jr., and Tessier-Lavigne,M. (1994). Netrins are diffusible chemotropic factors for commissural axons in the embryonic spinal cord. Cell *78*, 425-435.

Kidd,T., Bland,K.S., and Goodman,C.S. (1999). Slit is the midline repellent for the robo receptor in Drosophila. Cell *96*, 785-794.

Kikkawa,U., Takai,Y., Tanaka,Y., Miyake,R., and Nishizuka,Y. (1983). Protein kinase C as a possible receptor protein of tumor-promoting phorbol esters. J.Biol.Chem. *258*, 11442-11445.

Kim,J.H., Liao,D., Lau,L.F., and Huganir,R.L. (1998). SynGAP: a synaptic RasGAP that associates with the PSD-95/SAP90 protein family. Neuron *20*, 683-691.

Kim,M.D., Kolodziej,P., and Chiba,A. (2002). Growth cone pathfinding and filopodial dynamics are mediated separately by Cdc42 activation. J.Neurosci. *22*, 1794-1806.

Kimura,K., Ito,M., Amano,M., Chihara,K., Fukata,Y., Nakafuku,M., Yamamori,B., Feng,J., Nakano,T., Okawa,K., Iwamatsu,A., and Kaibuchi,K. (1996). Regulation of myosin phosphatase by Rho and Rho-associated kinase (Rho-kinase). Science *273*, 245-248.

Kiosses,W.B., Daniels,R.H., Otey,C., Bokoch,G.M., and Schwartz,M.A. (1999). A role for p21-activated kinase in endothelial cell migration. J.Cell Biol. *147*, 831-844.

Knoll,B. and Drescher,U. (2002). Ephrin-As as receptors in topographic projections. Trends Neurosci. *25*, 145-149.

Kolodney,M.S. and Elson,E.L. (1995). Contraction due to microtubule disruption is associated with increased phosphorylation of myosin regulatory light chain. Proc.Natl.Acad.Sci.U.S.A *92*, 10252-10256.

Kozma,R., Ahmed,S., Best,A., and Lim,L. (1995). The Ras-related protein Cdc42Hs and bradykinin promote formation of peripheral actin microspikes and filopodia in Swiss 3T3 fibroblasts. Mol.Cell Biol. *15*, 1942-1952.

Kozma,R., Ahmed,S., Best,A., and Lim,L. (1996). The GTPase-activating protein n-chimaerin cooperates with Rac1 and Cdc42Hs to induce the formation of lamellipodia and filopodia. Mol.Cell Biol. *16*, 5069-5080.

Kozma,R., Sarner,S., Ahmed,S., and Lim,L. (1997). Rho family GTPases and neuronal growth cone remodelling: relationship between increased complexity induced by Cdc42Hs, Rac1, and acetylcholine and collapse induced by RhoA and lysophosphatidic acid. Mol.Cell Biol. *17*, 1201-1211.

Kranenburg,O., Poland,M., van Horck,F.P., Drechsel,D., Hall,A., and Moolenaar,W.H. (1999). Activation of RhoA by lysophosphatidic acid and Galpha12/13 subunits in neuronal cells: induction of neurite retraction. Mol.Biol.Cell *10*, 1851-1857.

Leeuwen,F.N., Kain,H.E., Kammen,R.A., Michiels,F., Kranenburg,O.W., and Collard,J.G. (1997). The guanine nucleotide exchange factor Tiam1 affects neuronal morphology; opposing roles for the small GTPases Rac and Rho. J.Cell Biol. *139*, 797-807.

Leisner,T.M., Wencel-Drake,J.D., Wang,W., and Lam,S.C. (1999). Bidirectional transmembrane modulation of integrin alphaIIbbeta3 conformations. J.Biol.Chem. *274*, 12945-12949.

Lena,J.Y., Bamburg,J.R., Rabie,A., and Faivre-Sarrailh,C. (1991). Actin-depolymerizing factor (ADF) in the cerebellum of the developing rat: a quantitative and immunocytochemical study. J.Neurosci.Res. *30* , 18-27.

Krause,M., Dent,E.W., Bear,J.E., Loureiro,J.J., and Gertler,F.B. (2003). Ena/VASP proteins: regulators of the actin cytoskeleton and cell migration. Annu.Rev.Cell Dev.Biol. *19*, 541-564.

Kureishi,Y., Kobayashi,S., Amano,M., Kimura,K., Kanaide,H., Nakano,T., Kaibuchi,K., and Ito,M. (1997). Rho-associated kinase directly induces smooth muscle contraction through myosin light chain phosphorylation. J.Biol.Chem. *272*, 12257-12260.

Lambrechts,A., Kwiatkowski,A.V., Lanier,L.M., Bear,J.E., Vandekerckhove,J., Ampe,C., and Gertler,F.B. (2000). cAMP-dependent protein kinase phosphorylation of EVL, a Mena/VASP relative, regulates its interaction with actin and SH3 domains. J.Biol.Chem. *275*, 36143-36151.

Lanier,L.M., Gates,M.A., Witke,W., Menzies,A.S., Wehman,A.M., Macklis,J.D., Kwiatkowski,D., Soriano,P., and Gertler,F.B. (1999). Mena is required for neurulation and commissure formation. Neuron *22*, 313-325.

Laurent,V., Loisel,T.P., Harbeck,B., Wehman,A., Grobe,L., Jockusch,B.M., Wehland,J., Gertler,F.B., and Carlier,M.F. (1999). Role of proteins of the Ena/VASP family in actin-based motility of Listeria monocytogenes. J.Cell Biol. *144*, 1245-1258.

Lee,S., Kim,J.H., Lee,C.S., Kim,J.H., Kim,Y., Heo,K., Ihara,Y., Goshima,Y., Suh,P.G., and Ryu,S.H. (2002). Collapsin response mediator protein-2 inhibits neuronal phospholipase D(2) activity by direct interaction. J.Biol.Chem. *277*, 6542-6549.

Leonardo,E.D., Hinck,L., Masu,M., Keino-Masu,K., Ackerman,S.L., and Tessier-Lavigne,M. (1997). Vertebrate homologues of C. elegans UNC-5 are candidate netrin receptors. Nature *386*, 833-838.

Leung,T., How,B.E., Manser,E., and Lim,L. (1994). Cerebellar beta 2-chimaerin, a GTPase-activating protein for p21 ras-related rac is specifically expressed in granule cells and has a unique N-terminal SH2 domain. J.Biol.Chem. *269*, 12888-12892.

Leung,T., Manser,E., Tan,L., and Lim,L. (1995). A novel serine/threonine kinase binding the Ras-related RhoA GTPase which translocates the kinase to peripheral membranes. J.Biol.Chem. *270*, 29051-29054.

Leung,T., Chen,X.Q., Manser,E., and Lim,L. (1996). The p160 RhoA-binding kinase ROK alpha is a member of a kinase family and is involved in the reorganization of the cytoskeleton. Mol.Cell Biol. *16*, 5313-5327.

Leung,T., Chen,X.Q., Tan,I., Manser,E., and Lim,L. (1998). Myotonic dystrophy kinase-related Cdc42-binding kinase acts as a Cdc42 effector in promoting cytoskeletal reorganization. Mol.Cell Biol. *18*, 130-140.

Leung,T., Ng,Y., Cheong,A., Ng,C.H., Tan,I., Hall,C., and Lim,L. (2002). p80 ROKalpha binding protein is a novel splice variant of CRMP-1 which associates with CRMP-2 and modulates RhoA-induced neuronal morphology. FEBS Lett. *532*, 445-449.

Lewis,A.K. and Bridgman,P.C. (1992). Nerve growth cone lamellipodia contain two populations of actin filaments that differ in organization and polarity. J.Cell Biol. *119*, 1219-1243.

Li,X., Saint-Cyr-Proulx,E., Aktories,K., and Lamarche-Vane,N. (2002). Rac1 and Cdc42 but not RhoA or Rho kinase activities are required for neurite outgrowth induced by the Netrin-1 receptor DCC (deleted in colorectal cancer) in N1E-115 neuroblastoma cells. J.Biol.Chem. *277*, 15207-15214.

Li,X., Meriane,M., Triki,I., Shekarabi,M., Kennedy,T.E., Larose,L., and Lamarche-Vane,N. (2002). The adaptor protein Nck-1 couples the netrin-1 receptor DCC (deleted in colorectal cancer) to the activation of the small GTPase Rac1 through an atypical mechanism. J.Biol.Chem. *277*, 37788-37797.

Li,Z., Aizenman,C.D., and Cline,H.T. (2002). Regulation of rho GTPases by crosstalk and neuronal activity in vivo. Neuron *33* , 741-750.

Liebl,E.C., Forsthoefel,D.J., Franco,L.S., Sample,S.H., Hess,J.E., Cowger,J.A., Chandler,M.P., Shupert,A.M., and Seeger,M.A. (2000). Dosage-sensitive, reciprocal genetic interactions between the Abl tyrosine kinase and the putative GEF trio reveal trio's role in axon pathfinding. Neuron *26*, 107-118.

Lim,L., Manser,E., Leung,T., and Hall,C. (1996). Regulation of phosphorylation pathways by p21 GTPases. The p21 Ras-related Rho subfamily and its role in phosphorylation signalling pathways. Eur.J.Biochem. *242*, 171-185.

Liu,N.J., Chakrabarti,S., and Gintzler,A.R. (2004). Chronic morphine-induced loss of the facilitative interaction between vasoactive intestinal polypeptide and delta-opioid: involvement of protein kinase C and phospholipase Cbetas. Brain Res. *1010*, 1-9.

Loisel,T.P., Boujemaa,R., Pantaloni,D., and Carlier,M.F. (1999). Reconstitution of actin-based motility of Listeria and Shigella using pure proteins. Nature *401*, 613-616.

Loo,D.T., Kanner,S.B., and Aruffo,A. (1998). Filamin binds to the cytoplasmic domain of the beta1-integrin. Identification of amino acids responsible for this interaction. J.Biol.Chem. *273*, 23304-23312.

Lu,Q., Sun,E.E., Klein,R.S., and Flanagan,J.G. (2001). Ephrin-B reverse signaling is mediated by a novel PDZ-RGS protein and selectively inhibits G protein-coupled chemoattraction. Cell *105*, 69-79.

Luo,L. (2000). Rho GTPases in neuronal morphogenesis. Nat.Rev.Neurosci. *1*, 173-180.

Ma,L., Rohatgi,R., and Kirschner,M.W. (1998). The Arp2/3 complex mediates actin polymerization induced by the small GTP-binding protein Cdc42. Proc.Natl.Acad.Sci.U.S.A *95*, 15362-15367.

Machesky,L.M. and Insall,R.H. (1998). Scar1 and the related Wiskott-Aldrich syndrome protein, WASP, regulate the actin cytoskeleton through the Arp2/3 complex. Curr.Biol. *8*, 1347-1356.

Machesky,L.M., Mullins,R.D., Higgs,H.N., Kaiser,D.A., Blanchoin,L., May,R.C., Hall,M.E., and Pollard,T.D. (1999). Scar, a WASp-related protein, activates nucleation of actin filaments by the Arp2/3 complex. Proc.Natl.Acad.Sci.U.S.A *96*, 3739-3744.

Machesky,L.M. and Insall,R.H. (1999). Signaling to actin dynamics. J.Cell Biol. *146*, 267-272.

Madaule,P., Furuyashiki,T., Reid,T., Ishizaki,T., Watanabe,G., Morii,N., and Narumiya,S. (1995). A novel partner for the GTP-bound forms of rho and rac. FEBS Lett. *377*, 243-248.

Maekawa,M., Ishizaki,T., Boku,S., Watanabe,N., Fujita,A., Iwamatsu,A., Obinata,T., Ohashi,K., Mizuno,K., and Narumiya,S. (1999). Signaling from Rho to the actin cytoskeleton through protein kinases ROCK and LIM-kinase. Science *285*, 895-898.

Manser,E., Leung,T., Monfries,C., Teo,M., Hall,C., and Lim,L. (1992). Diversity and versatility of GTPase activating proteins for the p21rho subfamily of ras G proteins detected by a novel overlay assay. J.Biol.Chem. *267*, 16025-16028.

Manser,E., Leung,T., Salihuddin,H., Zhao,Z.S., and Lim,L. (1994). A brain serine/threonine protein kinase activated by Cdc42 and Rac1. Nature *367*, 40-46.

Manser,E., Huang,H.Y., Loo,T.H., Chen,X.Q., Dong,J.M., Leung,T., and Lim,L. (1997). Expression of constitutively active alpha-PAK reveals effects of the kinase on actin and focal complexes. Mol.Cell Biol. *17*, 1129-1143.

Manser,E., Loo,T.H., Koh,C.G., Zhao,Z.S., Chen,X.Q., Tan,L., Tan,I., Leung,T., and Lim,L. (1998). PAK kinases are directly coupled to the PIX family of nucleotide exchange factors. Mol.Cell *1*, 183-192.

Masliah,E., Terry,R., and Buzsaki,G. (1989). Thalamic nuclei in Alzheimer disease: evidence against the cholinergic hypothesis of plaque formation. Brain Res. *493*, 240-246.

Masuda,T., Tsuji,H., Taniguchi,M., Yagi,T., Tessier-Lavigne,M., Fujisawa,H., Okado,N., and Shiga,T. (2003). Differential non-target-derived repulsive signals play a critical role in shaping initial axonal growth of dorsal root ganglion neurons. Dev.Biol. *254*, 289-302.

Matsudaira,P., Mandelkow,E., Renner,W., Hesterberg,L.K., and Weber,K. (1983). Role of fimbrin and villin in determining the interfilament distances of actin bundles. Nature *301*, 209-214.

Mazia,D., Schatten,G., and Sale,W. (1975). Adhesion of cells to surfaces coated with polylysine. Applications to electron microscopy. J.Cell Biol. *66*, 198-200.

McGlade,J., Brunkhorst,B., Anderson,D., Mbamalu,G., Settleman,J., Dedhar,S., Rozakis-Adcock,M., Chen,L.B., and Pawson,T. (1993). The N-terminal region of GAP regulates cytoskeletal structure and cell adhesion. EMBO J. *12*, 3073-3081.

Messersmith,E.K., Leonardo,E.D., Shatz,C.J., Tessier-Lavigne,M., Goodman,C.S., and Kolodkin,A.L. (1995). Semaphorin III can function as a selective chemorepellent to pattern sensory projections in the spinal cord. Neuron *14*, 949-959.

Miao,H., Burnett,E., Kinch,M., Simon,E., and Wang,B. (2000). Activation of EphA2 kinase suppresses integrin function and causes focal-adhesion-kinase dephosphorylation. Nat.Cell Biol. *2*, 62-69.

Michaelson,D., Silletti,J., Murphy,G., D'Eustachio,P., Rush,M., and Philips,M.R. (2001). Differential localization of Rho GTPases in live cells: regulation by hypervariable regions and RhoGDI binding. J.Cell Biol. *152*, 111-126.

Michiels,F., Habets,G.G., Stam,J.C., van der Kammen,R.A., and Collard,J.G. (1995). A role for Rac in Tiam1-induced membrane ruffling and invasion. Nature *375*, 338-340.

Miki,H., Miura,K., and Takenawa,T. (1996). N-WASP, a novel actin-depolymerizing protein, regulates the cortical cytoskeletal rearrangement in a PIP2-dependent manner downstream of tyrosine kinases. EMBO J. *15*, 5326-5335.

Miki,H., Suetsugu,S., and Takenawa,T. (1998). WAVE, a novel WASP-family protein involved in actin reorganization induced by Rac. EMBO J. *17*, 6932-6941.

Mikule,K., Gatlin,J.C., de la Houssaye,B.A., and Pfenninger,K.H. (2002). Growth cone collapse induced by semaphorin 3A requires 12/15-lipoxygenase. J.Neurosci. *22*, 4932-4941.

Minamide,L.S., Striegl,A.M., Boyle,J.A., Meberg,P.J., and Bamburg,J.R. (2000). Neurodegenerative stimuli induce persistent ADF/cofilin-actin rods that disrupt distal neurite function. Nat.Cell Biol. *2*, 628-636.

Ming,G., Song,H., Berninger,B., Inagaki,N., Tessier-Lavigne,M., and Poo,M. (1999). Phospholipase C-gamma and phosphoinositide 3-kinase mediate cytoplasmic signaling in nerve growth cone guidance. Neuron *23*, 139-148.

Minturn,J.E., Fryer,H.J., Geschwind,D.H., and Hockfield,S. (1995). TOAD-64, a gene expressed early in neuronal differentiation in the rat, is related to unc-33, a C. elegans gene involved in axon outgrowth. J.Neurosci. *15*, 6757-6766.

Mitchell,K.J., Doyle,J.L., Serafini,T., Kennedy,T.E., Tessier-Lavigne,M., Goodman,C.S., and Dickson,B.J. (1996). Genetic analysis of Netrin genes in Drosophila: Netrins guide CNS commissural axons and peripheral motor axons. Neuron *17*, 203-215.

Mitsui,N., Inatome,R., Takahashi,S., Goshima,Y., Yamamura,H., and Yanagi,S. (2002). Involvement of Fes/Fps tyrosine kinase in semaphorin3A signaling. EMBO J. *21*, 3274-3285.

Miyata,H., Nishiyama,S., Akashi,K., and Kinosita,K., Jr. (1999). Protrusive growth from giant liposomes driven by actin polymerization. Proc.Natl.Acad.Sci.U.S.A *96*, 2048-2053.

Mizuno,K., Okano,I., Ohashi,K., Nunoue,K., Kuma,K., Miyata,T., and Nakamura,T. (1994). Identification of a human cDNA encoding a novel protein kinase with two repeats of the LIM/double zinc finger motif. Oncogene *9*, 1605-1612.

Mizuno,K., Okano,I., Ohashi,K., Nunoue,K., Kuma,K., Miyata,T., and Nakamura,T. (1994). Identification of a human cDNA encoding a novel protein kinase with two repeats of the LIM/double zinc finger motif. Oncogene *9*, 1605-1612.

Mogilner,A. and Oster,G. (1996). Cell motility driven by actin polymerization. Biophys.J. *71*, 3030-3045.

Monnier,P.P., Sierra,A., Schwab,J.M., Henke-Fahle,S., and Mueller,B.K. (2003). The Rho/ROCK pathway mediates neurite growth-inhibitory activity associated with the chondroitin sulfate proteoglycans of the CNS glial scar. Mol.Cell Neurosci. *22*, 319-330.

Moulder,G.L., Huang,M.M., Waterston,R.H., and Barstead,R.J. (1996). Talin requires beta-integrin, but not vinculin, for its assembly into focal adhesion-like structures in the nematode Caenorhabditis elegans. Mol.Biol.Cell *7*, 1181-1193.

Mukai,M., Togawa,A., Imamura,F., Iwasaki,T., Ayaki,M., Mammoto,T., Nakamura,H., Tatsuta,M., and Inoue,M. (2002). Sustained tyrosine-phosphorylation of FAK through Rho-dependent adhesion to fibronectin is essential for cancer cell migration. Anticancer Res. *22*, 3175-3184.

Mullins,R.D., Heuser,J.A., and Pollard,T.D. (1998). The interaction of Arp2/3 complex with actin: nucleation, high affinity pointed end capping, and formation of branching networks of filaments. Proc.Natl.Acad.Sci.U.S.A *95*, 6181-6186.

Mullins,R.D., Kelleher,J.F., Xu,J., and Pollard,T.D. (1998). Arp2/3 complex from Acanthamoeba binds profilin and cross-links actin filaments. Mol.Biol.Cell *9*, 841-852.

Nakagawa,H., Miki,H., Ito,M., Ohashi,K., Takenawa,T., and Miyamoto,S. (2001). N-WASP, WAVE and Mena play different roles in the organization of actin cytoskeleton in lamellipodia. J.Cell Sci. *114*, 1555-1565.

Nakamura,T., Komiya,M., Sone,K., Hirose,E., Gotoh,N., Morii,H., Ohta,Y., and Mori,N. (2002). Grit, a GTPase-activating protein for the Rho family, regulates neurite extension through association with the TrkA receptor and N-Shc and CrkL/Crk adapter molecules. Mol.Cell Biol. *22*, 8721-8734.

Nakayama,T., Goshima,Y., Misu,Y., and Kato,T. (1999). Role of cdk5 and tau phosphorylation in heterotrimeric G protein-mediated retinal growth cone collapse. J.Neurobiol. *41*, 326-339.

Newsome,T.P., Schmidt,S., Dietzl,G., Keleman,K., Asling,B., Debant,A., and Dickson,B.J. (2000). Trio combines with dock to regulate Pak activity during photoreceptor axon pathfinding in Drosophila. Cell *101*, 283-294.

Nguyen Ba-Charvet,K.T., Brose,K., Marillat,V., Kidd,T., Goodman,C.S., Tessier-Lavigne,M., Sotelo,C., and Chedotal,A. (1999). Slit2-Mediated chemorepulsion and collapse of developing forebrain axons. Neuron *22*, 463-473.

Nguyen Ba-Charvet,K.T., Brose,K., Ma,L., Wang,K.H., Marillat,V., Sotelo,C., Tessier-Lavigne,M., and Chedotal,A. (2001). Diversity and specificity of actions of Slit2 proteolytic fragments in axon guidance. J.Neurosci. *21*, 4281-4289.

Niederost,B., Oertle,T., Fritsche,J., McKinney,R.A., and Bandtlow,C.E. (2002). Nogo-A and myelin-associated glycoprotein mediate neurite growth inhibition by antagonistic regulation of RhoA and Rac1. J.Neurosci. *22*, 10368-10376.

Nikolic,M., Chou,M.M., Lu,W., Mayer,B.J., and Tsai,L.H. (1998). The p35/Cdk5 kinase is a neuron-specific Rac effector that inhibits Pak1 activity. Nature *395*, 194-198.

Nishida,E., Maekawa,S., and Sakai,H. (1984). Cofilin, a protein in porcine brain that binds to actin filaments and inhibits their interactions with myosin and tropomyosin. Biochemistry *23*, 5307-5313.

Nishimura,T., Fukata,Y., Kato,K., Yamaguchi,T., Matsuura,Y., Kamiguchi,H., and Kaibuchi,K. (2003). CRMP-2 regulates polarized Numb-mediated endocytosis for axon growth. Nat.Cell Biol. *5*, 819-826.

Nobes,C.D. and Hall,A. (1995). Rho, rac, and cdc42 GTPases regulate the assembly of multimolecular focal complexes associated with actin stress fibers, lamellipodia, and filopodia. Cell *81*, 53-62.

Nobes,C.D. and Hall,A. (1999). Rho GTPases control polarity, protrusion, and adhesion during cell movement. J.Cell Biol. *144* , 1235-1244.

Nogales,E., Whittaker,M., Milligan,R.A., and Downing,K.H. (1999). High-resolution model of the microtubule. Cell *96*, 79-88.

Obermeier,A., Ahmed,S., Manser,E., Yen,S.C., Hall,C., and Lim,L. (1998). PAK promotes morphological changes by acting upstream of Rac. EMBO J. *17*, 4328-4339.

Ochs,H.D. (1998). The Wiskott-Aldrich syndrome. Semin.Hematol. *35*, 332-345.

Ohashi,K., Nagata,K., Maekawa,M., Ishizaki,T., Narumiya,S., and Mizuno,K. (2000). Rho-associated kinase ROCK activates LIM-kinase 1 by phosphorylation at threonine 508 within the activation loop. J.Biol.Chem. *275*, 3577-3582.

Oinuma,I., Katoh,H., Harada,A., and Negishi,M. (2003). Direct interaction of Rnd1 with Plexin-B1 regulates PDZ-RhoGEF-mediated Rho activation by Plexin-B1 and induces cell contraction in COS-7 cells. J.Biol.Chem. *278*, 25671-25677.

Okano,I., Hiraoka,J., Otera,H., Nunoue,K., Ohashi,K., Iwashita,S., Hirai,M., and Mizuno,K. (1995). Identification and characterization of a novel family of serine/threonine kinases containing two N-terminal LIM motifs. J.Biol.Chem. *270*, 31321-31330.

Orr,J.W., Keranen,L.M., and Newton,A.C. (1992). Reversible exposure of the pseudosubstrate domain of protein kinase C by phosphatidylserine and diacylglycerol. J.Biol.Chem. *267*, 15263-15266.

Owesson,C., Pizzey,J., and Tonge,D. (2000). Sensitivity of NGF-responsive dorsal root ganglion neurons to semaphorin D is maintained in both neonatal and adult mice. Exp.Neurol. *165*, 394-398.

Ozaki,M., Deshpande,S.S., Angkeow,P., Suzuki,S., and Irani,K. (2000). Rac1 regulates stress-induced, redox-dependent heat shock factor activation. J.Biol.Chem. *275*, 35377-35383.

Palazzo,A.F., Cook,T.A., Alberts,A.S., and Gundersen,G.G. (2001). mDia mediates Rho-regulated formation and orientation of stable microtubules. Nat.Cell Biol. *3*, 723-729.

Palmer,A., Zimmer,M., Erdmann,K.S., Eulenburg,V., Porthin,A., Heumann,R., Deutsch,U., and Klein,R. (2002). EphrinB phosphorylation and reverse signaling: regulation by Src kinases and PTP-BL phosphatase. Mol.Cell *9*, 725-737.

Pantaloni,D. and Carlier,M.F. (1993). How profilin promotes actin filament assembly in the presence of thymosin beta 4. Cell *75*, 1007-1014.

Pasterkamp,R.J., Anderson,P.N., and Verhaagen,J. (2001). Peripheral nerve injury fails to induce growth of lesioned ascending dorsal column axons into spinal cord scar tissue expressing the axon repellent Semaphorin3A. Eur.J.Neurosci. *13*, 457-471.

Penzes,P., Beeser,A., Chernoff,J., Schiller,M.R., Eipper,B.A., Mains,R.E., and Huganir,R.L. (2003). Rapid induction of dendritic spine morphogenesis by trans-synaptic ephrinB-EphB receptor activation of the Rho-GEF kalirin. Neuron *37*, 263-274.

Perrot,V., Vazquez-Prado,J., and Gutkind,J.S. (2002). Plexin B regulates Rho through the guanine nucleotide exchange factors leukemia-associated Rho GEF (LARG) and PDZ-RhoGEF. J.Biol.Chem. *277*, 43115-43120.

Pfaff,M., Liu,S., Erle,D.J., and Ginsberg,M.H. (1998). Integrin beta cytoplasmic domains differentially bind to cytoskeletal proteins. J.Biol.Chem. *273*, 6104-6109.

Plump,A.S., Erskine,L., Sabatier,C., Brose,K., Epstein,C.J., Goodman,C.S., Mason,C.A., and Tessier-Lavigne,M. (2002). Slit1 and Slit2 cooperate to prevent premature midline crossing of retinal axons in the mouse visual system. Neuron *33*, 219-232.

Pollard,T.D., Blanchoin,L., and Mullins,R.D. (2000). Molecular mechanisms controlling actin filament dynamics in nonmuscle cells. Annu.Rev.Biophys.Biomol.Struct. *29*, 545-576.

Pollard,T.D., Borisy,G.G. (2003) Cellular Motility Driven by Assembly and Disassembly of Actin Filaments. Cell, *112*, 453-465.

Polleux,F., Morrow,T., and Ghosh,A. (2000). Semaphorin 3A is a chemoattractant for cortical apical dendrites. Nature *404*, 567-573.

Pond,A., Roche,F.K., and Letourneau,P.C. (2002). Temporal regulation of neuropilin-1 expression and sensitivity to semaphorin 3A in NGF- and NT3-responsive chick sensory neurons. J.Neurobiol. *51*, 43-53.

Priddle,H., Hemmings,L., Monkley,S., Woods,A., Patel,B., Sutton,D., Dunn,G.A., Zicha,D., and Critchley,D.R. (1998). Disruption of the talin gene compromises focal adhesion assembly in undifferentiated but not differentiated embryonic stem cells. J.Cell Biol. *142*, 1121-1133.

Quinn,C.C., Chen,E., Kinjo,T.G., Kelly,G., Bell,A.W., Elliott,R.C., McPherson,P.S., and Hockfield,S. (2003). TUC-4b, a novel TUC family variant, regulates neurite outgrowth and associates with vesicles in the growth cone. J.Neurosci. *23*, 2815-2823.

Reagan,L.P., Ye,X.H., Mir,R., DePalo,L.R., and Fluharty,S.J. (1990). Up-regulation of angiotensin II receptors by in vitro differentiation of murine N1E-115 neuroblastoma cells. Mol.Pharmacol. *38*, 878-886.

Ren,X.D., Kiosses,W.B., and Schwartz,M.A. (1999). Regulation of the small GTP-binding protein Rho by cell adhesion and the cytoskeleton. EMBO J. *18*, 578-585.

Reza,J.N., Gavazzi,I., and Cohen,J. (1999). Neuropilin-1 is expressed on adult mammalian dorsal root ganglion neurons and mediates semaphorin3a/collapsin-1-induced growth cone collapse by small diameter sensory afferents. Mol.Cell Neurosci. *14*, 317-326.

Ricard,D., Rogemond,V., Charrier,E., Aguera,M., Bagnard,D., Belin,M.F., Thomasset,N., and Honnorat,J. (2001). Isolation and expression pattern of human Unc-33-like phosphoprotein 6/collapsin response mediator protein 5 (Ulip6/CRMP5): coexistence with Ulip2/CRMP2 in Sema3a- sensitive oligodendrocytes. J.Neurosci. *21*, 7203-7214.

Ridley,A.J., Paterson,H.F., Johnston,C.L., Diekmann,D., and Hall,A. (1992). The small GTP-binding protein rac regulates growth factor-induced membrane ruffling. Cell *70*, 401-410.

Ridley,A.J. and Hall,A. (1992). The small GTP-binding protein rho regulates the assembly of focal adhesions and actin stress fibers in response to growth factors. Cell *70*, 389-399.

Ridley,A.J., Self,A.J., Kasmi,F., Paterson,H.F., Hall,A., Marshall,C.J., and Ellis,C. (1993). rho family GTPase activating proteins p190, bcr and rhoGAP show distinct specificities in vitro and in vivo. EMBO J. *12*, 5151-5160.

Riento,K., Guasch,R.M., Garg,R., Jin,B., and Ridley,A.J. (2003). RhoE binds to ROCK I and inhibits downstream signaling. Mol.Cell Biol. *23*, 4219-4229.

Rodriguez Fernandez,J.L. and Ben Ze'ev,A. (1989). Regulation of fibronectin, integrin and cytoskeleton expression in differentiating adipocytes: inhibition by extracellular matrix and polylysine. Differentiation *42*, 65-74.

Rodriguez,O.C., Schaefer,A.W., Mandato,C.A., Forscher,P., Bement,W.M., and Waterman-Storer,C.M. (2003). Conserved microtubule-actin interactions in cell movement and morphogenesis. Nat.Cell Biol. *5*, 599-609.

Rohatgi,R., Ma,L., Miki,H., Lopez,M., Kirchhausen,T., Takenawa,T., and Kirschner,M.W. (1999). The interaction between N-WASP and the Arp2/3 complex links Cdc42-dependent signals to actin assembly. Cell *97*, 221-231.

Rohm,B., Rahim,B., Kleiber,B., Hovatta,I., and Puschel,A.W. (2000). The semaphorin 3A receptor may directly regulate the activity of small GTPases. FEBS Lett. *486*, 68-72.

Ron,D., Zannini,M., Lewis,M., Wickner,R.B., Hunt,L.T., Graziani,G., Tronick,S.R., Aaronson,S.A., and Eva,A. (1991). A region of proto-dbl essential for its transforming activity shows sequence similarity to a yeast cell cycle gene, CDC24, and the human breakpoint cluster gene, bcr. New Biol. *3*, 372-379.

Roof,D.J., Hayes,A., Adamian,M., Chishti,A.H., and Li,T. (1997). Molecular characterization of abLIM, a novel actin-binding and double zinc finger protein. J.Cell Biol. *138*, 575-588.

Rosenblatt,J., Agnew,B.J., Abe,H., Bamburg,J.R., and Mitchison,T.J. (1997). Xenopus actin depolymerizing factor/cofilin (XAC) is responsible for the turnover of actin filaments in Listeria monocytogenes tails. J.Cell Biol. *136*, 1323-1332.

Rozelle,A.L., Machesky,L.M., Yamamoto,M., Driessens,M.H., Insall,R.H., Roth,M.G., Luby-Phelps,K., Marriott,G., Hall,A., and Yin,H.L. (2000). Phosphatidylinositol 4,5-bisphosphate induces actin-based movement of raft-enriched vesicles through WASP-Arp2/3. Curr.Biol. *10*, 311-320.

Safer,D. and Nachmias,V.T. (1994). Beta thymosins as actin binding peptides. Bioessays *16*, 473-479.

Sahay,A., Molliver,M.E., Ginty,D.D., and Kolodkin,A.L. (2003). Semaphorin 3F is critical for development of limbic system circuitry and is required in neurons for selective CNS axon guidance events. J.Neurosci. *23*, 6671-6680.

Sander,E.E., van Delft,S., ten Klooster,J.P., Reid,T., van der Kammen,R.A., Michiels,F., and Collard,J.G. (1998). Matrix-dependent Tiam1/Rac signaling in epithelial cells promotes either cell-cell adhesion or cell migration and is regulated by phosphatidylinositol 3-kinase. J.Cell Biol. *143*, 1385-1398.

Sarner,S., Kozma,R., Ahmed,S., and Lim,L. (2000). Phosphatidylinositol 3-kinase, Cdc42, and Rac1 act downstream of Ras in integrin-dependent neurite outgrowth in N1E-115 neuroblastoma cells. Mol.Cell Biol. *20*, 158-172.

Sasaki,Y., Cheng,C., Uchida,Y., Nakajima,O., Ohshima,T., Yagi,T., Taniguchi,M., Nakayama,T., Kishida,R., Kudo,Y., Ohno,S., Nakamura,F., and Goshima,Y. (2002). Fyn and Cdk5 mediate semaphorin-3A signaling, which is involved in regulation of dendrite orientation in cerebral cortex. Neuron *35*, 907-920.

Schachner,M. (1991). Cell surface recognition and neuron-glia interactions. Ann.N.Y.Acad.Sci. *633*, 105-112.

Schafer,D.A., Jennings,P.B., and Cooper,J.A. (1996). Dynamics of capping protein and actin assembly in vitro: uncapping barbed ends by polyphosphoinositides. J.Cell Biol. *135*, 169-179.

Scheffzek,K., Ahmadian,M.R., and Wittinghofer,A. (1998). GTPase-activating proteins: helping hands to complement an active site. Trends Biochem.Sci. *23*, 257-262.

Seeger,M., Tear,G., Ferres-Marco,D., and Goodman,C.S. (1993). Mutations affecting growth cone guidance in Drosophila: genes necessary for guidance toward or away from the midline. Neuron *10*, 409-426.

Serafini,T., Kennedy,T.E., Galko,M.J., Mirzayan,C., Jessell,T.M., and Tessier-Lavigne,M. (1994). The netrins define a family of axon outgrowth-promoting proteins homologous to C. elegans UNC-6. Cell *78*, 409-424.

Serafini,T., Colamarino,S.A., Leonardo,E.D., Wang,H., Beddington,R., Skarnes,W.C., and Tessier-Lavigne,M. (1996). Netrin-1 is required for commissural axon guidance in the developing vertebrate nervous system. Cell *87*, 1001-1014.

Serini,G., Valdembri,D., Zanivan,S., Morterra,G., Burkhardt,C., Caccavari,F., Zammataro,L., Primo,L., Tamagnone,L., Logan,M., Tessier-Lavigne,M., Taniguchi,M., Puschel,A.W., and Bussolino,F. (2003). Class 3 semaphorins control vascular morphogenesis by inhibiting integrin function. Nature *424*, 391-397.

Shamah,S.M., Lin,M.Z., Goldberg,J.L., Estrach,S., Sahin,M., Hu,L., Bazalakova,M., Neve,R.L., Corfas,G., Debant,A., and Greenberg,M.E. (2001). EphA receptors regulate growth cone dynamics through the novel guanine nucleotide exchange factor ephexin. Cell *105*, 233-244.

Shamah,S.M., Lin,M.Z., Goldberg,J.L., Estrach,S., Sahin,M., Hu,L., Bazalakova,M., Neve,R.L., Corfas,G., Debant,A., and Greenberg,M.E. (2001). EphA receptors regulate growth cone dynamics through the novel guanine nucleotide exchange factor ephexin. Cell *105*, 233-244.

Shekarabi,M. and Kennedy,T.E. (2002). The netrin-1 receptor DCC promotes filopodia formation and cell spreading by activating Cdc42 and Rac1. Mol.Cell Neurosci. *19*, 1-17.

Simpson,J.H., Kidd,T., Bland,K.S., and Goodman,C.S. (2000). Short-range and long-range guidance by slit and its Robo receptors. Robo and Robo2 play distinct roles in midline guidance. Neuron *28*, 753-766.

Song,H., Ming,G., He,Z., Lehmann,M., McKerracher,L., Tessier-Lavigne,M., and Poo,M. (1998). Conversion of neuronal growth cone responses from repulsion to attraction by cyclic nucleotides. Science *281*, 1515-1518.

Sonnenfeld,M.J. and Jacobs,J.R. (1994). Mesectodermal cell fate analysis in Drosophila midline mutants. Mech.Dev. *46*, 3-13.

Stein,E. and Tessier-Lavigne,M. (2001). Hierarchical organization of guidance receptors: silencing of netrin attraction by slit through a Robo/DCC receptor complex. Science *291*, 1928-1938.

Struckhoff,E.C. and Lundquist,E.A. (2003). The actin-binding protein UNC-115 is an effector of Rac signaling during axon pathfinding in C. elegans. Development *130*, 693-704.

Sumi,T., Matsumoto,K., Takai,Y., and Nakamura,T. (1999). Cofilin phosphorylation and actin cytoskeletal dynamics regulated by rho- and Cdc42-activated LIM-kinase 2. J.Cell Biol. *147*, 1519-1532.

Svitkina,T.M., Verkhovsky,A.B., McQuade,K.M., and Borisy,G.G. (1997). Analysis of the actin-myosin II system in fish epidermal keratocytes: mechanism of cell body translocation. J.Cell Biol. *139*, 397-415.

Swiercz,J.M., Kuner,R., Behrens,J., and Offermanns,S. (2002). Plexin-B1 directly interacts with PDZ-RhoGEF/LARG to regulate RhoA and growth cone morphology. Neuron *35*, 51-63.

Symons,M., Derry,J.M., Karlak,B., Jiang,S., Lemahieu,V., McCormick,F., Francke,U., and Abo,A. (1996). Wiskott-Aldrich syndrome protein, a novel effector for the GTPase CDC42Hs, is implicated in actin polymerization. Cell *84*, 723-734.

Takahashi,T., Fournier,A., Nakamura,F., Wang,L.H., Murakami,Y., Kalb,R.G., Fujisawa,H., and Strittmatter,S.M. (1999). Plexin-neuropilin-1 complexes form functional semaphorin-3A receptors. Cell *99*, 59-69.

Takahashi,T. and Strittmatter,S.M. (2001). Plexina1 autoinhibition by the plexin sema domain. Neuron *29*, 429-439.

Tamagnone,L., Artigiani,S., Chen,H., He,Z., Ming,G.I., Song,H., Chedotal,A., Winberg,M.L., Goodman,C.S., Poo,M., Tessier-Lavigne,M., and Comoglio,P.M. (1999). Plexins are a large family of receptors for transmembrane, secreted, and GPI-anchored semaphorins in vertebrates. Cell *99*, 71-80.

Tanelian,D.L., Barry,M.A., Johnston,S.A., Le,T., and Smith,G.M. (1997). Semaphorin III can repulse and inhibit adult sensory afferents in vivo. Nat.Med. *3*, 1398-1401.

Taniguchi,M., Yuasa,S., Fujisawa,H., Naruse,I., Saga,S., Mishina,M., and Yagi,T. (1997). Disruption of semaphorin III/D gene causes severe abnormality in peripheral nerve projection. Neuron *19*, 519-530.

Tawil,N.J., Houde,M., Blacher,R., Esch,F., Reichardt,L.F., Turner,D.C., and Carbonetto,S. (1990). Alpha 1 beta 1 integrin heterodimer functions as a dual laminin/collagen receptor in neural cells. Biochemistry *29*, 6540-6544.

Terman,J.R., Mao,T., Pasterkamp,R.J., Yu,H.H., and Kolodkin,A.L. (2002). MICALs, a family of conserved flavoprotein oxidoreductases, function in plexin-mediated axonal repulsion. Cell *109*, 887-900.

Tessier-Lavigne,M. and Goodman,C.S. (1996). The molecular biology of axon guidance. Science *274*, 1123-1133.

Tigyi,G., Fischer,D.J., Sebok,A., Yang,C., Dyer,D.L., and Miledi,R. (1996). Lysophosphatidic acid-induced neurite retraction in PC12 cells: control by phosphoinositide-Ca2+ signaling and Rho. J.Neurochem. *66*, 537-548.

Tilney,L.G., Bonder,E.M., and DeRosier,D.J. (1981). Actin filaments elongate from their membrane-associated ends. J.Cell Biol. *90*, 485-494.

Tominaga,T., Meng,W., Togashi,K., Urano,H., Alberts,A.S., and Tominaga,M. (2002). The Rho GTPase effector protein, mDia, inhibits the DNA binding ability of the transcription factor Pax6 and changes the pattern of neurite extension in cerebellar granule cells through its binding to Pax6. J.Biol.Chem. *277*, 47686-47691.

Tsubakimoto,K., Matsumoto,K., Abe,H., Ishii,J., Amano,M., Kaibuchi,K., and Endo,T. (1999). Small GTPase RhoD suppresses cell migration and cytokinesis. Oncogene *18*, 2431-2440.

Tsuji,T., Ishizaki,T., Okamoto,M., Higashida,C., Kimura,K., Furuyashiki,T., Arakawa,Y., Birge,R.B., Nakamoto,T., Hirai,H., and Narumiya,S. (2002). ROCK and mDia1 antagonize in Rho-dependent Rac activation in Swiss 3T3 fibroblasts. J.Cell Biol. *157*, 819-830.

Tyska,M.J. and Warshaw,D.M. (2002). The myosin power stroke. Cell Motil.Cytoskeleton *51*, 1-15.

Ueda,T., Kikuchi,A., Ohga,N., Yamamoto,J., and Takai,Y. (1990). Purification and characterization from bovine brain cytosol of a novel regulatory protein inhibiting the dissociation of GDP from and the subsequent binding of GTP to rhoB p20, a ras p21-like GTP-binding protein. J.Biol.Chem. *265*, 9373-9380.

Uehata,M., Ishizaki,T., Satoh,H., Ono,T., Kawahara,T., Morishita,T., Tamakawa,H., Yamagami,K., Inui,J., Maekawa,M., and Narumiya,S. (1997). Calcium sensitization of smooth muscle mediated by a Rho-associated protein kinase in hypertension. Nature *389*, 990-994.

van Horck,F.P., Lavazais,E., Eickholt,B.J., Moolenaar,W.H., and Divecha,N. (2002). Essential role of type I(alpha) phosphatidylinositol 4-phosphate 5-kinase in neurite remodeling. Curr.Biol. *12*, 241-245.

Van Raay,T.J., Foskett,S.M., Connors,T.D., Klinger,K.W., Landes,G.M., and Burn,T.C. (1997). The NTN2L gene encoding a novel human netrin maps to the autosomal dominant polycystic kidney disease region on chromosome 16p13.3. Genomics *41*, 279-282.

Vastrik,I., Eickholt,B.J., Walsh,F.S., Ridley,A., and Doherty,P. (1999). Sema3A-induced growth-cone collapse is mediated by Rac1 amino acids 17-32. Curr.Biol. *9*, 991-998.

Vignjevic,D., Yarar,D., Welch,M.D., Peloquin,J., Svitkina,T., and Borisy,G.G. (2003). Formation of filopodia-like bundles in vitro from a dendritic network. J.Cell Biol. *160*, 951-962.

Vikis,H.G., Li,W., He,Z., and Guan,K.L. (2000). The semaphorin receptor plexin-B1 specifically interacts with active Rac in a ligand-dependent manner. Proc.Natl.Acad.Sci.U.S.A *97*, 12457-12462.

Voncken,J.W., van Schaick,H., Kaartinen,V., Deemer,K., Coates,T., Landing,B., Pattengale,P., Dorseuil,O., Bokoch,G.M., Groffen,J., and . (1995). Increased neutrophil respiratory burst in bcr-null mutants. Cell *80*, 719-728.

Wahl,S., Barth,H., Ciossek,T., Aktories,K., and Mueller,B.K. (2000). Ephrin-A5 induces collapse of growth cones by activating Rho and Rho kinase. J.Cell Biol. *149*, 263-270.

Waldmann,R., Nieberding,M., and Walter,U. (1987). Vasodilator-stimulated protein phosphorylation in platelets is mediated by cAMP- and cGMP-dependent protein kinases. Eur.J.Biochem. *167*, 441-448.

Wang,K.H., Brose,K., Arnott,D., Kidd,T., Goodman,C.S., Henzel,W., and Tessier-Lavigne,M. (1999). Biochemical purification of a mammalian slit protein as a positive regulator of sensory axon elongation and branching. Cell *96*, 771-784.

Wang,L.H. and Strittmatter,S.M. (1996). A family of rat CRMP genes is differentially expressed in the nervous system. J.Neurosci. *16*, 6197-6207.

Wang,L.H. and Strittmatter,S.M. (1997). Brain CRMP forms heterotetramers similar to liver dihydropyrimidinase. J.Neurochem. *69*, 2261-2269.

Ward,Y., Yap,S.F., Ravichandran,V., Matsumura,F., Ito,M., Spinelli,B., and Kelly,K. (2002). The GTP binding proteins Gem and Rad are negative regulators of the Rho-Rho kinase pathway. J.Cell Biol. *157*, 291-302.

Watanabe,N., Madaule,P., Reid,T., Ishizaki,T., Watanabe,G., Kakizuka,A., Saito,Y., Nakao,K., Jockusch,B.M., and Narumiya,S. (1997). p140mDia, a mammalian homolog of Drosophila diaphanous, is a target protein for Rho small GTPase and is a ligand for profilin. EMBO J. *16*, 3044-3056.

Watanabe,N., Kato,T., Fujita,A., Ishizaki,T., and Narumiya,S. (1999). Cooperation between mDia1 and ROCK in Rho-induced actin reorganization. Nat.Cell Biol. *1*, 136-143.

Waterman-Storer,C.M., Worthylake,R.A., Liu,B.P., Burridge,K., and Salmon,E.D. (1999). Microtubule growth activates Rac1 to promote lamellipodial protrusion in fibroblasts. Nat.Cell Biol. *1*, 45-50.

Waterman-Storer,C.M. and Salmon,E. (1999). Positive feedback interactions between microtubule and actin dynamics during cell motility. Curr.Opin.Cell Biol. *11*, 61-67.

Welch,M.D., Iwamatsu,A., and Mitchison,T.J. (1997). Actin polymerization is induced by Arp2/3 protein complex at the surface of Listeria monocytogenes. Nature *385*, 265-269.

Welch,M.D., Mallavarapu,A., Rosenblatt,J., and Mitchison,T.J. (1997). Actin dynamics in vivo. Curr.Opin.Cell Biol. *9*, 54-61.

Welch,M.D., DePace,A.H., Verma,S., Iwamatsu,A., and Mitchison,T.J. (1997). The human Arp2/3 complex is composed of evolutionarily conserved subunits and is localized to cellular regions of dynamic actin filament assembly. J.Cell Biol. *138*, 375-384.

Wells,A.L., Lin,A.W., Chen,L.Q., Safer,D., Cain,S.M., Hasson,T., Carragher,B.O., Milligan,R.A., and Sweeney,H.L. (1999). Myosin VI is an actin-based motor that moves backwards. Nature *401*, 505-508.

Wennerberg,K., Forget,M.A., Ellerbroek,S.M., Arthur,W.T., Burridge,K., Settleman,J., Der,C.J., and Hansen,S.H. (2003). Rnd proteins function as RhoA antagonists by activating p190 RhoGAP. Curr.Biol. *13*, 1106-1115.

Williamson,T.L. and Cleveland,D.W. (1999). Slowing of axonal transport is a very early event in the toxicity of ALS-linked SOD1 mutants to motor neurons. Nat.Neurosci. *2*, 50-56.

Winberg,M.L., Mitchell,K.J., and Goodman,C.S. (1998). Genetic analysis of the mechanisms controlling target selection: complementary and combinatorial functions of netrins, semaphorins, and IgCAMs. Cell *93*, 581-591.

Winberg,M.L., Tamagnone,L., Bai,J., Comoglio,P.M., Montell,D., and Goodman,C.S. (2001). The transmembrane protein Off-track associates with Plexins and functions downstream of Semaphorin signaling during axon guidance. Neuron *32*, 53-62.

Winter,C.G., Wang,B., Ballew,A., Royou,A., Karess,R., Axelrod,J.D., and Luo,L. (2001). Drosophila Rho-associated kinase (Drok) links Frizzled-mediated planar cell polarity signaling to the actin cytoskeleton. Cell *105*, 81-91.

Wong,K., Ren,X.R., Huang,Y.Z., Xie,Y., Liu,G., Saito,H., Tang,H., Wen,L., Brady-Kalnay,S.M., Mei,L., Wu,J.Y., Xiong,W.C., and Rao,Y. (2001). Signal transduction in neuronal migration: roles of GTPase activating proteins and the small GTPase Cdc42 in the Slit-Robo pathway. Cell *107*, 209-221.

Worthylake,R.A. and Burridge,K. (2003). RhoA and ROCK promote migration by limiting membrane protrusions. J.Biol.Chem. *278*, 13578-13584.

Wright,D.E., White,F.A., Gerfen,R.W., Silos-Santiago,I., and Snider,W.D. (1995). The guidance molecule semaphorin III is expressed in regions of spinal cord and periphery avoided by growing sensory axons. J.Comp Neurol. *361*, 321-333.

Yamaguchi,Y., Katoh,H., Yasui,H., Mori,K., and Negishi,M. (2001). RhoA inhibits the nerve growth factor-induced Rac1 activation through Rho-associated kinase-dependent pathway. J.Biol.Chem. *276*, 18977-18983.

Yamashiro,S., Totsukawa,G., Yamakita,Y., Sasaki,Y., Madaule,P., Ishizaki,T., Narumiya,S., and Matsumura,F. (2003). Citron kinase, a Rho-dependent kinase, induces di-phosphorylation of regulatory light chain of myosin II. Mol.Biol.Cell *14*, 1745-1756.

Yamashita,T., Tucker,K.L., and Barde,Y.A. (1999). Neurotrophin binding to the p75 receptor modulates Rho activity and axonal outgrowth. Neuron *24*, 585-593.

Yamashita,T., Higuchi,H., and Tohyama,M. (2002). The p75 receptor transduces the signal from myelin-associated glycoprotein to Rho. J.Cell Biol. *157*, 565-570.

Yang,N., Higuchi,O., Ohashi,K., Nagata,K., Wada,A., Kangawa,K., Nishida,E., and Mizuno,K. (1998). Cofilin phosphorylation by LIM-kinase 1 and its role in Rac-mediated actin reorganization. Nature *393*, 809-812.

Yarar,D., To,W., Abo,A., and Welch,M.D. (1999). The Wiskott-Aldrich syndrome protein directs actin-based motility by stimulating actin nucleation with the Arp2/3 complex. Curr.Biol. *9*, 555-558.

Yasui,H., Katoh,H., Yamaguchi,Y., Aoki,J., Fujita,H., Mori,K., and Negishi,M. (2001). Differential responses to nerve growth factor and epidermal growth factor in neurite outgrowth of PC12 cells are determined by Rac1 activation systems. J.Biol.Chem. *276*, 15298-15305.

Yoshida,H., Watanabe,A., and Ihara,Y. (1998). Collapsin response mediator protein-2 is associated with neurofibrillary tangles in Alzheimer's disease. J.Biol.Chem. *273*, 9761-9768.

Yuan,X.B., Jin,M., Xu,X., Song,Y.Q., Wu,C.P., Poo,M.M., and Duan,S. (2003). Signalling and crosstalk of Rho GTPases in mediating axon guidance. Nat.Cell Biol. *5*, 38-45.

Yuasa-Kawada,J., Suzuki,R., Kano,F., Ohkawara,T., Murata,M., and Noda,M. (2003). Axonal morphogenesis controlled by antagonistic roles of two CRMP subtypes in microtubule organization. Eur.J.Neurosci. *17*, 2329-2343.

Zallen,J.A., Cohen,Y., Hudson,A.M., Cooley,L., Wieschaus,E., and Schejter,E.D. (2002). SCAR is a primary regulator of Arp2/3-dependent morphological events in Drosophila. J.Cell Biol. *156*, 689-701.

Zanata,S.M., Hovatta,I., Rohm,B., and Puschel,A.W. (2002). Antagonistic effects of Rnd1 and RhoD GTPases regulate receptor activity in Semaphorin 3A-induced cytoskeletal collapse. J.Neurosci. *22*, 471-477.

Zhang,W., Vazquez,L., Apperson,M., and Kennedy,M.B. (1999). Citron binds to PSD-95 at glutamatergic synapses on inhibitory neurons in the hippocampus. J.Neurosci. *19*, 96-108.

Zheng,J.Q., Felder,M., Connor,J.A., and Poo,M.M. (1994). Turning of nerve growth cones induced by neurotransmitters. Nature *368*, 140-144.

Zhou,F.Q., Waterman-Storer,C.M., and Cohan,C.S. (2002). Focal loss of actin bundles causes microtubule redistribution and growth cone turning. J.Cell Biol. *157*, 839-849.

Zou,Y., Stoeckli,E., Chen,H., and Tessier-Lavigne,M. (2000). Squeezing axons out of the gray matter: a role for slit and semaphorin proteins from midline and ventral spinal cord. Cell *102*, 363-375.